ISSN 0021-9673

VOL. 678 NO. 2 SEPTEMBER 2, 1994

THIS ISSUE COMPLETES VOL. 678

JOURNAL OF CHROMATOGRAPHY A

INCLUDING ELECTROPHORESIS AND OTHER SEPARATION METHODS

ELSEVIER

JOURNAL OF CHROMATOGRAPHY A

INCLUDING ELECTROPHORESIS AND OTHER SEPARATION METHODS

Scope. The *Journal of Chromatography A* publishes papers on all aspects of **chromatography, electrophoresis** and related methods. Contributions consist mainly of research papers dealing with chromatographic theory, instrumental developments and their applications. In the *Symposium volumes*, which are under separate editorship, proceedings of symposia on chromatography, electrophoresis and related methods are published. *Journal of Chromatography B: Biomedical Applications* —This journal, which is under separate editorship, deals with the following aspects: developments in and applications of chromatographic and electrophoretic techniques related to clinical diagnosis or alterations during medical treatment; screening and profiling of body fluids or tissues related to the analysis of active substances and to metabolic disorders; drug level monitoring and pharmacokinetic studies; clinical toxicology; forensic medicine; veterinary medicine; occupational medicine; results from basic medical research with direct consequences in clinical practice.

Submission of Papers. The preferred medium of submission is on disk with accompanying manuscript (see *Electronic manuscripts* in the Instructions to Authors, which can be obtained from the publisher, Elsevier Science B.V., P.O. Box 330, 1000 AH Amsterdam, Netherlands). Manuscripts (in English; *four* copies are required) should be submitted to: Editorial Office of *Journal of Chromatography A*, P.O. Box 681, 1000 AR Amsterdam, Netherlands, Telefax (+31-20) 5862 304, or to: The Editor of *Journal of Chromatography B: Biomedical Applications*, P.O. Box 681, 1000 AR Amsterdam, Netherlands. Review articles are invited or proposed in writing to the Editors who welcome suggestions for subjects. An outline of the proposed review should first be forwarded to the Editors for preliminary discussion prior to preparation. Submission of an article is understood to imply that the article is original and unpublished and is not being considered for publication elsewhere. For copyright regulations, see below.

Publication information. *Journal of Chromatography A* (ISSN 0021-9673): for 1994 Vols. 652–682 are scheduled for publication. *Journal of Chromatography B: Biomedical Applications* (ISSN 0378-4347): for 1994 Vols. 652–662 are scheduled for publication. Subscription prices for *Journal of Chromatography A*, *Journal of Chromatography B: Biomedical Applications* or a combined subscription are available upon request from the publisher. Subscriptions are accepted on a prepaid basis only and are entered on a calendar year basis. Issues are sent by surface mail except to the following countries where air delivery via SAL is ensured: Argentina, Australia, Brazil, Canada, China, Hong Kong, India, Israel, Japan, Malaysia, Mexico, New Zealand, Pakistan, Singapore, South Africa, South Korea, Taiwan, Thailand, USA. For all other countries airmail rates are available upon request. Claims for missing issues must be made within six months of our publication (mailing) date. Please address all your requests regarding orders and subscription queries to: Elsevier Science B.V., Journal Department, P.O. Box 211, 1000 AE Amsterdam, Netherlands. Tel.: (+31-20) 5803 642; Fax: (+31-20) 5803 598. Customers in the USA and Canada wishing information on this and other Elsevier journals, please contact Journal Information Center, Elsevier Science Inc., 655 Avenue of the Americas, New York, NY 10010, USA, Tel. (+1-212) 633 3750, Telefax (+1-212) 633 3764.

Abstracts/Contents Lists published in Analytical Abstracts, Biochemical Abstracts, Biological Abstracts, Chemical Abstracts, Chemical Titles, Chromatography Abstracts, Current Awareness in Biological Sciences (CABS), Current Contents/Life Sciences, Current Contents/Physical, Chemical & Earth Sciences, Deep-Sea Research/Part B: Oceanographic Literature Review, Excerpta Medica, Index Medicus, Mass Spectrometry Bulletin, PASCAL-CNRS, Referativnyi Zhurnal, Research Alert and Science Citation Index.

US Mailing Notice. *Journal of Chromatography A* (ISSN 0021-9673) is published weekly (total 52 issues) by Elsevier Science B.V., (Sara Burgerhartstraat 25, P.O. Box 211, 1000 AE Amsterdam, Netherlands). Annual subscription price in the USA US$ 4994.00 (US$ price valid in North, Central and South America only) including air speed delivery. Second class postage paid at Jamaica, NY 11431. **USA POSTMASTERS**: Send address changes to *Journal of Chromatography A*, Publications Expediting, Inc., 200 Meacham Avenue, Elmont, NY 11003. Airfreight and mailing in the USA by Publications Expediting.

See inside back cover for Publication Schedule, Information for Authors and information on Advertisements.

0021-9673/94/$07.00

Printed in the Netherlands

VOL. 678, NO. 2 JOURNAL OF CHROMATOGRAPHY A SEPTEMBER 2, 1994

CONTENTS

(Abstracts/Contents Lists published in Analytical Abstracts, Biochemical Abstracts, Biological Abstracts, Chemical Abstracts, Chemical Titles, Chromatography Abstracts, Current Awareness in Biological Sciences (CABS), Current Contents/Life Sciences, Current Contents/Physical, Chemical & Earth Sciences, Deep-Sea Research/Part B: Oceanographic Literature Review, Excerpta Medica, Index Medicus, Mass Spectrometry Bulletin, PASCAL-CNRS, Referativnyi Zhurnal, Research Alert and Science Citation Index)

REVIEW

REGULAR PAPERS

Column Liquid Chromatography

Gas Chromatography

(Continued overleaf)

Contents (continued)

ELSEVIER

Journal of Chromatography A, 678 (1994) 189–200

JOURNAL OF CHROMATOGRAPHY A

Review

Retrieval of structure information from retention index

C.T. Peng[1]

Department of Pharmaceutical Chemistry, School of Pharmacy, University of California, San Francisco, CA 94143-0446, USA and Department of Chemistry and Nuclear Science Facility, San Jose State University, San Jose, CA 95192-0163, USA

First received 10 January 1994; revised manuscript received 26 April 1994

Abstract

The chromatographic identity of a compound can be determined by four parameters, namely, I, A, Z and (GRF). These are interrelated in a linear regression equation, given in the paper as Eq. 8. The retrieval of structural information from retention data requires the introduction of a new meaning to the Kováts retention index, the use of column difference (ΔI) to characterize functional groups, the redefinition of the role of electronegative oxygen and nitrogen atoms, and the division of retention index (I) into contributions from atoms and from functional groups. The separation of retention index (I) into molecular and interaction contributions is a necessary condition for retention index prediction from structure and also for structure information retrieval from retention data. According to Eq. 8 the retention index is uniquely determined by three parameters, namely A, Z and (GRF). For prediction of retention index, the A value is assigned a value of 100 index units (i.u.), the Z value is obtained directly from the compound, and the (GRF) value is pre-calibrated. In Eq. 10, the m and n values represent the pre-calibrated terms for a quantitative structure–retention index relationship. These terms account for the positive and negative retention contributions from polar and polarizable atom groups. All atom groups that are different from methylene and methyl groups will interact with the stationary phase and contribute to retention. The m and n values for various functional, polar and polarizable atom groups and their column differences (ΔI values) are the results of interactions between the solute and the stationary phase and are structure dependent. The interaction increases with increasing polarities of the solute and the stationary phase. The column difference not only reflects the strength of the interaction, but is also characteristic of the functional and polarizable groups. The retrieval of structural information from retention data is equivalent to obtaining Z and (GRF) values from known I and ΔI values, which is straightforward for monofunctional compounds. For multi-functional compounds, additional data will be needed for retrieval of structural information. These can be obtained from derivatization of the unknown compound, from its chemical reactions with other reagents, from GC–MS analysis and from structure match using internal or external standards. The additional data required will depend upon the complexity of the unknown structure. This approach demonstrates that a system can be devised to utilize GC retention characteristics uniquely for structure elucidation.

[1] Address for correspondence: Department of Pharmaceutical Chemistry, School of Pharmacy, University of California, San Francisco, CA 94143-0446, USA.

0021-9673/94/$07.00
SSDI 0021-9673(94)00431-8

Contents

1. Introduction

Gas chromatography (GC) can separate complex mixtures of closely related components into individual chromatographic peaks by differential adsorption and partition on a chromatographic column but it provides no systematic means for identifying these peaks except by co-chromatography with authentic samples or by mass spectrometric (MS) analysis. The fact that each compound shows a characteristic emergence or retention time corresponding to the structure under given GC conditions, implies that there is structural information in GC retention data. The question is how can a system be devised to extract structural information from retention index. This report will focus on this subject, and the content will be divided into three parts. The first part will review briefly the current status of correlation between retention and structure for predictive purpose to show that not all correlations can be used to retrieve structural information from retention data. The second part will review our work on the prediction of retention index from structure and will point out the conceptual difference between the conventional approach and our approach, which can lead to a system that can be applied conversely. The third part will discuss the retrieval of structural information from retention data and will show a simple procedure for identifying monofunctional compounds. For more complex molecules, additional information from chromatographic retention on different stationary phases, from chemical reactions of the unknown compounds, from GC–MS and from other sources are needed for elucidating unknown structures.

2. Historical background

Gas–liquid chromatography [GLC or may be abbreviated as gas chromatography (GC)] was introduced in 1952 by James and Martin [1]. Its high resolving power and the ease of operation have rapidly gained world-wide acceptance. According to Takács and co-workers, the number of papers published on GC and its applications exceeded 70 000 up to 1983 [2], and there were over 100 important retention index research establishments in 28 countries over the world in 1989 [3]. The Twelfth Collective Index of *Chemical Abstracts* listed over 9000 references under Gas Chromatography in a 5-year span from 1987

to 1991. Numerous reviews, books and conference proceedings on the topic were published [2–6]. These activities are testimony to the importance of GC as a separation and analytical tool.

Aside from various applications, the central interest of GC research has been (i) the study of the influence on retention of carrier gas flow-rate, sample size, temperatures of injector, column and detector, column length, the nature, polarity and film thickness of stationary liquid phase, and the nature of solid support, etc., (ii) the use of retention index systems for reporting of retention data free of influences of experimental parameters for reproducibility and inter-laboratory comparison and (iii) the correlations between retention data and structure and between retention data and physico-chemical properties of the compounds under study. With the introduction of modern column technology and modern GC instrumentation, experimental parameters can be precisely controlled and reproduced and no longer represent a central focus of research interest. The retention data are reported in the literature in terms of equivalent chain length, methylene unit, relative retention with respect to *n*-nonane, retention index, etc. These retention values, while free of the influence of experimental parameters, are difficult to interconvert among one another. The Kováts retention index system, using *n*-alkanes as calibration standards, is the most favored and widely adopted. Other polar calibration standards, such as 1-alkanols [7], 2-alkanones [8], propyl ethers [9], fatty acid methyl esters [10], etc. have been recommended. Their usage is not suitable for prediction of retention index from structure and conversely for retrieval of structural information from retention data. Correlations of retention, structure and physico-chemical properties have been intensively studied. For clarity we will review them briefly separately below:

2.1. Correlation of retention index and physico-chemical properties

Retention and retention index and their correlations with physico-chemical properties have been the subject of many reviews [2–6]. According to Evans and Haken [4], "all the correlations of retention indices and the various physico-chemical properties are of relatively short order (i.e, there are few correlations), or with application being restricted to a particular functional class of functional classes", and "despite much work and many reports it is obvious that no realistic scheme of wide application is available for the precalculation of retention indices". Substantive review articles by Takács and co-workers [2,3] and by Evans and Haken [4] cited over 2200 references and discussed many aspects of retention and all retention index systems. These systems known as generalised retention index, homologous index, unified retention index, standard retention index, invariant retention index, universal retention index, molecular retention index, dispersion and selectivity indexes [2–6] and electric topological index [11], correlate retention with column temperature, boiling points, flow-rate, equivalent molecular mass or physico-chemical quantities, etc.. Evans and Haken [4,6] have given a concise, thorough account of different systems for reporting retention data and the retention index systems in GC. The application of these retention index systems has been limited generally to hydrocarbons on non-polar stationary phases. When retrieving structural information, retention data on at least two columns of different polarities are required to determine the nature of functional groups in the unknown molecule. If the correlations from the above systems are polynomial in nature or only valid for a non-polar column, then these correlations will be unsuitable to use for retrieving structural information from retention data.

Recent studies using molecular descriptors have predicted the retention indexes of 86 olefins and 144 diverse drugs on non-polar columns [12,13]. The molecular descriptors are derived for the molecular structure from a set of parameters consisting of electron density, charge separation, molecular mass, X moment of inertia, molecular connectivity, molecular refractivity, partition coefficient, etc., and are assigned numerical values for a given class of compounds to represent a molecule's properties. This multidescriptor approach can predict the retention in-

dexes of polychlorinated biphenyls [14,15] and nitrated polynuclear hydrocarbons [16]. According to Ong and Hites [17], a linear combination of molecular polarizability, the ionization potential and the square of the dipole moment of the molecule can predict the retention indexes of polycyclic aromatic hydrocarbons, polychlorinated biphenyls, polychlorinated dibenzo-*p*-dioxins and dibenzofurans. These examples show that although the physico-chemical properties of these compounds can be correlated with GC retention data, their relationships cannot be utilized to retrieve structural information from retention data.

2.2. Correlation of retention index and structure

The earliest structure–retention relationship in GC is the correlation of retention and the carbon number of members of a homologous series [18]. In the isothermal mode, the components of a homologous series will emerge logarithmically spaced from the adjacent peaks. Plotting the logarithmic retention time ($\log t_R$) against the carbon number (n) of the homologues gives a linear relationship, as shown below:

$$\log t_R = an + b \quad (I = 100n) \tag{1}$$

where a and b are constants. The equation in the bracket, $I = 100n$, defines the Kováts I values for the retention calibration standards, n-alkanes [19]. The Kováts I value is calculated from the isothermal retention time by the following equation:

$$I = 100i \cdot \frac{\log X_t - \log t_n}{\log t_{n+i} - \log t_n} + 100n \tag{2}$$

where n represents the number of carbon atoms in n-alkanes used as markers; X_t, t_n and t_{n+i} are the adjusted retention times (corrected for the air peak) of the analyte solute, the n-alkane marker with n carbon atoms eluting before and that with $n+i$ carbon atoms eluting after the analyte, respectively; i usually has the value of 1 or 2.

In temperature-programmed GC, the temperature is linearly increased with time, and the components of a homologous series emerge approximately equally spaced from adjacent peaks. Plotting the adjusted retention time (t'_R) with the carbon number (n) gives the following linear regression equation [20]:

$$t'_R = cn + d \tag{3}$$

where c and d are constants. The retention index can be calculated from the temperature-programmed retention time by the following equation:

$$I = 100i \cdot \frac{X - M_n}{M_{n+i} - M_n} + 100n \tag{4}$$

where n is the number of carbon atoms in n-alkanes used as markers; X, M_n and M_{n+i} are, respectively, the retention times of the solute, the n-alkane marker with n carbon atoms eluting before and that with $n+i$ carbon atoms eluting after the analyte, respectively; i usually has the value of 1 or 2.

Both Eqs. 1 and 3 are basic equations relating retention time to carbon number. The four constants a, b, c and d are arbitrary constants with no obvious significance to structure. The intercept b of Eq. 1 has been equated to a thermodynamic quantity [21].

A different approach to correlate retention with structure is adopted in the use of retention increments or the retention indexes of molecular fragments to compose the retention index of a molecule for which the authentic example is not available. Schomburg and Dielmann [22–24] applied retention increments to predict the retention indexes of saturated and unsaturated cyclopropane hydrocarbons by means of the Kováts indexes of isomers or of compounds with the same number of carbon atoms but with cyclopropane ring, double bond, chain branching, etc. in different positions of the molecule. Schomburg [24] also applied this correlation to aliphatic acid methyl esters and showed that different functional groups have characteristic column differences (ΔI values). Cook and Raushel [25] and West and Hall [26] used the same approach to pre-calculate retention indexes of benzene and benzene derivatives. Buchman et

al. [27] identified substituted cyclohexenes formed in tritium labeling using predicted retention index. Dimov and Moskovkina [28] correlated the retention with the structure of benzodiazepines. In the molecular fragment approach, the correlation found for one single class of compounds cannot be extended to other classes. It limits the general application of the retention increments for the molecular fragments. Our studies show that the retention increments contain mixed contributions of interaction and molecular retention.

2.3. A theoretical approach to retention index (I)

Garcia-Raso et al. [29] studied the GC behaviour of alkenes based on molecular orbital calculations, using the total energy, binding energy, energies and coefficients of highest occupied and lowest unoccupied molecular orbitals, etc. to arrive at the conclusion that the retention index (I) can be represented as:

$$I = I_m + I_i \quad (5)$$

where I_m is the molecular contribution and I_i the contribution from solute–stationary phase interaction. It shows that a linear combination of these two retention contributions can be used for structure information retrieval.

Attempts to sub-divide the retention index were made by Takács and co-workers [30–32] who divided the retention contribution into three components, thus:

$$I^{\text{st.ph.}}_{\text{substance}}(T) = I_a + I_b + I_i^{\text{st.ph.}}(T) \quad (6)$$

where I is retention index under isothermal conditions, at column temperature T, I_a atomic index contribution, I_b bond index contribution, and I_i interaction index contribution from a given stationary phase (st.ph.). Without the bond index contribution term I_b, this equation would have been identical to Eq. 5 given above. Souter [33] commented on the impracticality of using the bond index contribution in Eq. 6 for predicting retention index.

Evans and Smith [34,35] divided the retention index into two components, thus:

$$I = I_M + I^* \quad (7)$$

where I_M is the dispersion index, also known as the molecular index, defined as the retention index of a hypothetical n-alkane having the same molecular mass as the solute (M_e). I^* is the selectivity index which reflects the combined effects of molecular shape and functionality and is also given as the carbon number equivalent of ΔM_e. Eq. 7 appears to be identical to Eq. 5 in appearance but the meaning of the terms in these equations differs widely. The concept of effective molecular mass of the solute M_e was first introduced to correlate the relative retention index based on n-nonane (R_{09}) and the molecular mass of the compound (M) by the relation $\Delta M_e = M_e - M$. The correlation achieved by this system is between retention and molecular mass rather than between retention and structure. Retrieving structural information from retention data by the molecular and selectivity index systems, under such circumstances, would be difficult if the molecular mass is not known.

From the above brief survey, one may perceive that these retention index systems provide no direct link of retention data to structure in a manner that allows the process to work conversely to retrieve structural information from retention data.

3. Structure and retention

When the Kováts retention index (I) of members of a homologous series is plotted against the number of atoms in the molecule (Z), a straight line is obtained. We found that his linear correlation holds for homologous series of acids, alcohols, esters, amines, aromatic hydrocarbons, etc. on both non-polar and polar columns [36,37]. The linearity of the plot is expected because each member of the homologous series differs from its nearest neighbors by a methylene group, thus allowing the same retention mechanism to prevail and leading to the observed

linear relationship between the retention index value and the number of atoms (Z) in the molecule. This linear relationship may be represented by the following linear regression equation:

$$I = AZ + (\mathrm{GRF})_Z \quad (8)$$

where A is the regression coefficient and (GRF) the intercept. The $(\mathrm{GRF})_Z$ stands for the group retention factor when the atom number is Z. Eq. 8 is essentially identical to Eq. 5. The AZ term represents the molecular contribution and the (GRF) term the interaction contribution. Eq. 8 is the basis for predicting retention index from structure [36,37] and conversely, for retrieving structural information from retention data.

3.1. The applications of Eq. 8

The four parameters I, A, Z, and (GRF) in Eq. 8 can characterize the chromatographic identity of a compound. According to the Kováts convention, A can be arbitrarily assigned a value of 100 i.u. The three remaining parameters I, Z and (GRF) can be determined under given conditions. Eq. 8 can be used (i) to determine the (GRF) values of functional groups, (ii) to predict the retention index (I) from structure, and (iii) to retrieve structural information from retention data.

3.2. Redefinition of terms

Separation of the retention index into molecular and interaction contributions is essential, in order to ensure the general application of the (GRF) values. Eq. 8 has been successfully applied to predict the retention indexes of compounds of many functional classes on non-polar and polar columns [36–38].

3.2.1. The Kováts index (I).

The Kováts index is unbiased, that is, the index changes when the structure has a different connectivity and is different from methylene and methyl groups. For retrieval of structural information from retention data only unbiased retention index can be used. The Kováts retention index system uses chemically inert n-alkanes as calibration standards [19] and can detect structure features that are different from methylene and methyl groups. The concern that n-alkanes are poorly soluble on polar columns and adsorbed at the liquid–solid interface [40], and that a set of polar compounds can serve as better retention calibration standards for polar compounds on polar columns, may be overly cautious because the adsorption at the liquid–solid interface is difficult to measure, and the poor solubility occurs only when the column is overloaded. From the viewpoint of chemical inertness and general utility, the n-alkanes remain the least problematic retention calibration standards for information retrieval. Polar calibration standards can generate biased retention index, and their use is unsuitable for structure information retrieval.

In element-specific and electron capture detectors which are insensitive to n-alkanes, the use of polar retention calibration standards, such as 1-bromoalkanes [41], 1-nitroalkanes [42], n-alkyl trichloroacetates [43], etc. may be necessary. Conversion of retention data from one system to another is available [20,42].

Conventionally, the Kováts index marks the interpolated position between the time limits set by two adjacent n-alkanes. When used for structural information retrieval, the value of the retention index can also convey a sense of structure. For example, one may view the molecule of benzene as hypothetically formed from n-hexane; it has a retention index of 654 i.u. on a DB-1 column, of which 600 i.u. is the molecular contribution from the 6 carbon atoms, and 54 i.u. is the interaction contribution from the phenyl ring. On DB-Wax column the retention index (I) for benzene is 950 i.u., of which 600 i.u. is the molecular contribution from the 6 carbon atoms, and 350 i.u. is the interaction contribution from the phenyl ring. When predicting retention index from structure, it is necessary to have the structure built up from an n-alkane through a number of change steps. The predicted retention index will be a sum total of the molecu-

lar contribution and the interaction contributions from all the change steps.

3.2.2. The AZ term

The regression coefficient A in the AZ term in Eq. 8 is defined as the retention index increment for atom addition [36,37]. This value is arbitrarily assigned a value of 100 i.u. according to the Kováts convention, meaning that the addition of a carbon atom to the molecule will increase the retention index by 100 i.u. This rule is generally valid for all homologues and all classes of compounds when the methylene group is not influenced by adjacent electronegative groups. The A value will change if the connectivity of the carbon atoms differs from those of methylene and methyl groups, such as chain branching, quaternary carbon atom, etc. The A values are usually less than 100 i.u. when compounds contain adjacent functional groups or highly electronegative groups [36,37,44]. The carbon atoms in the alkyl chain of the phenylalkanes have A values slightly higher than 100 i.u. [45]. The silylated acid amide homologues have the lowest observed A value of 55 i.u. [44].

The parameter Z in the AZ term is the atom number or the number of atoms which include carbon as well as oxygen, nitrogen and other atoms in the molecule [36]. Inclusion of all the atoms in Z is a significant departure from the past convention which uses only the number of carbon atoms for structure correlation. The mass of oxygen and nitrogen atoms contributes to molecular retention, and at the same time, the non-bonding electrons in O and N atoms interact strongly with the stationary phase and contribute to interaction retention. All the functional groups contain O or N atoms or both. If the carbon number (n) is used in Eq. 5 for Z, the regression coefficient A will not change, but the (GRF) value will increase, in which case the (GRF) value will contain mixed interaction and molecular retention components. As such it will vitiate the devised system for retention index prediction from structure and conversely for retrieval of structural information from retention data.

3.2.3. The (GRF) term

The (GRF) term is the group retention factor or the functionality constant of functional groups. The (GRF) values for the functional groups are considerably larger than those for atom groups containing only carbon atoms. Functional groups containing two oxygen atoms or one nitrogen and one oxygen atom, such as carboxyl or acid amide group have larger (GRF) values than functional groups containing one nitrogen atom or one oxygen atom, such as $-NH_2$, $-OH$, $-CHO$ or $-CO$ groups. The non-bonding electrons can interact strongly with the stationary liquid phase. This interaction is characteristic of the functional group. The functional groups on non-polar DB-1 column can be arranged in the order of decreasing (GRF) values as follows [38]:

acid amides > acids > primary alcohols > primary amines > secondary amines = secondary alcohols > aldehydes, ketones > tertiary alcohols > tertiary amines > esters.

The polarity and polarizability of the functional groups can be modified by derivatization. The (GRF) value of the highly polar carboxyl group is about 257 i.u. on a DB-1 column and about 994 i.u. on a DB-Wax column. The former decreases to zero when the carboxyl group is esterified. The ester group has two oxygen atoms which can still interact with the polar stationary phase. This residual polarizability gives the methyl ester a (GRF) value of about 260 i.u. on the polar DB-Wax column.

The (GRF) values for functional groups are usually obtained from a homologous series. When the homologues for a given functional group are unavailable, the retention index increment value (δI) can be used instead. The δI value is the difference in retention index between a compound with the substituent ($I_{subst.}$) and the one without it (I_0) on the same stationary phase, and it should exclude any molecular contribution from atoms [36], thus:

$$\delta I = I_{subst.} - I_0 \quad (9)$$

Both δI and (GRF) are interaction terms, representing the interaction between solute and stationary phase.

3.3. An extension of Eq. 8

The linear regression Eq. 8 for predicting the retention indexes of homologues is not applicable to compounds not members of the homologous series. A general equation for prediction of retention indexes is given below [36–38] :

$$I_p = 100Z + \sum m_i - \sum n_j \quad (10)$$

where I_p is the predicted I value, and Z the atom number, which includes carbon atoms and carbon atom equivalents of oxygen, nitrogen and other atoms in the molecule. The term m_i is the group retention factor of any of the following functions and atom groups: acid, alcohol, aldehyde, amine, ketone, phenol, alicyclic and aromatic ring formation and ring fusion, etc. The presence of these functions and groups in the molecule contribute to a positive interaction term. The term n_j is the group retention factor of any of the following groups: quaternary carbon atom, carbon chain branching or tertiary carbon atom, terminal carbon–carbon double bond,"ortho effect b", fluorine atoms, etc. The presence of these groups in a molecule contribute to a negative interaction term. The m_i and n_j are essentially δI values, obtainable from reference compounds. Significant deviation of the A value from 100 i.u. can seriously affect the accuracy of Eq. 10 for retention index prediction.

4. Retrieval of structural information from retention data

Retention data collected from one column do not contain sufficient information for structure elucidation. For monofunctional compounds, at least two columns of different polarities should be used. Comparison of these retention data can reveal the nature of the functional groups. Additional information are obtained by derivatization and chemical reactions to modify the functional groups. From the chromatographic retention characteristics of these derivatives, one can obtain additional information to deduce the structure of an unknown compound.

4.1. The column difference (ΔI)

The column difference (ΔI) is defined as the difference between two I values of the same compound on two columns of different polarities, thus:

$$\Delta I = I_{\text{more polar}} - I_{\text{less polar}} \quad (11)$$

where $I_{\text{more polar}}$ and $I_{\text{less polar}}$ are retention indexes on more polar and less polar columns, respectively. The column difference (ΔI) is characteristic of the functional group and the column polarity. According to the Kováts convention the molecular contribution on these columns will be the same but the interaction contribution will increase with the polarity of the column. Combining Eq. 8 with Eq. 11 gives the following:

$$\Delta I = (\text{GRF})_{\text{more polar}} - (\text{GRF})_{\text{less polar}} \quad (12)$$

The largest value of ΔI will be between polar DB-Wax and non-polar DB-1 columns. Huber et al. [46] showed that chemical warfare agents, precursors and decomposition products can be identified using a number of stationary phases of low correlation coefficient and that these columns of different retention characteristics can be selected by applying information theory. This indicates that column difference (ΔI) is an important source for structural information. The Rohrschneider and McReynolds constants for characterizing the selectivities of various stationary liquid phases [47–49] are essentially column differences of selected solutes, such as benzene, nitropropane, butanol, pyridine, etc. on polar and non-polar columns. The column difference was first used to define the degree of unsaturation in fatty acids by James [18].

The procedure based on the use of column difference (ΔI) to identify the functionality of an unknown compound from retention data is given as follows: (i) chromatograph the sample on polar and non-polar columns; (ii) compute the retention indexes from the retention times on both columns using Eq. 4; (iii) obtain the column difference by Eq. 11 and compare this value with the values on the list of compiled column differences for functional groups. If the column

difference (ΔI) of the unidentified functional group is found to match that of the primary alcohol group, this information can be confirmed by derivatization; (iv) silylate the unknown compound by preparing trimethylsilylated and *tert.*-butyldimethylsilylated derivatives; (v) chromatograph the silylated derivatives separately on both polar and non-polar columns; (vi) confirm that all polar groups have been masked and that the trimethylsilyl and *tert.*-butyldimethylsilyl derivatives have identical I values on polar and non-polar columns, a condition characteristic of the silylated ether derivatives from alcohols; (vii) obtain the number of atoms (Z) of the unknown alkanol from the I values of these silylated derivatives by dividing by 100. This gives Z and (GRF) values, which concludes the identification.

4.2. The (GRF) and ΔI values and structure

The example given above for retrieving structural information from retention data is based on Eq. 8 which applies only to monofunctional compounds. For compounds containing other polarizable atom groups in addition to functional groups, Eq. 10 is used. This equation contains a number of (GRF) values in summation terms. To determine each of the (GRF) values, additional data will be required.

The magnitudes of the (GRF) and ΔI values are interrelated. Functional groups give large (GRF) and ΔI values. The polarizable atom groups containing only carbon atoms, such as alicyclic and aromatic rings, fused rings, conjugated systems, branched chain, ternary carbon atoms, etc. have small (GRF) and ΔI values. Conjugated systems containing π-electrons can give large ΔI values. A knowledge of the presence of these groups in the molecule can greatly simplify the process of identification. The use of an element-selective detector to detect the presence of nitrogen and halogen atoms and also conjugated bond systems will be extremely useful. The values of (GRF) and ΔI can characterize the polarizable atom groups by the ΔI values from a number of columns of different polarities. Structural atom groups can also be classified into six classes, as listed in the following from groups 1 to 6 in order of approximately increasing ΔI values. These values are based on DB-Wax and DB-1 columns [36,37]:

(1) Carbon atoms with different bond linkages (molecular connectivity), such as double and triple bonded and branch-chained carbon atoms, etc.

(2) Halogen atoms in the molecule.

(3) Aggregates of carbon atoms in single ring formation and polynuclear ring formation.

(4) The configuration of the whole molecule.

(5) An isolated functional group.

(6) A multiplicity of functional groups in the molecule.

This list is incomplete. Only a small portion of ΔI values for the various functional and polarizable atom groups in the above classes are known [36,37,44]. This will be an area for future investigation.

4.3. Retention index and molecular structure

The advantage of correlating retention index and structure is that a set of rules can be formulated from the published data to serve as guidelines, either to predict retention index from structure or to retrieve structural information from retention data [36]. These rules are:

(1) The retention index of a molecule containing Z atoms cannot be less than its base value (i.e., $100Z$) unless the molecule contains fluorine atoms, quaternary carbon atoms and derivatized functional groups in close proximity.

(2) Molecules which contain multiple O and N atoms will have higher I values than molecules that do not.

(3) Molecules which have highly conjugated systems containing N and O atoms tend to give higher I values than those that do not.

(4) Molecules which contain quaternary carbon atoms and functional groups connected to secondary or tertiary carbon atoms have lower I values than those that do not.

(5) Highly substituted molecules tend to yield lower I values than those that do not.

The above rules show that nitrogen and oxygen atoms by virtue of their non-bonding elec-

trons can form hydrogen bond and interact strongly with polar stationary phase by dipole–dipole, dipole–induced dipole, etc. interactions to give high values of interaction retention. Implicit in the observed data is that electron density, molecular planarity and molecular compactness (i.e., spherical shape) can play a very important role in determining the retention of a molecule.

4.4. Derivatization and chemical reactions

Highly polar compounds, such as amino acids, sugars, etc. cannot be analyzed by GC without derivatization. Their polarity can be modified by acylation, methylation, alkylation and silylation. Derivatization can mask the functionality of the polar groups to such an extent that these derivatives behave chromatographically as *n*-alkanes and have practically the same I values on polar and non-polar columns [44]. In the case of alcohols, the molecule has only one oxygen atom in the functional group, and the silyl group is highly electronegative so that after silylation the silylated ether has no residual polarity or polarizability and can behave chromatographically as an *n*-alkane. If the silyl group is replaced with an alkyl group, the resultant ether group will have a residual polarizability on polar column to give a small (GRF) value and also a small ΔI value. Since the nature of the chemical reactions and the structure of the reagents are known, the identity of the functional group can be deduced from the retention indexes (I) and the column differences (ΔI) of the derivatives. Different derivatives of the same functional group can be prepared to corroborate the identification. Commonly used reagents for derivatization are: (i) bromine (for probing double bond), (ii) hydrogenation (for probing double bond and reducible groups); (iii) silylating agents (for masking hydroxyl, carboxyl and amino groups): trimethylsilyl- and *tert.*-butyldimethyl silyl-; (iv) acylating agents (for masking hydroxyl and amino groups): acetic anhydride, trifluoroacetic anhydride, pentafluoropropionic anhydride and heptafluorobutyric anhydride; (v) methylating agents (for masking hydroxyl, carboxyl and amino groups): diazomethane, methyl iodide, dimethyl sulfate and alkyl chloroformates [50]; and (vi) Schiff's base formation (for masking amino or keto groups)

This list of reactions and reagents is not exhaustive. The reaction products should be well defined and amenable to chromatography, and their retention characteristics should be understood and can reflect the structure of the unknown compound.

4.5. Structure match using internal or external standards

Another source from which to obtain structural information is by comparing and matching the chromatographic retention characteristics of a known structure with that of an unknown structure under various conditions. Complex molecules such as natural products contain oxygenated ring structures. The oxygen atom can appear as ring oxygen as well as hydroxyl and carboxyl group. The functional groups can be derivatized to eliminate their retention contribution. But the (GRF) values of the atom groups, such as the ring system and the ring oxygen atom would not be affected by derivatization. These (GRF) values will vary when the compound is chromatographed on columns of different polarities. If the changes in (GRF) and ΔI values for the standard and the unknown compound can match each other on various columns, it would be a good indication that the standard and the unknown may have similar structural features.

4.6. Applications

One of the great challenges in analytical and organic chemistry is structure elucidation. UV/IR spectrophotometry can identify structures of chromophores by absorption bands. MS can identify unknown structures by fragment ions and molecular ions. Identification by these measurements is not without ambiguities because UV/IR spectrophotometry can only identify the chromophoric group but not the rest of the molecule, and MS has difficulty in differentiating not only between isomers but also between

diverse compounds that have similar fragmentation patterns [39]. In comparison, high-resolution GC can separate both homologues and isomers. The retention index (I) and column difference (ΔI) can reveal the size of the molecule and the nature of the functional groups. Derivatization and chemical reactions can yield additional structural information about the polarizable atom groups. In structure elucidation, any information is useful. For example, in the study of the mechanism of tritium labeling radioimpurities and radioactive by-products can be successfully identified by the use of quantitative structure–retention index relationship because these products are derived from one known compound.

By convention, GC serves only as a separation tool for the GC–MS technique and not as a source for structure information, but GC can complement MS and contribute to structure elucidation. For example, the search of a mass spectrum library for a structure to match the mass spectrum of an unknown compound can result in several different possible structures. The correct structure is selected on the basis that its predicted retention index and column difference (ΔI) values match the observed values of the unknown chromatographic peak [39]. Retrieving structural information from retention data can be a more efficient way for structural analysis because this method is not limited to analyzing one unknown compound at a time. It can simultaneously analyze many unknown chromatographic peaks in a multi-component unknown mixture, since all the components are similarly processed and chromatographed on various columns, and all the retention data are available for characterization of the unknown peaks. This approach has been successfully applied to identify solvent components in liquid scintillation cocktails [39].

5. Conclusions

With the use of an unbiased retention index system and a quantitative structure–retention index relationship one can obtain structural information from GC retention data. In this system the four parameters I, A, Z and (GRF) given in Eq. 8 can define the chromatographic identity of a compound. Based on this system, it is straightforward to identify an unknown monofunctional compounds from retention data, but to identify an unknown multi-functional compound from retention data alone may depend on the complexity of the molecular structure and the number of atom groups it contains. Each atom group needs a piece of chromatographic information to identify it uniquely. Chromatographic information generated from derivatization and chemical reactions of the unknown compound, from column differences on different stationary phases can identify polar and polarizable atom groups. Together with related information from GC–MS and other sources it can lead to structural identification. MS analysis does not always provide sufficient information for structural assignment, but a combination of analytical data from GC and MS can overcome the shortcoming and elucidate structures of unknown compounds.

Acknowledgement

This publication was made possible by grant number CA 33537 from the National Cancer Institute.

References

[1] A.T. James and A.J.P. Martin, *Biochem. J.*, 50 (1952) 679.
[2] M.V. Budahegyi, E.R. Lombosi, T.S. Lombosi, S.Y. Mészaros, Sz. Nyiredy, G. Tarján, I. Timár and J.M. Takács, *J. Chromatogr.*, 271 (1983) 213.
[3] G. Tarján, Sz. Nyiredy, M. Györ, E.R. Lombosi, T.S. Lombosi, S.Y. Budahegyi, S.Y. Mészáros and J.M. Takács, *J. Chromatogr.*, 472 (1989) 1.
[4] M.B. Evans and J.K. Haken, *J. Chromatogr.*, 472 (1989) 93.
[5] E. Kováts, *Adv. Chromatogr.*, 1 (1965) 229.
[6] J.K. Haken, *Adv. Chromatogr.*, 14 (1967) 367.
[7] A. Gröbler, *J. Chromatogr. Sci.*, 10 (1972) 128.
[8] R.G. Ackman, *J. Chromatogr. Sci.*, 10 (1972) 535.
[9] S.J. Hawkes, *J. Chromatogr. Sci.*, 10 (1972) 536.

[10] F.P. Woodford and C.M. van Gant, *J. Lipid Res.*, 1 (1960) 187.
[11] K. Ośmialowski, J. Halkeiewicz and R. Kaliszan, *J. Chromatogr.*, 361 (1986) 63.
[12] R.H. Rohrbaugh and P.C. Jurs, *Anal. Chem.*, 57 (1985) 2770.
[13] R.H. Rohrbaugh and P.C. Jurs, *Anal. Chem.*, 60 (1988) 2249.
[14] A. Robbat, Jr., G. Xyrafas, and D. Marshall, *Anal. Chem.*, 60 (1988) 982.
[15] M.N. Hasan and P.C. Jurs, *Anal. Chem.*, 62 (1990) 2318.
[16] A. Robbat, Jr., N.P. Corso, P.J. Doherty and D. Marshall, *Anal. Chem.*, 58 (1986) 2072.
[17] V.S. Ong and R.A. Hites, *Anal. Chem.*, 63 (1991) 2829.
[18] A.T. James, *J. Chromatogr.*, 2 (1959) 552.
[19] E. Kováts, *Helv. Chim. Acta*, 206 (1958) 1915.
[20] H. Van den Dool and P.D. Kratz, *J. Chromatogr.*, 11 (1963) 463.
[21] R.V. Golovnya and D.N. Grigoryeva, *Chromatographia*, 17 (1983) 613.
[22] G. Schomburg and G. Dielmann, *Anal. Chem.*, 45 (1973) 1647.
[23] G. Schomburg and G. Dielmann, *J. Chromatogr. Sci.*, 11 (1973) 151.
[24] G. Schomburg, *J. Chromatogr.*, 14 (1964) 157.
[25] L.E. Cook and F.M. Raushel, *J. Chromatogr.*, 65 (1972) 556.
[26] S.D. West and R.C. Hall, *J. Chromatogr. Sci.*, 13 (1975) 5.
[27] O. Buchman, G.-Y. Cao and C.T. Peng, *J. Chromatogr.*, 312 (1984) 75.
[28] N. Dimov and M. Moskovkina, *J. Chromatogr.*, 552 (1991) 59.
[29] A. García-Raso, F. Saura-Calixto and M.A. Raso, *J. Chromatogr.*, 302 (1984) 107.
[30] J. Takács, C. Szita and G. Tarján, *J. Chromatogr.*, 56 (1971) 1.
[31] J. Takács, I. Tálas, I. Bernáth, Gy. Czako and A. Fisher, *J. Chromatogr.*, 67 (1972) 203.
[32] J.M. Takács, *J. Chromatogr. Sci.*, 11 (1973) 210.
[33] P. Souter, *J. Chromatogr. Sci.*, 11 (1974) 418.
[34] M.B. Evans and J.F. Smith, *Nature*, 190 (1961) 905.
[35] M.B. Evans and J.F. Smith, *J. Chromatogr.*, 8 (1962) 303.
[36] C.T. Peng, S.F. Ding, R.L. Hua and Z.C. Yang, *J. Chromatogr.*, 436 (1988) 137.
[37] C.T. Peng, Z.C. Yang and S.F. Ding, *J. Chromatogr.*, 586 (1991) 85.
[38] C.T. Peng, *J. Radioanalyt. Nucl. Chem.*, 160 (1992) 449.
[39] C.T. Peng and S.Q. Liu, in J.E. Noakes, F. Schönhofer and H.A. Polach (Editors), *Liquid Scintillation Spectrometry 1992*, Radiocarbon, Tucson, AZ, 1993, pp. 157–164.
[40] D.F. Fritz, A. Sahil and E. Kováts, *J. Chromatogr.*, 186 (1979) 63.
[41] A. Yasuhara, M. Morita and K. Fuwa, *J. Chromatogr.*, 328 (1985) 35.
[42] R. Aderjan and M. Bogusz, *J. Chromatogr.*, 454 (1988) 345.
[43] T.R. Schwartz, J.D. Petty and E.M. Kaiser, *Anal. Chem.*, 55 (1983) 1839.
[44] C.T. Peng, Z.C. Yang and D. Maltby, *J. Chromatogr.*, 586 (1991) 113.
[45] C.T. Peng, R.L. Hua and D. Maltby, *J. Chromatogr.*, 589 (1992) 231.
[46] J.F.K. Huber, E. Kenndler, G. Reich, W. Hack and J. Wolf, *Anal. Chem.*, 65 (1993) 2903.
[47] L. Rohrschneider, *J. Chromatogr. Sci.*, 11 (1973) 160.
[48] W.O. McReynolds, *J. Chromatogr. Sci.*, 8 (9170) 685.
[49] S.K. Poole, B.R. Kersten, R.M. Pomaville and C.F. Poole, *LC·GC*, 6 (1988) 400.
[50] P. Hušek, J.A. Rijks, P.A. Leclercq and C.A. Cramers, *J. High Resolut. Chromatogr.*, 13 (1990) 633.

ELSEVIER

Journal of Chromatography A, 678 (1994) 201–212

JOURNAL OF CHROMATOGRAPHY A

Phosphorimetry and its potential for the study of surface heterogeneity of chromatographic silica-based stationary phases

Laura A. Ciolino, John G. Dorsey*,[1]

Department of Chemistry, University of Cincinnati, Cincinnati, OH 45221-0172, USA

First received 1 February 1994; revised manuscript received 11 May 1994

Abstract

Phosphorimetry was applied to the study of silica-based chromatographic phase surface heterogeneity by determining the phosphorescence response of a phenanthrene probe as a function of loading on underivatized silica and reversed and ion-exchange phases. The phosphorescence response was used to "titrate" and estimate the number of strong adsorption sites on underivatized silica. By incorporating covalent vs. ionic heavy atom/ion enhancers onto derivatized silicas, it was demonstrated that the probe molecules adsorb at residual silanols at lower loadings but associate with alkyl chains at higher loadings. Suggestions for further phosphorimetric studies are given.

1. Introduction

The understanding of adsorption and partitioning processes for chromatographic surfaces is critical to their continued development and use. Silica-based stationary phases continue to function as the workhorse tool for all analytical separations as evidenced by both user testimony [1] and column manufacturers' new product introductions [2]. Adsorption and partitioning processes for silica-based phases are a function of many factors including the nature of bare and derivatized silica surfaces and their interactions with adsorbates, solvents and solutes. A key question concerning silica-based phases is the degree of surface heterogeneity associated with adsorption and partitioning sites.

A variety of spectroscopic techniques are used for the study of silica-based stationary phases beyond characterization of the phases for analytical or quality control purposes. Fourier transform (FT) IR spectroscopy has been used to observe hydrogen bonding interactions between some population of covalently bound ligands and residual silanols on the silica surface for acetoacetamide [3] and cyanoalkyl [4,5] derivatized phases. FT-IR has also been used to study alkyl chain conformations as a function of temperature for reversed phases of varying length by determining the number of infrared "gauche defects" [6].

^{29}Si Cross polarization magic angle spinning (CP-MAS) solid-state NMR has been used to examine bare silica surfaces as a function of dehydration and rehydration [7]. In all cases, the spectra showed a heterogeneous distribution of silanols (Si–OH), geminal silanols [Si = $(OH)_2$] and siloxanes (Si–O–Si). ^{13}C FT-NMR has been

* Corresponding author.

[1] Present address: Department of Chemistry, Florida State University, Tallahassee, FL 32306-3006, USA.

0021-9673/94/$07.00
SSDI 0021-9673(94)00460-Q

used to study the mobility of reversed-phase bonded alkyl chains in the solvated state via line shape analysis or measurement of the spin-lattice relaxation time, t_1, for various moieties or portions of the chain [8–14]. These experiments have been conducted as a function of position along the chain [8,9], bonding density [9,12], solvent viscosity [10], mobile phase composition [11,12] and temperature [13] and the results have been related to retention data [12,14].

Deuterium NMR line shape analysis has also been used for the study of alkyl chain mobility for C_{18} reversed phases [15] and alkoxysilane phases ranging from C_1 to C_{16} [16] in both dry and solvated states. Deuterium NMR of ^2H_2O–methanol and ^2H_2O–acetonitrile mobile phases in contact with C_{18} stationary phases has been used to probe the degree of water association as a function of mobile phase composition via the change in t_1 [17,18]. A similar study was conducted in which the degree of association of methanol or acetonitrile with the phase was probed by using deuterated organic modifiers [19].

Much recent information concerning the heterogeneity of silica-based stationary phase surfaces has come from studies using fluorescent probe molecules which are either physisorbed or covalently bound to the phase. Lochmuller et al. [20,21] covalently attached the fluorescent probe, dansyl amide, to study the surfaces of LiChrospher Si 100 and reversed-phase silicas. Bauer et al. [22] studied the adsorption of pyrene on Merck 60 silica gel both in the absence and presence of long-chain alcohol coadsorbates using fluorescence excitation, emission and decay techniques. Lochmuller et al. [23] determined the proximity and distribution of silica surface silanols by observing the fluorescence of chemically bound pyrene as a function of pyrene-ligand bonding density. In a later study [24], the same authors used time-dependent fluorescence to resolve the pyrene fluorophores into three distinct populations and estimated the relative amount of each population. Oelkrug et al. [25] studied the adsorption of N-heterocycles onto silica from either the gas phase or solution as a function of temperature and surface hydroxyl concentration using a combination of transient absorption, fluorescence and phosphorescence decay measurements.

In separate studies, Stahlberg and Almgren [26] and Carr and Harris [27] used the fluorescence vibronic structure of pyrene to probe the polarity of a C_{18}-derivatized silica surface as a function of mobile phase composition (methanol–water). Further sorption site information was obtained by Carr and Harris [28] from studies in which ionic (prefers mobile phase) vs. non-ionic (prefers stationary phase) fluorescence quenchers were added.

These studies reveal that the surface of silica-based phases is comprised of a heterogeneous distribution of sites, whether they be adsorptive or chemically reactive sites for underivatized silica [22–25], reacted vs. residual sites for derivatized silicas [20,21], or partitioning sites for reversed phases [28]. There are a small percentage of strongly adsorptive/reactive sites [22] and there is a tendency for adsorption or reaction to occur in clusters even at low surface coverages [23,24]. The non-uniform interactions of silica-based phases with solvents and solutes is attributed, at least in part, to the surface heterogeneity [26–28]. There remains considerable controversy as to the specific "structure" of the various adsorption sites on silica as detailed in two comprehensive reviews by Nawrocki [29,30].

We recently investigated the feasibility of designing substrates for room temperature phosphorimetry (RTP) based on the coderivatization of silica with analyte- and heavy ion-binding ligands [31]. (Certain heavy ions are known to enhance phosphorescence quantum yields). In these experiments, we measured the phosphorescence of a model analyte (phenanthrene) as a function of amount analyte deposited on both derivatized and underivatized silica thin-layer phases. While the approach yielded limited success for the design of analytically useful RTP substrates, our research demonstrated that phosphorimetry is a powerful tool for studying adsorption processes on silica and derivatized silicas and should also be applicable to the study of partitioning processes.

Because of the inherently long lifetimes of excited triplet states, phosphorescence is extremely sensitive to the microenvironment of the

phosphor including its state of rigidity and number of collisions it experiences. A strong surface–phosphor interaction results in a rigidly held phosphor experiencing less motion and providing a higher phosphorescence yield. By using a low-surface-area base silica (ca. 2 m^2/g), even higher phosphorescence signals are obtained, making the use of conventional room temperature fluorescence (RTF)/phosphorescence instrumentation feasible for these studies. Our results confirmed the heterogeneous nature of silica-based phases, but also provided specific information concerning the adsorption site of phenanthrene as a function of the amount deposited on underivatized, reversed-phase and ion-exchange phases. Based on these studies, phosphorimetry should be pursued as a fundamental tool for the study of chromatographic surface processes.

2. Experimental

2.1. Reagents

Phenanthrene (Sigma, >96%), sodium dodecyl sulfate (SDS; Fluka, >98%) and thallium nitrate (Alfa, 99.5%) were used as received. Sodium iodide (Fisher) was recrystallized twice from acetone–diethyl ether and dried under vacuum at 50°C before use. Dichloromethane and toluene (Fisher) were distilled under nitrogen over P_2O_5 and $CaCl_2$, respectively. All silanes were purchased from Huls America, desiccated under nitrogen and used as needed. Dimethylaminopyridine (Nepera) was dried overnight at 80°C and desiccated. Peroxyoctanoic acid was prepared as needed from caproic acid (Sigma) and 30% hydrogen peroxide (Fisher) in concentrated sulfuric acid and extracted into diethyl ether for immediate use according to Parker et al. [32] and Fazio et al. [33].

2.2. Derivatized silicas

The base silica used for all RTP studies was a 1.5-μm non-porous silica donated by Keystone Scientific. This silica has a low specific surface area of 2.04 m^2/g (BET analysis, krypton adsorption, Micromeritics Materials Analysis Laboratory) which allows high sensitivity for phosphorescence measurements. *n*-Butyl-, *n*-octyl-, *n*-octadecyl-, 2-(3-cyclohexenyl)ethyl-, 3-iodopropyl- and thallium propylsulfonate-derivatized Keystone silica phases were prepared in our laboratory as described below. Because of the low surface area of the Keystone silica, elemental analysis and other conventional techniques were not sensitive enough to characterize derivatized phases made using this silica. Therefore, derivatization conditions were developed and tested using higher surface silicas and then applied to the Keystone silica. Silicas used to develop derivatization conditions were Waters Nova 5-μm (114 m^2/g) and 12-μm (119 m^2/g) silicas, Waters Resolve 5-μm silica (175 m^2/g) and Davisil 20–30-μm silica (300 m^2/g). Bonding densities obtained for the higher surface area silicas are given in Table 1.

Table 1
Bonding densities obtained for derivatized silicas

Ligand	Silica	Huls silane	Bonding density (μmol/m^2)
n-Butyl	Waters Nova 12 μm	*n*-Butyldimethylchlorosilane	3.5[a]
n-Octyl	Waters Nova 5 μm	*n*-Octyldimethylchlorosilane	3.2[a]
n-Octadecyl	Waters Nova 12 μm	Dimethyl-*n*-octadecylchlorosilane	3.3[a]
Cyclohexenyl	Waters Nova 12 μm	[2-(3-Cyclohexenyl)ethyl]dimethylchlorosilane	3.2[a]
Iodopropyl	Waters Resolve 5 μm	3-Iodopropyltrimethoxysilane	2.6[a]
Propylsulfonic acid	Davisil 20–30 μm		0.94[b]

[a] Calculated from %C analysis.
[b] Active capacity based on acid–base titration. Total bonding density is 1.2 μmol/m^2 based on %S.

Prior to derivatization, all silicas were acid washed by refluxing in 0.1 *M* HNO_3 overnight and rinsing to neutrality with water and subsequently dried at 105–110°C overnight. Reversed-phase derivatized silicas were prepared by reacting the silica with the appropriate alkyldimethylmonochlorosilane overnight in refluxing dichloromethane, using dimethylaminopyridine (DMAP) as catalyst. A 4:1 molar ratio of silane and 6:1 molar ratio of DMAP were used assuming a reactive silanol surface density of 5 μmol/m^2. Iodopropyl-derivatized silicas were prepared by reacting the silica with a 4:1 molar ratio of 3-iodopropyltrimethoxysilane overnight in refluxing toluene. Propylsulfonic acid-derivatized Keystone silica was prepared by reacting the silica with a 4:1 molar ratio of 3-mercaptopropyltrimethoxysilane overnight in refluxing toluene, followed by peroxyoctanoic acid oxidation of the thiol to the sulfonic acid following the basic procedure of Fazio et al. [33]. Bonding densities obtained for the higher-surface-area silicas are given in Table 1. The propylsulfonic acid-derivatized silica was converted to its Tl^+ form by washing 6 g of the phase with 100-ml portions of 0.01 *M* $TlNO_3$ (6×), water (6×), methanol (1×) and then air drying.

2.3. Sample spotting and phosphorescence measurement

For use as RTP substrates, the silica and derivatized silicas were cast into 200-μm thickness thin-layer phases using a low level of cornstarch binder. Details of the procedures for thin-layer phase casting are reported elsewhere [31]. Thin-layer phases were prepared for spotting by marking off a 6.25 mm circular area (hole punch size) using a technical drawing pen (no ink) and a template. A 1-μl volume of the appropriate solution was then spotted (3–4 replicates per sample load) onto the center of the area using a Hamilton microsyringe. The spotting volume was chosen so that the liquid would spread to fill the marked area without bleeding onto the surrounding phase. The spotting solution used for all experiments was either methanol (for bare substrate experiments) or 0.08 *M* SDS–0.024 *M* $TlNO_3$ (for coadsorbed surfactant experiments). After spotting, the sample was dried and mounted onto a sample holder. The area of illumination was reduced to a 5 mm circular area by using a flat black mask.

The instrument used for all phosphorescence measurements was a Hitachi F-4010 fluorescence spectrophotometer equipped with a phosphorescence accessory capable of resolving signals with lifetimes $\geq$1 ms. A semi-closed system comprising the optical Dewar assembly normally used for low-temperature measurements was used for inert gas purging with high-purity nitrogen passed through a high-capacity drying tube (Fig. 1). With this purging system, the signal increases initially and then reaches a steady state which is stable for several minutes or more at nitrogen flow-rates of 2–3 l/min. The signal reported is the ratio of the sample steady-state signal to the blank silica or derivatized silica phase steady-state signal. Although the residual humidity and oxygen levels present during purging were not measured in the sample chamber, the same purging conditions (pressure and flow-rate) were used for all measurements in a given study. λ_{ex} was 295 nm for all phosphorescence measurements. λ_{em} varied from 502 to 507 nm as noted in the figure captions.

The relative standard deviation of the average phosphorescence intensity for a given sample load ranged from 5 to 50%. Despite the large

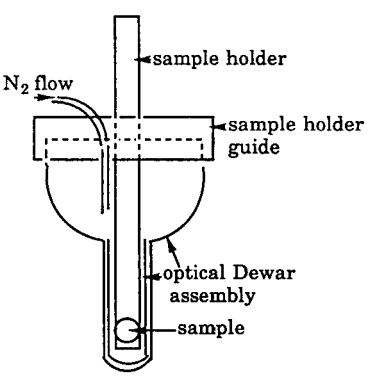

Fig. 1. Inert gas purging design. The sample is positioned in the optical path. Source and detector geometry is 45° from surface normal.

variation among individual measurements, the average phosphorescence intensity for a given sample load was reproducible. While the surface heterogeneity of silica makes a large contribution to the measurement variability, the presence of binder in the thin-layer phases is another source of variability. Other researchers are advised against the use of binder-containing thin-layer phases in fundamental studies.

3. Results and discussion

Phenanthrene was chosen as the probe for several reasons. Phenanthrene is a strong phosphor which previously has been studied in several different sampling modes including low-temperature phosphorimetry [34,35], micelle-stabilized RTP [36,37] and solid-substrate RTP, both with filter paper [38–40] and commercial silica thin-layer phase [41] substrates. Because it is a neutral molecule and has no functional groups, it enables the study of surface–adsorbate interactions uncomplicated by pH effects or specific functional group interactions. Also, because of its non-polar nature, phenanthrene represents a good test case for interaction with surfactant alkyl chains and reversed phases.

The main mode of interaction of phenanthrene with a surface is expected to occur via its aromatic π-electron system. There are a variety of silica surface hydroxyl structures, but in general, they are weak, inorganic acids. Hydrogen bonding between weakly acidic silanols and the electronegative π-system is a favorable interaction. Ramasamy and Hurtubise [42] obtained IR spectra for phenanthrene on polyacrylic acid which were consistent with a hydrogen bonding interaction between phenanthrene π-electrons and the polymer carboxylic acid groups.

The photophysics of phenanthrene adsorbed on bare silica have only recently been studied by Liu et al. [43–45], who studied six polyaromatic hydrocarbons (PAHs), including phenanthrene, adsorbed on silica gel. Because their research has direct bearing on the present work, it is reviewed with respect to phenanthrene in the next section. Liu et al.'s research confirms that phenanthrene is an ideal probe to study adsorption on silica because its photophysics, including phosphorescence yield, are extremely sensitive to the surface–adsorbate interactions.

3.1. Photophysical studies of Liu et al.

Lui et al. determined the fluorescence lifetime distribution [44], fluorescence quantum yield [45] and rates of total decay, fluorescence decay and non-radiative decay [45] for phenanthrene adsorbed on both "wet" and "dry" Kieselgel-60 silica gel. "Wet" silica refers to a pretreatment of 8 h at 25°C under vacuum; the resultant surface is assumed to be hydroxylated and contain a high density of hydrogen-bonded hydroxyl groups. "Dry" silica refers to the same pretreatment except at a temperature of 800°C; the resultant surface is assumed to be highly dehydroxylated containing significantly fewer hydroxyl groups, of which most or all are isolated hydroxyl groups [44].

The fluorescence spectrum and fluorescence lifetime distribution profile for phenanthrene on wet silica were similar to those obtained in polar solvents. However, a dramatic decrease in the fluorescence lifetime distribution profile [44] and large increases in both the rate of non-radiative decay [45] and the phosphorescence quantum yield relative to the fluorescence quantum yield [44] were observed for phenanthrene in going from wet to dry silica (phosphorescence quantum yields were not actually measured but phosphorescence increased dramatically relative to fluorescence). The fluorescence spectrum was also broadened on the dry silica [44].

The results for phenanthrene and the other PAHs were interpreted in terms of the adsorbate–surface interactions and the symmetry properties of the lowest excited singlet state [44,45]. The PAHs were classified into two groups according to whether or not the S_0–S_1 transition is symmetry allowed or forbidden. Phenanthrene has a symmetry-forbidden S_0–S_1 transition with a molar extinction coefficient (ϵ_{max}) of only 250 [44].

On wet silica, adsorbed phenanthrene ex-

periences an environment similar to polar solvents due to association with hydrogen-bonded hydroxyl groups. The symmetry properties of the lowest excited singlet state are not significantly perturbed relative to polar solvents. The situation changes for dry silica. The authors theorized that formation of a surface complex between phenanthrene and isolated hydroxyls on dry silica causes a perturbation of symmetry-forbidden singlet states leading to a "mixed state" with increased rates of S_1–T_1 intersystem crossing. This perturbation is consistent with all of the observed changes in the measured photophysical parameters of phenanthrene in going from wet to dry silica, including the larger increase in phosphorescence quantum yield relative to fluorescence quantum yield. The photophysical parameters for PAHs with symmetry-allowed S_0–S_1 transitions were similar on wet and dry silica [44,45].

3.2. Adsorption on underivatized silica: bare vs. coadsorbed surfactant studies

The spotting solution used in our early RTP studies contained 0.08 *M* SDS, a long-chain surfactant. Based on studies with reversed-phase derivatized silicas (discussed in the next section), we suspected that the long-chain surfactant was attenuating adsorbate–silica interactions, resulting in an overall lower phosphorescence yield for the adsorbate. To address this question, we determined the phosphorescence response of phenanthrene as a function of the amount deposited on bare silica (phenanthrene spotted from methanol) and compared the results to the coadsorbed surfactant case (phenanthrene spotted from 0.08 *M* SDS–0.024 *M* $TlNO_3$).

The results are plotted in Fig. 2 and clearly demonstrate a higher response on bare silica over the entire range tested (0–180 ng phenanthrene), confirming that the coadsorbed surfactant attenuates the phosphor–silica interactions. Furthermore, the response on bare silica is discontinuous while the response in the presence of coadsorbed surfactant is continuous. The implication is a more heterogeneous adsorption surface for bare silica and a more homogeneous adsorption surface with weaker surface–adsorbate interactions in the presence of coadsorbed surfactant. The strong surface–adsorbate interactions for bare silica were also confirmed by the appearance of vibrational fine structure in the phenanthrene phosphorescence spectra (Fig. 3). This fine structure was absent in the spectra for the coadsorbed surfactant case, with the phos-

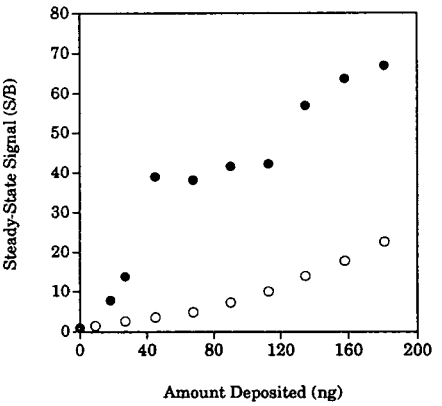

Fig. 2. Phenanthrene phosphorescence response on underivatized Keystone silica phases, bare substrate (●) vs. coadsorbed surfactant case (○). Bare substrate is spotted from methanol, coadsorbed surfactant case is spotted from 0.08 *M* SDS–0.024 *M* $TlNO_3$. λ_{em} is 502 nm for both phases.

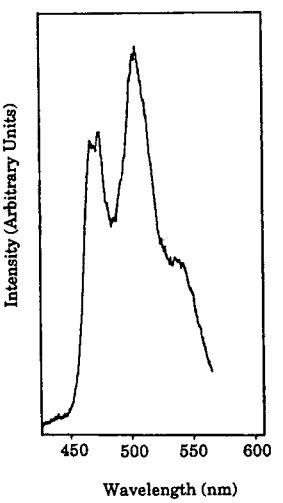

Fig. 3. Phenanthrene phosphorescence spectrum on bare, underivatized silica thin-layer phase. Phenanthrene is deposited from methanol at 180 ng. Excitation and emission bandpasses are both 5 nm.

phorescence emissions centered at 472 and 502 nm appearing as two smooth bands.

These results are wholly consistent with the fluorescence studies conducted by Bauer et al. [22] for pyrene adsorbed on silica. Bauer et al. [22] demonstrated that the surface of silica comprises a heterogeneous distribution of adsorption sites of which a small percentage can be characterized as strong, preferred adsorption sites. They further demonstrated that the adsorption surface becomes more uniform in the presence of glycerol or 1-decanol coadsorbed at greater than 50% surface coverage, evidently via the blockage of the strong adsorption sites. The surface coverage of SDS in our experiments is estimated to be 340% based on a contact surface area of 39 nm^2 per SDS micelle. It is assumed that the three-dimensional solution micelle structure collapses upon adsorption and drying to give a contact area ($2\pi r^2$) with the silica surface which is equal to one half the micelle surface area. This is a reasonable assumption for two reasons: first, the silica used in the study is non-porous so that penetration into the particle is not expected and second, dodecyl sulfate micelles are known to be "dry" or devoid of water even in solution [46]. Other pertinent parameters used in this calculation are micelle radius of 2.5 nm [47], aggregation number 62 [48], critical micelle concentration of 0.0081 *M* [48] and surface area available for adsorption on silica of 0.008 m^2 (calculated from specific surface area of silica and mass of silica in spotted disc). The estimated surface coverage does not include the additional surface area occupied by surfactant monomer.

Examination of the discontinuous response on bare silica reveals three distinct regions: a steep response region from 0–45 ng, a flat response region from 45–115 ng and another dynamic region above 115 ng. Loadings above 180 ng were not tested. The last point for each of the lower two regions represent 0.032 and 0.081 μmol of phenanthrene per m^2 of silica, respectively. Assuming a molecular area of 150 $Å^2$ for phenanthrene based on Snyder's method [49], the corresponding percent surface area coverages are 3 and 8%, respectively. A plausible explanation for the steep response region is that it represents the filling of the strongest adsorption sites. The "titration" of strong adsorption sites using phosphorescence gives similar results to the gas-phase titration technique used by Nawrocki [30]. Nawrocki observed multi-tiered "titration curves" in which the strongest adsorption sites representing the first tier ranged from 0.035–0.095 μmol of diethyl ketone per m^2 of silica for three different silicas. If the 3% surface area coverage from strong adsorption sites from our study is used to calculate the area density of strong adsorption sites, the result is 0.24 μmol/m^2 based on a total silanol bonding density [50] of 8 μmol/m^2.

The two higher loading regions are more difficult to interpret. A key question is whether adsorption occurs randomly or in aggregates. In general, adsorption from a solution phase occurs favors aggregation [25]. Lochmuller et al. [23] found that pyrene based silanes react on the surface of silica in clusters at surface coverages as low as 1%. If clustered adsorption does occur in our experiments, then the second dynamic range could represent strong interactions among aggregated molecules. It is important to note that the phosphorescence spectra of adsorbed phenanthrene on bare silica did not change to any significant extent as a function of loading.

3.3. Adsorption on reversed phases in presence of coadsorbed surfactant

Reversed phases were investigated to determine if alkyl chain–analyte interactions would decrease the rate of phosphorescence-quenching processes for a non-polar analyte such as phenanthrene. The spotting solution used in the reversed-phase experiments was again 0.08 *M* SDS–0.024 *M* $TlNO_3$. However, due to the hydrophobicity of the reversed phases, it was necessary to prespot with methanol to promote wetting. The phosphorescence response of phenanthrene was determined as a function of the amount deposited on *n*-butyl, *n*-octyl and *n*-octadecyl phases. A cyclohexenyl phase in which the cyclohexenyl moiety was attached via

a two-carbon spacer was also tested to determine if the ring structure would result in a higher phosphorescence response for phenanthrene owing to a more rigid environment and/or more favorable interactions.

The results for the *n*-butyl phase are given in Fig. 4 vs. the underivatized phase. For both phases, there is a general increase in phosphorescence intensity with increased phenanthrene loading, but the response on the *n*-butyl phase shows significant scatter, especially at higher phenanthrene loadings. The intensity of the response is about the same in the lower loading region (0–70 ng) for the two phases, but is slightly lower for the *n*-butyl phase in the higher loading region (70–180 ng). Evidence that the lower loading region corresponds to adsorption at unreacted silica surface sites and the higher loading region corresponds to association with the alkyl chains was obtained in subsequent experiments. The higher scatter for the *n*-butyl phase is indicative of a more heterogeneous environment, as is expected for a derivatized silica surface. The scatter may also be due to bulk phase inhomogeneity because it was more difficult to obtain homogeneous casting dispersions for the reversed phases.

Results for the *n*-octyl and cyclohexenyl phases are given in Fig. 5 vs. the *n*-butyl phase. For clarity, the *n*-octadecyl phase results are not plotted. The response for the *n*-octyl, cyclohexenyl and *n*-octadecyl phases were lower than the *n*-butyl phase over the entire loading range with the trend *n*-octadecyl $\approx$ cyclohexenyl $\ll$ *n*-octyl $<$ *n*-butyl. Phosphorescence was barely detectable for the *n*-octadecyl phase (signal/background near 1) although the actual spectrum of phenanthrene was distinguishable vs. the blank spectrum even at the lowest loading tested (0.2 ng). These results indicate that the interactions of phenanthrene with reversed phases is weaker than for underivatized silica and the interactions become weaker as chain length increases. The response for the cyclohexenyl phase with a total of 8 carbons is much less than the C_8 straight chain phase and almost as low as the C_{18} phase. This behavior is actually consistent with a rigid phase and probably indicates that penetration of phenanthrene into the phase did not occur under the conditions of this experiment. Both phase wetting and penetration from an aqueous surfactant solution are expected to decrease as the hydrophobicity of the phase increases. The lower phosphorimetric response on reversed phases

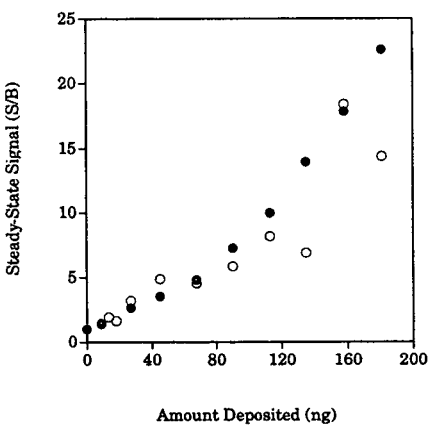

Fig. 4. Phenanthrene phosphorescence response on underivatized (●) and *n*-butyl-derivatized (○) Keystone silica phases. Both phases were spotted from 0.08 *M* SDS–0.024 *M* $TlNO_3$. λ_{em} is 502 nm for the underivatized phase and 504 nm for the *n*-butyl phase.

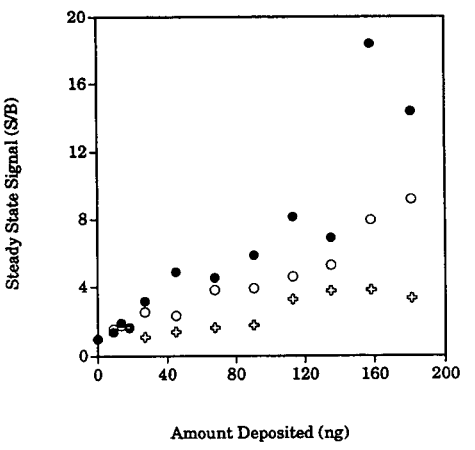

Fig. 5. Phenanthrene phosphorescence response on reversed phases: *n*-butyl (●), *n*-octyl (○) and cyclohexenyl (+). All phases were spotted from 0.08 *M* SDS–0.024 *M* $TlNO_3$. λ_{em} is 504 nm for the *n*-butyl and *n*-octyl phases, and 507 nm for the cyclohexenyl phase.

also represents a further attenuation of the strong phosphor–bare silica interactions.

3.4. Heavy atom/ion derivatized silica phases

One goal of this research was to determine the feasibility of incorporating heavy ion enhancers onto a phase by derivatizing silica with ion-exchange ligands. Whether or not a given heavy ion will cause net enhancement for a given phosphor is largely empirical and depends on the relative change in rates of intersystem crossing, collisional deactivation and phosphorescence caused by the heavy ion perturber [51] which is a function of the relative amounts of phosphor and heavy ion perturber [52]. Thallous ion was determined to provide net enhancement of phosphorescence for phenanthrene adsorbed on underivatized Keystone silica in previous experiments [31], with loadings of 1–60 μmol/m^2 thallous ion providing a minimum of 2.5 times enhancement.

A thallium propylsulfonate-derivatized silica phase with an estimated thallous ion loading of 0.9 μmol/m^2 was subsequently prepared and the phosphorescence response of phenanthrene as a function of loading on this phase was determined. An iodopropyl-derivatized silica phase with an estimated iodine loading of 2.6 μmol/m^2 was also prepared and tested. Iodine was tested in its covalent form because iodide was determined to be unstable on silica surfaces [31], probably due to the surface acidity.

The results for the thallium propyl sulfonate and iodopropyl phases are given in Fig. 6 vs. the underivatized phase and are split out into the lower loading region (0–45 ng, Fig. 6A) and the higher loading region (45–180 ng, Fig. 6B). All phases were spotted from methanol so that no coadsorbed surfactant was present. The net result for the thallium propylsulfonate phase is almost no difference vs. the underivatized phase in the lower loading region, but a lower response in the higher loading region. The net response for the iodopropyl phase is almost no difference vs. the underivatized phase in the lower loading region, but a higher response in the higher loading region.

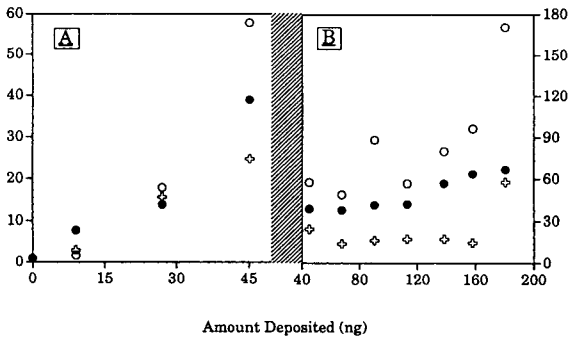

Fig. 6. Phenanthrene phosphorescence response on iodopropyl (○), thallium propylsulfonate (+) and underivatized (●) Keystone silica phases for both low (A) and high (B) loading regions. All phases were spotted from methanol. λ_{em} is 502 nm for the iodopropyl and underivatized phases, and 503 nm for the thallium propylsulfonate phase. Note the difference in both x- and y-axis scales for the two plots. y-Scale is intensity in arbitrary units.

These results provide information regarding the general adsorption sites of the phosphor and provide further evidence that the lower loading region corresponds to unreacted surface sites. Enhancement of phosphorescence should only occur if the analyte and heavy ion/atom are in close enough proximity. The heavy atom for the iodopropyl phase is covalently attached to the alkyl chain ligands. The fact that no enhancement occurs in the lower loading region indicates that the phosphor is associated with unreacted surface silanols. Enhancement in the higher loading region indicates a closer association of the analyte with the alkyl chain ligands for these loadings. The enhancement from the heavy atom is sufficient to provide a net phosphorescence increase despite the attenuation caused by the alkyl chains.

The heavy ion for the thallium propylsulfonate phase is not covalently linked to the propylsulfonate ligand. It is free to migrate according to its relative attraction to the silica surface and the sulfonate counterion and its proximity to the alkyl chains is expected to be much less vs. the iodopropyl phase. The fact that no enhancement occurs in the lower loading region and net attenuation occurs in the higher loading region

for the thallium propylsulfonate phase is again consistent with close association of the phosphor with the unreacted silica surface at low loadings and association with the alkyl chains at higher loadings.

4. Conclusions and suggestions for further study

When comparing results from different researchers, it is imperative to consider the different ranges of surface coverage that the experiments comprise, as well as the mode of attachment (adsorptive or covalent) of the probe molecules to the surface. Our research comprises surface coverages (0–0.14 μmol of phenanthrene per m^2 of silica) that are most similar to Nawrocki's [30]. A summary of the surface coverages and probe conditions used by the other researchers cited in this paper is given in Table 2. Surface coverages for the other researchers' work are estimated from the information given in the references.

It is significant that no decrease in phosphorescence occurred in the lower loading regions for any of the short alkyl chain (C_3 or C_4) derivatized phases (reversed phases, heavy ion/atom phases), providing a consistent picture in which strong residual adsorption sites are present and accessible for these phases. It is also important to emphasize that these experiments were designed to test the analytical utility of silica phases and not to study fundamental adsorption processes. For fundamental adsorption studies, powdered samples rather than thin-layer phases should be used to eliminate unwanted interferences from binders. Precise measurement as well as control of humidity and oxygen levels should be made in the sample chamber.

Despite the limitations of the present study, the use of phosphorimetry for the study of surface heterogeneity and adsorption processes has clearly been demonstrated. The degree of surface heterogeneity is examined by "titrating" the surface with adsorbate and observing the change in phosphorescence signal, which is directly related to the average strength of surface–adsorbate interactions. The adsorption site as a function of adsorbate loading can be probed on derivatized phases by selective incorporation of heavy atom/ion enhancers. These types of studies can be extended to other base silicas, derivatized silicas and adsorbates. The effect of various silica pretreatments and derivatization processes on surface heterogeneity can be determined. It is important to note that phosphorescence sensitivity is also a function of silica specific surface area [31], with lower surface area silicas giving higher sensitivity.

The type of information which can be gained from phosphorimetric studies supplements and/or complements information obtained from IR and fluorescence studies and alleviates some restrictions. The type and strength of bonding

Table 2
Experimental conditions for silica surface studies

Ref.	Probe molecule	Mode of attachment	Surface coverage (reported units)[a]	Surface coverage (μmol/m^2)[b]
[20]	Dansyl amide	Covalent	0.07–0.31 (mmol/g)	0.29–1.3
[21]	Dansyl amide	Covalent	$1.5 \cdot 10^{-11}$ (mol/cm^2)	0.15
[22]	Pyrene	Adsorption	0.2–3 (%)	0.002–0.03
[23,24]	Pyrene	Covalent	0.13–1.10 (μmol/m^2)	0.13–1.10
[30]	Diethyl ketone	Adsorption	0.01–0.18 (μmol/m^2)	0.01–0.18
[44,45]	Phenanthrene and other PAHs	Adsorption	0.22 (mg/g) (phenanthrene)	0.0019
Present work	Phenanthrene	Adsorption	0–180 (ng/spot)	0–0.14

[a] Ranges and units reported in cited reference.
[b] Converted to μmol of probe molecule per m^2 of silica based on information given in reference.

interactions have been probed by IR, but the large silica background severely limits the accessible IR region and the ability to make quantitative measurements. Surface heterogeneity has been examined using fluoresence spectroscopy, but there is the need to choose probes which have critical interaction distances or whose spectral features are polarity or environmentally sensitive. By comparison, the background phosphorescence of silica is minimal and virtually all phosphorescent probes are sensitive to environment due to the inherent lifetimes of excited triplet states. Fluorescence and phosphorescence studies can easily be combined using today's conventional RTF/RTP instruments to gain the maximum information. Fluorescence quenching and phosphorescence enhancement measurements can be made on the same samples. The phosphorescence behavior of pyrene probes can be examined to determine the relationship between pyrene–pyrene interaction distances and strength of surface–pyrene interactions.

The application of phosphorimetry to the study of partitioning processes is also feasible. It is known that phosphorescence is easily quenched in the fluid state. An exception is micellar solutions in which PAH phosphors are protected from quenching processes by partitioning into the long-chain micelles. (Heavy ion enhancers must also be present.) It is therefore feasible that phosphorimetry be used to probe two types of analagous partitioning processes which are thought to occur in reversed-phase LC: intercalation of flat, rigid aromatics into C_{18} chains [53] and the collapse of C_{18} chains in the presence of high-water mobile phases [54,55].

Both theory [54] and experiment [53,55] support the model that C_{18} chains exist in an extended "bristle" state when they are fully solvated but exist in a collapsed state in the presence of high-polarity, high-water mobile phases. Recently, Montgomery et al. [56] provided evidence that C_{18} chains are wetted but neither fully solvated nor extended in the presence of low organic mobile phases. Shape selectivity is highest for high bonding density and/or polymeric phases in the extended state because only flat, rigid molecules are able to intercalate between the extended chains [53]. The extended chain state is frequently described [53–55] as being "rigid", "stiff" or "ordered", but Bayer et al.'s [12] ^{13}C NMR studies showed a higher mobility for the extended state than the collapsed state. While shape selectivity is low for phases in the collapsed state, partitioning of solutes into the stationary phase is still possible for these phases and it is predicted that the solute distribution will follow classical liquid–liquid partitioning [54]. Assuming that intercalation and partitioning do occur, the phosphorescence of solute probes will be sensitive to the rigidity of C_{18} chains in the extended or collapsed state. In this regard, phosphorimetric studies would supplement NMR studies of alkyl chain mobility.

Finally, it may be possible to directly study bonded phase rigidity as a function of mobile phase composition by preparing a phosphorescent stationary phase. Such a phase will necessarily contain aromatic moieties, but Lochmuller et al. [55] have shown that a dipentylbiphenyl aromatic phase may be a good model for studying the bonded chain rigidity of C_{18} stationary phases.

Acknowledgements

The authors are grateful for support of this work by The National Forensic Chemistry Center of the FDA and NIEHS-04908. Thanks to Keystone Scientific for donation of the silica used in this work. J.G.D. also gratefully acknowledges Pfizer, Inc. for continued support of our research.

References

[1] R.E. Majors, *LC·GC*, 6 (1988) 298.
[2] R.E. Majors, *LC·GC*, 11 (1993) 188.
[3] D.E. Leyden, D.S. Kendall, L.W. Burggraf, F.J. Pern and N. DeBello, *Anal. Chem.*, 54 (1982) 101.
[4] B.R. Suffolk and R.K. Gilpin, *Anal. Chem.*, 57 (1985) 596.
[5] B.R. Suffolk and R.K. Gilpin, *Anal. Chim. Acta*, 181 (1986) 259.

[6] L.C. Sander, J.B. Callis and L.R. Field, *Anal. Chem.*, 55 (1983) 1068.
[7] D.W. Sindorf and G.E. Maciel, *J. Am. Chem. Soc.*, 105 (1983) 1487.
[8] R.K. Gilpin and M.E. Gangoda, *J. Chromatogr. Sci.*, 21 (1983) 352.
[9] R.K. Gilpin and M.E. Gangoda, *Anal. Chem.*, 56 (1984) 1470.
[10] R.K. Gilpin and M.E. Gangoda, *J. Magn. Reson.*, 64 (1985) 408.
[11] M.E. McNally and L.B. Rogers, *J. Chromatogr.*, 331 (1985) 23.
[12] E. Bayer, A. Paulus, B. Peters, G. Laupp, J. Reiners and K. Albert, *J. Chromatogr.*, 364 (1986) 25.
[13] M. Gangoda, R.K. Gilpin and B.M. Fung, *J. Magn. Reson.*, 74 (1987) 134.
[14] P. Shah, L.B. Rogers and J.C. Fetzer, *J. Chromatogr.*, 388 (1987) 411.
[15] R.C. Ziegler and G.E. Maciel, *J. Am. Chem. Soc.*, 113 (1991) 6349.
[16] E.C. Kelusky, *J. Am. Chem. Soc.*, 108 (1986) 1746.
[17] D.B. Marshall and W.P. McKenna, *Anal. Chem.*, 56 (1984) 2090.
[18] D.M. Bliesner and K.B. Sentell, *Anal. Chem.*, 65 (1993) 1819.
[19] D.M. Bliesner and K.B. Sentell, *J. Chromatogr.*, 631 (1993) 23.
[20] C.H. Lochmuller, D.B. Marshall and J.M. Harris, *Anal. Chim. Acta*, 130 (1981) 31.
[21] C.H. Lochmuller, J.M. Harris and D.B. Marshall, *Anal. Chim. Acta*, 131 (1981) 263.
[22] R.K. Bauer, P. de Mayo, W.R. Ware and K.C. Wu, *J. Phys. Chem.*, 86 (1982) 3781.
[23] C.H. Lochmuller, A.S. Colborn, M.L. Hunnicutt and J.M. Harris, *Anal. Chem.*, 55 (1983) 1344.
[24] C.H. Lochmuller, A.S. Colborn, M.L. Hunnicutt and J.M. Harris, *J. Am. Chem. Soc.*, 106 (1984) 4077.
[25] D. Oelkrug, S. Uhl, M. Gregor, R. Lege, G. Kelley and F. Wilkinson, *J. Mol. Struct.*, 218 (1990) 435.
[26] J. Stahlberg and M. Almgren, *Anal. Chem.*, 57 (1985) 817.
[27] J.W. Carr and J.M. Harris, *Anal. Chem.*, 58 (1986) 626.
[28] J.W. Carr and J.M. Harris, *Anal. Chem.*, 59 (1987) 2546.
[29] J. Nawrocki, *Chromatographia*, 31 (1991) 177.
[30] J. Nawrocki, *Chromatographia*, 31 (1991) 193.
[31] L.A. Ciolino and J.G. Dorsey, *Anal. Chem.*, (1994) in press.
[32] W.E. Parker, C. Ricciuti, C.L. Ogg and D. Swern, *J. Am. Chem. Soc.*, 77 (1955) 4037.
[33] S.D. Fazio, J.B. Crowther and R.A. Hartwick, *Chromatographia*, 18 (1984) 216.
[34] S.P. McGlynn, B.T. Neely and C. Neely, *Anal. Chim. Acta*, 28 (1963) 472.
[35] G.D. Boutilier and J.D. Winefordner, *Anal. Chem.*, 51 (1979) 1391.
[36] R. Weinberger, P. Yarmchuk and L.J. Cline Love, *Anal. Chem.*, 54 (1982) 1552.
[37] R.A. Femia and L.J. Cline Love, *Spectrochim. Acta*, 42A (1986) 1239.
[38] G.R. Ramos, M.C.G. Alvarez-Coque, A.M. O'Reilly, I.M. Khasawneh and J.D. Winefordner, *Anal. Chem.*, 60 (1988) 416.
[39] D.A. White and T. Vo-Dinh, *Appl. Spec.*, 42 (1988) 285.
[40] A.D. Campiglia, A. Berthod and J.D. Winefordner, *J. Chromatogr.*, 508 (1990) 37.
[41] C.D. Ford and R.J. Hurtubise, *Anal. Chem.*, 52 (1980) 656.
[42] S.M. Ramasamy and R.J. Hurtubise, *Anal. Chim. Acta*, 152 (1983) 83.
[43] Y.S. Liu and W.R. Ware, *J. Phys. Chem.*, 97 (1993) 5980.
[44] Y.S. Liu, P. de Mayo and W.R. Ware, *J. Phys. Chem.*, 97 (1993) 5987.
[45] Y.S. Liu, P. de Mayo and W.R. Ware, *J. Phys. Chem.*, 97 (1993) 5995.
[46] K.A. Dill, D.E. Koppel, R.S. Cantor, J.D. Dill, D. Bendedouch and S. Chen, *Nature*, 309 (1984) 42.
[47] G.L. McIntire, *CRC Rev. Anal. Chem.*, 21 (1990) 257.
[48] J.H. Fendler and E.J. Fendler, *Catalysis in Micellar and Macromolecular Systems*, Academic Press, New York, 1975.
[49] L.R. Synder, *Principles of Adsorption Chromatography*, Marcel Dekker, New York, 1968, p. 199.
[50] K.K. Unger, *Porous Silica*, Elsevier, Amsterdam, New York, 1979.
[51] S.P. McGlynn, J. Daigre and F.J. Smith, *J. Chem. Phys.*, 39 (1963) 675.
[52] T. Vo-Dinh and J.R. Hooyman, *Anal. Chem.*, 51 (1979) 1915.
[53] S.A. Wise and L.C. Sander, *J. High Resolut. Chromatogr. Chromatogr. Commun.*, 8 (1985) 248.
[54] D.E. Martire and R.E. Boehm, *J. Phys. Chem.*, 87 (1983) 1045.
[55] C.H. Lochmuller, M.L. Hunnicutt and J.F. Mullaney, *J. Phys. Chem.*, 89 (1985) 5770.
[56] M.E. Montgomery, M.A. Green and M.J. Wirth, *Anal. Chem.*, 64 (1992) 1170.

ELSEVIER

Journal of Chromatography A, 678 (1994) 213–221

JOURNAL OF CHROMATOGRAPHY A

Computer-assisted rapid development of gradient high-performance liquid chromatographic methods for the analysis of antibiotics

R. Bonfichi

Marion Merrell Dow Research Institute, Lepetit Research Center, I-21040 Gerenzano (VA), Italy

First received 25 March 1994; revised manuscript received 20 May 1994

Abstract

Computer simulation by DryLab G/plus has proved to be an invaluable tool in the rapid development of analytical HPLC methods for antibiotics. A glycopeptide antibiotic under study at this Research Center was taken into consideration as a case study. Retention data from two preliminary experiments have allowed us to perform several simulations which greatly shortened the time normally required for the identification of the optimum gradient conditions. The "key steps" in the simulation process have been experimentally verified and a more than satisfactory agreement between calculated and experimental retention times was consistently found.

This article presents the preliminary results obtained and proposes an HPLC method for the analysis of a glycopeptide antibiotic.

Because of its general approach, the DryLab concept can be extended to any class of chemical compounds not only shortening impressively the HPLC method development time, but also making it possible to adjust/develop a method which takes into account the typical features of the instrument to be used. This last aspect means, among other things, that: (1) HPLC methods already optimized can be transferred from one laboratory to another, differently equipped, without any "local" further adjustment or development work and (2) HPLC methods can be optimized "at a distance" for other laboratories once a few instrumental parameters have been determined and two exploratory runs have been carried out.

1. Introduction

Glycopeptide antibiotics are a family of antibiotics which have recently acquired relevant clinical importance as a result of a specific and high pharmacological activity against many Gram-positive pathogens and highly gentamicin-resistant Enterococci. Among the members of this family, teicoplanin represents the last member introduced into clinical practice [1–10].

Glycopeptide antibiotics are usually (i) characterized by a highly modified sugar-containing heptapeptidic structure and are

(ii) naturally produced by fermentation where they occur as mixtures, called complexes, of closely chemically related substances or factors.

Because of the intrinsic structural complexity and the large number of components normally constituting these mixtures, the development of a reliable and robust analytical method is normally a challenging and time-consuming task.

In spite of protracted development efforts, the

0021-9673/94/$07.00
SSDI 0021-9673(94)00475-O

final chromatogram often provides inadequate overall resolution. An example which supports this statement is the HPLC chromatogram (Fig. 1) of a glycopeptide antibiotic complex currently under study at this Research Center, which has shown pharmacological activity against aerobic and anaerobic Gram-positive microorganisms.

The chromatogram shown in Fig. 1, shows bands which are poorly resolved in spite of a gradient time (t_g) of 45 min. Resolution, in particular, is very low for the bands which elute close to the main peak, or factor B of the complex. Chromatograms shown later in this article will in fact demonstrate that close to the main peak several other factors of the complex are eluted (e.g., factor B1, demannosyl factor B, etc.) for which separation and quantification are essential for a correct definition of the quantitative HPLC profile.

The achievement of high chromatographic resolution is a prerequisite that cannot be disregarded particularly when dealing with complex mixtures of natural substances such as the glycopeptide antibiotics. In fact the chromatograms, usually quite confused, are often further complicated by the onset of new peaks related to new chemical substances synthesized by the strains as a result of even slight changes in the fermentation conditions.

Recent reports in the literature have shown the successful applicability of the predictive software DryLab G/plus [11] to the rapid development of reliable and robust HPLC methods concerning complex mixtures of natural substances [12,13].

On the basis of the previous considerations, and (i) the task of our laboratory being the development of analytical methods to be used at both the development and production levels, and (ii) the HPLC method available for the antibiotic under evaluation, still used at the time this study was started, being unsatisfactory, we have chosen DryLab G/plus to rapidly develop and optimize an HPLC method for the glycopeptide antibiotic under study.

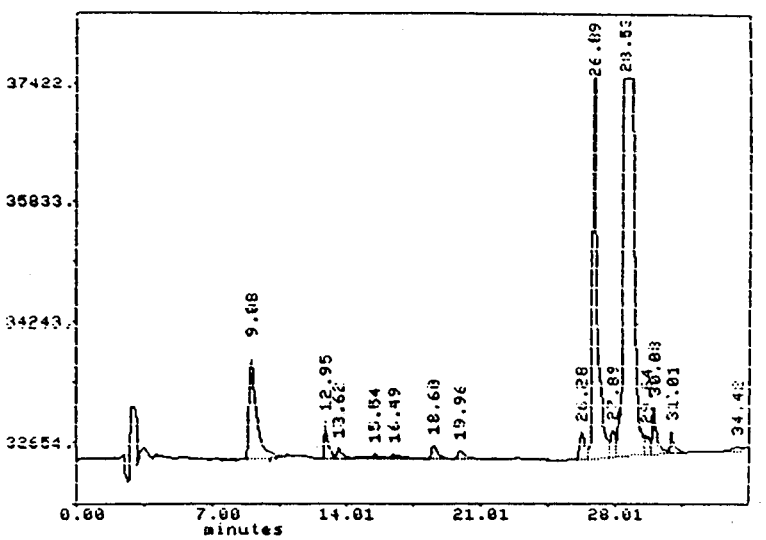

Fig. 1. HPLC chromatogram of the gycopeptide antibiotic under evaluation (batch 1) available at the beginning of this study. Instrument, Hewlett-Packard Model 1084; column, Bakerbond C_8 (250 × 4.6 mm); mobile phase A, NaH_2PO_4 20 m*M*–CH_3CN (95:5, v/v); mobile phase B, NaH_2PO_4 20 m*M*–CH_3CN (25:75, v/v); gradient profile: %B (*t*, min): 10 (0), 30 (10), 30 (20), 65 (30), 90 (40), 90 (45), 10 (48); flow-rate, 1 ml/min.

2. Experimental

Conditions: instrument, liquid chromatograph Model 1090A (Hewlett-Packard); column, Hypersil ODS 5 μm (Shandon) 250 mm × 4.6 mm I.D.; mobile phase A, phosphate buffer 12.5 m*M* pH 7.8–CH_3CN (90:10, v/v); mobile phase B, phosphate buffer 12.5 m*M* pH 7.8–CH_3CN (50:50, v/v). Gradient profile: at 0 min, 16% B; at 5 min, 37% B; at 15 min, 45% B; at 19.3 min, 45% B; at 21.3 min, 60% B; at 26.3 min, 70% B. Flow-rate, 1 ml/min; detector, UV diode array; plotted wavelength, 254 nm; injected volume, 10 μl; temperature, 22°C. *Sample preparation:* a solution, the concentration of which was about 1 mg/ml, was prepared by dissolving the sample in mobile phase A. No further pH adjustments were required, while 15 min sonication were, at least, necessary. *Phosphate buffer (12.5 mM, pH 7.8) solution preparation:* 2 l of 12.5 m*M* pH 7.8 phosphate buffer were prepared by diluting with water 870 ml of a 25 m*M* solution of Na_2HPO_4 to which were added 130 ml of a 25 m*M* solution of NaH_2PO_4. The two mother solutions were prepared as follows: 25 m*M* Na_2HPO_4: 17.92 g of $Na_2HPO_4 \cdot 12 H_2O$ to 2 l with water; 25 m*M* NaH_2PO_4: 6.9 g of $NaH_2PO_4 \cdot H_2O$ to 2 l with water. Acetonitrile used was of HPLC grade, water was from Milli-Q and phosphate salts were of analytical-reagent grade.

2.1. Instrumentation

The HPLC system used for this study was a Hewlett-Packard (Palo Alto, CA, USA) Model 1090A liquid chromatograph equipped with a UV photodiode array detector. Although chromatograms were monitored at 254, 280 and 350 nm with a sampling interval of 320 ms, the plotted wavelength is always 254 nm. Data were collected and integrated on a Hewlett-Packard Model 79994A analytical workstation and plotted on a Hewlett-Packard Model 7470A plotter.

DryLab G/plus software (LC Resources, Lafayette, CA, USA; in Europe: Molnar Institute for Applied Chromatography, Berlin, Germany) was operated on an IBM PS/2 Model 57 SX personal computer equipped with a Hewlett-Packard (Avondale, CA, USA) Laser Jet Model IIIp PCL5 printer.

2.2. Reagents and materials

The batches numbered 1 and 2 of the antibiotic under study were obtained from our Chemical Development Department (Lepetit Research Center). All the solvents used during this study were of HPLC grade (Carlo Erba, Milan, Italy) while the salts were reagents of analytical grade (Carlo Erba). Water was obtained from a Milli-Q purification system (Millipore, USA).

All the chromatograms were obtained by using a 250 × 4.6 mm I.D. Hypersil ODS 5 μm (Shandon Scientific, Runcorn, UK).

2.3. Chromatographic parameters of the analytical system

Beside some more basic chromatographic parameters (e.g., column length, column internal diameter, flow-rate, etc.) the DryLab G/plus software also requires as input data: dwell (or gradient delay) volume, extra-column band broadening and efficiency of the column.

The dwell (or gradient delay) volume of the equipment [14] was measured by running a 10-min gradient from CH_3CN–(CH_3CN + 0.2%, v/v, acetone) (90:10, v/v) to CH_3CN–(CH_3CN + 0.2%, v/v, acetone) (10:90, v/v) without the column and was shown to be $V_D = 0.6$ ml (vs. a 0.3–0.5 ml value for V_D as measured by the Manufacturer —courtesy of Hewlett-Packard).

Extra-column band broadening, σ_{ex}, was measured by injecting, without column and with MeOH–water (60:40, v/v) as mobile phase, 5 μl of a solution containing 10 μl of toluene in 10 ml of methanol at different flow-rates (i.e., 0.9, 1,

1.1, 1.2 ml/min). The σ_{ex} value used for DryLab G/plus simulations was that determined by extrapolation of previous experimental data at zero flow-rate and was shown to be: $\sigma_{ex} = 59$ μl.

Despite the very well known limitations of the approach used for σ_{ex} determination, the good agreement between simulated and experimental data, consistently found in the course of this study, has implicitly confirmed the validity of the value of 59 μl obtained.

The efficiency of the chromatographic column was determined by measuring the number of theoretical plates corresponding to the toluene peak. The theoretical plate number was calculated by using the classical expression $N = 5.54(t_R/w_{1/2})^2$ where t_R and $w_{1/2}$ indicate, respectively, the retention time and the width at half height of the toluene peak. In practice, efficiency was measured by injecting 10 μl of a solution containing 10 μl of toluene in 10 ml of methanol and using MeOH–water (60:40, v/v) as mobile phase. The flow-rate was 0.5 ml/min. Under these conditions an average value of 5000 theoretical plates was obtained. As was the case for extra-column band-broadening determination, the approach for measuring the column efficiency could also be a matter of opinion. However, as previously noted, the good agreement consistently found during this study between simulated and experimental data has implicitly confirmed the correctness of the efficiency value used. For the purposes of the simulation, an estimate of a suitable value for N can also be made by simply comparing the shape of the two initial exploratory chromatograms and how they look when represented by DryLab G/plus. The N value can then be changed with respect to the default value ($N = 10\,000$) so that experimental and DryLab chromatograms will look nearly the same.

For X = ratio of the volume of mobile phase outside the pores to the total volume of mobile phase, Y = ratio of solute diffusion coefficients inside and outside the pores, A = Knox parameter (sometimes called the "multipath term") which describes the effects of eddies and voids within the column packing and which value depends primarily on how well a particular column was packed, values are required for computer band-width predictions; the following data were respectively used: $X = 0.75$, $Y = 0.40$ and $A = 0.80$.

2.4. Chromatographic conditions and sample preparation

On the basis of previous experience, suitable HPLC solvents were prepared to run the preliminary separations. Mobile phase A was phosphate buffer 12.5 m*M* pH 7.84–CH_3CN (90:10, v/v) while mobile phase B was phosphate buffer 12.5 m*M* pH 7.84–CH_3CN (50:50, v/v). The Na_2HPO_4–NaH_2PO_4 buffer solution used for mobile phases preparation was that according to Gomori [14] and Sørensen [15,16], i.e., known amounts of a 25 m*M* Na_2HPO_4 solution and of a 25 m*M* NaH_2PO_4 solution were mixed and diluted to reach the desired pH of 7.8.

Other preliminary trials performed by using mobile phase B containing progressively increasing amounts of CH_3CN have not eluted further peaks from the column.

The glycopeptide antibiotic samples were dissolved in mobile phase A. All the experiments were carried out by injecting 10 μl of a sample solution with an average concentration of ca. 1 mg/ml (equivalent to ca. 6 nmol directly injected).

3. Results and discussion

As the first step in the method development process, two linear gradients characterized by different steepnesses (i.e., $t_g = 20$ min and $t_g = 60$ min) were run varying the percentage of component B of the mobile phase in the range 0–100% and using batch 1 as a sample.

The two chromatograms shown in Figs. 2a and b displayed the same peak sequence and this made an easy identification of twelve bands possible which were used as a starting set for carrying out the optimization work. The retention data for the twelve bands selected in the two initial runs and the area values (those which were measured in the run with $t_g = 60$ min) are summarized in Table 1.

To begin the optimization process the data of

SUBSCRIBER!

Please cut out and paste on page 312 of Vol. 668, No. 2

Erratum

Characterization of stationary phases used in reversed-phase and hydrophobic interaction chromatography [*Journal of Chromatography A*, 668 (1994) 301–312]

G. Rippel, E. Alattyani, L. Szepesy

Page 312 of this article was erroneously left blank. The text on this page should read:

[33] R.M. Smith, *J. Chromatogr.*, 236 (1982) 313.
[34] R.M. Smith, *Anal. Chem.*, 56 (1984) 256.
[35] B.A. Bidlingmeyer, S.N. Deming, W.P. Price, B. Sachok and M. Petrusek, *J. Chromatogr.*, 186 (1979) 419.
[36] P.J. Schoenmakers, H.A.H. Billiet and L. de Galan, *J. Chromatogr.*, 185 (1979) 179.
[37] T.L. Hafkenscheid and E. Tomlinson, *J. Chromatogr.*, 264 (1983) 47.
[38] P.J. Schoenmakers, *Optimization of Chromatographic Selectivity*, Elsevier, Amsterdam, 1986, p. 64.
[39] P.J. Schoenmakers, A. Bartha and H.A.H. Billiet, *J. Chromatogr.*, 550 (1991) 425.
[40] L. Szepesy and G. Rippel, *Chromatographia*, 34 (1992) 391.
[41] G. Rippel and L. Szepesy, *J. Chromatogr. A*, 664 (1994) 27.
[42] A. Drouen, J.W. Dolan, L.R. Snyder, A. Poile and P.J. Schoenmakers, *LC · GC Int.*, 5, No. 2 (1992) 28.
[43] L. Szepesy and G. Rippel, *J. Chromatogr. A*, 668 (1994) 337.

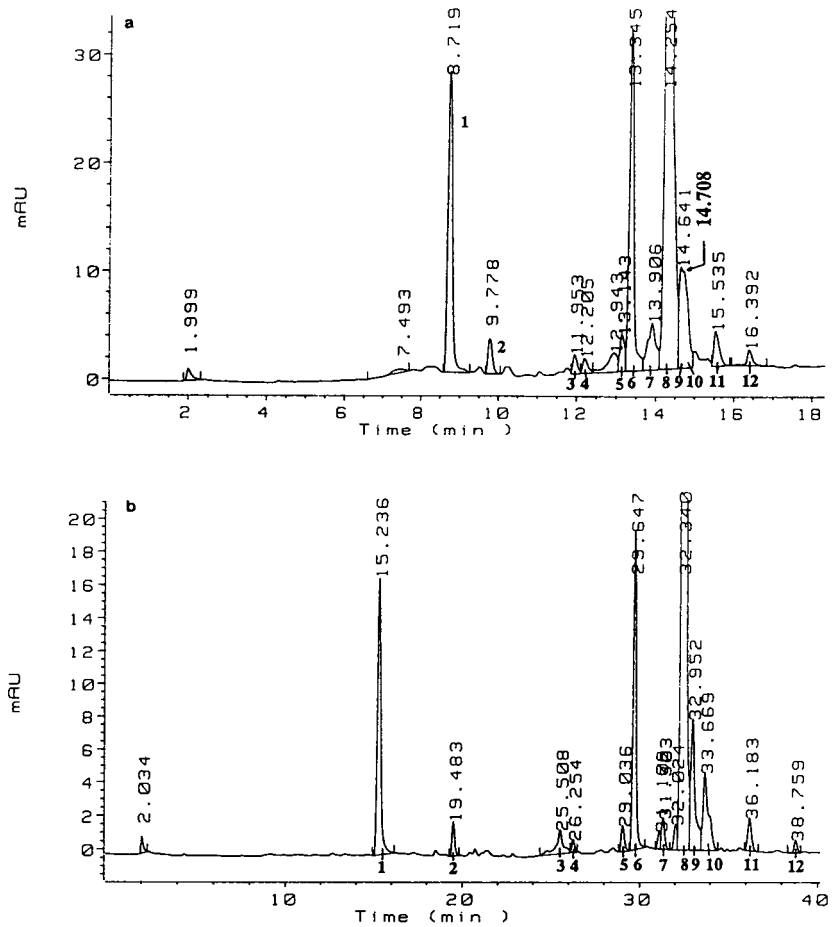

Fig. 2. (a) First exploratory HPLC chromatogram, $t_g = 20$ min, of batch 1. Column, Hypersil ODS 5 μm (250 × 4.6 mm); mobile phase A, phosphate buffer 12.5 m*M* pH 7.8–CH_3CN (90:10, v/v); mobile phase B, phosphate buffer 12.5 m*M* pH 7.8–CH_3CN (50:50, v/v); gradient profile: %B (*t*, min): 0 (0), 100 (20), 0 (25), 0 (35); flow-rate, 1 ml/min. (b) Second exploratory HPLC chromatogram, $t_g = 60$ min, of batch 1. Column, mobile phases and flow-rate as in (a); gradient profile: %B (*t*, min): 0 (0), 100 (60), 0 (65), 0 (75).

Table 1 and the chromatographic parameters of the analytical system (see the corresponding paragraph) were entered. On the basis of these input data the relative resolution map (RRM), calculated by DryLab G/plus, is depicted in Fig. 3. It clearly shows that (i) on the whole, a fairly acceptable resolution ($R_s \approx 1.4$), at least at the beginning, can be achieved at a gradient time of ca. 50 min, (ii) the resolution for bands 9 and 10 increases as the gradient time increases and (iii) the separation of the critical pair 8 and 9 can be improved by short and steep gradients.

As a direct consequence of the previous considerations a segmented gradient should be used to achieve a final successful separation.

As a starting point for the development of a segmented gradient the minimum gradient time for which the critical pair 5 and 6 (Fig. 3) shows $R_s \approx 1.4$ was chosen. This minimum gradient time is 23.8 min and it was automatically determined by DryLab G/plus starting from the gradient time corresponding to the maximum of the RRM shown in Fig. 3 and trimming off any waste time.

Table 1
Input retention data for DryLab G/plus simulations

Band	Run 1 (t_R, min)	Run 2 (t_R, min)	Area (counts)
1 (mannosyl aglycone)	8.72	15.24	224.63
2	9.78	19.48	22.36
3	11.95	22.51	34.29
4	12.21	26.25	12.48
5 (factor A1)	13.14	29.04	19.00
6 (factor A)	13.35	29.65	225.81
7	13.91	31.30	25.14
8 (factor B)	14.25	32.34	2133.94
9 (factor B1)	14.64	32.95	139.78
10	14.71	33.67	102.34
11	15.54	36.18	29.10
12	16.39	38.76	16.69

Run 1: $t_g = 20$ min; run 2: $t_g = 60$ min.

Table 2
Comparison between calculated (DryLab G/plus) and experimentally determined retention times when running the linear gradient from 15.6 to 63.2% mobile phase B in 23.8 min

Band	DryLab G (t_R, min)	Experimental (t_R, min)
1 (mannosyl aglycone)	7.30	6.84
2	9.77	9.50
3	14.67	14.56
4	15.28	15.17
5 (factor A1)	17.57	17.47
6 (factor A)	18.07	17.97
7	19.44	19.36
8 (factor B)	20.30	20.18
9 (factor B1)	20.90	20.69

$t_g = 23.8$ min; 15.6–63.2% B linear gradient.

The retention times of the twelve bands of interest, estimated by DryLab G/plus and those experimentally determined for the minimum gradient time, are compared in Table 2. The agreement between the two data sets is more than satisfactory. The examination of the experimental chromatogram, depicted in Fig. 4, still shows, however, an unresolved cluster of bands eluted after the main peak ($t_R = 20.18$ min) and characterized by an overall $\Delta t_R \approx 1.4$ min measured between the shoulder of band 10 and the main peak (or band 8). In order to resolve this cluster of bands better, several simulations using linear segmented gradients were attempted. The experimental chromatogram corresponding to the final simulation is shown in Fig. 5 and displays a $\Delta t_R \approx 2.5$ min between the peak eluted at 19.87 min (which corresponds to the shoulder of band 10 in Fig. 4) and the main peak ($t_R = 17.38$ min, Fig. 5). The

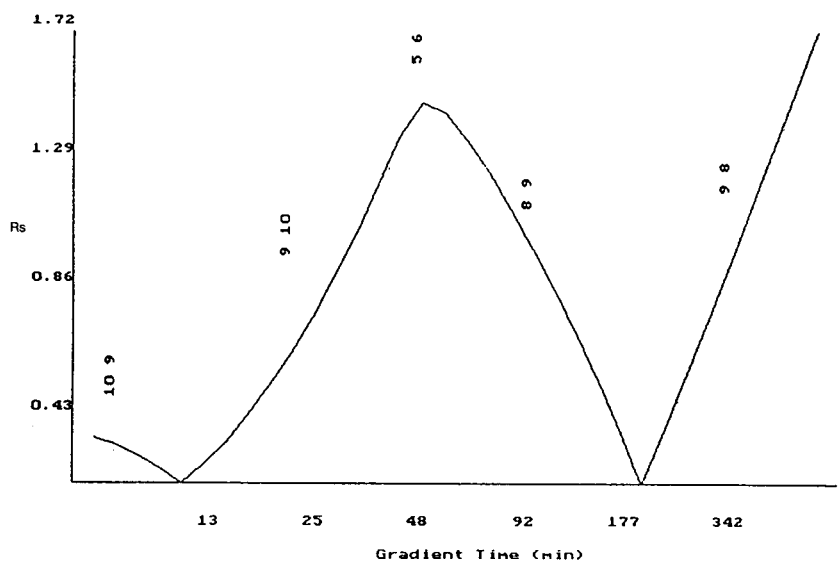

Fig. 3. Relative resolution map (0 to 100% B gradient) calculated by DryLab G/plus with $N = 5000$.

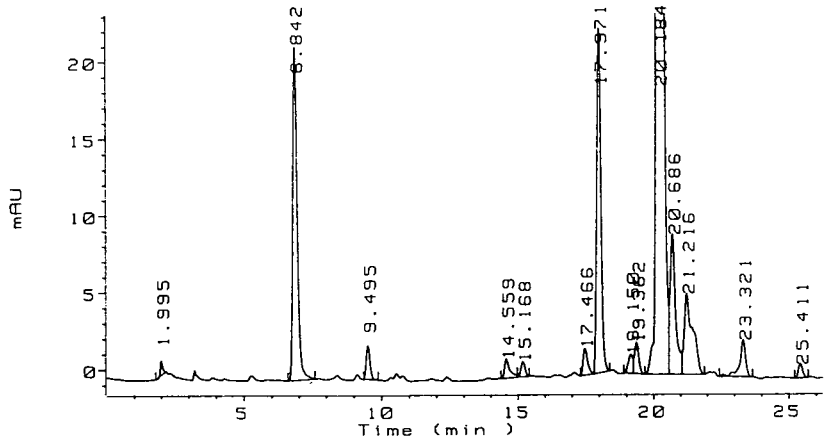

Fig. 4. HPLC chromatogram corresponding to the minimum linear gradient time $t_g = 23.8$ min, automatically calculated by DryLab G/plus in correspondence with the maximum of the relative resolution map shown in Fig. 3. Sample, batch 1; column, Hypersil ODS 5 μm (250 × 4.6 mm); mobile phase A, phosphate buffer 12.5 m*M* pH 7.8–CH_3CN (90:10, v/v); mobile phase B, phosphate buffer 12.5 m*M* pH 7.8–CH_3CN (50:50, v/v); gradient profile: %B (t, min): 15.6 (0), 63.2 (23.8), 63.2 (23.8), 15.6 (30), 15.6 (35); flow-rate, 1 ml/min.

peak separated at $t_R = 19.87$ min in Fig. 5 is particularly important because it corresponds to the demannosyl derivative of factor B.

The calculated and experimentally determined retention times for the most relevant bands are shown in Table 3. Again good agreement between the two data sets was obtained.

The elution conditions, under which the chromatogram depicted in Fig. 5 was obtained, were then slightly changed in order to partially smooth a variation on the baseline observed in the range $t_R \approx 20$–22.5 min and caused by the steepness of the gradient in that time interval.

This adjustment, which has increased the overall gradient time by 4 min [$t_g = 26.3$ min (Fig. 6) *vs.* $t_g = 22.3$ min (Fig. 5)], has however improved at 3.3 min the separation, Δt_R, between the peaks corresponding to factor B (main

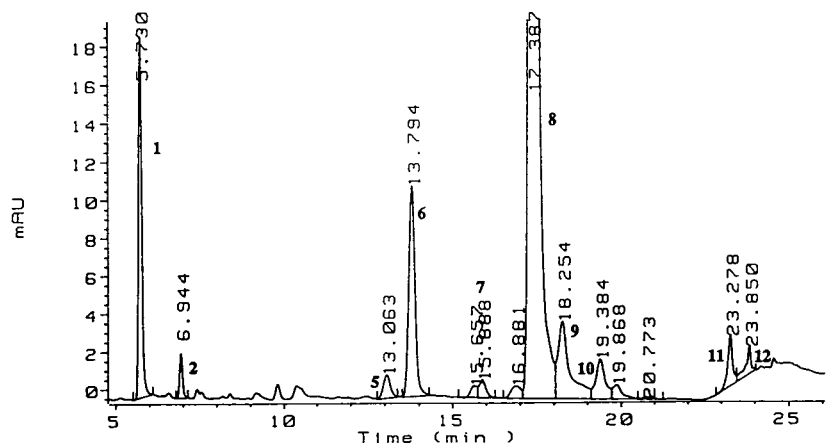

Fig. 5. HPLC chromatogram corresponding to the optimized linear segmented gradient: %B (t, min): 16 (0), 37 (5), 48 (16.6), 48 (19.3), 98 (22.3); column: Hypersil ODS 5 μm (250 × 4.6 mm); mobile phase A, phosphate buffer 12.5 m*M* pH 7.8–CH_3CN (90:10, v/v); mobile phase B, phosphate buffer 12.5 m*M* pH 7.8–CH_3CN (50:50, v/v); flow-rate, 1 ml/min.

Table 3
Comparison between calculated (DryLab G/plus) and experimentally determined retention times when running the optimized linear gradient: %B (t, min): 16 (0), 37 (5), 48 (16.6), 48 (19.3), 98 (22.3).

Band	DryLab G (t_R, min)	Experimental (t_R, min)
5 (factor A1)	13.89	13.06
6 (factor A)	14.61	13.79
7	16.69	15.89
8 (factor B)	18.11	17.38
9 (factor B1)	18.97	18.25
10	20.05	19.38
11	23.06	23.28
12	23.62	23.85

t_g = 22.3 min. Only the data regarding the most relevant bands are reported.

peak or band 8) and its demannosyl derivative (t_R = 21.41 min, Fig. 6). The chromatogram displayed by the batch 1 under the new conditions is plotted in Fig. 6. The gradients employed in Figs. 5 and 6 represent the last steps in this optimization process. The same gradient profile which was adopted in Fig. 6 was then used for the analysis of the batch 2, Fig. 7, allowing a clear identification of the peak due to the demannosyl B derivative and confirming the presence of a further peak which elutes at $t_R \approx$ 20.7 min. The elution conditions under which the chromatograms reported in Figs. 6 and 7 were obtained, are summarized in the Appendix and they represent a proposed method for the HPLC analysis of glycopeptide antibiotic subject of this study.

4. Conclusions

DryLab G/plus software has proved to be a very practical and useful tool for shortening the time required to develop analytical HPLC methods including analysis of complicated mixtures of natural substances such as the glycopeptide antibiotics.

A method has been rapidly developed which allows a satisfactory chromatographic resolution of the most important factors of the complex glycopeptide antibiotic.

It must also be pointed out that the usefulness of the DryLab approach is even more evident if it is taken into account that (i) it does not refer to any definite class of chemical substances, (ii) once a few equipment parameters required for computer simulations are determined (i.e., dwell volume, extra-column band broadening, plate number of the chromatographic column) and if parts, when changed, are replaced with their

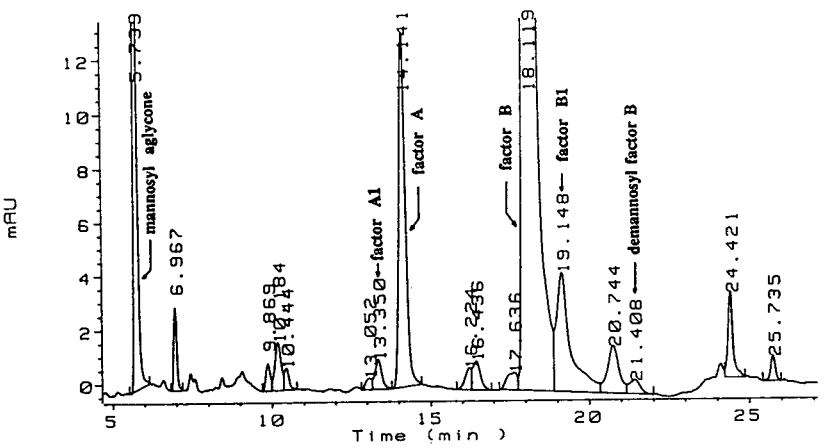

Fig. 6. HPLC chromatogram corresponding to the optimized linear segmented gradient: %B (t, min): 16 (0), 37 (5), 45 (15), 45 (19.3), 60 (21.3), 70 (26.3); sample, batch 1; column: Hypersil ODS 5 μm (250 × 4.6 mm); mobile phase A, phosphate buffer 12.5 mM pH 7.8–CH_3CN (90:10, v/v); mobile phase B, phosphate buffer 12.5 mM pH 7.8–CH_3CN (50:50, v/v); flow-rate, 1 ml/min.

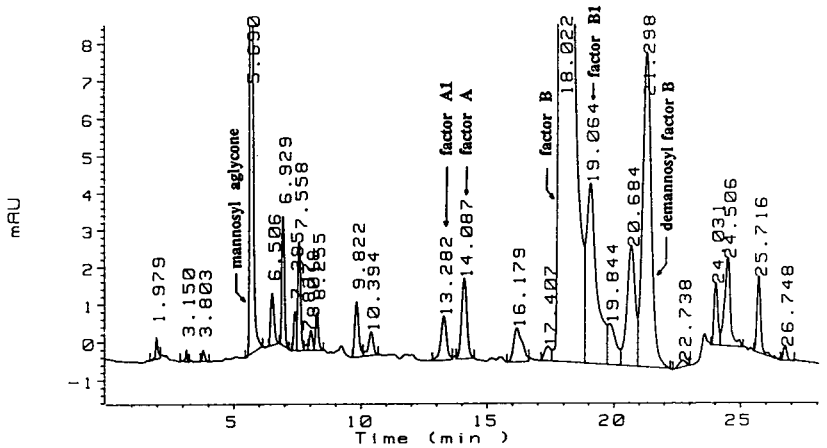

Fig. 7. HPLC chromatogram corresponding to the optimized linear segmented gradient: %B (t, min): 16 (0), 37 (5), 45 (15), 45 (19.3), 60 (21.3), 70 (26.3); sample, batch 2; column: Hypersil ODS 5 μm (250 × 4.6 mm); mobile phase A, phosphate buffer 12.5 mM pH 7.8–CH_3CN (90:10, v/v); mobile phase B, phosphate buffer 12.5 mM pH 7.8–CH_3CN (50:50, v/v); flow-rate, 1 ml/min.

equivalent, any further method developed on that instrument only requires two initial exploratory gradient runs (e.g., see those shown in Fig. 2a and b) [17], (iii) the RRM that can be easily calculated from the initial retention data shows not only the poorest-resolved band-pair, but also indicates the success probabilities that the elution conditions chosen will have, and (iv) any HPLC gradient method developed on a certain instrument can easily be adjusted to any other equipment, wherever located, once its characteristics (basically: dwell volume and extra-column band broadening) are known [17].

References

[1] F. Parenti, G. Beretta, M. Berti and V. Arioli, *J. Antibiot.*, 31 (1978) 276.
[2] C. Coronelli, G.G. Gallo and B. Cavalleri, *Il Farmaco, Ed. Sci.*, 42 (1987) 767.
[3] A. Del Favero and F. Menichetti, *Drugs Today*, 24 (1988) 641.
[4] D. Speller, D. Greenwood and P.J. Daly (Editors), *J. Antimicrob. Chemother.*, 21 (Suppl. A) (1988) 1.
[5] F. Fraschini, *J. Chemother.*, 1 (Suppl. 4) (1989) 590.
[6] D.M. Campoli-Richards, R.N. Brogden and D. Faulds, *Drugs*, 40 (1990) 449.
[7] A.H. Hunt, R.M. Molloy, J.L. Occolowitz, G.G. Marconi and M. Debono, *J. Am. Chem. Soc.*, 106 (1984) 4891.
[8] J.C.J. Barna, D.H. Williams, D.J.M. Stone, T.-W.C. Leung and D.M. Doddrell, *J. Am. Chem. Soc.*, 106 (1985) 4895.
[9] S.L. Heald, L. Müller and P.W. Jeffs, *J. Magn. Res.*, 72 (1987) 120.
[10] R. Pallanza, M. Berti, B.P. Goldstein, E. Mapelli, E. Randisi, R. Scotti and V. Arioli, *J. Antimicrob. Chemother.*, 11 (1983) 419.
[11] T.H. Jupille, J.W. Dolan and L.R. Snyder, *Drylab G/plus User's Manual*, LC Resources, Lafayette, CA, 1989; and references cited therein.
[12] I. Molnar, K.H. Gober and B. Christ, *J. Chromatogr.*, 550 (1991) 39.
[13] T.H. Dzido, E. Soczewinski and J. Gudej, *J. Chromatogr.*, 550 (1991) 71.
[14] G. Gomori, *Methods Enzymol*, 1 (1955) 143.
[15] S.P.L. Sørensen, *Biochem Z.*, 21 (1909) 131.
[16] S.P.L. Sørensen, *Biochem. Z.*, 22 (1909) 352.
[17] L.R. Snyder and J.W. Dolan, *LC·GC*, 8 (1990) 524.

ELSEVIER

Journal of Chromatography A, 678 (1994) 223–231

JOURNAL OF CHROMATOGRAPHY A

Determination of phenolic compounds in surface water using on-line liquid chromatographic precolumn-based column-switching techniques

E.R. Brouwer*, U.A.Th. Brinkman

Department of Analytical Chemistry, Free University, De Boelelaan 1083, 1081 HV Amsterdam, Netherlands

First received 1 March 1994; revised manuscript received 11 May 1994

Abstract

Gradient LC–diode array UV detection, combined on-line with a PLRP-S and an ENVI-Chrom P precolumn in series, enables the on-line trace-level determination and provisional identification of phenol and 13 substituted phenols in surface water. Additional selectivity has been incorporated into the system by properly utilizing the breakthrough properties of phenol over the PLRP-S precolumn. With 50-ml sample volumes, the limits of detection for all analytes are at the low- to sub-μg/l level.

1. Introduction

Phenolic compounds, including phenol, are ubiquitous environmental contaminants. They can be released to the environment by many industrial processes and also as a result of degradation of, e.g., chlorophenoxy acids, a well known group of pesticides. Since many substituted phenols are toxic to aquatic organisms, both the European Union and the US Environmental Protection Agency include many phenolic compounds in their lists of priority pollutants. Consequently, the trace-level determination of these compounds in surface water is of primary concern. In the literature, several procedures are reported which use either capillary gas chromatography (both without and with derivatization) [1–6] or column liquid chromatography [7–10]. In order to comply with tolerance levels typically encountered today for individual pesticides, e.g. 1–3 μg/l in surface water, it is necessary to introduce either an enrichment step or selective derivatization of the analytes [11–13]. At present, solid-phase extraction (SPE) is the preferred method for the enrichment of polar environmental pollutants, because it combines the advantages of convenience, low cost and minimal consumption of organic solvents. Besides, SPE-based procedures can easily be incorporated into fully on-line set-ups which facilitates automation.

Over the years, a wide variety of sorbents, such as graphitized carbon black, ion-exchange materials, octadecyl-bonded silicas, cyclohexyl-bonded silicas and polymer resins, has been used for the isolation of phenols from water samples. Unfortunately, because of a lack of selectivity, several of the reported procedures are not really suitable for the trace-level monitoring of phenols in complex matrices. Therefore, current research aims at using selective sorbents [14] or at instal-

* Corresponding author.

0021-9673/94/$07.00
SSDI 0021-9673(94)00513-9

ling two precolumns in series [10]. Recently a new packing material, ENVI-Chrom P, was introduced. This non-ionic styrene–divinylbenzene copolymer ($d_p = 80–160$ μm), which has excellent chemical and mechanical stability, contains a relatively large number of active aromatic sites which enhances interaction with the aromatic phenols, and, thus, improves the enrichment of many of these analytes. It is well known that the sorption on styrene–divinylbenzene-based sorbents, e.g. the ENVI-Chrom P material in this study, is based on rather selective $\pi-\pi$ interactions. That is analytes not bearing an aromatic ring do not sorb properly on such materials. When using this sorbent, salting out is not necessary anymore. According to Nolan [14], loading 100-ml samples on a tube containing 500 mg of ENVI-Chrom P gave recoveries of 96–106% for 13 phenolic compounds (including phenol). However, off-line methods such as that referred to here have several disadvantages: because an aliquot of the final sample extract is injected only, and losses are prone to occur during (partial) evaporation of the extract, off-line concentration techniques tend to be less sensitive and less reproducible than on-line methods. On-line SPE utilizes small precolumns typically containing 50 mg of the preferred sorbent, from which the analyte can be desorbed and transported directly to the analytical column, either in the forward- or the back-flush mode.

In the present project we studied the use of ENVI-Chrom P as a selective sorbent in an on-line SPE–LC-based analytical system for the sorption of phenols from surface water samples, with final determination by means of diode-array UV detection. Recently we developed several methods for the determination of organic pollutants in surface water within the framework of the international Rhine Basin Program (Amsterdam/Waldbronn) [15–18]. In these studies a polymer-based PLRP-S precolumn was often used because this type of highly hydrophobic sorbent strongly retains many compounds of interest. In the present study the PLRP-S and ENVI-Chrom P sorbents were compared with respect to sorption strength and band broadening of the analytes after on-line desorption. The experimental results led us to construct an analytical system which utilizes two precolumns in series, one containing PLRP-S, the other ENVI-Chrom P material.

2. Experimental

2.1. Reagents and materials

Phenol, 3-nitrophenol, 2,4-dinitrophenol, 2,3-dimethylphenol and 4-chlorophenol were from Fluka (Buchs, Switzerland). 2,6-Dichlorophenol, 2,3,4-trichlorophenol, 2,3,5-trichlorophenol, 2,3,6-trichlorophenol and 2,3,5,6-tetrachlorophenol were purchased from Aldrich (Beerse, Belgium). Dinoseb, dinoterb, 4,6-dinitro-*ortho*-cresol and bromoxynil came from Riedel-de Haën (Seelze, Germany). HPLC gradient-grade acetonitrile, HPLC-grade methanol, and nitric acid were obtained from Baker (Deventer, Netherlands). Buffer solutions were prepared by mixing 1 *M* stock solutions of potassium dihydrogen phosphate and dipotassium hydrogen phosphate (Baker) to the appropriate pH and subsequent dilution to 10 m*M*. All aqueous solutions were prepared with demineralized water, purified with a Milli-Q (Millipore, Bedford, MA, USA) ultrafiltration system.

Stock solutions were prepared by dissolving about 3 mg of the analyte in 15 ml of methanol and stored at 4°C. Surface water samples were spiked by diluting the stock solutions to the appropriate concentration and adjusted to pH 3 with a 1 *M* solution of nitric acid. Prior to use the surface water samples were filtered over a 0.45-μm filter (Schleicher and Schuell, Dassel, Germany). Three 250 × 4.6 mm I.D. stainless-steel analytical columns, i.e., Supelco ABZ, Supelco LC-18 and Supelco LC-18-DB, were a gift from Supelchem (Leusden, Netherlands). Two 250 × 4.6 mm I.D. base-deactivated octadecyl-bonded silica (Chromspher B and Inertsil) stainless-steel analytical columns were a gift from Chrompack (Middelburg, Netherlands). Home-made stainless-steel precolumns (10 mm × 3.0 or 2.0 mm I.D.) were manually slurry packed, using methanol as the slurry liquid, with 15–25 μm PLRP-S (Polymer Lab-

oratories, Church Stretton, UK), 80–160 μm ENVI-Chrom P (Supelchem) or two experimental phases denoted as 1038A and 1038B (Supelchem).

2.2. Set-up and procedures

The LC system consisted of a Gynkotek (Germering, Germany) Model 300 pump to deliver the aqueous sample (3 ml/min) and methanol–acetonitrile (50:50, v/v) for cleaning and wetting of the precolumn. The LC analyses were performed with an HP 1090 (Hewlett Packard, Waldbronn, Germany) LC gradient system equipped with a ternary solvent-delivery system, and an injection valve with a 25-μl loop. For detection an HP 1040 (Hewlett Packard) diode array detection (DAD) apparatus, set at various wavelengths (cf. Table 1), with a 10-mm flow cell was used. Two home-made six-port injection valves were used. The data were evaluated by a Hewlett Packard Pascal workstation using the Chemstation software.

The total analytical set-up is shown in Fig. 1. The final procedure is as follows. Pump P1 delivers the methanol–acetonitrile mixture and the aqueous sample at a flow-rate of 3 ml/min. The precolumn(s) (Pr1 and Pr2) are percolated with 5 ml of the methanol–acetonitrile mixture, to condition the packing material and subsequently 2 ml of Milli-Q water. Prior to loading of the aqueous sample the ENVI-Chrom P precolumn (Pr2) is switched in the analytical system via valve V2 ("inject" position). Subsequently, the PLRP-S precolumn (Pr1) is loaded with 50 ml of sample (at 3 ml/min) by switching valve V1 to the "load" position. When 45 ml of sample have passed the precolumn, valve V2 is switched to the "load" position, and the final 5 ml of sample are loaded with the two precolumns in series. Next, valve V2 is switched to the "inject" position, and the analytes trapped on precolumn Pr2 are desorbed by the LC gradient. After 8.50 min the analytes trapped on the PLRP-S precolumn are desorbed by the LC gradient by switching valve V1 to the "inject" position.

The LC gradient was prepared by mixing an aqueous phosphate buffer (10 m*M*, pH 3; A) and acetonitrile (B). The gradient profile for the desorption of the analytes from both precolumns and the subsequent separation on the analytical

Table 1
Validation data for total SPE–LC–DAD-UV procedure for the determination of phenolic compounds using two precolumns in series

No.	Compound	Detection wavelength (nm)	Recovery (%)	R.S.D. (%) ($n = 6$)	Detection limit (μg/l)
1	Phenol	195	92	5.0	1.0
2	3-Nitrophenol	210	103	8.0	0.8
3	2,4-Dinitrophenol	268	100	2.5	0.8
4	4-Chlorophenol	195	98	3.5	0.05
5	2,3-Dimethylphenol	195	90	3.5	0.1
6	2,6-Dichlorophenol	204	95	3.0	0.3
7	Bromoxynil	210	92	4.5	0.5
8	4,6-Dinitro-*ortho*-cresol	268	94	1.5	0.4
9	2,3,6-Trichlorophenol	204	105	3.0	0.6
10	2,3,4-Trichlorophenol	204	100	2.5	0.3
11	2,3,5-Trichlorophenol	204	93	1.0	0.3
12	2,3,5,6-Tetrachlorophenol	210	96	1.0	0.3
13	Dinoseb	268	105	0.5	0.5
14	Dinoterb	268	103	1.0	0.5

Samples: 50-ml surface water; for other conditions, see text.

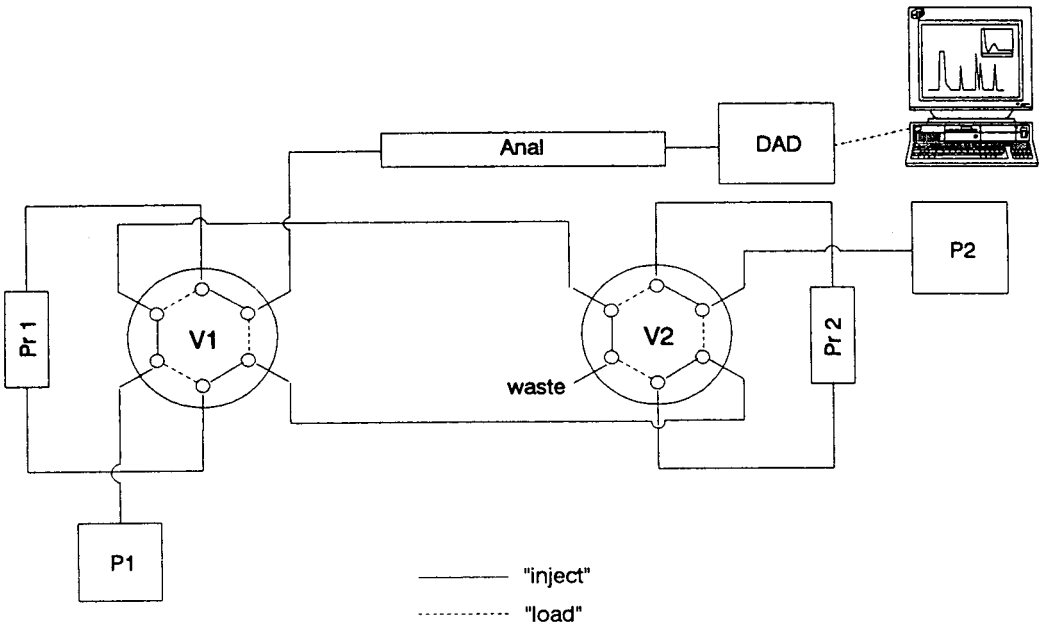

Fig. 1. Set-up of on-line trace enrichment–LC–DAD-UV system; V1, V2: six-port injection valves; Pr1: 10 × 3 mm I.D. precolumn containing 15–25 μm PLRP-S; Pr2: 10 × 3 mm I.D. precolumn containing 80–160 μm ENVI-Chrom P; P1: pump delivering methanol, Milli-Q water and aqueous samples; P2: gradient LC pump; Anal: 250 × 4.6 mm I.D. analytical column; DAD: diode array UV detector.

column was: A–B (80:20) (0 min) which was changed linearly to A–B (39:61) in 45 min, and subsequently to A–B (10:90) (50 min). All separations were carried out at 40°C, using the column oven of the HP 1090 LC system and a flow-rate of 1 ml/min (pump P2).

3. Results and discussion

3.1. Analytical column

In order to obtain optimum sensitivity and selectivity, the selection of the analytical column that has to be used in combination with the enrichment cartridge, is of primary importance. In general alkyl-bonded silica analytical columns provide better separation efficiency than polymer columns and therefore are preferred in most instances. However, it is well known that amines and related compounds often yield very broad non-gaussian peaks as a result of interaction with free silanol groups when non-deactivated silicas are used. In order to solve this problem, a variety of base-deactivated silica columns has been marketed in the last decade. Initially, the separation efficiency of the base-deactivated analytical columns could not compare with that of conventional alkyl-bonded silicas. Today, however, separation efficiencies are similar. Recent experience in our, and also in other laboratories, has shown that problems with non-gaussian peak shapes also occur with phenolic compounds. Therefore, several analytical columns were selected for the present study, viz. four base-deactivated columns (LC-18-DB, LC-ABZ, Chromspher B and Inertsil), along with one non-deactivated column (LC-18). All columns had the same dimensions (250 × 4.6 mm I.D.) and they all contained 5-μm particles.

Since it was our intention to study a wide range of phenolic compounds, the test set included both highly polar analytes such as phenol and several nitrophenols, and apolar phenols such as higher-substituted chlorophenols. Consequently an LC gradient had to be used to effect

the required separation. The final separation conditions, which were the same for the five analytical columns tested, are given in section 2.2. As can be seen from Fig. 2 all selected phenols were baseline-separated when using either the Chromspher B or Inertsil column, although there was a reversal in the order of elution (peaks 6 and 7). However, when the Supelcosil LC-18-DB column, which has successfully been used by us for many applications in the area of polar pesticides [16,17], was tested using the same LC gradient, broad tailing peaks appeared, especially for the late eluting compounds. These broad peaks can not be attributed to working at an unfavourable pH value since the LC gradient was the same as with the two Chrompack columns. In order to test whether the agent used for endcapping the analytical columns caused secondary interactions with the phenols, a non-deactivated Supelcosil LC-18 column was included in the study. However, the peak shapes did not improve. Finally a Supelcosil LC-ABZ column was tested. With this column silanol deactivation is based on electrostatic shielding, a polar group being embedded covalently in the phase. In our hands the LC-ABZ column has been shown to be quite efficient for the separation of neutral, acidic, basic and zwitterionic compounds without the use of additives such as amines or silanol-suppressing LC eluent conditions [19,20]. In the present

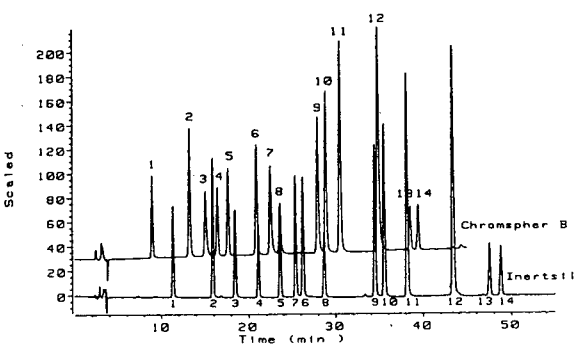

Fig. 2. LC–DAD-UV chromatogram of standard mixture of 14 phenols after loop injection (15 μl; 14 mg/l of each phenol) on 250 × 4.6 mm I.D. Inertsil and Chromspher B analytical columns. For peak assignment, see Table 1; for experimental conditions, see text.

study, the LC-ABZ column provided sharp peaks for most phenolic compounds, but the four dinitrophenols (compounds 3, 8, 13 and 14, Table 1) still gave broad tailing peaks. Since the above data suggest that the non-gaussian peak shapes are not primarily due to the deactivation process, the role of the modifier was also briefly studied. Although the use of methanol instead of acetonitrile did improve the peak shapes for several analytes (e.g., 2,3-dimethylphenol and 2,3,4-trichlorophenol) on the LC-18 and LC-18-DB columns, the results for the dinitrophenols, and also bromoxynil, still were not satisfactory. This observation is in line with data recently published [16].

On the basis of the above results, the Chromspher B column, with its relatively short time of analysis was selected for all further work.

3.2. DAD-UV absorbance detection

In order to determine the optimum wavelengths for DAD-UV detection, UV spectra were recorded for all analytes (data not shown). For most of the test analytes, the wavelength of maximum absorption was selected. It is well known, however, that in surface water analysis co-eluting peaks or bands especially interfere at these low-UV wavelengths. Therefore, for all phenolic compounds featuring a sufficiently intense secondary maximum at a higher wavelength (compounds 3, 8, 13 and 14; Table 1), the latter maximum was preferred. The wavelengths selected for each single analyte are given in Table 1.

3.3. Analyte trace enrichment

In our laboratory several LC-based systems have been developed for the determination of a variety of polar pesticides [15–18]. In most instances, a single precolumn is used to trap the analytes of interest, with a polymer-based sorbent such as PLRP-S being the preferred packing material because of its high and broad-range retention power. Besides, this type of sorbent can be used over the pH range of 0–14. In this study we also tested the recently introduced

ENVI-Chrom P, another styrene–divinylbenzene-based sorbent, which has been modified to increase the retention of polar aromatic compounds. Initially a set-up containing a single precolumn was used; that is, valve V2 (and precolumn Pr2; cf. Fig. 1) was not included. In order to test the retention power and/or selectivity of both sorbents, 50 ml of river Meuse water, spiked with 5 μg/l of all test analytes, was passed through the precolumn at 3 ml/min. Two striking differences are observed when comparing the chromatograms recorded in Fig. 3 (a–d: PLRP-S; e: ENVI-Chrom P). When using the PLRP-S precolumn sharp peaks are obtained at the four wavelengths selected for the efficient detection of the test compounds. Phenol, however, which elutes at $t_R = 8$ min, does not show up. When, instead of PLRP-S, the ENVI-Chrom P material was used, the detection of phenol presented no problems. However, distinctly broader peaks were observed for all analytes and the detectability of especially the late-eluting peaks now left much to be desired (Fig. 3e). The additional band broadening can be explained by the high retention power of ENVI-Chrom P compared with PLRP-S.

For all analytes breakthrough volumes were determined on both sorbents. To this end, increasing volumes of river Meuse water, spiked at the 25 μg/l level, were pumped through the precolumn. For PLRP-S the breakthrough volumes for phenol and 3-nitrophenol were 1 and 50 ml, respectively, while all other analytes had breakthrough volumes of over 50 ml. For ENVI-Chrom P breakthrough of phenol occurred after 5 ml of the sample has been passed through the precolumn. All other analytes had breakthrough volumes over 50 ml, which was the maximum volume tested. Obviously, if analyte trace-enrichment from 50 ml of sample is sufficient to achieve detection limits of ca. 1 μg/l or below (see below), both sorbents behave rather similarly. However, ENVI-Chrom P is to be preferred because of its distinctly higher retention of phenol, while PLRP-S is the better choice in terms of final separation efficiency. It was therefore decided to combine both precolumns in one set-up with the ENVI-Chrom P precolumn inserted between the PLRP-S precolumn and the analytical column (cf. Fig. 1).

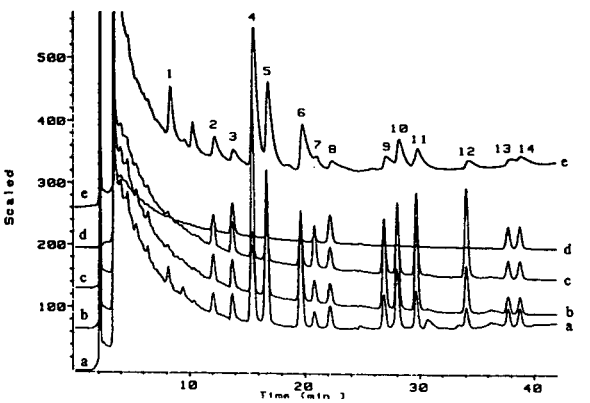

Fig. 3. On-line trace enrichment–LC–DAD-UV chromatogram of 50 ml surface water spiked with 14 phenols (5 μg/l each), using a single precolumn. (a–d) 10 × 3 mm I.D. PLRP-S precolumn, a: $\lambda = 195$ nm, b: $\lambda = 204$ nm, c: $\lambda = 210$ nm, d: $\lambda = 268$ nm; e: 10 × 3 mm I.D. ENVI-Chrom P precolumn, $\lambda = 195$ nm. For peak assignment, see Table 1.

Usually when two precolumns are used in series, the total amount of sample is pumped through both precolumns. However, in the present case this was not the proper solution. In order to prevent breakthrough of phenol only 5 ml of sample can be pumped through the ENVI-Chrom P precolumn. For all other test analytes, however, a larger sample volume is preferred to obtain lower detection limits. Therefore the total, i.e. 50-ml sample was pumped through the PLRP-S precolumn by switching valve V1 to the "load" position and valve V2 to the "inject" position. When 45 ml of the sample had passed the first precolumn —with phenol obviously displaying breakthrough at this point— the second precolumn was inserted in-line by switching valve V2 to the "load" position. In other words, only the final 5 ml of sample were pumped through both precolumns in series, and the recovery is essentially quantitative for all analytes (cf. the data included in Table 1). After trace enrichment of the analytes, the ENVI-Chrom P precolumn was analysed first. To this end, valve V2 was switched to the "inject" position to start LC gradient elution. After 8.50 min, analysis of the PLRP-S precolumn was

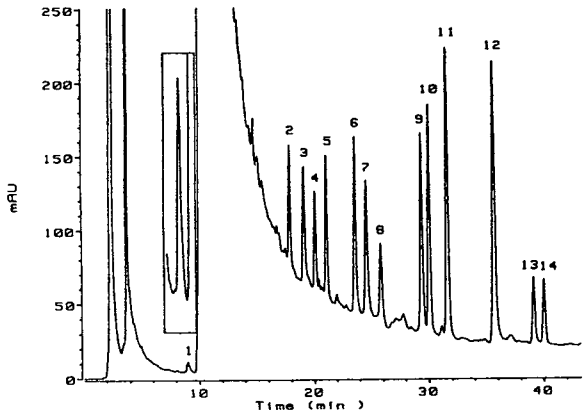

Fig. 4. On-line trace enrichment–LC–DAD-UV chromatogram ($\lambda = 210$ nm) of 50 ml surface water, spiked with 14 phenols (5 μg/l each), using two precolumns in series. The insert shows a blow up of peak 1 (phenol). For conditions, see text. For peak assignment, see Table 1.

started by switching valve V1 to the "inject" position and valve V2 to the "load" position. Comparison of Fig. 4 with Fig. 3 illustrates that (i) the dual-precolumn set-up provides additional selectivity in the early part of the chromatogram, enabling the detection of phenol at 195 nm (!), and (ii) the slightly more complicated set-up does not detract from the performance of the total analytical system.

Analytical performance

Calibration curves were constructed for all analytes in surface water samples over the range 0–25 μg/l using the dual-precolumn set-up of Fig. 1. The plots (six data points; $n = 2$) were linear for all analytes with R^2 values of over 0.99. In order to determine the precision of the total analytical procedure, six consecutive analyses were performed of river Meuse water spiked with a mixture of all test solutes at the 5 μg/l level. Although valve-switching was done manually, the precision for all analytes was quite satisfactory with a mean R.S.D. value of 3% (range 0.6–7.8%; cf. Table 1). Detection limits (signal-to-noise ratio 3:1) in real-life samples typically were ca. 0.5 μg/l (range, 0.05–1.0 μg/l).

In order to test the applicability of the present trace-enrichment–LC–DAD-UV system several surface water samples were analysed. Fig. 5 shows four chromatograms obtained after preconcentration of 50 ml of water from the rivers Meuse (Keizersveer, Netherlands), Rhine (Lobith, Netherlands), Danube (Bratislava, Slovakia) and Nitra (Nizne Krstenany, Slovakia). No phenols were found in these samples at or above the detection limits quoted in Table 1. When an automated library search was performed with spectral match as the only key for peak identification, diuron, a well known phenylurea herbicide, was found to be present in river Meuse water (cf. Fig. 5a). Unfortunately, none of the DAD-UV libraries available to us (polar pesticides, polynuclear aromatics, pyrethroids, sulphonic acids) provided a clue with regard to the nature of the several large peaks showing up in the samples, especially in the river Nitra sample.

4. Conclusions

An on-line trace enrichment–LC system with diode-array UV detection has been developed for the monitoring of a large series of phenolic compounds in surface water at low- to sub-μg/l levels. The procedure involves the preconcentration of 50 ml of surface water on a non-selective and a selective precolumn coupled in series. Because of the early breakthrough of phenol on the first precolumn, only an appropriate 5-ml portion of the total sample is pumped through the second precolumn. This helps to increase the selectivity of the procedure for phenol itself, allowing UV detection even at 195 nm (even for surface water). Besides, compared with literature studies, a wider range of analytes can be analysed using this technique. With the present set-up detection limits are between 1 (phenol) and 0.05 (4-chlorophenol) μg/l; the precision of the total analytical procedure is quite satisfactory. Future research will focus on the use of ENVI-Chrom P material with a smaller particle size than the present 80–160 μm. Two experimental phases, denoted 1038A and 1038B, are currently being tested. First results are quite promising; that is, band broadening

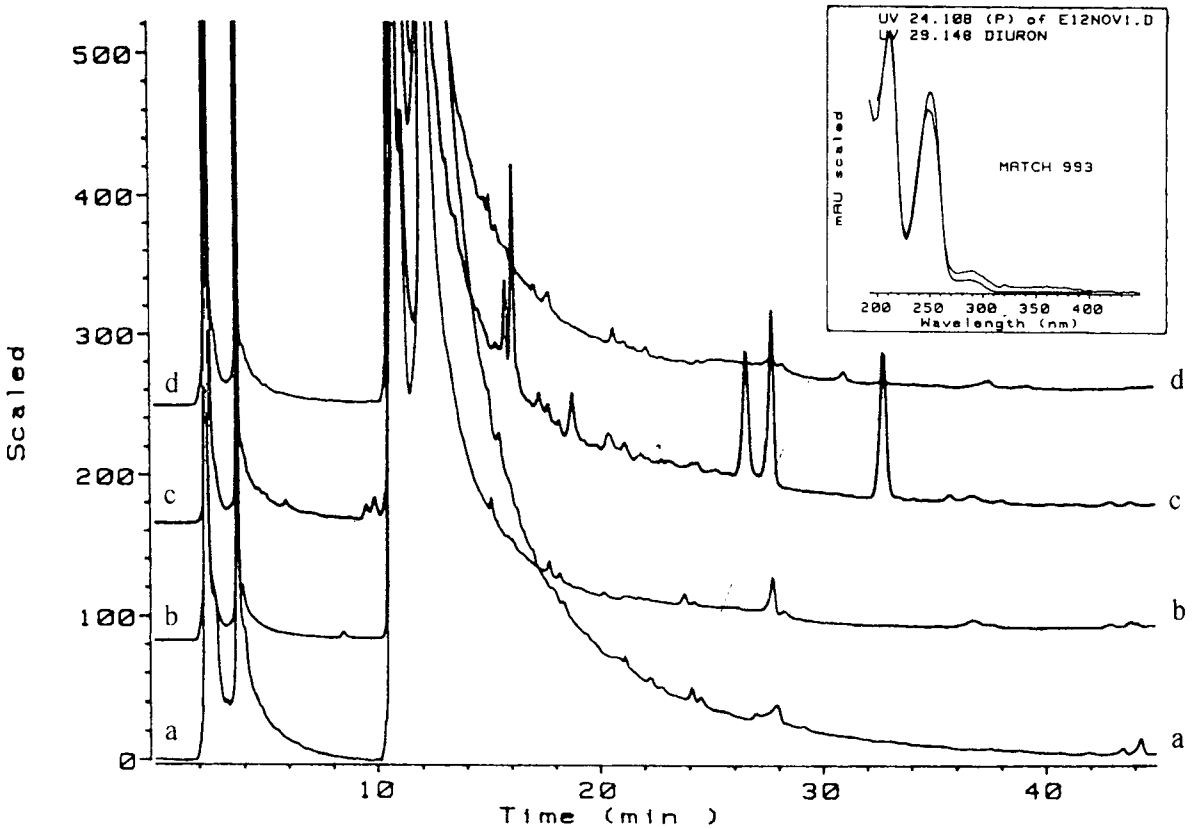

Fig. 5. On-line dual-precolumn trace enrichment–LC–DAD-UV chromatograms ($\lambda = 210$ nm) of 50 ml blank surface water samples. (a) river Meuse; (b) river Danube; (c) river Nitra; (d) river Rhine. The insert shows the library DAD-UV spectrum of diuron and the spectrum recorded for the peak at $t_R = 24.1$ min in trace a. For experimental conditions, see text.

which was the major disadvantage of the ENVI-Chrom P material used in this study, is considerably reduced.

Acknowledgements

We like to thank the Rhine Basin Program for their financial support. J. Brands (Supelchem, Leusden, Netherlands) and L. Nolan (Supelco, Bellefonte, PA, USA) are acknowledged for their useful comments and the gift of several sorbents and analytical columns. J.-W. Marinissen (Chrompack, Middelburg, Netherlands) is acknowledged for the gift of the Chromspher B and Inertsil columns.

References

[1] H.B Lee, R.L. Hong-You and P.J.A. Fowlie, *J. Assoc. Off. Anal. Chem.*, 72 (1989) 339–342.
[2] V. Janda and K. Krijt, *J. Chromatogr.*, 283 (1984) 309–314.
[3] US EPA Method 604, *Fed. Regist.*, 49 (1984) 43290.
[4] US EPA Method 625, *Fed. Regist.*, 49 (1984) 153.
[5] C. Borra, A. Di Corcia, M. Marchetti and R. Samperi, *Anal. Chem.*, 58 (1986) 2048–2052.
[6] K.D. Buchholz and J. Pawliszyn, *Environ. Sci. Technol.*, 27 (1993) 2844–2848.
[7] V. Coquart and M.-C. Hennion, *J. Chromatogr.*, 600 (1992) 195–203.
[8] A. Hagen, J. Mattusch and G. Werner, *Fresenius J. Anal. Chem.*, 339 (1991) 26–29.
[9] B. Schultz, *J. Chromatogr.*, 269 (1983) 208–212.
[10] A. Di Corcia, S. Marchese and R. Samperi, *J. Chromatogr.*, 642 (1993) 175–184.

[11] A. Di Corcia and M. Marchetti, *Anal. Chem.*, 63 (1991) 580–585.
[12] C. de Ruiter, J.N.L. Tai Tin Tsoi, U.A.Th. Brinkman and R.W. Frei, *Chromatographia*, 26 (1988) 267–273.
[13] C. de Ruiter, R.R. Otten, U.A.Th. Brinkman and R.W. Frei, *J. Chromatogr.*, 436 (1988) 429–436.
[14] L. Nolan, *Supelco Reporter*, 12 (1993) 10–11.
[15] E.R. Brouwer, T.M. Tol, H. Lingeman and U.A.Th. Brinkman, *Quim. Anal.*, 12 (1993) 88–95.
[16] J. Slobodnik, M.G.M. Groenewegen, E.R. Brouwer, H. Lingeman and U.A.Th. Brinkman, *J. Chromatogr.*, 642 (1993) 359–370.
[17] I. Liska, E.R. Brouwer, A.G.L. Ostheimer, H. Lingeman U.A.Th. Brinkman, R.B. Geerdink and W.H. Mulder, *Int. J. Environ. Anal. Chem.*, 47 (1992) 267–291.
[18] E.R. Brouwer, A.N.J. Hermans, H. Lingeman and U.A.Th. Brinkman, *J. Chromatogr. A*, 669 (1994) 45–57.
[19] N. Snippe, N.C. van de Merbel, F.P.M. Ruiter, H. Lingeman and U.A.Th. Brinkman, in preparation.
[20] T.L. Ascah, *Supelco Reporter*, 11 (1992) 23–24.

ELSEVIER

Journal of Chromatography A, 678 (1994) 233–240

JOURNAL OF CHROMATOGRAPHY A

Separations of basic amino acid benzyl esters by pH-zone-refining counter-current chromatography

Ying Ma, Yoichiro Ito*

Laboratory of Biophysical Chemistry, National Heart, Lung, and Blood Institute, National Institutes of Health, Building 10, Room 7N322, Bethesda, MD 20892, USA

(First received March 1st, 1994; revised manuscript received May 11th, 1994)

Abstract

pH-Zone-refining counter-current chromatography was applied to the separation of basic amino acid benzyl esters. The method uses a retainer base in the stationary phase to retain analytes in the column and an eluent acid to elute the analytes in the decreasing order of pK_a and hydrophilicity. The preparative capability of the method is demonstrated in the separation of a 10-g quantity of the sample.

1. Introduction

pH-Zone-refining counter-current chromatography (CCC) [1–6] is a new preparative CCC method which yields a characteristic elution pattern of analytes comparable to that observed in displacement chromatography [7]. The method uses a retainer acid or base in the stationary phase (or sample solution) to retain analytes which are then eluted with the mobile phase containing the respective counterion. The analytes are eluted as a succession of highly concentrated rectangular peaks with minimum overlap. In the past, applications were limited to the separation of acidic compounds including dinitrophenyl (DNP) amino acids [1–6], various hydroxyxanthene dyes [2,8–12], indole auxins [3], etc.

In this paper pH-zone-refining CCC is applied to basic compounds to illustrate its wider domain. After equilibration of a two-phase solvent system composed of methyl *tert.*-butyl ether and water, triethylamine (retainer base) was added to the upper organic stationary phase and HCl (eluent acid) to the lower aqueous mobile phase. Using a set of amino acid benzyl esters, the separation was obtained by varying the concentrations of both retainer base and eluent acid. The preparative capability is then demonstrated in the separation of a 10-g sample. Its success with these bases suggests its possible application to the separation of natural products such as alkaloids.

2. Experimental

2.1. CCC apparatus

A commercial model (Ito multilayer coil separator/extractor, P.C. Inc., Potomac, MD, USA) of the high-speed CCC centrifuge was

* Corresponding author.

0021-9673/94/$07.00
SSDI 0021-9673(94)00463-J

used throughout the present studies. The detailed design of the apparatus was given elsewhere [13]. The apparatus holds a multilayer coil separation column and a counterweight symmetrically at a distance of 10 cm from the central axis of the centrifuge. The column holder is equipped with a plastic planetary gear which is engaged to an identical stationary sun gear mounted around the central axis of the apparatus. This gear arrangement produces the desired planetary motion to the column holder, i.e. rotation about its own axis and revolution around the centrifuge axis in the same direction at the same rate. This planetary motion also prevents the flow tubes from twisting during revolution, thus permitting the elution of the mobile phase through the column without the use of rotary seals.

The separation column consists of a single piece of 160 m × 1.6 mm I.D. long polytetrafluoroethylene (PTFE) tubing (Zeus Industrial Products, Raritan, NJ, USA) wound around the column holder hub forming 16 layers with 325 ml capacity. Each terminal of the column was connected to a flow tube (0.85 mm I.D. PTFE) (Zeus) by the aid of a set of tube connectors (Upchurch Scientific, Oak Harbor, WA, USA) which were rigidly mounted on the holder flange. A narrow-bore PTFE tube (5 m × 0.3 mm I.D.) (Zeus) was placed at the outlet of the column to stabilize the effluent flow, thus facilitating the recording of elution curves.

The speed of the apparatus was regulated with a speed controller (Bodine Electric, North Chicago, IL, USA).

2.2. Reagents

Methyl *tert.*-butyl ether, methanol and triethylamine were glass-distilled chromatographic grade (Baxter Healthcare, Muskegon, MI, USA). Hydrochloric acid and acetic acid were of reagent grade (Fisher Scientific, Fair Lawn, NJ, USA). Amino acid benzyl esters used in the present studies include: Gly(OBzl)·Tos, Ala(OBzl)·Tos, Leu(OBzl)·Tos, Val(OBzl)·Tos, Glu(OBzl)–OBzl·Tos, Phe(OBzl)·Tos, Asp(OBzl)–OBzl·Tos, Ile(OBzl)·Tos (OBzl = benzyl ester, Tos = *p*-toluenesulfonic acid) (Peninsula Labs., Belmont, CA, USA).

2.3. Preparation of solvent phases and sample solutions

The solvent pair was prepared as follows: methyl *tert.*-butyl ether and distilled water were thoroughly equilibrated in a separatory funnel at room temperature and the two phases were separated. Triethylamine (2.5–40 m*M*) was added to the upper organic phase which was then used as the stationary phase. The lower aqueous phase was acidified with HCl (5–40 m*M*) and used as the mobile phase.

Sample solutions were prepared by dissolving a set of amino acid benzyl esters *p*-toluenesulfonic acid salts in 10–50 ml solvent, usually consisting of about equal volumes of upper organic phase and water. The solution was neutralized by an addition of triethylamine in an appropriate amount and sonicated for several minutes before injection into the column.

2.4. Separation procedure

In each separation, the column was first entirely filled with the organic stationary phase containing triethylamine. Then the sample solution was injected through the sample port and the acidified aqueous mobile phase was eluted through the column in the head-to-tail elution mode at a flow-rate of 3.0 ml/min (metering pump from Rainin Instruments, Emeryville, CA, USA) while the apparatus rotated. In order to minimize the carryover loss of the stationary phase from the column, the revolution speed was initially set at 600 rpm which was increased to 800 rpm after 20 min of elution. The effluent from the column was continuously monitored by absorbance at 206 nm (Uvicord S; LKB, Bromma/Stockholm, Sweden) and collected at 3.0 ml/tube (Ultrorac fraction collector, LKB). After all peaks were eluted, the centrifuge was stopped and the column contents were collected into a graduated cylinder by connecting the inlet of the column to a nitrogen line at 80 p.s.i. (1 p.s.i. = 6894.76 Pa). The retention of the stationary

phase relative to the total column capacity was computed from the volume of the stationary phase collected from the column (80–65%).

2.5. Studies on effects of eluent acid and retainer base concentrations

A series of experiments was carried out with a set of three amino acid benzyl esters *p*-toluenesulfonic acid salts (monobenzyl esters of glycine and leucine and dibenzyl ester of glutamic acid) to study the effects of the eluent acid (HCl) and retainer base (triethylamine) on the separation. In the first series the effect of the eluent acid was studied by varying the HCl concentration in the aqueous mobile phase from 5 to 40 m*M* while the concentration of triethylamine in the organic stationary phase was kept constant at 5 m*M*. In the second series, the effect of the retainer base was investigated by varying the concentration of triethylamine in the organic stationary phase from 2.5 to 40 m*M* while the HCl concentration in the mobile phase was fixed at 10 m*M*.

In each separation, the column was first filled with the organic stationary phase followed by injection of a sample mixture containing 0.5 mmol of each component in 10 ml solvent (5 ml upper phase and 5 ml water). In order to neutralize the sample solution, 200 μl of triethylamine was added. Then the column was rotated at 600 rpm and eluted with the acidified organic phase at a flow-rate of 3.0 ml/min. As mentioned earlier, the revolution speed was increased to 800 rpm after 20 fractions were collected (20 min). The effluent from the column was continuously monitored with a UV monitor at 206 nm. The average solute concentration in each fraction was estimated from the width of each peak. The partition coefficient of the retainer base was also computed from its retention volume and the volume of the stationary phase retained in the column [6].

2.6. Continuous UV monitoring

As previously described [3], the elution curve produced by the continuous UV monitoring with an LKB Uvicord S needs further explanation: this monitor uses an interference filter (206 nm) which actually passes some light in a broad range, even extending to the visual region. This particular feature allows us to monitor elution curves at several wavelengths. Thus the lower portion of the absorbance scale correctly reflects the 206 nm absorption when this is the major chromophore present. At the higher sample concentrations found in pH-zone-refining CCC, the sample may be opaque to 206 nm light but the detection will still respond to absorption of other frequencies. Thus, impurities absorbing at different wavelengths can be detected above the main plateau as sharp peaks at the zone boundaries. (In the present study no impurities were detected in this fashion.) The actual absorbance values at the tops of the peaks (not shown) were determined using a Zeiss PM6 spectrophotometer at 206 nm after diluting the fraction with methanol. These values were about 200 absorbance units and obviously could not be directly monitored by an ordinary UV monitor. For this reason, we do not indicate absorbance values in the chromatogram.

2.7. Analysis of CCC fractions

The pH value of each fraction was manually determined with a portable pH meter (Accumet portable laboratory; Fisher Scientific, Pittsburgh, PA, USA).

The amino acid benzyl esters were identified by their partition coefficients, K_{std}, in a standard two-phase system composed of *n*-hexane–ethyl acetate–MeOH–0.1 *M* NaOH (1:1:1:1, v/v). An aliquot of each fraction (usually 1 ml) was delivered into a test tube and dried under vacuum (Speed Vac concentrator; Savant Instruments, Hicksville, NJ, USA). Then 2 ml of the standard solvent system (1 ml of each phase) were added to each tube and the contents vigorously shaken to equilibrate the solute. An aliquot of each phase (usually 100–200 μl) was diluted with 2 ml of methanol and the absorbance determined at 260 nm. The standard partition coefficient, K_{std}(U/L) or K_{std}, was expressed as solute concentration in the upper

phase (U) divided by that in the lower phase (L). The peak fractions were also analyzed by TLC (Kieselgel 60 F_{254}, EM Separations, Gibbstown, NJ, USA) with a chloroform–methanol–32% acetic acid (16:4:1, v/v) system and detection at 254 nm.

3. Results and discussion

Fig. 1 shows a typical chromatogram of amino acid benzyl esters obtained by the present method. Seven components (each 0.5 mmol) were eluted together as a broad rectangular peak (Fig. 1A) due to detector saturation (see above). Partition coefficient measurement, K_{std}(U/L), revealed that it consisted of a series of narrow rectangular peaks of the individual components with minimum overlap in the same fashion as observed in separation of acidic analytes [1–3]. Although the chromatogram in Fig. 1A indicates sharp boundaries between neighboring peaks, the TLC analyses (Fig. 1B) of fractions show that each boundary actually consists of several milliliters of the mixing zone. Each component formed a pH plateau in a downward staircase fashion. Considerable irregularity of the pH plots at some peaks was caused by the carryover of organic stationary phase which, however, did not affect the peak resolution. The results indicate that basic amino acids with similar structures can be separated in decreasing order of their pK_a and hydrophilicity since these two parameters determine the pH of the eluted solute zone [3].

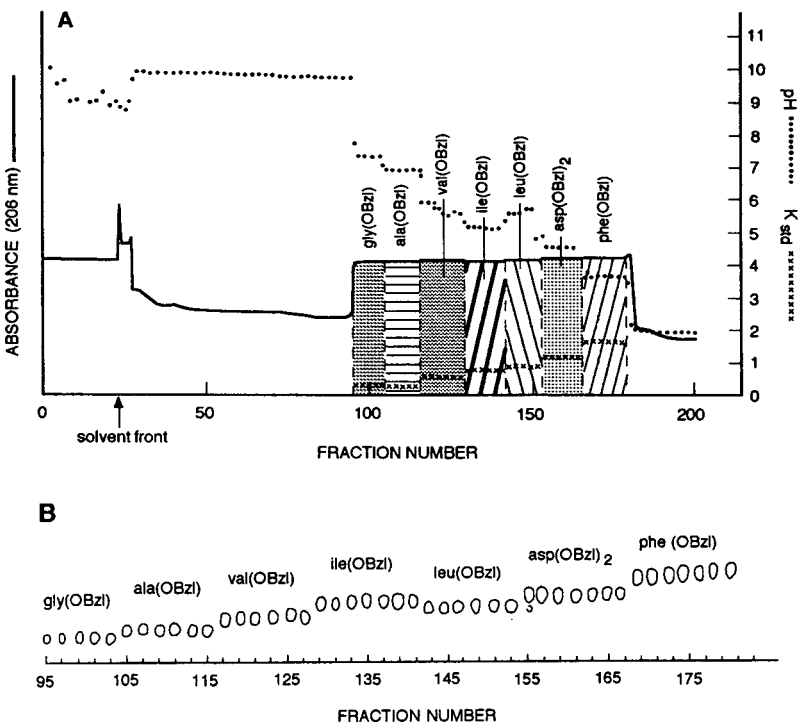

Fig. 1. Separation of seven amino acid benzyl esters by pH-zone-refining CCC. (A) Elution profile. Experimental conditions: apparatus: high-speed CCC centrifuge; column: semipreparative multilayer coil, 160 m × 1.6 mm I.D., 325 ml capacity; solvent system: methyl *tert.*-butyl ether, 10 m*M* triethylamine in upper organic stationary phase and 10 m*M* hydrochloric acid in lower aqueous mobile phase; sample: a synthetic mixture of 7 amino acid benzyl esters as labelled in the chromatogram, each 100 mg dissolved in 20 ml solvent; flow-rate: 3 ml/min; revolution: 800 rpm; retention of stationary phase: 71.2%. (B) TLC analysis of peak fractions. TLC plate: Kieselgel 60 F_{254}, EM Separations; solvent: chloroform–methanol–32% acetic acid (16:4:1, v/v).

A series of experiments was performed to investigate the effects of concentration of the eluent acid and retainer base on those of the eluted analytes. The effects of the eluent acid concentration are shown in Fig. 2A where molar concentrations of three analytes are plotted against those of HCl (eluent acid) in the mobile phase. As the HCl concentration is increased from 5 to 40 m*M*, all analytes increase their concentrations at a nearly 1:1 molar ratio suggesting that the eluent acid acts as the counterion to effectively determine the analyte concentration in the mobile phase. On the other hand, the increased HCl concentration causes a sharp decrease of the partition coefficient (K) of the retainer base (triethylamine) resulting in the reduced retention time of the analyte peaks.

Fig. 2B similarly shows the effects of the retainer base (triethylamine) concentration in the stationary phase while the concentration of the eluent acid (HCl) in the mobile phase is fixed at 10 m*M*. In this case, the concentrations of all analytes were almost unaltered with the increased triethylamine concentration by maintaining a near 1:1 molar ratio to the eluent acid that serves as the counterion mentioned above. The increase in concentration of the retainer base, however, causes the increase of the partition coefficient (K), thus enhancing the retention of the analytes. As described elsewhere [3], the partition coefficient (K) of the retainer is equal to those for all analytes within the succeeding pH zones. This fact indicates that the increased retainer base concentration increases the analyte concentration in the stationary phase while it produces no change in that in the mobile phase.

In short, the eluent acid determines the analyte concentration in the mobile phase while the retainer base modifies that in the stationary phase. The retention time of the analyte is counterbalanced by concentrations of the retainer base and the eluent acid. A short retention time may result in incomplete resolution between the early-eluting zones. On the other hand, an excessively long retention time may cause decomposition of the analyte which follows immediately behind the retainer base by hydrolysis of these benzyl esters by the exposure to high pH. This complication may be avoided by using a suitable spacer which occupies the column space between the retainer base and the analytes.

Fig. 3 shows the separations of three amino acid benzyl esters in three different sample sizes of 0.6 g (A), 3 g (B) and 6 g (C) under otherwise similar experimental conditions. Separations

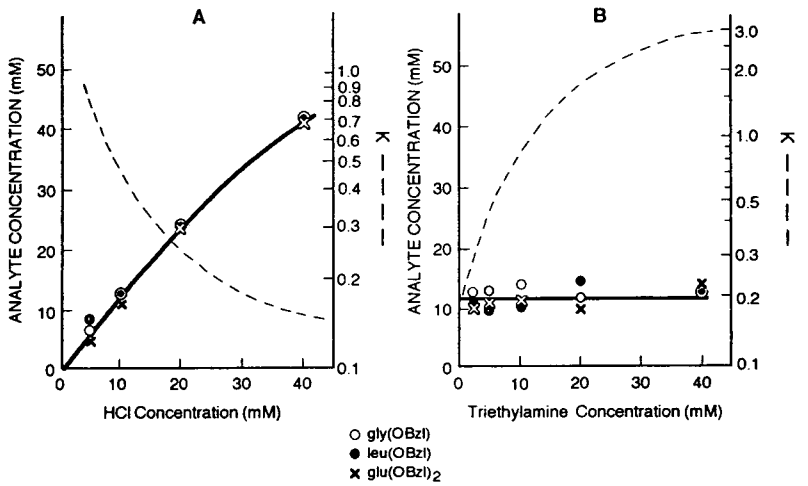

Fig. 2. Effects of eluent acid (A) and retainer base (B) on analyte concentrations in the mobile phase. (A) Analyte concentration in the mobile phase was plotted against the concentration of the eluent acid from 5 to 40 m*M* while the concentration of the retainer base was fixed at 10 m*M*. (B) Analyte concentration in the mobile phase was plotted against the concentration of the retainer acid from 5 to 40 m*M* while the eluent acid concentration was fixed at 10 m*M*.

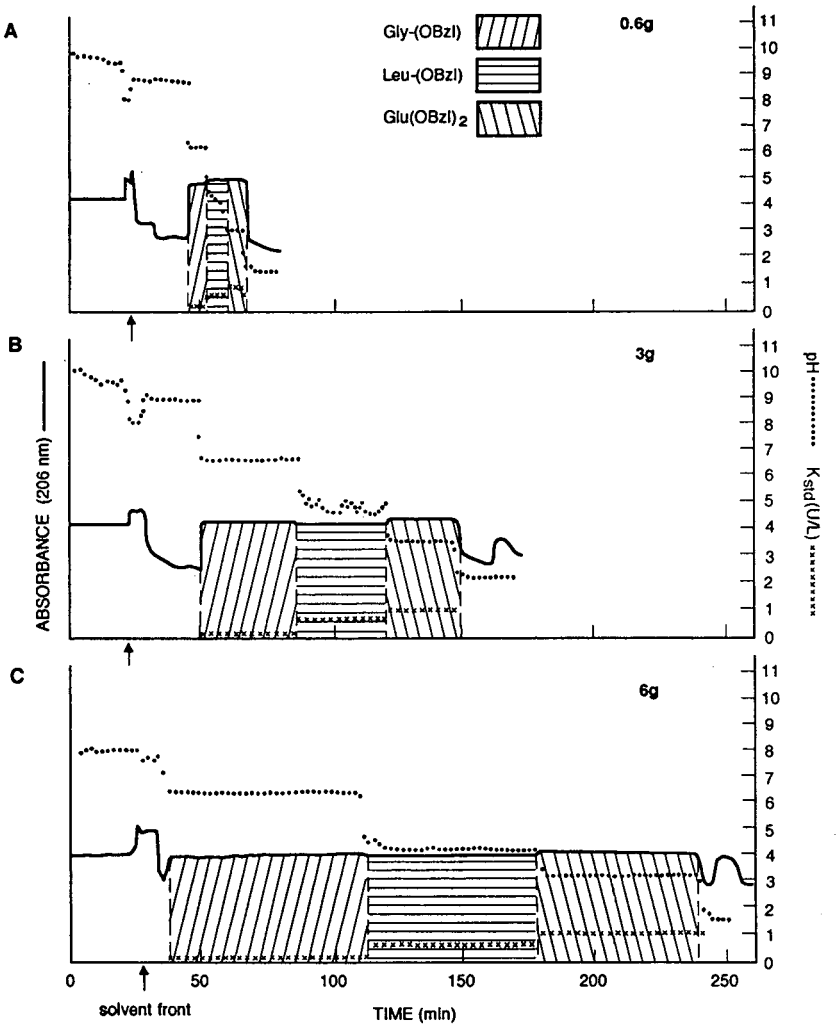

Fig. 3. Separation of three amino acid benzyl esters by pH-zone-refining CCC. Experimental conditions: apparatus and columns as in Fig. 1; solvent system: methyl *tert.*-butyl ether, 5 m*M* triethylamine in the upper organic stationary phase and 20 m*M* hydrochloric acid in the lower aqueous mobile phase; sample: Gly(OBzl)·Tos, Leu(OBzl)·Tos and $Glu(OBzl)_2$·Tos, each 0.2 g (A), 1 g (B) and 2 g (C); flow-rate: 3 ml/min; revolution: 800 rpm; retention of stationary phase: 76.5% (A), 68.3% (B) and 77.8% (C).

were performed with a methyl *tert.*-butyl ether–water system by adding triethylamine (retainer base) to the upper organic stationary phase at 5 m*M* and hydrochloric acid (eluent acid) to the lower aqueous mobile phase at 20 m*M*. In order to normalize the retention time of the analytes, the sample solution was neutralized with triethylamine (0.2, 1.0 and 2.0 ml were added for A, B and C, respectively). Under a flow-rate of 3.0 ml/min and a revolution speed of 800 rpm, the separations were completed in about 1.1, 2.5 and 4.0 h for the sample sizes of 0.6 g, 3 g and 6 g, respectively. In all separations, three components were eluted together as fused rectangular peaks with sharp boundaries as indicated by the abrupt transition of the partition coefficient (K_{std}) and pH levels (dotted line) in the diagrams. The results show that with a given

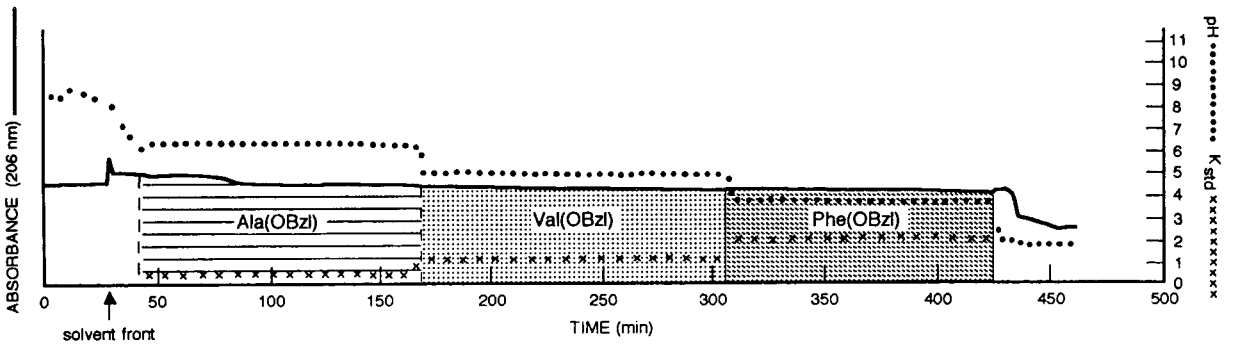

Fig. 4. Preparative separation of three amino acid benzyl esters by pH-zone-refining CCC. Sample: Ala(OBzl)·Tos, Val(OBzl)·Tos, and Phe(OBzl)·Tos each 3.3 g in 100 ml solvent. Other experimental conditions as in Fig. 3.

concentration of the retainer base and eluent acid the analyte concentrations stay similar regardless of the sample size. Consequently the length of each peak increases nearly proportional to the applied sample size while the widths of the mixing zones between the neighboring peaks are not significantly altered. This allows one to harvest a greater overall yield of pure product by increasing the sample size.

Fig. 4 shows a chromatogram of three amino acid benzyl esters at a sample size of 10 g by the present method. Each component is well resolved and eluted in slightly over 7 h. The stable pH plateau in each analyte zone indicates that no carryover of the stationary phase occurred. The partition coefficient measurement, K_{std}, revealed that the mixing zone at each peak boundary amounts no more than several milliliters. This separation is the first case in our laboratory where a sample size of 10 g was successfully separated using a semipreparative multilayer coil with a 325-ml total capacity.

4. Conclusions

The overall result of our studies indicates that pH-zone-refining CCC can be successfully applied to basic amino acid benzyl esters. The present method provides more than a 10-fold increase in sample capacity for a given column. Separation of three components from a 10 g sample size was achieved using a 325 ml capacity column in about 7 h. The method should be applicable to other basic compounds such as alkaloids from the natural products.

Acknowledgement

The authors wish to thank Dr. Henry M. Fales for his help in editing the manuscript.

References

[1] Y. Ito, K. Shinomiya, H.M. Fales, A. Weisz and A.L. Scher, presented at the *1993 Pittsburgh Conference and Exposition on Analytical Chemistry and Applied Spectroscopy, Atlanta, GA, March 8–12, 1993*, abstract 054P.

[2] A. Weisz, A.L. Scher, K. Shinomiya, H.M. Fales and Y. Ito, *J. Am. Chem. Soc.*, 116 (1994) 704, 1994.

[3] Y. Ito, K. Shinomiya, H.M. Fales, A. Weisz and A.L. Scher, in W.D. Conway and S.G. Petrosky (Editors), *Countercurrent Chromatography (ACS Monographs)*, American Chemical Society, Washington, DC, in preparation.

[4] A.L. Scher and Y. Ito, in W.D. Conway and S.G. Petrosky (Editors), *Countercurrent Chromatography (ACS Monographs)*, American Chemical Society, Washington, DC, in preparation.

[5] Y. Ito, in Y. Ito and W.D. Conway (Editors), *High-Speed Countercurrent Chromatography*, Wiley-Interscience, New York, in press.

[6] Y. Ito and Y. Ma, *J. Chromatogr. A*, 672 (1994) 101.

[7] Cs. Horváth, A. Nahum and J.H. Frenz, *J. Chromatogr.*, 218 (1981) 365.

[8] A. Weisz, K. Shinomiya and Y. Ito, presented at the *1993 Pittsburgh Conference and Exposition on Analytical Chemistry and Applied Spectroscopy, Atlanta, GA, March 8–12, 1993*, abstract 865.
[9] A. Weisz, D. Andrzejewski and Y. Ito, *J. Chromatogr. A*, (1994) in press.
[10] A. Weisz, A.L. Scher, D. Andrzejewski, and Y. Ito, presented at the *10th International Symposium on Preparative Chromatography, Arlington, VA, June 14–16, 1993.*
[11] A. Weisz, D. Andrzejewski, R.J. Highet and Y. Ito, *J. Chromatogr. A*, 658 (1994) 505–510.
[12] A. Weisz, in Y. Ito and W.D. Conway (Editors), *High-Speed Countercurrent Chromatography*, Wiley-Interscience, in press.
[13] Y. Ito, in N.B. Mandava and Y. Ito (Editors), *Countercurrent Chromatography: Theory and Practice*, Marcel Dekker, New York, 1988, pp. 79–442.

ELSEVIER

Journal of Chromatography A, 678 (1994) 241–247

JOURNAL OF CHROMATOGRAPHY A

Precolumn fluorescence derivatization of carnitine and acylcarnitines with 4-(2-aminoethylamino)-7-nitro-2,1,3-benzoxadiazole prior to high-performance liquid chromatography

Kojiro Matsumoto[a,*], Yukako Ichitani[a], Noriko Ogasawara[a], Hidetaka Yuki[a], Kazuhiro Imai[b]

[a]*Clinical Chemistry, School of Pharmaceutical Sciences, Toho University. 2-2-1 Miyama, Funabashi, Chiba 274, Japan*
[b]*Analytical Chemistry, Faculty of Pharmaceutical Sciences, University of Tokyo, 7-3-1 Hongo, Tokyo 113, Japan*

First received 21 September 1993; revised manuscript received 11 May 1994

Abstract

4-(2-Aminoethylamino)-7-nitro-2,1,3-benzoxadiazole (NBD-ED) was synthesized as a precolumn fluorescence derivatization reagent for the high-performance liquid chromatographic determination of carnitine and acylcarnitines. Carnitine and acylcarnitines were reacted with NBD-ED (2.0 m*M*) and 1-ethyl-3-(3-dimethylaminopropyl)carbodiimide (35 m*M*) in pyridine–dimethylformamide (1:4) at room temperature for 2 h. The NBD-ED derivatives of carnitine and acylcarnitines were separated by gradient elution with water–acetonitrile containing 10 m*M* trifluoroacetic acid on a reversed-phase column and the eluate was monitored with excitation at 470–485 nm and emission at 530–540 nm. Carnitine and sixteen acylcarnitines were determined within 45 min. The detection limits (signal-to-noise ratio = 3) for the carnitine-related compounds were 10–100 fmol. Four other NBD-alkyldiamines were also studied.

1. Introduction

The determination of serum and urinary acylcarnitines in patients with organic acidurias is important for the diagnosis of genetic defects involving mitochondrial dehydrogenases or carboxylases [1,2]. A common feature in these patients is a decrease in free carnitine in serum and an increase in normal or abnormal acylcarnitines in serum and urine. Further, administration of L-carnitine increases considerably the excretion of acylcarnitines into urine, reflecting the washout of coenzyme A esters accumulated in the mitochondrion.

Several post- and precolumn derivatization methods have been developed for the high-performance liquid chromatographic (HPLC) determination of acylcarnitines. HPLC of coenzyme A esters formed by transesterification [3,4] and HPLC of [^{3}H]acylcarnitines produced by added [^{3}H]carnitine in the presence of coenzyme A [5–7] are limited to the catalytic

* Corresponding author.

0021-9673/94/$07.00
SSDI 0021-9673(94)00459-M

reaction of carnitine acetyltransferase to determine short-chain acylcarnitines. HPLC with a carboxylic acid analyser [8,9] or HPLC with mass spectrometry [10,11] requires expensive apparatus. Precolumn derivatization methods such as with bromophenacyl esters with 4′-bromophenacyl triflate [12] or 4-bromophenacyl bromide [13] have been applied to determine carnitine and acylcarnitines in biological samples [14–17].

Various fluorescent precolumn derivatization reagents have been developed for the HPLC determination of carboxylic acids, coumarin-type reagents such as 4-bromomethyl-7-methoxycoumarin [18–20], 4-bromomethyl-7-acetoxycoumarin [21,22] and 3-bromoacetyl-7-methoxycoumarin [23], diazomethane-type reagents such as 9-anthryldiazomethane [24,25] and 1-pyrenyldiazomethane [26], hydrazide-type reagents such as 6,7-dimethoxy-1-methyl-2(1*H*)-quinoxalinone-3-propionylcarboxylic acid hydrazide [27] and 4-(5,6-dimethoxy-2-benzimidazoyl)benzohydrazide [28] and aliphatic amine-type reagents such as dansyl semipiperazide [29], monodansylcadaverine [30] and 4-substituted-7-aminoalkylamino-2,1,3-benzoxadiazoles [31,32]. Among these reagents, the aliphatic amine-type reagents seem to be suitable for carboxylic acid determinations owing to their excellent stability and sensitivity.

We have developed an immobilized enzyme reactor of acylcarnitine hydrolase, carnitine dehydrogenase and diaphorase for the sensitive and selective HPLC determination of short-chain acylcarnitines [33]. However, the method needs an immobilized enzyme reactor and cannot determine medium- and long-chain acylcarnitines. In this paper, we report a precolumn derivatization method for the HPLC determination of carnitine and acylcarnitines with 4-(2-aminoethylamino)-7-nitro-2,1,3-benzoxadiazole (NBD-ED).

2. Experimental

2.1. Reagents

Chloride salts of D,L-carnitine and acetyl-, hexanoyl-, heptanoyl-, octanoyl-, nonanoyl-, decanoyl-, lauroyl-, myristoyl-, palmitoyl- and stearoyl-D,L-carnitine were purchased from Sigma (St. Louis, MO, USA). 4-Fluoro-7-nitro-2,1,3-benzoxadiazole (NBD-F), ethylenediamine (ED), 1,3-propanediamine (PD), piperazine (PZ), 1-ethyl-3(3-dimethylaminopropyl)carbodiimide (EDC), diethyl phosphorocyanidate (DEPC), triphenylphosphine (TPP), N,N′-dimethylformamide (DMF) for fluorescence analysis, pyridine for sequence analysis and methanol and acetonitrile for HPLC analysis were obtained from Wako (Osaka, Japan), putrescine (PS) and cadaverine (CD) from Nacalai Tesque (Kyoto, Japan) and diphenylphosphoroylazide (DPPA), 2,2′-dipyridyl disulphite (DPDS) and 2-chloro-1-methylpyridinium iodide (CMP) from Tokyo Kasei Kogyo (Tokyo, Japan). A TSKgel ODS 80Ts column (150 mm × 4.6 mm I.D., 5 μm particle size) and a Toyopak IC-SP S cartridge (0.15 ml gel bed, 0.06 mequiv.) were purchased from Tosoh (Tokyo, Japan). Other chemicals were of analytical-reagent grade.

2.2. HPLC

The HPLC system from Tosoh was composed of a Model CCPM-8000 pump, a Model AS-48 autosampler equipped with a 100-μl loop injector, a Model FS-8010 fluorescence detector and a Model CP-8000 chromatoprocessor.

2.3. Synthesis of acylcarnitines

Propionyl-, isobutyryl-, butyryl-, isovaleryl-, valeryl- and valproyl-D,L-carnitine hydrochloride were synthesized from the corresponding acid chlorides in trifluoroacetic acid (TFA) according to the method of Bohmer and Bremer [34].

2.4. Synthesis of NBD-alkyldiamine derivatives

NBD-F (10 mg, 55 μmol) in 10 ml of acetonitrile was added dropwise to a stirred solution of each alkyldiamine (550 μmol) in 10 ml of acetonitrile for 30 min at room temperature. After stirring for 2 h at room temperature, acetonitrile was evaporated under reduced pressure. The residue was acidified with 5% HCl and the NBD-alkyldiamine derivatives were purified several

times on a reversed-phase column with a linear gradient of 10 m*M* HCl–acetonitrile.

2.5. Comparison of activation agents for the derivatization reaction

NBD-ED (2.0 m*M*) was reacted with the carnitine mixture (D,L-carnitine and acetyl-, octanoyl- and palmitoyl-D,L-carnitine, 50 μM each) in 100 μl of DMF or acetonitrile in the presence of each activation agent: EDC (35 m*M*)–20% pyridine, DEPC (70 m*M*), DPPA (70 m*M*), DPDS (35 m*M*) and TPP (35 m*M*) or CMP (35 m*M*)–20% triethylamine (TEA). After reaction for 3 h at room temperature, the reaction mixture was diluted with 900 μl of 10 m*M* HCl in DMF–water (4:1, v/v), 100 μl of the solution was injected on to the column and the fluorescent peaks corresponding to the adducts were compared with each other.

2.6. Comparison of derivatization agents

The carnitine mixture (50 μM each) was reacted with EDC (35 m*M*) and the NBD-akyldiamine reagent (NBD-ED, NBD-PD, NBD-CD, NBD-PT or NBD-PZ, 2 m*M* each) at room temperature in 100 μl of pyridine–DMF (1:4, v/v). At fixed time intervals, the reaction was stopped by adding 9 volumes of 10 m*M* HCl in DMF–water (4:1, v/v), 100 μl of the solution were injected on to the column and the fluorescent peak areas corresponding to the adducts were measured at each maximum excitation and emission wavelength.

2.7. Spectral measurement of fluorescent adducts

The carnitine mixture (50 μM each) was reacted with 2 m*M* each of NBD-ED, NBD-PD, NBD-CD, NBD-PT or NBD-PZ in 100 μl of pyridine–DMF (1:4, v/v) in the presence of 35 m*M* EDC at room temperature for 2 h. The fluorescent peaks corresponding to the adducts separated by reversed-phase HPLC were collected. Excitation and emission spectra of the fluorescent adducts were measured with a Model F-3000 spectrofluorimeter (Hitachi, Tokyo, Japan).

2.8. Dependence of fluorescence intensities on organic solvent

The NBD-ED adducts corresponding to carnitine and acetyl-, octanoyl- and palmitoyl-D,L-carnitine separated on the reversed-phase column were collected and the eluates were evaporated to dryness. The residues were dissolved in 10 m*M* TFA with various ratios of acetonitrile and water. The fluorescence intensities were measured with excitation at 485 nm and emission at 540 nm with the spectrofluorimeter.

2.9. Purification of fluorescent adducts with a Toyopak IC-SP S cartridge

The reaction mixture of the NBD-ED adducts with carnitine and acylcarnitines diluted with 9 volumes of 10 m*M* HCl in methanol–water (4:1, v/v) was applied to a Toyopak IC-SP S cartridge, the cartridge was washed with 5 ml of 10 m*M* HCl–methanol (1:1, v/v) and the fluorescent adducts retained on the cartridge were eluted with 3 ml of TEA–acetate (1.0 *M*, pH 7.0) in methanol. The eluent was evaporated to dryness and the residue was dissolved in 1 ml of 0.1 *M* TFA–DMF (1:4, v/v) and an aliquot of the solution was injected on to the reversed-phase column.

2.10. HPLC conditions for NBD-ED adducts with acylcarnitines

The NBD-ED adducts with carnitine and acylcarnitines purified on the Toyopak IC-SP S cartridge and dissolved in 0.1 *M* TFA–DMF (1:4, v/v) were injected on to a TSKgel ODS-80Ts column and separated by the following gradient programme with solvents A = 10 m*M* TFA and B = water–acetonitrile (1:9, v/v) containing 10 m*M* TFA: 0–15% B for 1 min, 15–25% B for 9 min, 25–35% B for 10 min, 35–100% B for 20 min, 100% B for 2 min and 100–0% B for 1 min. The eluate was monitored with excitation at 485 nm and emission at 540 nm.

3. Results and discussion

3.1. Fluorescence properties of the NBD-alkyldiamine adducts with carnitine and acylcarnitines

The excitation and emission wavelengths for maximum fluorescence intensities of the NBD-alkyldiamine adducts with carnitine and acylcarnitines obtained using an eluent composed of acetonitrile–water (1:9 to 9:1, v/v) containing 10 m*M* TFA are given in Table 1. Acetonitrile caused blue shifts of both the excitation and emission maxima of the NBD-alkyldiamine adducts, 9–15 nm shorter in excitation and 4–10 nm shorter in emission of NBD-adducts with carnitine (eluted with 10% acetonitrile) than those of palmitoylcarnitine (in 90% acetonitrile).

Organic solvents markedly affected the fluorescence intensities of the NBD-ED adducts [35]. About a tenfold increase in the fluorescence intensities was obtained in acetonitrile containing 10 m*M* TFA compared with those in 10 m*M* TFA. Although accurate gradient control was necessary for reproducible determination, the dependence of the fluorescence intensities of the NBD-ED adducts on the concentrations of acetonitrile would be favourable for the simultaneous determination of carnitine and acylcarnitines in biological samples that contain higher contents of carnitine and short-chain acylcarnitines than long-chain acylcarnitines.

3.2. Reactivities and fluorescence intensities of NBD-alkyldiamine reagents with carnitine and acylcarnitines

The reactivities of NBD-alkyldiamine reagents with carnitine and acylcarnitines are shown in Fig. 1. The chain length of the acyl groups in acylcarnitines did not affect the derivatization reactivity with NBD-ED and the reaction reached a plateau after 1.5–6 h (Fig. 1a). Comparing the reaction rates of carnitine with five NBD-alkyldiamine reagents, NBD-ED reacted most rapidly and the reaction rate of NBD-PZ seemed to be similar to those of the other NBD-alkyldiamine reagents (Fig. 1b). The relative fluorescence intensities of the NBD-alkyldiamine adducts with carnitine and acylcarnitines were calculated for the peak areas at their maximum excitation and emission wavelengths and are given in Table 2. The fluorescence intensities of the NBD-ED adducts were highest and those of NBD-PZ were lowest among the five NBD-alkyldiamine reagents. These results were different from those for 4-(aminosulphonyl)-2,1,3-benzoxadiazolamine (ABD-amine) adducts with car-

Table 1
Wavelengths for maximum fluorescence intensities of NBD-alkyldiamine adducts with carnitine and acylcarnitines

NBD-diamine	Excitation/ emission	Wavelength (nm)			
		Free	Acetyl	Octanoyl	Palmitoyl
NBD-ED	Ex.	485	483	476	470
	Em.	540	540	536	533
NBD-PD	Ex.	488	487	479	475
	Em.	543	543	535	533
NBD-PS	Ex.	485	490	481	476
	Em.	542	546	536	533
NBD-CD	Ex.	485	484	481	476
	Em.	542	539	535	533
NBD-PZ	Ex.	493	493	487	484
	Em.	542	541	538	538

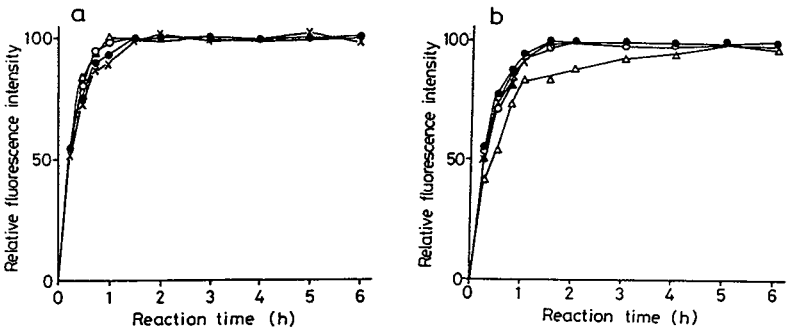

Fig. 1. Reactivities of the NBD-alkyldiamine derivatives with carnitine and acylcarnitines. (a) Reactivities of NBD-ED with carnitine and acylcarnitines in the presence of EDC and pyridine. ● = carnitine; × = acetylcarnitine; △ = octanoylcarnitine; ○ = palmitoylcarnitine. (b) Reactivities of NBD-alkyldiamines with carnitine in the presence of EDC and pyridine. ● = NBD-ED; ○ = NBD-PD; ▲ = NBD-PS; △ = NBD-CD; × = NBD-PZ. The relative fluorescence intensities are expressed with respect to maximum fluorescence intensities = 100.

boxylic acids in the presence of DEPC [32], which indicated that ABD-PZ reacted with carboxylic acids more slowly than ABD-ED and ABD-CD, while the fluorescence intensities of ABD-PZ adducts were highest among the three ABD-amines.

3.3. Derivatization reaction of NBD-ED with carnitine in the presence of activation agents

The five activation agents were compared for the reaction of NBD-ED with carnitine in acetonitrile or DMF and the results are given in Table 3. Among the five activation agents, EDC-pyridine and DPDS-TPP exhibited the highest activation in acetonitrile and DMF, respectively. In the activation of arachidic acid for derivatization with 4-(N,N-dimethylaminosulphonyl)-7-N-piperazino-2,1,3-benzoxazole (DBD-PZ), DEPC and DPDS-TPP exhibited the highest activation in acetonitrile and DMF, respectively [31]. As DPDS-TPP produced side-reaction peaks, EDC-pyridine in DMF was selected as an activation agent.

3.4. Optimized reaction conditions for derivatization of carnitine with NBD-ED

Fluorescent derivatization of carnitine with NBD-ED in the presence of EDC-pyridine was optimized with respect to the concentrations of NBD-ED, EDC, pyridine. The reaction time courses were also compared in acetonitrile and DMF. As shown in Fig. 2, the derivatization reactions reached plateaux with the use of over 2 m*M* of NBD-ED, 20 m*M* of EDC and 10% of

Table 2
Relative fluorescence intensities of NBD-alkyldiamine adducts with carnitine and acylcarnitines

NBD-diamine	Wavelength (nm)		Relative fluorescence intensity			
	Ex.	Em.	Free	Acetyl	Octanoyl	Palmitoyl
NBD-ED	485	540	100	100	100	100
NBD-PD	488	543	92	82	63	82
NBD-PS	485	542	74	59	27	55
NBD-CD	485	542	76	57	25	49
NBD-PZ	493	542	39	50	28	24

Table 3
Reactivities of activation agents in NBD-ED adducts with carnitine

Activation agent	Relative fluorescence intensity	
	Acetonitrile	Dimethylformamide
EDC	100	100
DPDS–TPP	89	101
CMP–TEA	24	48
DEPC	23	67
DPPA	56	61

pyridine in DMF at room temperature for 3 h. The reaction time courses reached plateaux after 1.5 and 2 h in acetonitrile and DMF, respectively. The derivatization conditions selected were 2 m*M* NBD-ED and 35 m*M* EDC in 20% pyridine–DMF at room temperature for 2 h.

3.5. HPLC of the NBD-ED adducts with carnitine and acylcarnitines

The main impurity peaks due to the side-reactions were eluted with the peaks of acetylcarnitine and myristoylcarnitine. Minor impurity peaks due to carboxylic acids hydrolysed from acylcarnitines were also detected after the peaks of the corresponding acylcarnitines. Pretreatment with a Toyopak IC-SP S cartridge was effective in eliminating these impurity peaks. The impurity peaks were easily washed out from the Toyopak IC-SP S cartridge with 5 ml of 10 m*M* HCl–methanol (1:1, v/v), whereas the NBD-ED adducts of carnitine and acylcarnitines retained on the cartridge were eluted with 3 ml of TEA–acetate (1.0 *M*, pH 7.0) in methanol.

As shown in Fig. 3, the NBD-ED adducts with carnitine and sixteen acylcarnitines were clearly separated within 45 min. The isomeric acylcarnitines such as isobutyryl- and butyryl-D,L-carnitine, isovaleryl- and valeryl-D,L-carnitine and valproyl- and octanoyl-D,L-carnitine were also clearly separated with faster retention times for the former acylcarnitines than for the latter. The detection limits for the NBD-ED adducts with carnitine and acylcarnitines were 100 fmol for carnitine and 10 fmol for stearoylcarnitine. The reproducibilities obtained in eight assays were 1.8–3.6, 1.6–4.4 and 1.6–3.2% (relative standard

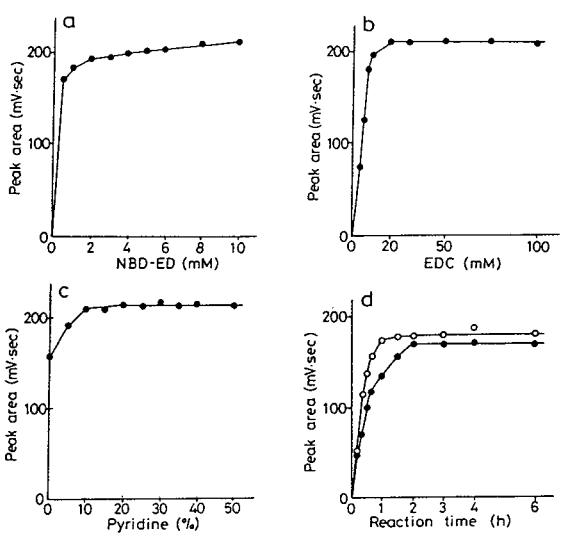

Fig. 2. Optimized reaction conditions for derivatization of carnitine with NBD-ED in the presence of EDC and pyridine. (a) Concentration of NBD-ED; (b) concentration of EDC; (c) concentration of pyridine; (d) reaction time course in acetonitrile and DMF. ● = DMF; ○ = acetonitrile.

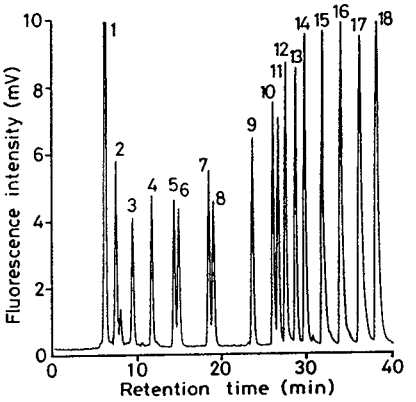

Fig. 3. Chromatogram of carnitine and acylcarnitines derivatized with NBD-ED. Carnitine and acylcarnitines (50 pmol each) were injected. HPLC conditions as described in the text. Peaks: 1 = NBD-ED; 2 = carnitine; 3 = acetylcarnitine; 4 = propionylcarnitine; 5 = isobutyrylcarnitine; 6 = butyrylcarnitine; 7 = isovalerylcarnitine; 8 = valerylcarnitine; 9 = hexanoylcarnitine; 10 = heptanoylcarnitine; 11 = valproylcarnitine; 12 = octanoylcarnitine; 13 = nonanoylcarnitine; 14 = decanoylcarnitine; 15 = lauroylcarnitine; 16 = myristoylcarnitine; 17 = palmitoylcarnitine; 18 = stearoylcarnitine.

deviations) for 25, 50 and 250 pmol of NBD-adducts with carnitine and sixteen acylcarnitines, respectively. Carnitine dicarboxylic acid esters such as glutarylcarnitine could not be eluted using the present HPLC conditions.

This method should be applicable to the simultaneous determination of carnitine and acylcarnitines in human urine and serum samples in combination with suitable pretreatment procedures [14–17].

References

[1] C.A. Stanley, *Adv. Pediatr.*, 34 (1987) 59.
[2] N. Siliprandi, L. Sartorelli, M. Ciman and F.D. Lisa, *Clin. Chim. Acta*, 183 (1989) 3.
[3] N. Takeyama, D. Takagi, K. Adachi and T. Tanaka, *Anal. Biochem.*, 158 (1986) 346.
[4] R.E. Dugan, M.J. Schmidt, G.E. Hoganson, J. Steele, B.A. Gilles and A.L. Shug, *Anal. Biochem.*, 160 (1987) 275.
[5] J. Kerner and L.L. Bieber, *Anal. Biochem.*, 134 (1983) 459.
[6] L.L. Bieber and J. Kerner, *Methods Enzymol.*, 123 (1986) 264.
[7] E. Schmidt-Sommerfeld, D. Penn, J. Kerner and L.L. Bieber, *Clin. Chim. Acta*, 181 (1989) 231.
[8] K. Kidouchi, N. Sugiyama, H. Morishita, Y. Wada, S. Nagai and J. Sakakibara, *J. Chromatogr.*, 423 (1987) 297.
[9] K. Kidouchi, T. Niwa, D. Nohara, K. Asai, N. Sugiyama, H. Morishita, M. Kobayashi and Y. Wada, *Clin. Chim. Acta*, 173 (1988) 263.
[10] A.L. Yergey, D.J. Liberato and D.S. Millington, *Anal. Biochem.*, 139 (1984) 278.
[11] D.S. Millington, D.L. Norwood, N. Kodo, C.R. Roe and F. Inoue, *Anal. Biochem.*, 180 (1989) 331.
[12] P.E. Minkler, S.T. Ingalls and C.L. Hoppel, *J. Chromatogr.*, 420 (1987) 385.
[13] M. Pourfarzam and K. Bartlett, *J. Chromatogr.*, 570 (1991) 253.
[14] A.K.M.J. Bhuiyan, S. Jackson, D.M. Turnbull, A. Aynsley-Green, J.V. Leonard and K. Bartlett, *Clin. Chim. Acta*, 207 (1992) 185.
[15] B.J.H.M. Poorthuis, T. Jille-Vlckova and W. Onkenhout, *Clin. Chim. Acta*, 216 (1993) 53.
[16] P.E. Minkler and C.L. Hoppel, *J. Chromatogr.*, 613 (1993) 203.
[17] P.E. Minkler and C.L. Hoppel, *Anal. Biochem.*, 212 (1993) 510.
[18] S. Lam and E. Grushka, *J. Chromatogr.*, 158 (1978) 207.
[19] J.B.F. Lloyd, *J. Chromatogr.*, 178 (1979) 249.
[20] W. Voelter, R. Huber and K. Zech, *J. Chromatogr.*, 217 (1981) 491.
[21] H. Tsuchiya, T. Hayashi, H. Naruse and N. Takagi, *J. Chromatogr.*, 234 (1982) 121.
[22] H. Tsuchiya, T. Hayashi, M. Sato, M. Tatsumi and N. Takagi, *J. Chromatogr.*, 309 (1984) 43.
[23] A. Takadate, T. Masuda, C. Tajima, C. Murata, M. Irikura and S. Goya, *Anal. Sci.*, 8 (1992) 663.
[24] S.A. Barker, J.A. Monti, S.T. Christian, F. Benington and R.D. Morin, *Anal. Biochem.*, 107 (1980) 116.
[25] N. Nimura and T. Kinoshita, *Anal. Lett.*, 13 (1980) 191.
[26] N. Nimura, T. Kinoshita, T. Yoshida, A. Uetake and C. Nakai, *Anal. Chem.*, 60 (1988) 2067.
[27] M. Yamaguchi, T. Iwata, K. Inoue, A. Hara and M. Nakamura, *Analyst*, 115 (1990) 1363.
[28] T. Iwata, M. Nakamura and M. Yamaguchi, *Anal. Sci.*, 8 (1992) 889.
[29] I. Yanagisawa, M. Yamane and T. Urayama, *J. Chromatogr.*, 345 (1985) 229.
[30] Y.M. Lee, H. Nakamura and T. Nakajima, *Anal. Sci.*, 5 (1989) 681.
[31] T. Toyo'oka, M. Ishibashi, Y. Takeda, N. Nakashima, S. Akiyama, S. Uzu and K. Imai, *J. Chromatogr.*, 558 (1991) 61.
[32] T. Toyo'oka, M. Ishibashi, Y. Takeda and K. Imai, *Analyst*, 116 (1991) 609.
[33] K. Matsumoto, M. Takahashi, N. Takiyama, H. Misaki, N. Matsuo, S. Murano and H. Yuki, *Clin. Chim. Acta*, 216 (1993) 135.
[34] T. Bohmer and J. Bremer, *Biochim. Biophys. Acta*, 152 (1968) 559.
[35] K. Imai, S. Uzu and T. Toyo'oka, *J. Pharm. Biomed. Anal.*, 7 (1989) 1395.

ELSEVIER

Journal of Chromatography A, 678 (1994) 249–257

JOURNAL OF CHROMATOGRAPHY A

Manipulation of ion-pairing reagents for reversed-phase high-performance liquid chromatographic separation of phosphorylated opioid peptides from their non-phosphorylated analogues

Chhabil Dass*, P. Mahalakshmi, Deidrea Grandberry[1]

The Charles B. Stout Neuroscience Mass Spectrometry Laboratory and Department of Neurology, University of Tennessee at Memphis, 956 Court Avenue, Memphis, TN 38163, USA

First received 25 February 1994; revised manuscript received 10 May 1994

Abstract

The use of reversed-phase high-performance liquid chromatography for the separation of a mixture of 14 phosphorylated and non-phosphorylated enkephalins is described. The influence of two homologous series of hydrophobic ion-pairing reagents, consisting of perfluorinated carboxylic (trifluoroacetic, pentafluoropropionic and hexafluorobutyric) acids and sodium salts of sulfonic (butane-, hexane- and heptane-) acids, on the retention of enkephalin peptides was investigated. The incorporation of the phosphate group reduces retention time in proportion with the resulting change in hydrophobicity of the peptide. All peptides exhibit increase in retention time with increase in the counter ion hydrophobicity. The increase is proportional to the number of positively charged groups present in a peptide. Phosphopeptides show small increases in retention times than their corresponding non-phospho derivatives. The near-neighbor effect of the Tyr–O–phosphate group is responsible for suppression of the ion-pairing interaction of the mobile phase counter ions with the positively charged terminal amino group of enkephalins.

1. Introduction

During their transport in the cell body, proteins undergo several covalent modifications, of which phosphorylation is the most important and ubiquitous. It serves as a mechanism to regulate the activity of many proteins, hormones and enzymes. Methionine enkephalin (MetEnk; YGGFM) and leucine enkephalin (LeuEnk; YGGFL) are neuropeptides that play a role in several biological processes, including nociception. Biochemically, they are synthesized in the cell body from a large precursor protein preproenkephalin A (ProEnk A), which also produces several C-terminally extended MetEnk and LeuEnk opioid peptides, including MetEnk–Lys (MetEnk-K), LeuEnk–Lys (LeuEnk-K), MetEnk–Arg (MetEnk-R), MetEnk–ArgPhe (MetEnk-RF) and MetEnk–ArgGlyLeu (Met-

* Corresponding author.

[1] An undergraduate summer fellow.

0021-9673/94/$07.00
SSDI 0021-9673(94)00453-G

Enk-RGL). It is important to know whether enkephalin peptides and their precursor molecules undergo phosphorylation at the tyrosine residue. However, before that question can be answered it is essential that an analytical method for their purification and separation is known.

Reversed-phase (RP) high-performance liquid chromatography (HPLC) has proven to be the most versatile method for rapid and effective separation of peptides and proteins and can be credited as a major contributing factor to advances made in several areas of peptide research, including synthesis and biomedical sciences. Selectivity in RP-HPLC analysis of peptides and proteins is achieved by exploiting the presence of free amino and carboxylic acid groups in those solutes. Previous researchers have shown that by taking advantage of the interaction of anionic and cationic counter ions present in the mobile phase with the amino and carboxylic groups of peptides, respectively, retention of peptides can be significantly altered. Typical additives used are perfluorinated carboxylic acids [1–4], alkylsulfonates [5–7], amine salts [8], tetraalkylammonium salts [4,7,9] perchloric acid [10] and phosphoric acid [5,11]. The incorporation of counter ions in the mobile phase has been a successful approach in isolation of several endogenous peptides from body tissues [4,12,13], in peptide mapping [14] and in preparative HPLC [3]; phosphorylated and non-phosphorylated forms of adrenocorticotropin (ACTH) [15] and corticotropic-like intermediate lobe peptide (CLIP) [16] have been resolved; and empirical sets of retention coefficients for amino acid residues have been developed [17–21], from which retention of peptides can be predicted [22].

As a first step in our quest for detection of the phosphorylation state of ProEnk A peptides, we report here the use of RP-HPLC for the analysis of Tyr–O–phosphate esters of the above listed enkephalins. The use of several perfluorinated carboxylic acids (trifluoroacetic, pentafluoropropionic and hexafluorobutyric) and sodium salts of sulfonic (butane-, hexane- and heptane-) acids as anionic ion-pairing reagents was exploited to effectively separate phosphorylated enkephalins from their non-phospho derivatives.

2. Experimental

2.1. Materials

All of the non-phosphorylated peptides were purchased from Sigma (St. Louis, MO, USA) except for MetEnk-R, which was obtained by trypsin digestion of MetEnk-RGL. The phosphorylated peptides were synthesized in our laboratory by solid-phase peptide synthesis protocol using 9-fluorenylmethoxycarbonyl (FMOC) chemistry, the details of which will be published elsewhere. They were purified by semi-preparative RP-HPLC. A further purification involved analytical RP-HPLC column. The purity of those synthetic peptides was checked by liquid secondary ionization mass spectrometry (LSI-MS).

Triethylamine was purchased from Pierce (Rockford, IL, USA), formic acid from Mallinckrodt (Paris, KY, USA), trifluoroacetic acid and heptafluorobutyric acid from Sigma, pentafluoropropionic acid and sodium salts of 1-butane-, 1-hexane- and 1-heptanesulfonic acids from Aldrich (Milwaukee, WI, USA) and acetic acid and acetonitrile from J.T. Baker (Phillipsburg, NJ, USA). All chemicals and solvents were of HPLC grade.

2.2. High-performance liquid chromatography

RP-HPLC was performed on an HP 1050 (Hewlett-Packard, CA, USA) instrument, consisting of a quaternary pumping system, a solvent degassing system, a Rheodyne 7125 manual injection valve, a photodiode-array based multiple-wavelength detector and an LC ChemStation data system. Samples were injected via a 20-μl sample loop onto a Vydac C_{18} analytical column (250 × 4.6 mm I.D. with 5 μm particle size and 300 Å pore size, purchased from Sigma fitted with PLRP-S guard column, containing poly(styrene–divinylbenzene) support (5 × 3 mm

I.D.; Polymer Labs., Amherst, MA, USA). Thus, two different column supports were used in tandem. The solvents were filtered through a 0.45-μm nylon-66 filter membrane (Pierce) and degassed by sparging with helium. The solvent reservoirs were maintained under helium atmosphere throughout the experiment. Chromatography was carried out at ambient temperatures with the mobile phase consisting of water–acetonitrile containing appropriate buffer and ion-pairing reagent flowing at 1.5 ml/min. The UV–visible multiple-wavelength detector was set at 200, 248 and 288 nm to monitor the absorbance due to the peptide bond, Tyr–O–phosphate and tyrosine residue, respectively. Water used was deionized in the laboratory, and was further purified by distillation using the Corning AG 11 system.

2.3. Ion-pairing reagents

The following seven ion-pairing reagent systems were studied: 0.1% trifluoroacetic acid (TFA), 0.1% pentafluoropropionic acid (PFPA), 0.1% heptafluorobutyric acid (HFBA), 0.1% sodium salts of butanesulfonic acid (BSA), hexanesulfonic acid (HxSA) and heptanesulfonic acid (HpSA) and triethylamine formate (TEAF; 0.04 *M* formic acid titrated with triethylamine to pH 3.12). The alkylsulfonates were dissolved in 0.02 *M* acetic acid to give a pH of 3.0.

3. Results

To understand the effect of ion-pairing reagents upon retention time in RP-HPLC, we studied a set of seven phosphorylated and the corresponding seven non-phosphorylated enkephalins. Those peptides, along with their sequence, the number of positive charges and the hydrophobicity/hydrophilicity indices, are listed in Table 1. A simple approach that uses the Bull and Breese (B and B) indices [23] for each individual amino acid is used to calculate the hydrophobicity/hydrophilicity index of a peptide. A more negative value of the B and B index reflects increased hydrophobicity. A num-

Table 1
Peptides studied

Peptide	Sequence of the peptide	Number of positively charged residues	Hydrophobicity/ hydrophilicity index (B and B index, cal/mol)
1	YGGFM	1	−398
1P	Y(P)GGFM	1	−268
2	YGGFL	1	−596
2P	Y(P)GGFL	1	−466
3	YGGFMK	2	−255
3P	Y(P)GGFMK	2	−147
4	YGGFLK	2	−420
4P	Y(P)GGFLK	2	−312
5	YGGFMR	2	−217
5P	Y(P)GGFMR	2	−109
6	YGGFMRF	2	−403
6P	Y(P)GGFMRF	2	−310
7	YGGFMRGL	2	−268
7P	Y(P)GGFMRGL	2	−187

Sequence is given in the single letter code: Y = tyrosine; G = glycine; F = phenylalanine; M = methionine; L = leucine; K = lysine; R = arginine; P in parentheses represents the phosphate group; the B and B index is calculated by adding the ΔF values (taken from ref. [23]) of individual amino acids and dividing the sum by the number of amino acids in the peptide; the contribution of the phosphate group ($\Delta F = +650$ cal/mol) is from ref. [31].

ber of other approaches have also been described in the literature to determine the overall hydrophobicity/hydrophilicity of a peptide [24–26]. The two homologous series of ion-pairing reagents (TFA, PFPA and HFBA and sodium salts of BSA, HxSA and HpSA) being used here are surface-active reagents and offer a range of gradually increasing hydrophobicity in a particular series.

The water–acetonitrile containing TFA as the ion-pairing reagent is the most commonly used RP-HPLC separation system for peptides and proteins because TFA offers the advantages of volatility, low UV transparency and excellent resolving power. Acetonitrile has been shown to be an excellent organic modifier for the analysis of peptides because it provides better resolution and selectivity than other common solvents such as 2-propanol and methanol [21]. The separation of a mixture of enkephalin peptides was first attempted using this system. A linear gradient, where acetonitrile content increased from 12% (at 0 min) at the rate of 0.5%/min, was found to give optimum separation of the complex mixture of 14 phosphorylated and non-phosphorylated enkephalin peptides; only phospho-MetEnk and phospho-LeuEnk-K coeluted under these conditions. The mobile phase contained 0.1% TFA to give pH 2.0. At this low pH, all carboxylic acids in a peptide are protonated and the positively charged amino groups are masked by the trifluoro group, increasing retention of the peptide via increased interaction with the hydrophobic stationary phase of the column. The effect of various other ion-pairing reagents mentioned above on the retention of those peptides was evaluated under the same chromatographic conditions except that the required amounts of those ion-pairing reagents were added to the mobile phase. As a typical example, the chromatogram obtained using the TFA ion-pairing system is shown in Fig. 1.

An aliquot (5 μl) of a mixture containing all of the 14 peptides (8–12 nmol/μl) was injected onto the RP-HPLC column. Fig. 2 is a pictorial depiction of relative retention times obtained using perfluorinated carboxylic acids (upper panel) and sodium alkylsulfonates (lower panel) as ion-pairing reagents. Each peak in the chromatogram was identified by analyzing separately mixtures of non-phosphorylated and phosphorylated enkephalin peptides. Sometimes to resolve ambiguity, individual peptides were injected. Recording of chromatogram at multiwavelengths also helped in identification of peaks. All non-phosphorylated peptides were easily distinguished in the mixture by monitoring the absorption at 288 nm, which is characteristic of tyrosine residue. Although no wavelength was found specific to the Tyr–O–phosphate group, that signal was recorded at 248 nm.

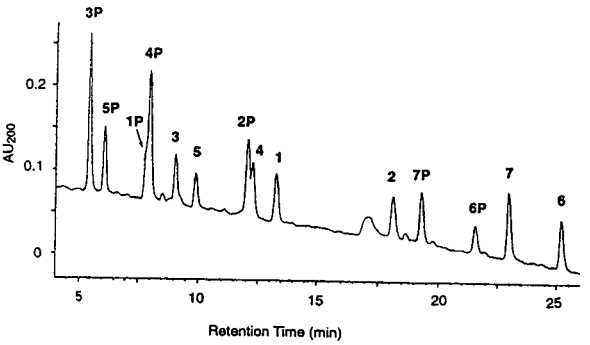

Fig. 1. A typical chromatogram of a mixture of 14 phosphorylated and non-phosphorylated enkephalin peptides. Mobile phase, water–acetonitrile containing 0.1% TFA; gradient, linear from 12% acetonitrile at 0 min to 32% at 40 min. The injection volume was 5 μl and contained 8–12 nmol/μl of each peptide. See Table 1 for peak identification.

With the above linear gradient, a clear separation of some of the peptides was not achieved in the TFA and HFBA systems, whereas the PFPA system completely resolved all of the 14 peptides under the same elution conditions. To obtain a baseline separation in the TFA and HFBA systems, a non-linear gradient was developed and the following gradient was found to provide optimum separations in both the systems: 12–20% acetonitrile, 0–18 min; 20–35% acetonitrile, 18–30 min; 35% acetonitrile, 30–40 min. Similarly, the above linear gradient was adequate to provide separation of all of the 14 peptides in the BSA and HpSA systems, whereas in the HxSA system all but LeuEnk and phospho-MetEnk-RGL were well resolved. In this system, the following non-linear gradient provided a clean separation of all of the peptides studied here: 12–18% acetonitrile, 0–12 min;

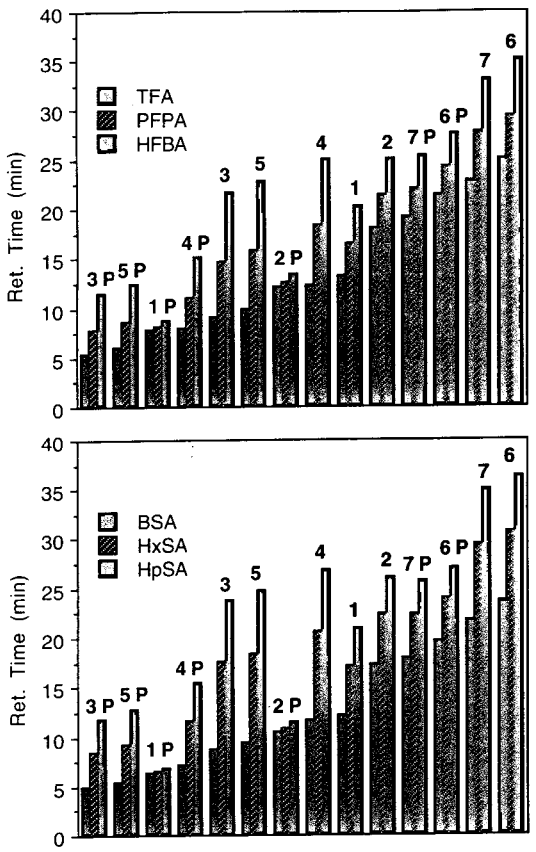

Fig. 2. Graphical representation of relative retention times of 14 phosphorylated and non-phosphorylated enkephalin peptides obtained using perfluorinated carboxylic acids (upper panel) and sodium salts of sulfonic acids (lower panel) as ion-pairing reagents under linear gradient conditions.

18–22% acetonitrile, 12–30 min; 22–35% acetonitrile, 30–35 min; 35% acetonitrile, 35–40 min.

The water–acetonitrile buffered by TEAF (pH 3.1) is frequently used in our laboratory for separation of neuropeptides from tissue extracts [27]. Similar to perfluorinated carboxylic acids, TEAF is also volatile. TEA is a weak hydrophobic ion-pairing reagent. This system was also tested for separation of phospho and non-phospho enkephalins. The following gradient of acetonitrile was found to resolve all of the 14 components of the mixture: 0–10 min, 10%; 10–20 min, 15%; 20–30 min, 15–30%; 30–40 min, 30%. The presence of a peptide in a biological extract is confirmed only when the amino acid sequence of that peptide is demonstrated. Therefore, our research uses MS as a highly specific post-column detector for analysis of peptides because it provides a precise knowledge of the molecular mass and amino acid sequence of the peptide [12,27]. However, it was found that the TEAF system may not be appropriate for MS analysis of phosphopeptides because the phosphate group is known to form adducts with TEA [28]. LSI-MS mass spectra of the lyophilized fractions of phosphopeptides also confirmed that, in addition to the usual $(M+H)^+$ ions of phosphopeptides, monoadducts with TEA are also formed.

4. Discussion

Peptides are polar molecules and contain both hydrophobic (leucine, methionine, phenylalanine, tyrosine, etc.) and hydrophilic (aspartic, glutamic, lysine, arginine, etc.) amino acids. The predominant factor involved in separation of peptides by RP-HPLC is the hydrophobic interaction between the non-polar hydrocarbonaceous matrix of the column material and the hydrophobic groups of the peptide. At any given pH, the RP-HPLC behavior of a peptide is determined by the relative contribution of hydrophobic and hydrophilic amino acids [17–22]. In the case of phosphorylated peptides, the polar phosphate group also contributes to hydrophilicity. Peptides with hydrophobic side chains are preferentially retained on the column material. Therefore, relatively hydrophilic peptides elute earlier with aqueous mobile phase, whereas those strongly retained hydrophobic peptides require increasing concentrations of an organic modifier in the mobile phase.

This initial behavior, however, can be altered by the addition of a suitable ion-pairing reagent [1–11]. Because peptides are charged molecules they form complexes with the auxiliary ions added to the solvent system; the anionic counter ions bind to the positively charged amino groups and the cationic ions bind to the negatively charged acidic groups. The ion-pair complex of a

peptide with the hydrophobic counter ions results in increased affinity of the peptide with the column, whereas the complex with the hydrophilic counter ions reduces that interaction [29]. In addition to the surface adsorption, the dynamic ion exchange can also play a role in determining retention of a solute on the RP-HPLC column [30]. Recently, Patthy [30] has shown that separation of small peptides, amines and acidic compounds in the TFA system is solely governed by surface adsorption, whereas in the HFBA system dynamic ion exchange is an important factor.

4.1. Perfluorinated carboxylic acids

The effect of hydrophobicity of amino acids on retention of peptides

From the data in Fig. 2, it is obvious that the hydrophobicity of peptides has a profound influence on their retention time in perfluorinated carboxylic acid systems. For example, amongst the pentapeptides, LeuEnk (B and B = −596 cal/mol; 1 cal = 4.184 J) elutes later than MetEnk (B and B = −398 cal/mol). All hexapeptides contain an additional hydrophilic basic amino group, and thus elute earlier than MetEnk and LeuEnk. MetEnk-RF and MetEnk-RGL also contain a basic amino acid but are retained more than the hexapeptides mainly due to the presence of additional hydrophobic amino acids (Phe and Leu, respectively). As expected, all phospho derivatives elute earlier than their non-phospho counterparts; the polar phosphate group contributes +650 cal/mol towards the hydrophobicity/hydrophilicity index of a peptide [31].

These observations are consistent with the findings of Guo and co-workers [21,22], who pointed out that RP-HPLC retention of peptides can be correlated with the summated relative retention coefficients of each amino acid residues. Under those experimental conditions, retention time of a peptide can be predicted from its amino acid composition. On the basis of the relative coefficients of each amino acids determined by them [21], MetEnK should elute earlier than LeuEnk, Metenk-K earlier than MetEnk-R and MetEnk-RGL earlier than MetEnk-RF; a similar retention behavior is noted in the present study.

The effect of hydrophobicity of ion-pairing reagents on retention of peptides

From Fig. 2, it is also obvious that retention of peptides of interest here can be significantly modified by the addition of various anionic reagents to the mobile phase. Fig. 3 is a plot of retention time versus length of the alkyl chain in the ion-pairing reagents; the latter is a direct measure of the hydrophobicity of the anionic counter ion. To avoid cluttering, the data for non-phosphorylated (Fig. 3A) and phosphorylated peptides (Fig. 3B) are plotted separately. Those plots illustrate a linear increase in retention time with increasing length of the alkyl

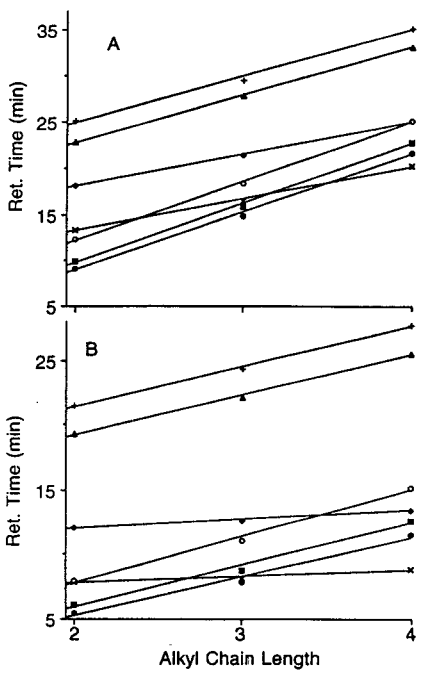

Fig. 3. Effect of counter ion hydrophobicity on the retention of enkephalin peptides, when TFA, PFPA and HFBA are used as the mobile phase additives. (A) Non-phospho enkephalins: × = MetEnk; ◆ = LeuEnk; ● = MetEnk-K; ○ = LeuEnk-K; ■ = MetEnk-R; + = MetEnk-RF; ▲ = MetEnk-RGL; (B) corresponding phospho derivatives.

chain, demonstrating clearly the effect of the hydrophobicity of the counter ions on retention of peptides. In view of the findings of Patthy [30], it is likely that dynamic ion exchange plays an increasing role in determining the retention of peptides when longer-chain perfluorinated carboxylic acid solvent systems are used.

As observed by Guo et al. [29], the magnitude of increase in retention time also depends upon the number of positively charged residues in peptides. For example, non-phosphopeptides that contain basic amino acid residues Arg or Lys show almost twice the increase in retention compared to MetEnk and LeuEnk; the slopes of the plots for peptides MetEnk-K, LeuEnk-K, and MetEnk-R vary from 6.34 to 6.51 and for peptides MetEnk-RF and MetEnk-RGL from 5.04 to 5.14, whereas the corresponding slope for pentapeptides is ca. 3.50.

In contrast, phospho-MetEnk and -LeuEnk show only a marginal change in retention time in moving from TFA to HFBA system; the slopes of their retention time versus counter ion hydrophobicity plots are 0.49 and 0.68, respectively. Similarly, the increase in retention time for other phosphopeptides is not as significant as with their non-phospho analogues. As a result, the elution order of peptides changes in progressing from TFA to HFBA. For example, phospho-MetEnk-K and -MetEnk-R both elute earlier than phospho-MetEnk in the TFA system, whereas in the HFBA system they elute after phospho-MetEnk.

The probable reason for the intriguing behavior for phosphopeptides is that the phosphate group is located in close proximity to the terminal amino group and as a result offers steric hindrance for the ion-pairing interaction of the counter ions with that amino group. Phospho-MetEnk and -LeuEnk behave as if no basic group is present. Likewise, the phosphorylated hexapeptides behave as if they contain only one basic amino acid. Fig. 4 demonstrates that the magnitude of the slope of the plot of retention time versus the counter ion hydrophobicity for these three phosphopeptides is nearly identical to that obtained for MetEnk and LeuEnk, in which the only positively charged site is the N-terminal amino group.

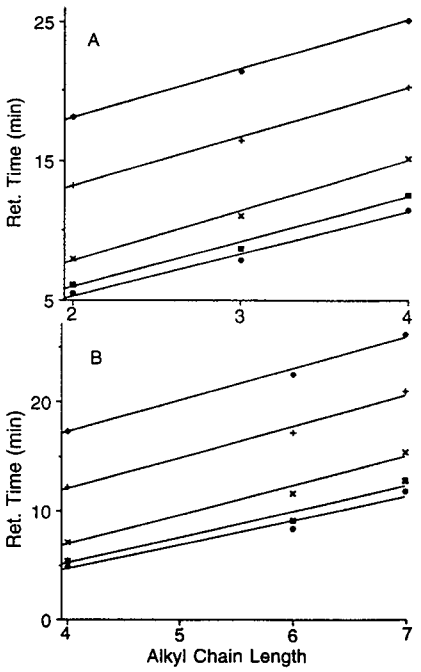

Fig. 4. Graphical representation of the near-neighbor effect on ion-pair interaction. The counter ion hydrophobicity vs. retention time curves for (O) phospho-MetEnk-K, (□) phospho-MetEnk-R and (×) phospho-LeuEnk-K are nearly parallel with those of (+) MetEnk and (◆) LeuEnk, indicating that phosphorylation of the N-terminal tyrosine suppresses the ion-pair interaction with the terminal amino group. (A) Perfluorinated carboxylic acids, (B) sodium salts of sulfonic acids.

The effect of phosphate group on the retention of peptides

The polar phosphate group also influences retention of enkephalin peptides. With the introduction of the phosphate group, the hydrophobic character of a peptide is reduced. Consequently, the interaction between a peptide and the hydrophobic sites on the HPLC column is diminished, resulting in early elution of the phosphopeptides. Introduction of a phosphate group produces a change in the hydrophobicity index of −130.0, −108.3, −92.9 and −81.2 cal/mol for penta-, hexa-, hepta- and octapeptides, respectively. The change in retention time upon phosphorylation is also roughly proportional to the resulting change in hydrophobicity. This aspect is demonstrated in

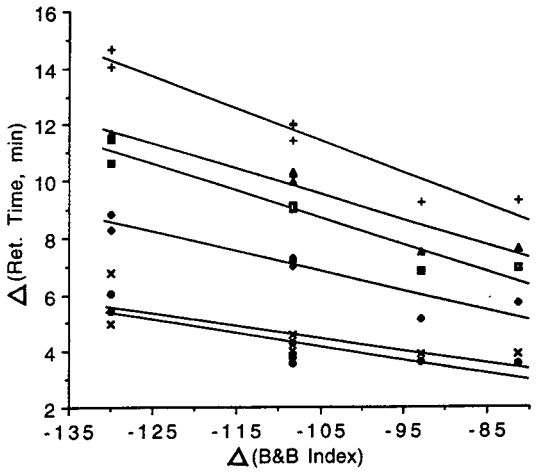

Fig. 5. Effect of phosphorylation on the retention of enkephalin peptides; the decrease in retention time is approximately linear with decrease in hydrophobicity of the peptide. ○ = TFA; ◆ = PFPA; ▲ = HFBA; × = BSA; □ = HxSA; + = HpSA.

Fig. 5. An approximately linear relation is observed between change in retention time and change in hydrophobicity for the ion-pairing systems used here.

4.2. Alkylsulfonates

The RP-HPLC elution profile of phospho and non-phospho enkephalin peptides in the alkylsulfonate solvent system is also parallel to the perfluorinated carboxylic acids solvent system. The hydrophilic peptides elute earlier than peptides with the hydrophobic character (Fig. 2), the increase in retention in progressing from butanesulfonate to heptanesulfonate system is proportional to the hydrophobicity of the counter ion (Fig. 6), and decrease in retention upon phosphorylation is commensurate with the decrease in the hydrophobicity (Fig. 5).

Thus, this study has demonstrated that RP-HPLC can be effectively used to separate phosphorylated and non-phosphorylated enkephalin peptides by either manipulation of the gradient or by changing the ion-pairing system. Although parallel results were obtained with the perfluorinated carboxylic acids and alkylsulfonates, the former system offers advantages because of

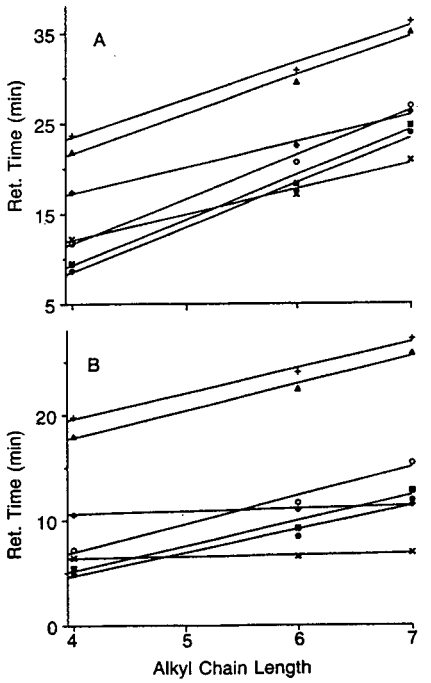

Fig. 6. Effect of counter ion hydrophobicity on retention time of enkephalin peptides, when BSA, HxSA and HpSA are used as the mobile phase additives. (A) Non-phospho enkephalins: × = MetEnk; ◆ = LeuEnk; ○ = MetEnk-K; ○ = LeuEnk-K; □ = MetEnk-R; + = MetEnk-RF; ▲ = MetEnk-RGL; (B) corresponding phospho derivatives.

volatility of the ion-pairing reagents. A volatile reagent does not interfere in the post-column detection of peptides by radioimmunoassay and MS, the two most commonly used detectors by us for analysis of peptides.

Acknowledgement

The research was supported by the grant (NS 28025) from the National Institutes of Health.

References

[1] W.M.M. Schaaper, D. Voskamp and C. Olieman, *J. Chromatogr.*, 195 (1980) 181.
[2] H.P.J. Bennett, C.A. Browne and S. Solomon, *J. Liq. Chromatogr.*, 3 (1980) 1353.

[3] H.P.J. Bennett, *J. Chromatogr.*, 266 (1983) 501.
[4] D.R.K. Harding, C.A. Bishop, M.F. Tarttellin and W.S. Hancock, *Int. J. Peptide Protein Res.*, 18 (1981) 214.
[5] W.S. Hancock, C.A. Bishop, L.J. Meyer, D.R.K. Harding and M.T.W. Hearn, *J. Chromatogr.*, 161 (1978) 291.
[6] E. Spindel, D. Pettibone, L. Fisher, J. Fernstrom and R. Wurtman, *J. Chromatogr.*, 222 (1981) 381.
[7] Z. Iskandarini, R.L. Smith and D.J. Pietrzyk, *J. Liq. Chromatogr.*, 7 (1984) 111.
[8] J.E. Rivier, *J. Liq. Chromatogr.*, 1 (1978) 342.
[9] W.S. Hancock, C.A. Bishop, J.E. Battersby, D.R.K. Harding and M.T.W. Hearn, *J. Chromatogr.*, 168 (1979) 377.
[10] M. Rubenstein, *Anal. Biochem.*, 98 (1979) 1.
[11] W.S. Hancock, C.A. Bishop, R.L. Prestidge, D.R.K. Harding and M.T.W. Hearn, *Science (Washington, D.C.)*, 200 (1089) 1168.
[12] D.M. Desiderio, J.J. Kusmierz, X. Zhu, C. Dass, D. Hilton, J.T. Robinson and H.S. Sacks, *Biol. Mass Spectrom.*, 22 (1993) 89.
[13] A.W. Burgess, J. Knesel, L.G. Sparrow, N.A. Nicola and E.C. Nice, *Proc. Natl. Acad. Sci. U.S.A.*, 79 (1982) 5753.
[14] J.D. Hockenhull-Johnson, M.S. Stern, P. Martin, C. Dass, D.M. Desiderio, J.B. Wittenberg, S.N. Vinogradov and D.A. Walz, *J. Protein Chem.*, 10 (1991) 609.
[15] H.P.J. Bennett, C.A. Browne and S. Solomon, *Biochemistry*, 20 (1981) 4530.
[16] C.A. Browne, H.P.J. Bennett and S. Solomon, *Biochemistry*, 20 (1981) 4538.
[17] J.L. Meek and Z.L. Rossetti, *J. Chromatogr.*, 211 (1981) 15.
[18] S.J. Su, B. Grego, B. Niven and M.T.W. Hearn, *J. Liq. Chromatogr.*, 4 (1981) 1745.
[19] C.A. Browne, H.P.J. Bennett and S. Solomon, *Anal. Biochem.*, 124 (1982) 201.
[20] T. Sasagawa, T. Okuyama and D.C. Teller, *J. Chromatogr.*, 240 (1982) 329.
[21] D. Guo, C.T. Mant, A.K. Taneja, J.M.R. Parker and R.S. Hodges, *J. Chromatogr.*, 359 (1986) 499.
[22] D. Guo, C.T. Mant, A.K. Taneja and R.S. Hodges, *J. Chromatogr.*, 359 (1986) 519.
[23] H.B. Bull and K. Breese, *Arch. Biochem. Biophys.*, 161 (1974) 665.
[24] J. Kyte and R.F. Doolittle, *J. Mol. Biol.*, 157 (1982) 105.
[25] D. Eisenberg and A.D. McLachlan, *Nature*, 319 (1986) 199.
[26] J.L. Cornette, K.B. Cease, H. Margalit, J.L. Spouge, J.A. Berzofsky and C. DeLisi, *J. Mol. Biol.*, 195 (1987) 659.
[27] C. Dass, G.H. Fridland, P.W. Tinsley, J.T. Killmar and D.M. Desiderio, *Int. J. Peptide Protein Res.*, 34 (1989) 81.
[28] G. Zardeneta, D. Chen., S.T. Weintraub and R.J. Klebe, *Anal. Biochem.*, 190 (1990) 340.
[29] D. Guo, C.T. Mant and R.S. Hodges, *J. Chromatogr.*, 386 (1987) 205.
[30] M. Patthy, *J. Chromatogr.*, 660 (1994) 17.
[31] L. Poulter, S.G. Ang, D.H. Williams and P. Cohen, *Biochim. Biophys. Acta*, 929 (1987) 296.

ELSEVIER

Journal of Chromatography A, 678 (1994) 259–263

JOURNAL OF CHROMATOGRAPHY A

Separation of 3-hydroxy-3-methylglutaryl-coenzyme A reductase inhibitor drug substance diastereomers, and their analogues on β-cyclodextrin stationary phase

Narendra Kumar[a,*], Vincent Windisch[a], Pravin Trivedi[a], Chris Golebiowski[b]

[a]*Department of Analytical and Physical Chemistry, Rhône-Poulenc Rorer Central Research, 500 Arcola Road, P.O. Box 1200 Collegeville, PA 19426-0107, USA*

[b]*Burroughs Wellcome, P.O. Box 1887, Greenville, NC 27834, USA*

First received 7 March 1994; revised manuscript received 8 April 1994

Abstract

β-Cyclodextrin stationary phases are extremely useful in the separation of complex diastereomeric mixtures under normal-phase chromatographic conditions. The retention behavior of the 3-hydroxy-3-methylglutaryl (HMG)-coenzyme A reductase inhibitor drug substances (I–IV) is influenced by the size and chain length of the polar alcohol modifier. Retention time changes caused by different alcohol modifiers can be explained by hydrogen bonding and steric effects involving the stationary phase, the analyte and the alcohol modifier.

1. Introduction

The utility of cyclodextrin stationary phases as chromatographic chiral selectors in the separation of enantiomers is well established [1–6]. In the reversed-phase mode of chromatography, the mechanism of chiral separation afforded by the cyclodextrin stationary phase is believed to involve the formation of an inclusion complex between the chiral analyte and the hydrophobic cavity of the cyclodextrin molecule [6,7]. This phenomenon of cavity inclusion complexation by cyclodextrins is not limited to its application as chiral separation agent. Recently, this property of cyclodextrins has become increasingly popular in enhancing the aqueous solubility, bioavailability, and stability of pharmaceutical drug substances [8,9]. In the reversed-phase mode of chromatography, the hydroxyl groups on the outer side of the cyclodextrin molecules play an important role by providing hydrogen-bonding controlled stabilization of the inclusion complex. In the normal-phase mode of chromatography employing a non-polar hydrocarbon solvent, the hydrophobic cavity of the cyclodextrin molecules is occupied by the non-polar solvent molecules, and this cyclodextrin–hydrocarbon complex offers a unique environment consisting of primary and secondary hydroxyl groups and ether oxygen atoms. β-Cyclodextrin has a C-7 symmetry axis and 14 hydroxyl groups situated about the mouth of the cavity. Seven of these are at the C-2 carbon of the glucose and orient in the clockwise direction, while those at C-3 position are anticlockwise. The opposite rim of the cavity has seven primary hydroxyl groups. The potential of

* Corresponding author.

0021-9673/94/$07.00
SSDI 0021-9673(94)00341-6

three types of functionalities in providing interactions with compounds possessing hydrogen bonding sites for unique chromatographic selectivities appears very attractive.

We have studied the utility of cyclodextrin stationary phases in the normal-phase mode of chromatography in the separation of a complex mixture of diastereomers of our HMG-coenzyme A (CoA) reductase inhibitor drug substance (RG 12561) and related compounds. Preclinical as well as clinical studies show that RG 12561, [4α,6β(*E*)]-(±)-6-[2-[2-(4-fluoro-3-methylphenyl)-4,4,6,6-tetramethyl-1-cyclohexen-1-yl)-ethynyl]tetrahydro-4-hydroxy-2H-pyran-2-one (I, Fig. 1) is an effective and potent HMG-CoA reductase inhibitor and hypocholesterolemic agent. RG 12561 possesses the β-hydroxy-4-lactoneethylenic moiety deemed necessary for the activity and present in the naturally occurring substances of this class. The drug substance RG 12561 is prodrug for the corresponding open-chain dihydroxy acid (IV, Fig. 1). Synthesis of RG 12561 involves stereospecific reduction of the hydroxyketo ester X or XI (Fig. 1) to produce the corresponding *syn*-dihydroxy esters VI and VIII, respectively, followed by de-esterification to the free acid (IV, Fig. 1) and lactonization. Under non-ideal conditions of reduction of the above two esters, the corresponding anti-dihydroxy esters (VII, IX, Fig. 1) could be formed. Also, the lactones I and II could be labile to hydrolytic and transesterification conditions and produce diastereomeric free acids IV and V, respectively, or the corresponding esters VI and VII, as the case may be. The formation of the product III is also observed under dehydration conditions. Development of RG 12561 required a chromatographic method which was capable of providing separation of the above diastereomeric compounds and III in one chromatographic run.

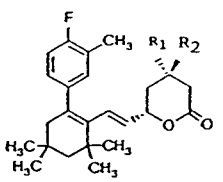

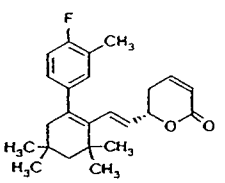

(I) R2 = OH, R1 = H, RG 12561
(II) R2 = H, R1 = OH

(III)

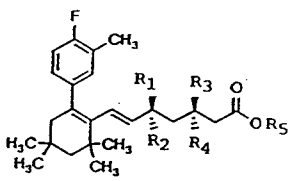

(IV) R1 = R3 = OH, R2 = R4 = R5 = H
(V) R1 = R4 = OH, R2 = R3 = R5 = H
(VI) R1 = R3 = OH, R2 = R4 = H, R5 = CH3
(VII) R1 = R4 = OH, R2 = R3 = H, R5 = CH3
(VIII) R1 = R3 = OH, R2 = R4 = H, R5 = t-Bu
(IX) R1 = R4 = OH, R2 = R3 = H, R5 = t-Bu
(X) R1 = OH, R2 = H, R3,R4 = O, R5 = CH3
(XI) R1 = OH, R2 = H, R3,R4 = O, R5 = t-Bu

Fig. 1. Structures of RG 12561, its stereoisomers and related compounds. t = *tert.*

2. Experimental

2.1. Chemicals

The drug substance RG 12561 and related compounds II–IX were synthesized by the Process Research Department at Rhône-Poulenc Rorer Central Research, Collegeville, PA, USA. HPLC-grade hexane, methylene chloride, isopropanol and trifluoroacetic acid and reagent-grade *n*-propanol, *n*-butanol, *tert.*-butanol and *tert.*-amyl alcohol were obtained from Fisher Scientific (Fair Lawn, NJ, USA). 2-Butanol was purchased from EM Science (Gibbstown, NJ, USA). 2-Pentanol was purchased from Aldrich (Milwaukee, WI, USA). Dioxane, analyzed reagent grade, was obtained from J.T. Baker (Phillipsburg, NJ, USA). Quantum Chemical (Tuscola, IL, USA) supplied ethanol, 200-proof dehydrated alcohol, USP.

2.2. Equipment

An HPLC pump (Spectra-Physics 8800 solvent-delivery system), an autosampler (Spectra-Physics 8800 Autoinjector) and a variable-wavelength UV detector (Spectra-Physics Forward optical scanning detector) were used. Data ac-

quisition was done with an integrator/computer (IBM PS/2 Model 70 equipped with Spectra Focus software). Other equivalent equipment, along with Waters Chromatography ExpertEase software, was also used.

2.3. Chromatographic conditions

The primary mobile phase consisted of hexane–ethanol (96:4, v/v; equivalent to 0.682 *M* ethanol) containing 0.1% (v/v) trifluoroacetic acid. Other mobile phases were prepared by mixing hexane and different alcohols at 0.682 *M* concentration and adding 0.1% (v/v) trifluoroacetic acid. The flow-rate was 2.0 ml/min. In a typical analysis, a 20-μl volume of the sample solution was injected into two serially linked Cyclobond I columns, each 250 × 4.6 mm I.D., 5 μm particle size (Advanced Separation Technologies, Whippany, NJ, USA). Detection was performed by a UV detector set at 245 nm. Retention characteristics measured as capacity factors (k') were computed from the equation $k' = t_R - t_0/t_0$, where t_R and t_0 are retention times of retained and unretained compounds, respectively. Methylene chloride was injected as a measure of the unretained compound.

2.4. Standard and sample preparations

Solutions of RG 12561 and related compounds were prepared in a diluent consisting of hexane–*tert.*-butanol (95:5, v/v). For the linearity study, a set of solutions of RG 12561 of concentrations 0.54, 0.79, 1.06, 1.25 and 1.53 mg/ml which range from approximately 50 to 150% of the target assay concentration of 1.0 mg/ml were prepared. To determine system precision of the method, a standard solution of 0.97 mg/ml was used. Method precision was determined using six solutions of concentrations ranging from 0.88 to 0.92 mg/ml. In order to study retention characteristics and the separation mechanism of four diastereomers on the Cyclobond I column using different polar alcohol modifiers in the mobile phase, a 1.0 mg/ml solution of RG 12561 containing approximately 0.1 mg/ml each of II (RG 12841), IV (RG 12839) and V (RG 14100) were prepared.

3. Results and discussion

Attempts to achieve the separation of compounds I–XI (Fig. 1), which include four diastereomeric pairs, under reversed-phase conditions of chromatography employing a variety of stationary phases met with difficulties due to partial or no separation of the above compounds. Use of two serially linked β-cyclodextrin columns in the normal-phase mode of chromatography employing a mobile phase consisting of hexane–ethanol containing 0.1% of trifluoroacetic acid produced the desired separation. A chromatogram showing the separation of related compounds, including four diastereomer pairs and compound III is depicted in Fig. 2. The capacity factors of these compounds under these

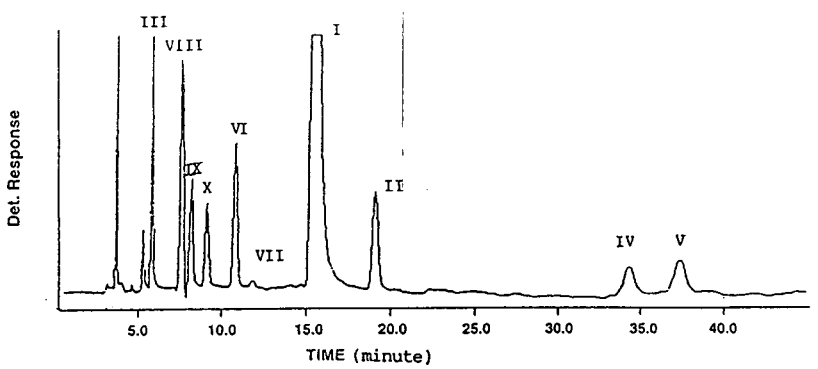

Fig. 2. HPLC Chromatogram of RG 12561 and related substances.

Table 1
Effect of alcohol modifiers on the retention times and capacity factors of RG 12561 and related compounds

Alcohol	Compounds							
	RG 12561 (I)		RG 12841 (II)		RG 12839 (IV)		RG 14100 (V)	
	t_R	k'	t_R	k'	t_R	k'	t_R	k'
Primary alcohols								
CH_3–CH_2–OH	16.39	4.6	20.28	5.9	35.54	11.1	38.96	12.3
CH_3–CH_2–CH_2–OH	15.05	4.0	18.53	5.2	30.46	9.2	32.95	10.0
CH_3–CH_2–CH_2–CH_2–OH	15.20	4.1	18.97	5.3	26.99	8.0	29.70	8.9
CH_3–CH_2–CH_2–CH_2–CH_2–OH	14.66	3.9	18.35	5.1	29.65	8.9	32.00	9.7
Secondary alcohols								
CH_3–CH(OH)–CH_3	16.94	4.6	21.15	6.0	29.36	8.8	32.53	9.8
CH_3–CH_2–CH(OH)–CH_3	18.62	5.7	23.80	7.6	29.96	9.8	33.47	11.0
CH_3–CH_2–CH_2–CH(OH)–CH_3	19.24	5.8	25.19	7.9	28.71	9.1	31.99	10.3
Tertiary alcohols								
$(CH_3)_3$–C–OH	23.36	7.0	30.89	9.6	31.72	9.9	34.92	11.0
$(CH_3)_2$–C(OH)–CH_2–CH_3	24.38	7.3	32.38	9.9	29.62	9.0	33.81	10.5

conditions of chromatography are listed in Table 1. Under the conditions described in this method, the two dihydroxy acids showed relatively large retention times. Validation studies were carried out with respect to RG 12561 (I). The method provided satisfactory validation parameters for quantitative use of the method. The validation data are summarized in Table 2. A linearity study was performed using five solutions of concentration ranging from 50 to 150% of the target concentration of 1.0 mg/ml. The correlation coefficient of the fitted line was 0.99999. System precision of six injections of a standard solution of 0.97 mg/ml concentration had an R.S.D. of 0.9%. Method precision determined for six different sample preparations ranging in concentration from 0.88 to 0.95 mg/ml showed an R.S.D. of 1.2%. Recovery studies were performed at nine levels of concentration covering the range of 50–150% of target assay concentration of 1.0 mg/ml. The mean recovery was 100.4% with an R.S.D. of 0.8%. The limit of detection of the method as determined by a signal-to-noise ratio of 3 was found to be 2 ng on column.

Compounds IV and V have three protic functional groups capable of hydrogen bonding. They are retained longer than the lactones. The retention of the anti-dihydroxy acid V is greater than the *syn*-diastereomer IV in all the mobile phase systems examined in this study. Intramolecular hydrogen bonding in the latter could possibly compete with the hydrogen-bonding interactions with the stationary phase. We

Table 2
Method validation data for RG 12561 (I)

Linearity	r (n = 5): 0.99999
Instrument precision	R.S.D. (n = 6): 0.9%
Method precision	R.S.D. (n = 6): 1.3%
Recovery	Mean assay (n = 9): 100.4%
	R.S.D. (n = 9): 0.8%
Limit of detection (RG 12561)	2 ng on column (signal/noise ratio = 3)

investigated the effect of chain length and steric bulk of the alcohol modifier on the retention times and capacity factors of the four key compounds, the lactones I and II, and their corresponding free acids IV and V. On increasing the chain length of the alcohol modifier from ethanol to *n*-butanol, the retention of the dihydroxy acids IV and V diminishes. Increase in the chain length is expected to increase the hydrophobic character of the hydrogen bonded complex including the protic groups of IV and V and the alcohol. The effect reverses with *n*-pentanol which provides retention greater than *n*-butanol for compounds IV and V. Possible inclusion of the long hydrophobic chain of *n*-pentanol in the cyclodextrin cavity and diminished efficiency of hydrogen bonding between the analyte and multiple *n*-pentanol molecules may be responsible for this reversal. The changes in retention times of the lactones I and II with the increasing alcohol chain length are relatively smaller. Among the homologous secondary and tertiary alcohols, the effect of increase of the carbon chain length of the alcohols on the retention times of IV and V is very small, but the lactones I and II show significant retention increases.

3.1. Effect of increase in the steric bulk of alcohols

On going from the straight-chain alcohols to their branched-chain isomers, the behavior of the acids IV and V and the lactones I and II is reversed. The branching has little influence on the retention times of IV and V but the retention times of the lactones I and II show a marked increase in propanol, butanol and pentanol series. In I and II, the hydrogen bonding with the first bulkier alcohol molecule may diminish the possibility of further hydrogen bonding due to steric hindrances. On the other hand, the dihydroxy acids IV and V have a much more flexible open chain. The inhibition of multiple hydrogen bonding due to steric crowding is expected to be relatively smaller.

The use of dioxane as the polar modifier resulted in the large retention of all of the compounds. Hydrogen-bonded interaction between the analyte, protic modifiers and cyclodextrin hydroxyl groups play a key role in the retention behavior of the analyte. In the absence of protic functionality in the mobile phase with dioxane, a large retention on the hydroxylic stationary phase is expected.

4. Conclusions

β-Cyclodextrin provides an excellent stationary phase for the normal-phase chromatographic separation of diastereomers possessing hydrogen-bonding sites. The separation mechanism appears to be dominated by the hydrogen-bonded interactions of the analyte with the cyclodextrin and the alcohol modifiers.

Acknowledgement

The authors thank Dr. F. DeLuccia for his valuable comments and Dr. L. Reilly and Dr. S. Golec for supplying material used in this study.

References

[1] D.W. Armstrong, W. Demond, A. Alak, W.L. Hinze, T.E. Riehl and K.H. Bui, *Anal. Chem.*, 57 (1985) 234.
[2] K. Vekama, F. Hirayama, K. Ikeda and K. Inaba, *J. Pharm. Sci.*, 66 (1977) 706.
[3] M. Gazdag, G. Szepesi and L. Huszar, *J. Chromatogr.*, 351 (1986) 128.
[4] M. Gazdag, G. Szepesi and L. Huszar, *J. Chromatogr.*, 371 (1986) 227.
[5] M. Gazdag, G. Szepesi and K. Mihalyfi, *J. Chromatogr.*, 436 (1988) 381.
[6] J. Zukowski, D. Sybilska, J. Bojarski and J. Szejtli, *J. Chromatogr.*, 436 (1988) 381.
[7] D.W. Armstrong, A. Alak, W. DeMond, W.L. Hinze and T.E. Riel, *J. Liq. Chromatogr.*, 8 (1985) 261.
[8] F. Liu, D.O. Kildsing and A.K. Mitna, *Pharm. Res.*, 7 (1990) 869.
[9] J.M.E.L. Hage Chaline, J.P. Bertingny and M.A. Schwaller, *J. Chem. Soc., Perkin Trans. II*, 6 (1989) 629.

ELSEVIER

Journal of Chromatography A, 678 (1994) 265–277

JOURNAL OF CHROMATOGRAPHY A

Quantitative aspects of a valve-based, multi-stage multidimensional gas chromatography–infrared spectroscopy–mass spectrometry system

Kevin A. Krock, Charles L. Wilkins*

Department of Chemistry, University of California, Riverside, Riverside, CA 92521-0403, USA

Received 27 April 1994

Abstract

Use of high-resolution capillary gas chromatography coupled with infrared and mass spectral detectors is a very powerful qualitative analytical technique. However, accurate qualitative analyses with spectroscopic detection requires that the separation system provide the detectors with pure components. Unfortunately, in very complex mixtures, this is virtually impossible when single-stage separations are employed. This paper describes the sample recycling capabilities of a valve-based multidimensional gas chromatography system equipped with both infrared and mass spectral detectors. Sample recycle efficiencies, valve adsorption effects and cycle-to-cycle reproducibility are considered. Mixtures including the Grob test mixture were analyzed and it was found that 35 out of the 40 total components examined could be recycled six times or more following injection of 500 ng or less of each component. Additionally, the first demonstration of a 23-stage recycling experiment with several components of a chlorinated hydrocarbon mixture is shown. This demonstrates the plausibility of performing GC^n experiments, where n is the number of separation stages, with values of n up to 23 for these components. It is also shown that mechanical valves generally do not have deleterious effects on the majority of these components. The main limitations of the system appear to be the design of the heating system and the manual control of the pressure and flow switching systems. The applicability of the present results to qualitative analyses are discussed.

1. Introduction

For over a decade, it has been established that the combination of capillary gas chromatography (GC) with infrared (IR) and mass spectral (MS) detectors can provide highly accurate qualitative information [1,2]. However, statistical examinations of complex chromatograms by Davis and Giddings [3] demonstrate that the probability of completely isolating every component of even relatively simple mixtures using a single-column separation is very low. In terms of the spectroscopic detection of effluents, incomplete separation yields IR and mass spectra of mixtures rather than pure components. Ultimately, the quality of the library search or spectral interpretation is compromised. Methods of improving the chromatographic resolution to provide the detectors with single-component peaks include use of longer capillary columns, smaller inner

* Corresponding author.

0021-9673/94/$07.00
SSDI 0021-9673(94)00476-P

diameter (I.D.) capillary columns, and multidimensional techniques.

Unfortunately, because of inherent restrictions on the chromatography imposed the sample size and flow requirements of IR lightpipe detectors, small I.D. capillary columns (≤ 300 μm) cannot be used. Although detection limits of IR detectors are in the low nanogram range, samples with a wide range of component concentrations require sample dilution to reduce chromatographic column overloading. Such dilutions reduce the amount of minor components and, if they are to be detected, critical minor components may have been diluted below the minimum identifiable quantity. Thus, smaller I.D. capillaries are incompatible with the requirements of the IR detector. On the other hand, long capillary columns with inner diameters compatible with a lightpipe can be used to improve the separation resolution, but the carrier gas pressure requirements for a column long enough to provide a sufficient number of theoretical plates to completely separate a mixture containing several hundred components would preclude the use of common injection techniques. As a consequence, methods other than column dimension adjustments must be employed to achieve improved separations.

Another option for improving chromatographic resolution while observing the constraints imposed by the detection system is multidimensional (MD) GC. This technique generates its improved chromatographic resolution by utilizing columns with different stationary phase selectivities between two or more stages of separation and by reducing the number of components separated in the higher order separations through selective sample transfer. Samples can be transferred from the first-stage column to a subsequent analytical column by utilizing either mechanical valves or a valveless pressure switching technique based on Deans' original design [4]. Both methods have positive and negative aspects, as previously discussed in detail by Bertsch [5]. However, it is generally accepted is that valveless switching is the best method for MD-GC sample transfer, even though several reports have shown that mechanical valve-based systems function just as well as their valveless counterparts [6–9].

The two main problems attributed to mechanical valves are their activity towards polar compounds at trace levels and band broadening. During the past several years, there have been numerous conflicting reports regarding the activity of mechanical valves in capillary GC [6–14]. In most of the reports, the activity of the valves was assessed by analysis of a Grob test mixture [15], but in other reports, subsets of the components of a Grob mixture were used. Several reports over the last 15 years have shown mild to severe activity of mechanical valves towards 2-ethylhexanoic acid [10], 2,3-butanediol [11], 2,6-dimethylaniline [11], dicyclohexylamine [11,12], octanoic acid [13], trichlorophenol [13], nitrophenol [13], 2-methoxyethanol [14], 2-ethoxyethanol [14] and 2-isopropylethanol [15]. On the other hand, others have reported a lack of activity towards the compounds previously listed [6–9]. Unfortunately, the reason for these differences is not obvious. The other difficulty, peak broadening, can result from the combined valve and transfer volumes being greater than that of the column, so that in effect, a mixing volume is created within the valve. This problem can be alleviated by approximately matching the capillary column I.D. with the valve passage diameter. For conventional-size capillaries (ca. 320 μm I.D.) and valves with internal volumes of 1–2 μl, the effect from peak broadening is insignificant [5].

The primary advantages mechanical valves have over valveless systems are their simplicity and lower cost. Fig. 1 shows a schematic diagram of the mechanical valve-based system utilized in the study. Here, a total of five mechanical valves were incorporated into the design in order to achieve the desired chromatographic flexibility. Equivalent chromatographic systems based upon valveless switching technology would be extremely complex and cost prohibitive. Previous research utilizing instrumentation similar to that shown in Fig. 1 revealed that the qualitative information generated is not affected by use of mechanical valves [16–18]. Additionally, two recent studies demonstrated the use of the sys-

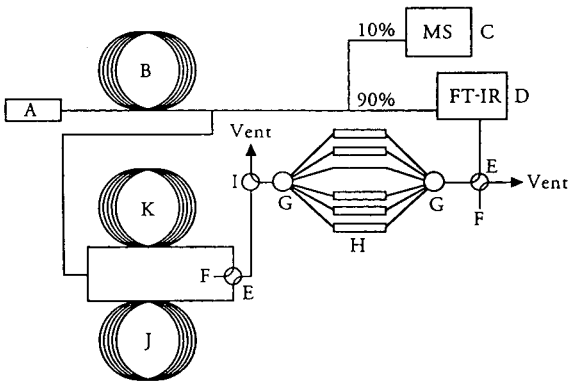

Fig. 1. Schematic diagram of the parallel cryogenic trap MD-GC–Fourier transform (FT) IR–MS system. A = Splitless injection port; B = Rt_x-1701 intermediate-polarity first separation stage column; C = HP 5970B mass-selective detector; D = HP 5965B IR detector; E = four-port, two-way valve (300°C maximum temperature); F = external auxilliary carrier gas; G = six-port selection valve (300°C maximum temperature); H = stainless-steel cryogenic traps; I = three-port, two-way valve (300°C maximum temperature); J = Stabilwax polar column; K = Rt_x-5 non-polar column.

tem for sample recycling to improve chromatographic resolution and component identification accuracy [17,18]. Even though the previous reports demonstrated the capability of using only three sample recycles (GC^3), they were the first demonstrations of the feasibility of sample recycling and GC^n experiments with the IR lightpipe of a combined MD-GC–IR–MS system.

Sample recycling through an IR lightpipe instrument was first demonstrated by Azarraga and Potter in 1981 [19], but literature references to this technique have been non-existent until very recently [17,18]. The system diagrammed in Fig. 1 was specifically designed to accommodate sample recycling, but most of the past research has been directed towards understanding and demonstrating the qualitative advantages of the system. The purpose of the present study is to examine the sample recycling process in order to determine whether or not there are any deleterious effects due to sample adsorption or trapping inefficiencies. Furthermore, it is of interest to characterize and along with the other results, a overall recycling efficiency.

2. Experimental

2.1. Instrumentation

A commercially available Hewlett-Packard (HP, Palo Alto, CA, USA) GC–IR–MS system was modified for MD-GC. The system consists of a HP 5890 series II gas chromatograph coupled in parallel with an HP 5965B IR detector and a HP 5970B mass-selective detector (Fig. 1). Effluent output from the lightpipe IR detector is either vented or collected into one of the five parallel cryogenic traps. For second and higher stages of analysis, trapped effluents are reinjected onto one of the analytical columns by turning off the liquid nitrogen flow to the selected trap and routing carrier gas flow to the trap with the selection valves. In the present configuration, the mechanical valve switching and carrier gas pressure adjustments required for multistage experiments are accomplished manually. Using the arrangement depicted in Fig. 1, the parallel cryogenic trapping multidimensional system does not interfere with normal operation of the GC–IR–MS system, so both IR and MS data are obtainable for eluting components resulting from any GC separation stage.

2.2. Samples

Five standard mixtures (Supelco, Bellefonte, PA, USA) were chosen to represent a broad cross-section of functionalities and reactivities. Table 1 summarizes the contents of each of the mixtures as well as the amount of material injected for each component. The Grob mixture was selected so that direct comparisons with previous reports on the activities of mechanical valves could be performed, and the other mixtures were chosen to probe the activity of the valves towards several different classes of compounds not present in the Grob mixture.

2.3. Mechanical valving system

Five mechanical valves are incorporated into the design of the system. The two valves used for cryogenic trap selection are Rheodyne Model

Table 1
Study mixture components and result summary

Mixture	Peak No.	Component	Quantity injected (ng)	Maximum number of recycles		R^2 for linear regression of 10 recycles		Slope-based recycle (%)	
				MS	IR	MS	IR	MS	IR
Grob Mixture	1	2,3-Butanediol	530	11	12	0.991	0.950	64	66
	2	Decane	280	18	18	0.999	0.999	75	77
	3	1-Octanol	360	13	16	0.997	0.999	69	73
	4	Undecane	290	18	18	0.999	1.00	74	76
	5	Nonanal	400	10	12	0.991	0.996	60	66
	6	2,6-Dimethylphenol	320	13	12	0.993	0.999	65	69
	7	2-Ethylhexanoic acid	380	6	6	0.957	0.990	45	60
	8	2,6-Dimethylaniline	320	8	6	0.992	0.996	46	50
	9	C_{10} Acid methyl ester	420	12	11	0.991	0.993	64	65
	10	C_{11} Acid methyl ester	420	9	9	0.943	0.971	48	55
	11	Dicyclohexylamine	310	1	1	N/A	N/A	N/A	N/A
	12	C_{12} Acid methyl ester	410	6	5	0.993	0.993	32	37
Hazardous substances mixture	13	Aniline	500	10	10	0.989	0.989	60	58
	14	Benzyl alcohol	500	11	10	0.990	0.991	61	62
	15	*p*-Chloroaniline	500	6	8	0.993	0.970	45	50
	16	2-Methylnaphthalene	500	11	8	0.971	0.972	59	68
	17	*m*-Nitroaniline	500	2	6	1.00	0.959	17	45
	18	Dibenzofuran	500	4	2	0.956	1.00	25	46
Phenol mixture	19	2-Chlorophenol	500	16	16	0.991	0.983	73	73
	20	2-Methylphenol	500	15	9	0.980	0.995	70	71
	21	4-Methylphenol	500	13	12	0.981	0.988	64	66
	22	2,4-Dimethylphenol	500	13	12	0.972	0.992	66	68
	23	2,6-Dichlorophenol	500	11	10	0.938	0.976	57	61
	24	2,4,5-Trichlorophenol	500	5	5	0.990	0.981	33	40
	25	2,3,4,6-Tetrachlorophenol	500	2	3	1.00	0.981	49	22
Base–neutrals mixture	26	N-Nitrosodimethylamine	500	12	11	0.993	0.989	70	69
	27	Di-2-chloroethyl ether	500	14	14	0.998	0.988	78	79
	28	Di-2-chloroisopropyl ether	500	14	14	0.970	0.999	80	80
	29	N-Nitrosodipropylamine	500	12	12	0.988	0.998	62	65
	30	2-Chloroethoxymethane	500	14	13	0.999	0.999	72	72
	31	Dimethyl phthalate	500	10	10	0.987	0.996	52	56
	32	Diethyl phthalate	500	9	6	0.909	0.986	46	32
	33	4-Chlorophenyl phenyl ether	500	6	6	0.969	0.982	30	30
Chlorinated hydrocarbon mixture	34	1,3-Dichlorobenzene	500	23	20	0.998	0.999	78	77
	35	1,4-Dichlorobenzene	500	23	20	0.999	0.998	76	75
	36	1,2-Dichlorobenzene	500	23	19	0.998	0.999	79	78
	37	Hexachloroethane	500	15	22	0.996	0.997	75	75
	38	1,2,4-Trichlorobenzene	500	23	14	0.997	0.999	71	71
	39	Hexachlorobutadiene	500	15	16	0.996	0.999	80	79
	40	2-Chloronaphthalene	500	12	4	0.987	0.962	35	36

N/A = Not applicable.

7060 selection valves with Vespel rotor seals. Each valve provides one common input/output line and six selectable trap lines (Rheodyne, Cotati, CA, USA; 300°C maximum temperature). The internal valve passages are 0.41 mm in diameter, and the internal volume of each of the valves is less than 2 μl. A three-port, two-position Valco Model 3N3WT valve (Houston, TX, USA; 350°C maximum temperature) is used to switch flow from the traps to either a vent or the higher separation stage columns. The last two valves in the system are four-port, two-position Valco Model 4C6WT valves (350°C maximum temperature). The first of these valves is used to direct flow from the lightpipe to either a vent or the cryogenic trap array. The other valve is used to control flow to either of the two higher separation stage columns.

2.4. External trap oven heating system

The cryogenic trapping array is situated inside a small oven on top of the GC oven, and a 0.75 m × 0.53 mm I.D. MXT-5 column (Restek, Bellefonte, PA, USA) carries sample from the valves in the GC oven to the trap array. Heating of the external trap oven is accomplished by three lengths of heating tape and variable-voltage regulators. Fig. 2 shows a top view scale drawing of the external trap oven on top of the GC oven. The boxed and lined areas show the heater placement, and the circles show where the resistive thermal devices (RTD) are placed in order to monitor the oven temperatures. The temperatures at the tips of the valves are maintained at 250°C to help reduce component condensation in the valve, and the transfer line temperature is also maintained at 250°C for identical reasons.

2.5. Chromatography

For separations, initial injections were 1.0-μl splitless injections followed by an injection port purge 55 s after injection. The amount of sample delivered to the first stage column was at the column's approximate sample capacity of 500 ng per component. This was done to provide

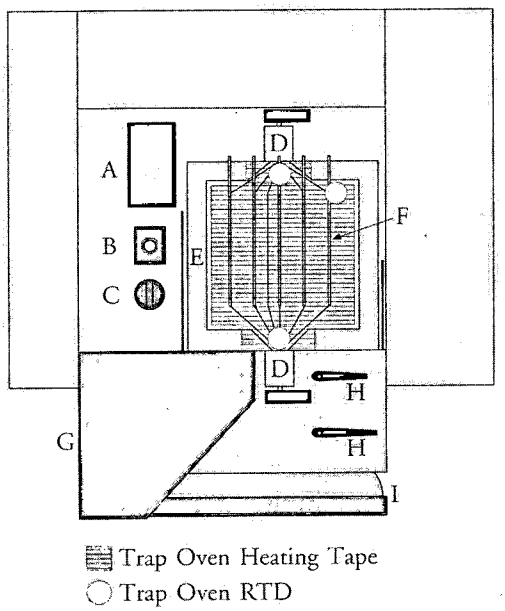

Fig. 2. Top view scale drawing of the GC oven and external trap oven. A = Injection port cooling fan; B = splitless injection port; C = three-port, two-way valve (300°C maximum temperature); D = six-port selection valve (300°C maximum temperature); E = external trap oven ceramic insulation; F = stainless-steel cryogenic traps; G = GC oven extension and bracket; H = four-port, two-way valve (300°C maximum temperature); I = GC oven door.

enough sample to obtain several recycles without grossly overloading the analytical column, in order to obtain a high number of sample recycles. Three columns were installed in the chromatograph: one first-stage separation column and two higher separation stage columns. The first-stage column was a Restek Rt_x-1701 intermediate polarity column (30 m × 0.32 mm, 1.0 μm film thickness), and the two higher separation stage columns were Restek polar Stabilwax and non-polar Rt_x-5 columns (both 30 m × 0.32 mm, 1.0 μm film thickness). Temperature programs utilized for the second and succeeding stages of separation for each of the standards are summarized in Table 2. Carrier gas linear velocities used in all parts of the study were approximately 30 cm/s at 70°c. Each standard was first separated on the intermediate-polarity column, and the entire sample was refocussed into a single cryogenic trap after

Table 2
Temperature programming for second and succeeding stage separations

Mixture	Initial oven temperature (°C)	Initial hold time (min)	Temperature ramp rate (°C/min)	Final oven temperature (°C)	Final hold time (min)	Infrared SWC range[a] (cm^{-1})
Grob	50	0	4	210	0.00	1000–3100
Hazardous substances	60	4	15	230	9.67	1300–1800
Phenol	100	2	15	230	14.33	1200–1600
Base–neutrals	100	2	15	230	14.33	1000–1600
Chlorinated hydrocarbons	45	7	10	190	1.50	779–1600

[a] SWC = Selective wavelength chromatogram.

detection. The subsequent sample recycle separation stages were performed using only the nonpolar column by utilizing a looping sequence to retrap all of the column effluents from a particular injection following detection. Because the purpose of the study was to examine valve interactions with mixture components, only one analytical column was used.

2.6. Spectrometry

IR spectra were collected by the HP 5965B IR detector at a rate of 10 scans per spectrum with 16 cm^{-1} optical resolution, corresponding to a rate of one spectrum per second. IR reconstructed chromatograms were produced using a second-derivative selective-wavelength reconstruction with the wavenumber ranges shown in Table 2. Mass spectra were recorded with the HP 5970B mass-selective detector in full scan mode scanning between 20 and 275 u, corresponding to an acquisition rate of approximately 1.3 spectra per second.

3. Results and discussion

As mentioned above, most of the previous research performed with the system diagrammed in Fig. 1 was focused on qualitative analysis applications. This is the first comprehensive report on the quantitative aspects of the system with regard to sample recycling and valve adsorption. Studies using initial versions of the MD-GC system [16–20] resulted in a number of improvements which are incorporated in the present design. As a consequence, it is possible to demonstrate a level of recycling performance previously not obtained.

The MD-GC system used in this study was developed with the intention of reducing the reported deleterious effects upon the chromatography due to the presence of mechanical valves while retaining the desired chromatographic flexibility. As can be seen in Fig. 1, the valves have been placed either after detection or immediately before the higher separation stage columns. By doing this, peak broadening at the detector due to the valve rotor mixing volume is dramatically reduced. Additional reduction of peak broadening is achieved by using 0.32 mm I.D. capillary columns and transfer lines throughout the system. Generally, the measured peak widths at half height for most components in the valve-based system are comparable to widths measured in a system without the valves.

Valve temperature effects and reactivity were also taken into account when developing the design, but neither of those effects were examined until this study. The temperatures of the trap selection valves and transfer line in the external trap oven were maintained at 250°C by use of heating tape. However, as Fig. 2 shows, the switching valves are placed inside the GC oven and their temperatures vary with the temperature GC oven programming. Valves inside of temperature-programmed GC ovens have been previously shown to have temperature lag problems when oven temperature ramps are greater than 2°C/min [9,11]. It is this lag that is expected

to cause an approximate loss of 2% of the sample per valve passage. Additionally, component condensation in the trap selection valves was designed to be minimized but, due to GC column (230°C) and trap selection valve temperature limits (300°C), high boiling point and late-eluting components were experimentally determined to be less efficiently transferred to the cryogenic traps. It is possible to differentiate between component reactivity towards the valves and component transfer inefficiencies due to condensation by comparing peak areas, valve temperature, and the maximum number of recycles for a particular component. A component was considered to have some activity towards valve surfaces if its elution temperature was below 230°C and it had a maximum recycle number of less than ten. On the other hand, components which eluted during the 230°C isothermal portion of the temperature programs and had maximum recycle numbers less than ten were considered to be affected by condensation in the valve passages, rather than activity.

As Table 1 shows, most of the components examined in the study had maximum recycle numbers equal to or greater than ten cycles. The last recycle for each component was identified as the last chromatogram in which the component peak could be integrated and a library searchable spectrum obtained. However, several components could not be recycled through the system more than six times. This apparent shortcoming must be examined in terms of the *qualitative* analysis of a sample. The maximum number of recycles required for a particular sample depends upon the number of analytical columns present in the system and the amount of information required from the analysis. For example, a system with two analytical columns would require a primary separation and one recycle of the entire sample on each of the two analytical columns to provide a total of three independent separations with three different sets of IR and mass spectra as well as three sets of retention times. Therefore, with a single sample injection, three complementary sets of data could be obtained using only two sample recycles. With this information, a more accurate qualitative analysis can be performed. Additionally, heartcuts can be made during any of the recycles, and those cuts can subsequently be recycled on each of the analytical columns. In the end, the practical number of recycles for a qualitative analysis is roughly six cycles per component, so for 35 of the 40 examined compounds, more than adequate recycling capability is provided.

Because the chromatographic system effluent is split in parallel to the IR and MS detectors as shown in Fig. 1, a loss of approximately 10% is expected due to the destructive nature of MS detection. In addition to detector losses, Miller [9] reported typical sample losses of about 2% per valve path, so approximately 10% more of the sample is expected to be lost due to valve losses. Therefore, if the system operates without additional losses due to reactivity, condensation, or other factors, the maximum recycle efficiency of the system should be about 80% per cycle. Based upon the expected consistent loss of 20% per cycle, there is an anticipated sample consumption which can be fitted to an exponential regression. That theoretical consumption curve is shown in Fig. 3. However, such an exponential fitting procedure does not provide easy access to information regarding the efficiency of the system. A plot of the natural logarithms of the integrated chromatographic peak areas versus the recycle number should give a straight line with the slope of the line (m) related to the percent efficiency per cycle of the system by:

$$\% \text{ Efficiency} = e^{m} \cdot 100\% \quad (1)$$

Additionally, the correlation coefficient (R^2, with an expected value of 1.00) of the linear regression provides some insight into the cycle-to-cycle behavior of the system. A lower correlation coefficient can be taken to be an indication of cycle-to-cycle variation of valve adsorption, component condensation, carrier gas pressure, or inadequate detector response.

The first test mixture examined was the Grob mixture. Fig. 4 is a series of total ion chromatograms showing the sample consumption of the various components from cycle-to-cycle. All but one of the components are apparent up to the fifth recycle, but dicyclohexylamine is completely missing following the first recycle. As previously

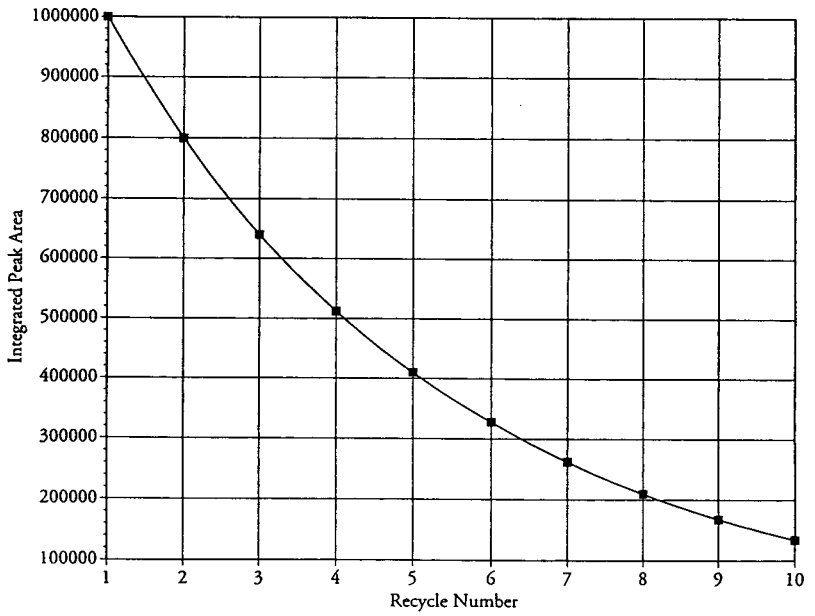

Fig. 3. Theoretical integrated peak area versus recycle number plot showing the exponential consumption of sample from cycle-to-cycle.

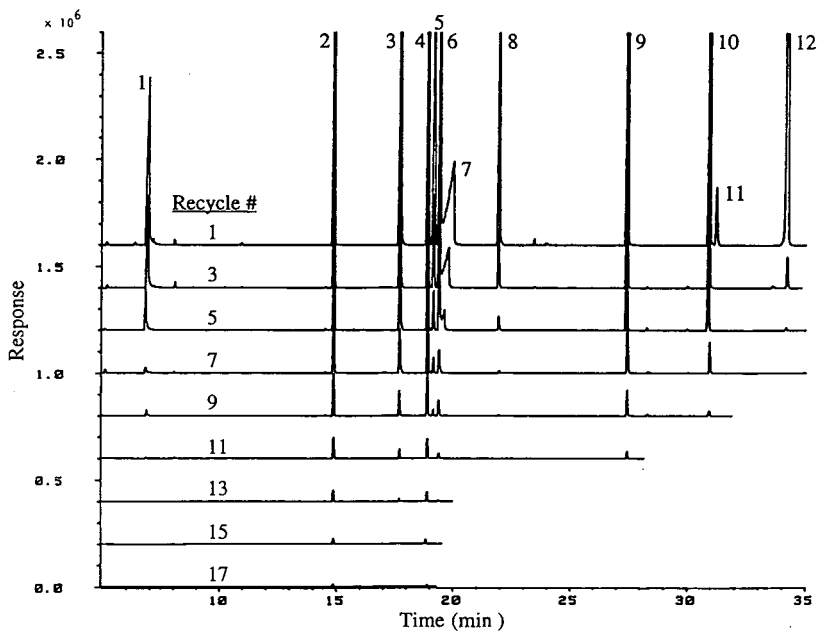

Fig. 4. MS total ion chromatograms of the Grob test mixture recycling experiments. In order to improve clarity, only every other separation is shown. Peak labels correspond to components listed in Table 1.

mentioned, there have been conflicting reports regarding interactions between mechanical valves and dicyclohexylamine. The present research is in agreement with those earlier reports demonstrating problems with the amine [11,12]. As expected, the non-polar components, decane and undecane, could be recycled most often (17 times) and, interestingly, 1-octanol could be recycled 15 times. The quantity of material in the last recycle for each of these three components is approximately 2 ng, close to the expected minimum identifiable quantities with the current configuration of the detector system. Fig. 5a and b are the recycle regression plots for the Grob mixture. The differing slopes between the IR and MS plots for the same compounds can be attributed to the differing responses of the detectors for different components. The correlation coefficients and recycle efficiencies obtained from the regression slopes are summarized in Table 1. Efficiencies for several of the components are above 50%, with a maximum of about 75% for decane. Correlation coefficients are also high, with most values between 0.95 and 1.00. For the majority of the components, the results are close to theory, but the acid methyl esters had values lower than expected. These lower values are thought to be the result of component condensation in the trap valves because elution times for these components were well into the 230°C isothermal temperature program. However, overall system performance appears to be within the expected range with the single exception of the strongly basic dicyclohexylamine.

Although the Grob mixture provides a broad spectrum of components and functionalities, there are several classes of compounds which are not included in the mixture. Therefore, four other mixtures were chosen to fill in some of the missing classes. The second mixture analyzed was a hazardous substances mixture. Regression plots similar to those in Fig. 5 were made from the integrated peak area data; Table 1 summarizes these results. The most noticeable differences between the Grob mixture and the hazardous substances mixture are the lower number of recycles achieved and the lower efficiencies per recycle. One possible reason for these lower values is that half of the compounds in this mixture have nitrogen containing groups and, like dicyclohexylamine and 2,6-dimethylaniline

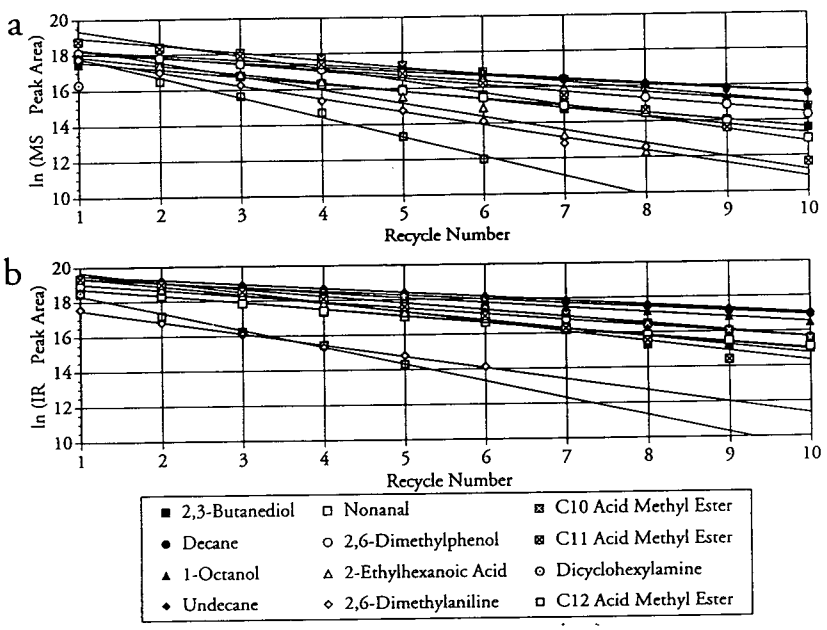

Fig. 5. Linear recycle regression plots for the Grob test mixture. (a) MS response data; (b) IR response data.

in the Grob mixture, it appears that some nitrogen-containing compounds may have lower efficiencies for reasons other than basicity. Dibenzofuran also has a low values for all three categories in Table 1, but the reason for these low values seems to be related to the valve temperature problems previously described. However, the recycling ability of the system for these types of compounds appears to be more than adequate.

A phenol mixture was the third sample analyzed. The results of the recycling were better than those of the hazardous substances mixture and, not surprisingly, similar to that obtained for 2,6-dimethylphenol in the Grob mixture. The values for the correlation coefficient and recycle efficiency summarized in Table 1 were obtained with the same data reduction methods used for the previous mixtures. A comparison of the recycle percentage results for 2,4-dimethylphenol and 2,6-dimethylphenol shows a great similarity, and their maximum number of recycles are also similar. However, because more 2,4-dimethylphenol was injected it was expected that it could be recycled more times than 2,6-dimethylphenol. The discrepancy between these two results may be due to an inaccurate estimate of injection volume which would lead to a lower amount of injected material, or it may be due to an unidentified initial loss of material between the first stage of separation and the latter stages. Phenols as a class do not appear to have serious interactions with mechanical valves. This can be seen by comparing both the maximum number of recycles and the recycle efficiencies obtained for the first five components. As for the last two components, they are high-temperature, late-eluting components that are probably hindered more by the temperature limitations of the system than by activity towards the valve surfaces.

The fourth mixture analyzed in this study was a base–neutrals mixture. The results obtained from the linear regression analysis of the results for this sample are also summarized in Table 1. It is interesting that all eight of the compounds are capable of being recycled a minimum of six times, and di-2-chloroethyl ether and di-2-chloroisopropyl ether have recycle efficiencies which are equal to or near to the expected maximum value of 80%. The two phthalates and 4-chlorophenyl phenyl ether have relatively low efficiencies, but the temperature limitations of the system seem to be the cause of the lower values for these two components. It is also interesting that the two nitrosamines present in the mixture have recycling efficiencies and recycle numbers much higher than those found for the other nitrogen- containing components in the study. The reason for this is not known, but it may be related to the relatively short retention times and low elution temperatures of the two components. This base–neutrals mixture provided the first data demonstrating that the expected maximum recycling efficiency could be reached.

Finally, the last mixture investigated in this study was a chlorinated hydrocarbon mixture. As with the other four mixtures, a summary of the linear regression analysis results appears in Table 1. Fig. 6 shows a series of IR selected-wavelength chromatograms for the first four components of the chlorinated hydrocarbon mixture. Of those first four components, only hexachloroethane is present at the 22nd cycle, where an estimated quantity of about 1 ng is detected. This amount of hexachloroethane would be expected to be present in the final cycle based on previously measured minimum identifiable quantities for these types of compounds [21]. In contrast, Fig. 7 shows a series of total ion chromatograms for the same four compounds, clearly demonstrating the difference between the IR and MS responses. Hexachloroethane appears to be completely absent by the 19th cycle in Fig. 7 as opposed to the 22nd cycle in Fig. 6. However, the three isomers of dichlorobenzene are present at the 22nd cycle in Fig. 7, yet they are gone by the 19th and 20th cycles in Fig. 6. Overall, the recycle efficiencies are very high for all but 2-chloronaphthalene, and several are equal to or close to the expected maximum efficiency. 2-Chloronaphthalene has a low recycle efficiency because of the system temperature limits and due to its high elution temperature and long retention time. The difference in the maximum number of recycles detected for this

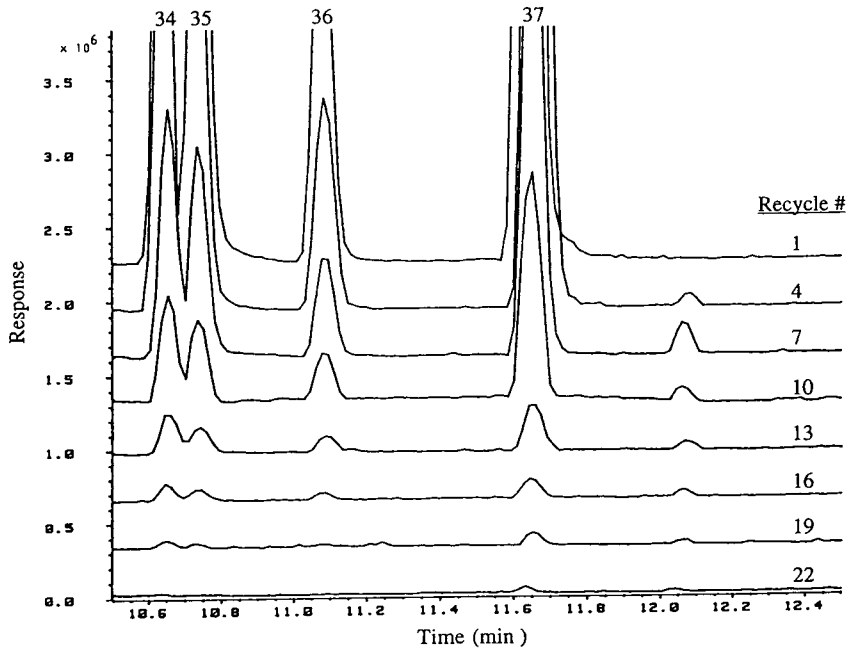

Fig. 6. IR total response chromatograms for the first four components of the chlorinated hydrocarbon mixture recycling experiments. In order to improve clarity, only every third separation is shown. Peak labels correspond to components listed in Table 1.

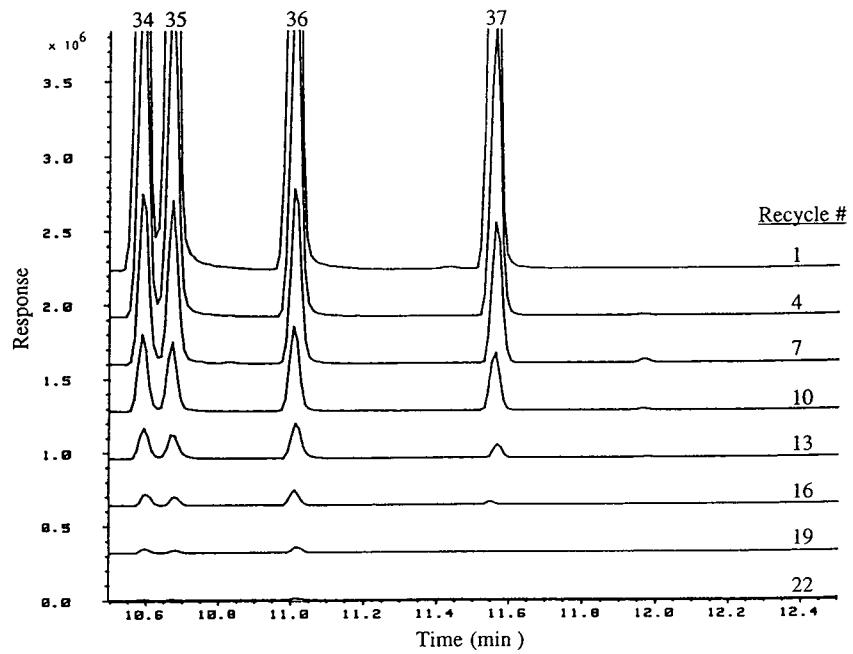

Fig. 7. MS total ion chromatograms for the first four components of the chlorinated hydrocarbon mixture recycling experiments. In order to improve clarity, only every third separation is shown. Peak labels correspond to components listed in Table 1.

compound is due to the choice of IR selected-wavelength chromatogram range used in the reconstruction. The strongest IR absorption band for 2-chloronaphthalene falls below the detector cutoff of 779 cm^{-1}, and the reconstruction range does not go high enough to incorporate the aromatic C–H stretch at approximately 3050 cm^{-1}. Out of all of the mixtures considered in this study, the chlorinated hydrocarbon mixture provides the most impressive data, demonstrating for the first time that it is possible to recycle the same components up to 23 times with a single injection, and this demonstrates the possibility of performing a GC^{23} experiment with these compounds. Additionally, five of the seven components could be recycled and detected at least 20 times using one detector or the other. For these compounds, the high correlation coefficients exhibit the fairly high cycle-to-cycle repeatability of the recycling. As these data show, chlorinated compounds appear to have the less activity towards mechanical valves than another other class of compounds studied other than alkanes.

4. Conclusions

For the first time, a comprehensive examination of component activity towards mechanical valves in a recycling MD-GC–IR–MS system has been performed. For most of the compounds in the study, very high to medium recycling efficiencies were determined and, as the correlation coefficients of the linear regressions demonstrate, most components have reasonably high cycle-to-cycle reproducibility. It therefore appears that mechanical valves do not introduce severe problems for a broad range of chemical classes, with the possible exception of certain types of nitrogen-containing compounds. In terms of recycling ability, the majority of components examined in this study can be recycled more times than should be required for typical qualitative analysis applications. This study also demonstrates the plausibility of GC^n where n is the number of stages of separation, with values of n routinely in excess of 6. Here it has been shown that a maximum of 23 recycles can be accomplished with a single injection of a mixture containing 500 ng each of 1,2-dichlorobenzene, 1,3-dichlorobenzene, 1,4-dichlorobenzene, and 1,2,4-trichlorobenzene. In general, the MD-GC system presented here provides unprecedented separation abilities for combined spectroscopic detection systems. However, there are aspects of the system which presently limit its widespread application.

One of the main difficulties with the current design is the temperature limitations imposed by some of the valves. The data presented in this study reveal that there are problems with late-eluting, high-elution-temperature components. With improved valves the present limitations may be removed. Another problem which needs to be addressed is the manually actuated nature of the switching and pressure system. Run-to-run and cycle-to-cycle reproducibility would be greatly improved by the addition of electronic pressure control to control the various carrier gas flows, and heartcut timing reproducibility would also be improved with computer-controlled valve actuators. Nevertheless, as a feasibility study, the results are very encouraging. The range of compounds examined were intended to demonstrate the wide applicability of the instrumentation applications outside of the previously studied areas of essential oil and petroleum analysis [16–18,20]. It is expected that, with further development of the hardware along the lines discussed here, it should be possible to develop a completely flexible computer-controlled MD-GC chromatographic system with IR and MS detection at each stage of separation. Such a system would provide the ability to separate components in very complex mixtures to any required resolution. Furthermore, in concert with improved data reduction algorithms, the resulting analytical tool will greatly improve and simplify overall qualitative analysis of complex volatile mixtures.

Acknowledgement

We gratefully acknowledge support from the National Science Foundation under grant CHE-92-01277.

References

[1] C.L. Wilkins, *Anal. Chem.*, 59 (1987) 571 A.
[2] C.L. Wilkins, *Anal. Chem.*, 65 (1994) 295 A.
[3] J.M. Davis and J.C. Giddings, *Anal. Chem.*, 55 (1983) 418.
[4] D.R. Deans, *Chromatographia*, 1 (1968) 18.
[5] W. Bertsch, in H.J. Cortes (Editor), *Multidimensional Chromatorgraph-Techniques and Applications (Chromatographic Science Series*, Vol. 50), Marcel Dekker, New York, Basel, 1990, Ch. 3., p. 74.
[6] S. Jacobsson and S. Berg, *J. High Resolut. Chromatogr. Chromatogr. Commun.*, 5 (1982) 236.
[7] W. Jennings, *J. Chromatogr. Sci.*, 22 (1984) 129.
[8] S.L. Smith, *Appl. Spectrosc.*, 40 (1986) 278.
[9] R.J. Miller, *J. High Resolut. Chromatogr. Chromatogr. Commun.*, 10 (1987) 497.
[10] B.M. Gordon, C.E. Rix and M.F. Borgerding, *J. Chromatogr. Sci.*, 23 (1985) 1.
[11] S.T. Adam, *J. High Resolut. Chromatogr. Chromatogr. Commun.*, 11 (1988) 85.
[12] D. Roberts and W. Bertsch, *J. Chromatogr.*, 477 (1989) 59.
[13] Q.W. Zhang, L. Hathcock and W. Bertsch, *J. High Resolut. Chromatogr.*, 13 (1990) 683.
[14] A.E. Stanley and J.B. Turner, *Appl. Spectrosc.*, 45 (1991) 133.
[15] K. Grob, Jr., G. Grob and K. Grob, *J. Chromatogr.*, 156 (1978) 1.
[16] K.A. Krock, N. Ragunathan and C.L. Wilkins, *J. Chromatogr.*, 645 (1993) 153.
[17] K.A. Krock, N. Ragunathan and C.L. Wilkins, *Anal. Chem.*, 66 (1994) 425.
[18] K.A. Krock, N. Ragunathan, C. Klawun, T. Sasaki and C.L. Wilkins, *Analyst*, 119 (1994) 483.
[19] L.V. Azarraga and C.A. Potter, *J. High Resolut. Chromatogr. Chromatogr. Commun.*, 4 (1981) 60.
[20] N. Ragunathan, K.A. Krock and C.L. Wilkins, *Anal. Chem.*, 65 1993) 1012.
[21] K.A. Krock and C.L. Wilkins, *Appl. Spectrosc.*, 46 (1992) 1621.

ELSEVIER

Journal of Chromatography A, 678 (1994) 279–288

JOURNAL OF CHROMATOGRAPHY A

Industrial-grade field-mountable gas chromatograph for process monitoring and control

Raymond Annino

AWS Associates, Box 118, Forrestdale, RI 02896, USA

First received 1 February 1994; revised manuscript received 17 May 1994

Abstract

A novel design is proposed for a field-mountable on-line process gas chromatograph. The chromatograph proper is constructed as a light, portable, plug-in cartridge in support of a rapid repair-by-replacement philosophy. The support structure is mounted close to the sampling point and consists of an explosion-proof section and an intrinsically safe oven that can be unbuttoned in the field without powering down the unit. The "cartridge" chromatograph is designed to support fast capillary column chromatography. A description of a prototype unit is given as well as performance chromatograms and a demonstration of its multicolumn analysis capability by its application to the rapid BTU (British Thermal Unit) analysis of natural gases.

1. Introduction

The differences that distinguish on-line process gas chromatography (PGC) systems from their laboratory counterparts have been discussed in the literature [1–3] and details for the design and operation of industrial-grade PGC systems can be found in a recently published text [4]. These analyzers are designed with the objective of providing up-to-date composition measurement information to enable proper control of the process.

The purpose of this paper is to propose a design for PGC systems that will better meet the monitoring and control objectives than have previous devices and to report our progress toward attaining this goal. This report will focus specifically on the design and performance of the analyzer (chromatograph) portion of the package.

The primary research goal was to design and test a truly field-mountable (FM) PGC systems that had the following attributes. It would (1) require none of the usual on-site trouble-shooting and repair that is common with currently manufactured PGC systems, (2) be truly field mountable (on a pipe stand) close to the sampling point, (3) provide updated analysis to the control system in seconds rather than minutes.

It was assumed early on in the research that their was no way to design a unit that would be maintenance free. It was anticipated that both user misuse, as well as unexpected process upsets, would continue to pose problems for the FMPGC system well into the future. Thus, to limit the exposure of maintenance personnel to the elements, a design was required that would allow for rapid replacement of the unit in the field rather than trouble shooting and replacing individual components as is the practice today.

0021-9673/94/$07.00
SSDI 0021-9673(94)00470-T

It was decided to design the analyzer so that there was only one rapidly replacement part. This part would include as a unit the columns, detector and sample/switching valves. The support structure consisting of the temperature controlled oven, calculation/communication/control section, and the basic sample-handling support structure would remain intact at the site.

Short analysis turnaround times would be insured by both short sample transport lines and an analyzer design that would support chromatography on 0.25 mm to 0.050 mm I.D. open tubular columns (OTCs).

2. Experimental

2.1. General description of the FMPGC system

The proposed FMPGC system illustrated in Fig. 1 is shown with its insulated oven cover unbuttoned and partially removed. The exploded view shown in Fig. 2 illustrates the separation of

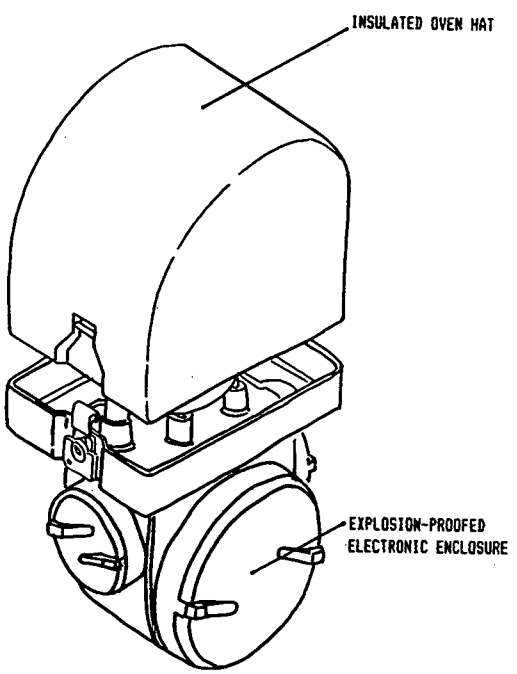

Fig. 1. Complete FMPGC package with GC oven's protective. Covering partially removed.

the intrinsically safe oven enclosure from the explosion-proofed electronics/communication module.

The oven, contained in the upper portion of the field-mounted support structure, is designed for static heating (thus eliminating yet another operating expense and customer burden, i.e., purge air). The oven housing includes a number of electrical heaters cast within its walls for maintaining the temperature of the environment surrounding the chromatograph. The power connections to these heaters as well as to the detector, sample/stream switching valves solenoid drivers, and associated electronics are made below, within the explosion-proof section. Thus, since not enough power is available within its environment to cause an explosion, the oven enclosure is intrinsically safe and can be unbuttoned in the field without powering down. This feature enables the maintenance technician to quickly replace a faulty GC cartridge and have the FMPGC system operational again in a very short time —a critical requirement for control applications.

The analyzer portion of the unit consisting of valves, columns, flow balancing restrictors and thermal conductivity detectors is configured on a manifold so as to form a modular unit that can be replaced easily. This cartridge assembly (shown in Fig. 2 in an exploded view) is lightweight and portable. It is attached in the oven enclosure to two posts (passages through these posts supply carrier gas, sample and vents for the analyzer) by means of two bolts. Thus, it can be easily removed, replaced with another unit and repaired later at a remote site. The individual components of the analyzer cartridge are surface mounted and can be easily replaced in the user's own maintenance shop or returned to the manufacturer for repair.

The idea of using a cartridge totally micromachined of silicon [5], while attractive at first glance, was ruled out for a number of reasons. Very few, if any users, have this technology available in house. Thus, either a manifold unit (consisting of valves, detectors and restrictors, but detachable columns) would have to be made cheap enough to be a "throwaway" item

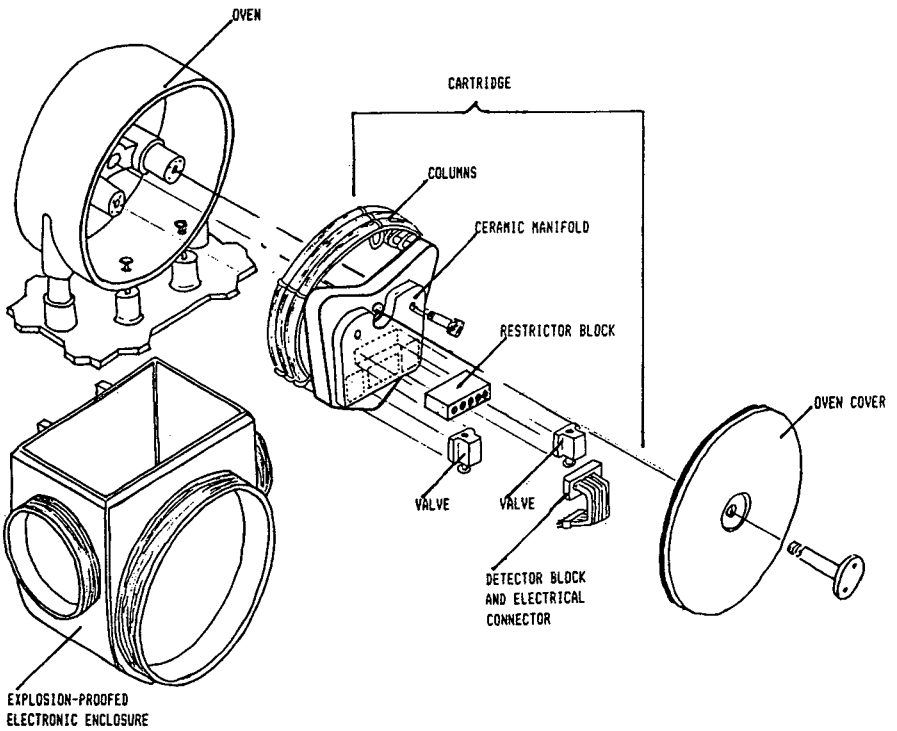

Fig. 2. Detailed view of the FMPGC system showing (as an exploded view) the elements of the cartridge and how it fits into the oven enclosure.

(not likely in the near future) or it would have to be sent back to the manufacturer for repair at additional expense. In addition, in order to accommodate a short turnaround repair time, a large inventory of spare cartridges would have to be kept on hand. We did not, however, rule out micromachining for specific parts of the unit.

2.2. Details of the GC cartridge

No-wrench replaceable chromatograph cartridge

Clearly, the cartridge concept, with its fixed geometry, will not provide the analyst with the flexibility in column, valve and detector arrangements that is now available in current PGC designs. The circuit shown in Fig. 3 was selected as the best compromise to this situation. It features two ten-port valves to be used for sample injection and column switching, balancing adjustable restrictors, and a bank of five thermal conductivity detectors. This circuit provides the unit with a powerful analysis capability as will be illustrated further on by its application to the measure of the calorific value of natural gas.

The cartridge consists of a chassis plate to which a manifold is coupled. The cartridge is fastened to the oven housing through the chassis by two bolts that are threaded into the bosses in the oven housing. The bosses also contain passageways for carrier gas, sample and vents. The gasketed faces of these bosses mate directly to the manifold to provide a simple leak-free connection of the services to the manifold.

The manifold is made of ceramic by means of the same technology perfected for manufacturing fluidic logic devices (Fluidics Products Department, Corning Glass Works, Corning, NY, USA) and is polished to a flat finnish (two light bands interference pattern) to accept the sliding faces of the sample/column switch valves.

It is essentially a pneumatic circuit board and

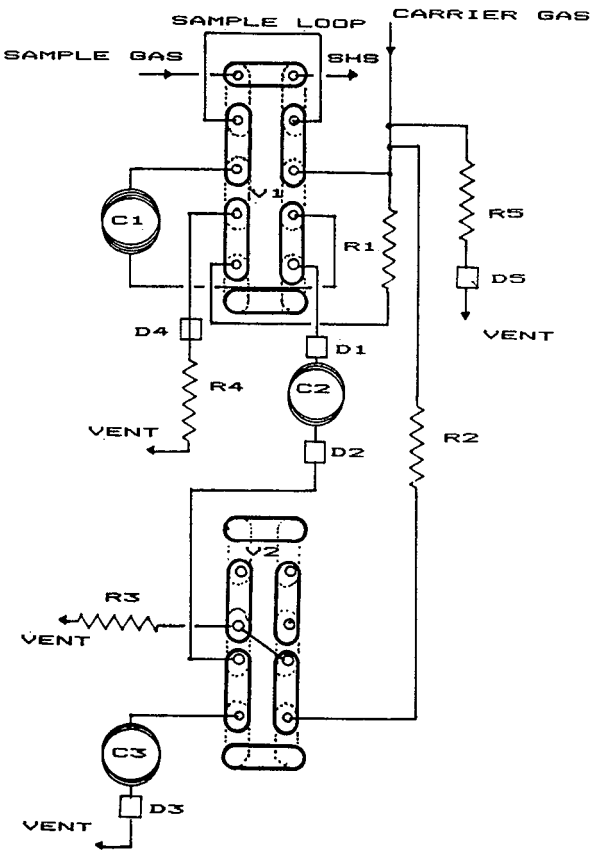

Fig. 3. Flow schematic of the circuit used in the FMPGC system. In the present position of valve 1 (V1) and valve 2 (V2), a portion of the process stream from the sample handling system (SHS) is being sent back to the SHS where it will be either returned to the process or vented. The injected sample of the process is being directed to columns C1, C2 and C3 and detectors D1, D2 and D3. The flow schematic for V1 in the backflush position and V2 in the stream divert position is given by the dotted lines (C1 is backflushed to vent through D4 and R4 and the remaining components in C2 are diverted to vent through R3 while the remaining components in C3 are eluted and detected by D3.

contains the connecting channels (0.015 in. I.D.; 1 in. = 2.54 cm) and holes (0.010 and 0.015 in. I.D.) for the columns, detectors, restrictors and valves that are surface mounted on it (see exploded view of the cartridge in Fig. 2).

Cartridge elements

Columns

Provision is made to support multicolumn analysis schemes using conventional fused-silica open tubular (FSOT) and micropacked columns. In order to retain user flexibility of column selection and replacement, the columns are not directly connected to the manifold. Rather the connection is made via standard 1/16-in. Valco capillary column connectors to stainless-steel column blocks that are themselves surface mounted on the manifold.

Injection and column switching valves

Even though fairly detailed operating characteristics of the no-moving part fluidic sample valve suggested by Gaspar et al. [6] are available [7], the use of this technology was ruled out because it requires the sample to be at an elevated pressure (the sample pressure in the fluidic valve must be larger than the column head pressure). Thus, to encompass applications where the sample is at atmospheric or lower pressures provision would have to be made to pressurize the sample. Besides the additional hardware required to do this, the pressurization might unduly complicate sampling streams with high dew points.

Based on the results of our previous experience with miniaturized versions of conventional valves and the preferred geometry of the valve in the cartridge, a slider type valve was chosen.

Two slider valves are mounted on the manifold. They are identical and miniature in size. Their Rulon II sliders are finished to 0.3 microns and have 0.020-in. wide slots to transfer gas from the 0.010-in. holes in the manifold to the appropriate channels. The sliders are attached to shafts that mate (through simple fastener free couplings) with those of the solenoid shafts. Switching times for this design were calculated to be less than 5 ms.

Before finalizing the design a prototype of the valve was tested and found to remain within specifications even after one million cycles.

Flow-adjusting restrictors

When using multicolumn analysis schemes, a means of balancing carrier gas flow-rates is

Table 1
Variation of sensitivity with excitation current

Current (mA)	Resistance (Ω)	Sensitivity (mV/mol% propane)	Temperature of filament (°C)[a]
7.64	147	22.2	119
9.99	162	30.3	161
12.0	178	38.0	206
13.6	196	43.8	257
15.1	215	51.0	311
16.5	237	57.6	372
16.9	242	59.5	388
17.8	262	63.9	444

[a] Temperature coefficient of the sensor was 0.354 Ω/°C.

required when switching from one column configuration to another. Five adjustable restrictors are provided for this purpose. They are contained in a stainless-steel restrictor block that is mounted on the manifold. These restrictors are identical and consist of stainless-steel mandrels which ride in plastic sleeves (with a 0.0005-in. interference fit). They are threaded with a variable-depth thread from 0.0035-in. deep at maximum to zero in five and one half turns.

Thermal conductivity detectors

Only four detectors are required to support the configuration outlined in Fig. 3 (a fifth is provided to be used as a reference detector if desired). They are identical, each consisting of a 1-μm platinum wire welded to two posts of a glass-to-metal-sealed header soldered to a brass metal holder. A cavity (approximately 0.08 μl volume) is previously ground (or etched) into the glass under the platinum wire. This open-faced detector block is attached to the manifold and connections to the appropriate holes in the manifold are made through the mounting gaskets.

The nominal room temperature resistance of the detector filament is 100 Ω. The characteristics of a typical detector element are given in Tables 1 and 2.

The slight variation of sensitivity with carrier gas flow-rate that was observed was attributed to the design requirement for a fast responding detector to support high-speed chromatography. This necessitated placement of the filament in the flow stream with a consequent increase in the specific heat, flow-sensitive, component of the detector signal. In any case, it was felt that the observed flow dependence was not large enough to constitute a problem.

As has been reported elsewhere [8], the rather large time constant of currently manufactured gas chromatographs seriously limits the performance of these systems to support high-speed analysis. Using a large 84-μl sample loop (to create a frontal chromatogram) to inject propane–helium (4.8:95.2) mixtures into the present detector, the time constants (time to reach 67% of the final peak height) at various flow-rates were determined and plotted versus the reciprocal of flow-rate (see ASTM E 516-74 [11]), The intercept of this plot yielded a system time constant of less than 0.5 ms.

Table 2
Variation of sensitivity with flow-rate of carrier gas

Flow-rate (ml/min)[a]	Sensitivity (mV/mol% propane)
1.7	43.9
2.5	44.0
3.2	43.9
4.3	44.4
5.6	44.3
7.0	44.8
8.0	44.9

[a] Flow-rate of propane–helium (1:99).

Table 3
Comparison of experimental vs. theoretical peak widths for a system time constant of 5 ms

Component	Flow-rate 3.6 ml/min				Flow-rate 6.9 ml/min			
	Retention time (s)		Peak width (s)		Retention time (s)		Peak width (s)	
	Theoretical	Experimental	Theoretical	Experimental	Theoretical	Experimental	Theoretical	Experimental
Unretained	8.19	8.40	0.14	0.15	4.71	4.74	0.07	0.08
Ethane	8.79	8.80	0.22	0.16	5.06	4.92	0.14	0.10
Propane	9.81	9.60	0.31	0.22	5.65	5.40	0.22	0.16

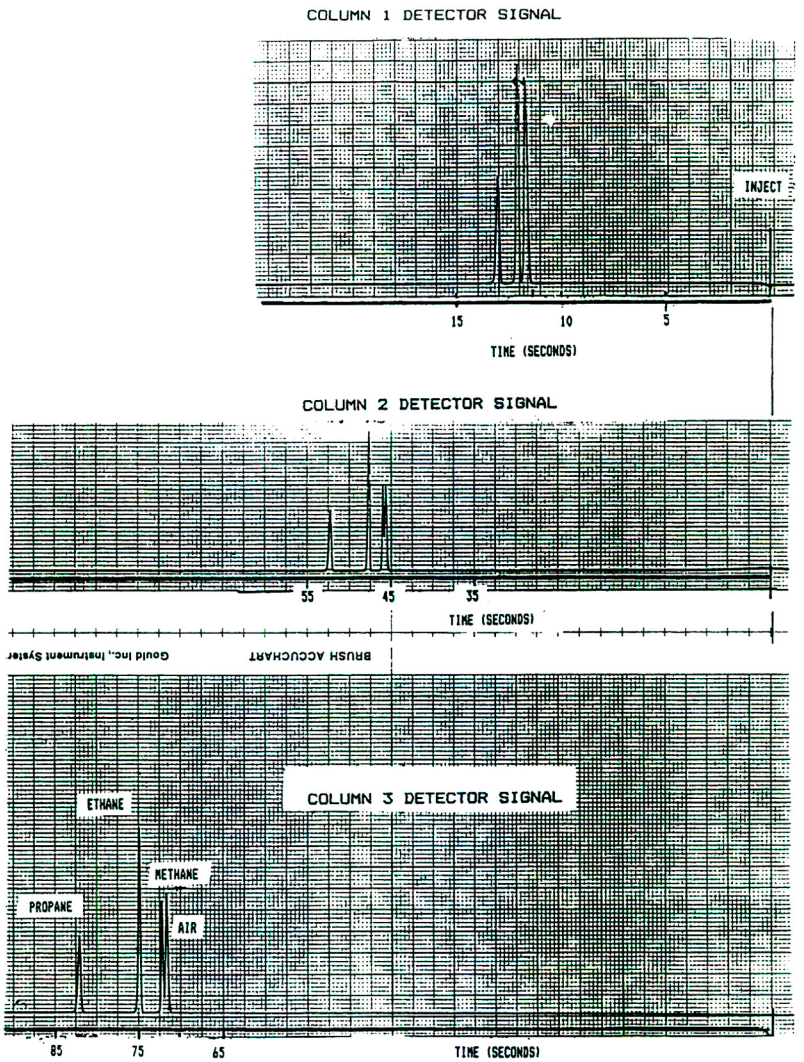

Fig. 4. Performance chromatograms obtained at D1, D2 and D3 for the flow configuration illustrated in Fig. 3. Stationary phase = GB-1 at film thickness 1.0 μm. FSOT column of 0.25 mm I.D., C1 = 7 m, C2 = 25 m, C3 = 27 m; temperature, ambient; carrier gas, helium at 34.65 p.s.i.g. (1 p.s.i. = 6894.76 Pa); sample: methane–ethane–propane–helium (10:10:8.5:71.5).

To determine the overall system time constant for the normally used impulse injection mode of operation, a sample loop of 0.06 μl was used to inject a ethane–propane–helium (10:8:82) mixture into a 7 m × 0.25 mm I.D., film thickness 1.0 μm, OV-1 column at various flow-rates of carrier gas. The observed peak widths were compared to that predicted from a theoretical model [9] for systems of various time constants. The closest correspondence was found to be for a system with a 5 ms time constant (see Table 3). This was well within the response that was required to support the projected chromatographic peak widths (50 to 100 ms) for which this unit was being designed.

As mentioned previously, the detectors were powered in the constant-resistance mode. This procedure insured not only a fast responding system, but one that was protected from burnout under large sample loads or when carrier gas was turned off. The time constant for the electronic portion of the package (with the detector element in the circuit) was found to be less than 0.2 ms.

With this system, when the filament was excited to yield a sensitivity of 3.3 μV/ppm (v/v) propane, the peak to peak noise level was found to be 14.9 μV. Thus, under these conditions the minimum detection level was calculated to be 9 ppm (v/v) propane.

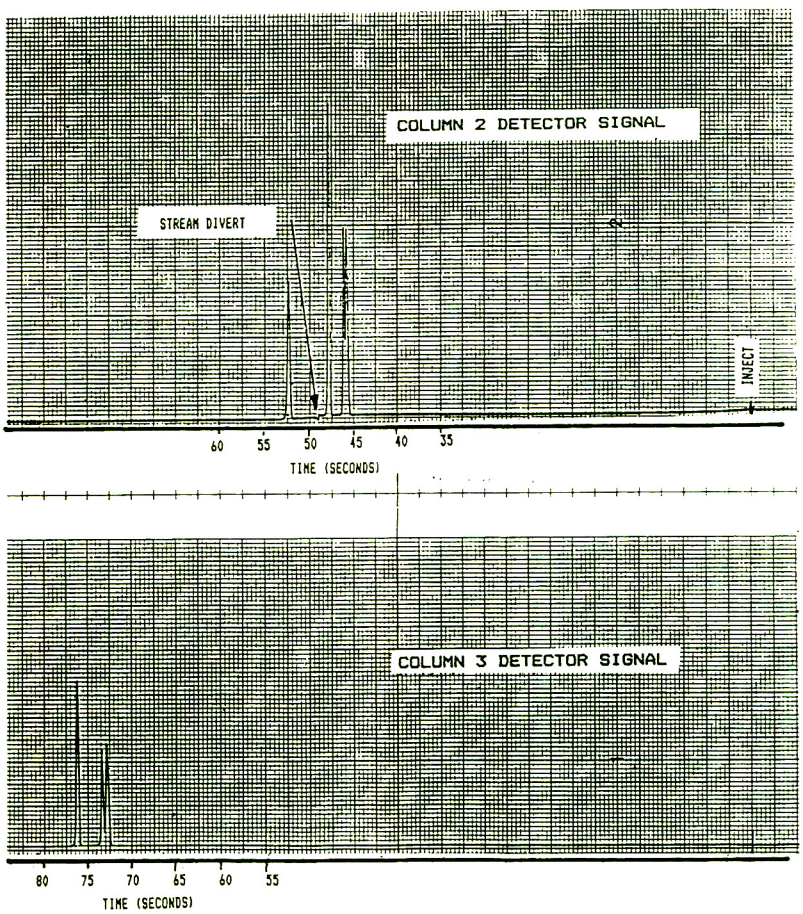

Fig. 5. Performance chromatograms obtained at D1, D2 and D3 when V2 is switched to the divert-to-vent position after the appearance of ethane. Propane is diverted to vent and never enters C3. Thus the chromatogram from D3 contains only air, methane and ethane peaks. Conditions are the same as described for Fig. 4.

3. Results

3.1. Performance of the system

Typical chromatograms obtained from the unit under a variety of column/detector switching arrangements are shown in Figs. 4–6. As can be seen by examining those signal channels that involve column switching, flow balancing was sufficiently accurate to eliminate significant baseline upsets during the switching.

Since many of the flow passages involve rather abrupt 90° changes in direction with consequent changes in the flow profile, it was expected that some degree of peak tailing would result.

And indeed, some asymmetry was observed. For example, a high-speed chromatogram of methane, ethane and propane on a 7.0 m × 0.25 mm OV-1 column of 1.0 μm film thickness produced asymmetries of 1.16, 1.19 and 1.30 for the respective peaks. As will be demonstrated in the following BTU application, this degree of asymmetry does not seriously limit the performance of the unit.

3.2. Application to the BTU determination of natural gas

The following experiments were performed on a prototype unit similar to that shown in Figs. 1 and 2. However, the electronics enclosure was empty except for the oven-temperature controller, valve solenoids and driver electronics. The detector power supply and data acquisition hardware were breadboarded and external to the unit.

Four columns were used for the British Thermal Unit (BTU; 1 BTU = 1054.35 J) determination of natural gas with the proper I.D., lengths and film thicknesses being determined by our computer-aided multicolumn design program [10]. Three of the columns were analysis columns

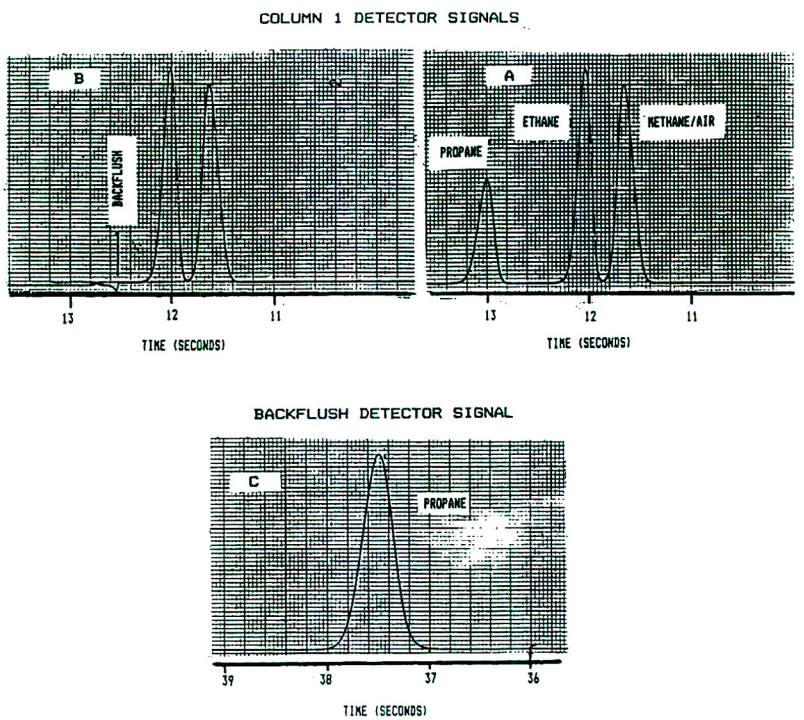

Fig. 6. Performance chromatograms obtained from D1 and D4 illustrate what is observed when V1 is returned to the backflush position after the detection of ethane at D1. Propane is backflushed from C1 and appears at D4. Conditions are the same as Figs. 4 and 5 except that for illustrative purposes a faster chart speed was used to record the chromatograms.

while the fourth, acted only to delay the appearance of any peaks at D3 until after the effluent from D2 had been diverted to vent. This simplified writing the "peak find/analysis" code since no provision was then necessary to allow for possible baseline perturbations during the stream-switching operation.

The chromatograms simultaneously recorded

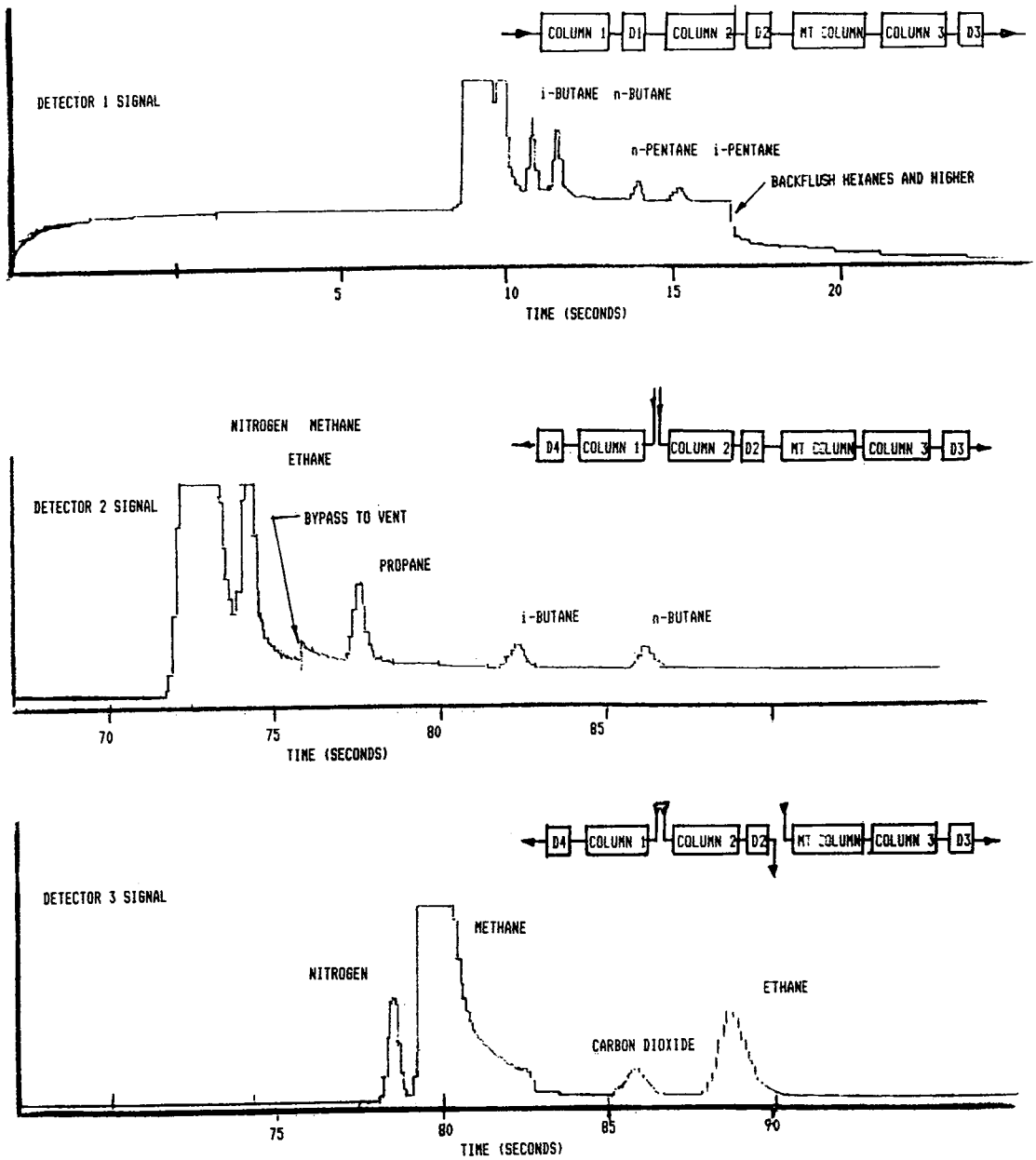

Fig. 7. Chromatograms available at D1, D2 and D3 during a natural gas BTU analysis. GB-1 at 1.0 μm film thickness are used in columns 1 (5 m × 0.25 mm) and 2 (25 m × 0.25 mm). A delay column of 2 m × 0.25 mm was used between D2 and the third column [40 cm × 0.56 mm, 140–170 mesh (105–88 μm), Hayes Sep. T]. Helium carrier gas at 48.5 p.s.i.g.; temperature, 60°C; sample described in Table 4; i = iso.

Table 4
Standard BTU gas sample

Component	Mol%
Nitrogen	2.52
Carbon dioxide	1.003
Methane	90.64
Ethane	3.99
Propane	0.994
Isobutane	0.302
n-Butane	0.298
Isopentane	0.101
n-Pentane	0.103
n-Hexane	0.050

at the various detectors for a typical analysis along with the pertinent column configurations are shown in Fig. 7. Not shown due to space restrictions is the chromatogram recorded at D4 (the regrouped heavies). Also the full recording of D2 would show the elution of *n*-pentane at 112 s and isopentane at 122 s.

The analysis was conducted at 60°C on a standard BTU sample whose composition is given in Table 4. Helium was used as carrier gas at 4.27 ml/min.

Analysis is complete in just over 2 min —much faster than can be obtained with other analyzers currently on the market. Typically, using a 3-min cycle the analysis of a 1036 BTU/ft^3 sample had a standard deviation of 0.87 BTUs/ft^3.

4. Conclusions

The successful design of a rapidly replaceable GC cartridge so necessary for a viable FMPGC system has been demonstrated by the results reported herein. Moreover, this design supports the high-speed chromatography needed for the short turnaround analysis time in control applications.

Acknowledgements

The author gratefully acknowledges the contributions of other members of the team, Mr. Edward Lewis for mechanical engineering, Mr. Mathew Phillips for package design and Mr. Bent Norlund and Mr. John Cox for electronic design. The column/detector/valve geometry was suggested by Mr. R. Villalobos.

References

[1] R. Villalobos, *Anal. Chem.*, 47 (1975) 983A.
[2] H.M. McNair, *Am. Lab.*, 19, No. 1 (1987) 17.
[3] R. Annino, *Am. Lab.*, 21, No. 10 (1989) 60.
[4] R. Annino and R. Villalobos, *Process Gas Chromatography, Fundamentals and Applications*, Instrument Society of America, Research Triangle Park, NC, 1992.
[5] S.C. Terry, J.H. Jerman and J.B. Angel, *IEEE Trans. Electr. Dev.*, 26 (1979) 1880.
[6] G. Gaspar, P. Arpino and G. Guiochon, *J. Chromatogr. Sci.*, 15 (1977) 256.
[7] R. Annino and J. Leone, *J. Chromatogr. Sci.*, 20 (1982) 19.
[8] R. Annino and R. Villalobos, presented at the *20th FACS Meeting, Detroit, MI, October 17–22, 1993.*
[9] R. Villalobos and R. Annino, *J. High Resolut. Chromatogr.*, 12 (1989) 149.
[10] R. Villalobos and R. Annino, *J. High Resolut. Chromatogr.*, 13 (1990) 764.
[11] ASTM Standards on Chromatography, American Society for Testing and Materials, Philadelphia, PA, 1st ed., 1981, method ASTM E 516-74.

ELSEVIER

Journal of Chromatography A, 678 (1994) 289–297

JOURNAL OF CHROMATOGRAPHY A

Large-volume injections in gas chromatography–atomic emission detection: an approach for trace-level detection in water analysis

F.D. Rinkema, A.J.H. Louter*, U.A.Th. Brinkman

Department of Analytical Chemistry, Free University, De Boelelaan 1083, 1081 HV Amsterdam, Netherlands

First received 15 March 1994; revised manuscript received 25 May 1994

Abstract

The ruggedness and analytical performance of on-line capillary gas chromatography–atomic emission detection (GC–AED) have been studied using 100-μl injections of sample solutions in ethyl acetate, via a loop-type interface. A series of organophosphorus compounds were selected as test analytes; they were monitored using the carbon, sulphur, nitrogen, chlorine, bromine and phosphorus channels. The system showed no flame-outs or other maintenance problems even after 300 large-volume injections. The analytical potential of the system, expressed in terms of repeatability, linearity and minimum detectable amount, was not affected and a 100-fold increase in analyte detectability, in terms of concentration units, compared with a conventional 1-μl injection was observed.

As an application, GC–AED was combined off-line with solid-phase extraction. Several environmental contaminants were preconcentrated from river and tap water samples, and 20% (100 μl) of the ethyl acetate eluent were directly analysed. With a sample volume of only 10 ml, the detection limits of the organophosphorus pesticides typically were ca. 0.1 μg/l.

1. Introduction

Atomic emission detection (AED) is a selective detection method specifically designed for capillary gas chromatography (GC) which is, in principle, capable of detecting any element except helium [1]. Although the minimum detectable amounts vary greatly per element [2] and, for several elements, are distinctly higher than are found with other selective detection systems such as nitrogen–phosphorus (NPD) or electron-capture (ECD) detection [3], the multi-element detection capability makes AED highly interesting for, e.g., rapid screening and surveying studies. The information so obtained will often be complementary to that collected by means of GC with mass spectrometric (MS) detection. In order to improve the analyte detectability of GC–AED and, also, to explore the potential of an on-line coupling of column liquid chromatography (LC) or LC-type solid-phase extraction (SPE) approaches, i.e. SPE–GC–AED (cf. Refs. [4–6]), the use of large-volume injections of, typically, 100 μl has been studied in this paper. Compared with the 1-μl injections conventionally used in capillary GC, such large-volume injections should improve analyte detectability (in concentration units) by about two

* Corresponding author.

0021-9673/94/$07.00
SSDI 0021-9673(94)00484-Q

orders of magnitude and, consequently, should make GC–AED highly suitable for trace-level environmental analysis. In the present project, from among the interfaces commonly used to enable large-volume injections [7], the loop-type interface was selected because it is the least complicated to operate and, actually, allows injection volumes up to several millilitres.

In work on on-line SPE–GC, ethyl acetate is often used as a desorption solvent [8–10]. Since SPE–GC–AED is one of the goals we have in mind (see above), ethyl acetate was also used in this study. The several approaches to large-volume injection GC and on-line SPE–GC have been discussed in the recent past [4–6]. Although there are apparently no real problems with such techniques irrespective of the detector selected, this will probably not be true for rather vulnerable detection devices such as a Fourier transform infrared detector or an AED system. The primary goal of the present study was therefore to test, and improve, the ruggedness of the GC–AED system. Eleven organophosphorus pesticides (OPPs) were selected as model compounds. They contain several hetero atoms (Cl, Br, S, P, N, O) which for the present study has the advantage that several AED channels can be tested. Finally, since OPPs can be extracted rather easily from water on C_{18}-bonded silica or polymer sorbents [11], the off-line combination of SPE and GC–AED was briefly studied as a first attempt to assess the practicality of on-line SPE–GC–AED.

2. Experimental

2.1. Chemicals

Benzothiazole, bromophos-ethyl, coumaphos, diazinon, ethion, fenchlorphos, mevinphos, parathion-ethyl, pyrazophos, sulphotep, tetrachlorvinphos, triazophos and triphenylphosphine oxide were obtained from Riedel-de Haën (Seelze, Germany). The structures of the analytes are shown in Fig. 1. Ethyl acetate and HPLC-grade water were purchased from J.T. Baker (Deventer, Netherlands) and methanol from Rathburn (Walkerburn, UK). High-purity helium gas (5.0 purity grade) was obtained from Union Carbide (Westerlo, Belgium). Stock solutions of the analytes were prepared in methanol and ethyl acetate. Spiked solutions were prepared by spiking water samples with an aliquot of the stock solution.

All river water samples were filtered over 0.45-μm membrane filters (Schleicher & Schuell, Dassel, Germany), Amsterdam tap water was directly used for preconcentration without any pretreatment.

2.2. GC equipment

A Hewlett-Packard (Avondale, CA, USA) Model 5890 Series II gas chromatograph with a Hewlett-Packard Model 5921 A atomic emission detector and a Hewlett-Packard Model 7673 autosampler were used for GC–AED.

The GC–AED large-volume injection system is shown in Fig. 2. It consists of a loop-type interface with a 100-μl stainless-steel loop, a 9 m $\times$ 0.53 mm I.D. diphenyltetramethyldisilazane-deactivated retention gap (BGB Analytik, Zurich, Switzerland), a 3 m $\times$ 0.32 mm I.D. DB-17 (J & W, Folsom, CA, USA) retaining precolumn with a film thickness of 0.25 μm and a 25 m $\times$ 0.32 mm I.D. DB-17 analytical column with a film thickness of 0.25 μm. Connections were made with press-frit connectors (Chrompack, Middelburg, Netherlands). The early solvent vapour exit (SVE) was opened and closed with a 24 V pinch solenoid valve (Type S 104; Sirai, Milan, Italy) which clamped a piece of 2 mm O.D. silicone tubing. Helium was used as carrier gas.

Large-volume injections with the loop-type interface were made at a head pressure of 200 kPa and a temperature of 100°C (6 min hold time), followed by temperature programming to 270°C (final hold time, 5 min) at a rate of 20°C /min. The SVE open time was 90 s. Relevant AED parameters are recorded in Table 1.

2.3. SPE system

Trace enrichment of the OPPs from water samples was performed on a Prospekt sample preparation system of Spark Holland (Emmen,

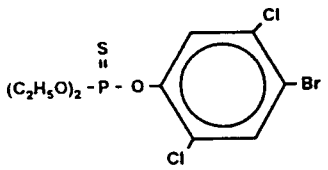

Bromophos-ethyl

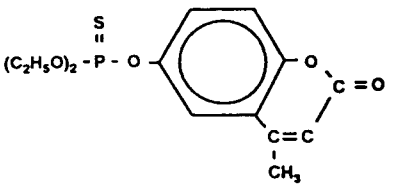

Coumaphos

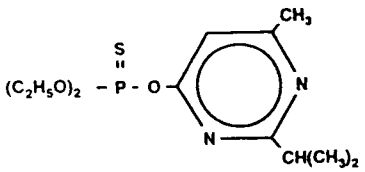

Diazinon

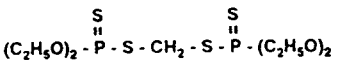

Ethion

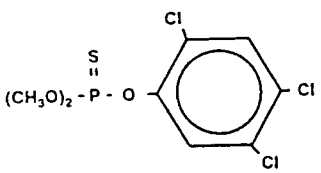

Fenchlorphos

Mevinphos

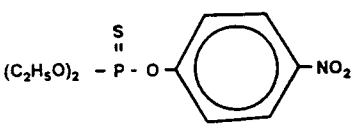

Parathion-ethyl

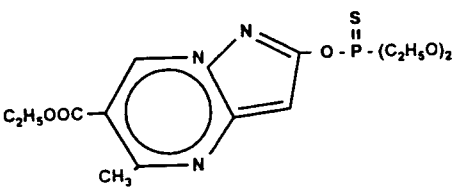

Pyrazophos

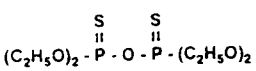

Sulphotep

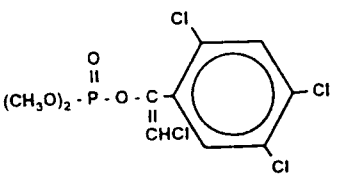

Tetrachlorvinphos

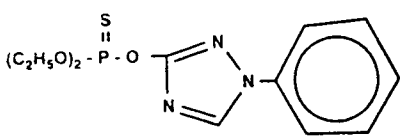

Triazophos

Fig. 1. Structural formulae of the organophosphorus pesticides used as test analytes.

Netherlands) [12]. The Prospekt system contains three pneumatic Rheodyne six-port valves, an automated cartridge exchanger and a solvent delivery unit equipped with a six-port solvent delivery valve and single-piston LC pump. Timed events such as valve switching, solvent

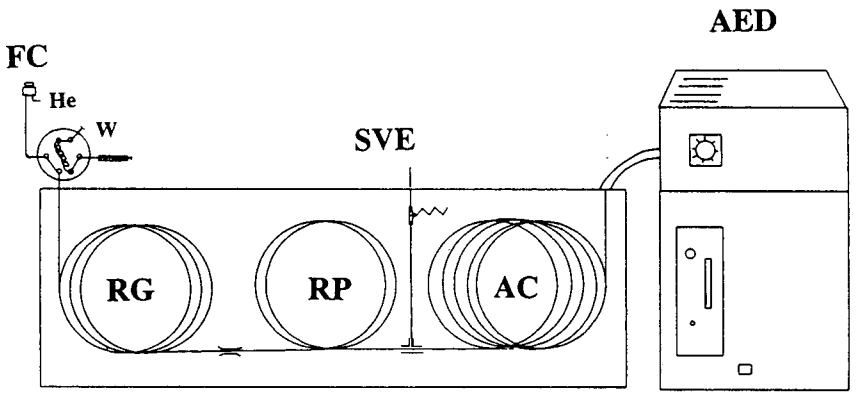

Fig. 2. Instrument configuration of large-volume injection GC–AED. AC = Analytical column; FC = flow controller; RG = retention gap; RP = retaining precolumn; SVE = solvent vapour exit; W = waste.

selection and on/off switching of auxiliary channels could be programmed via software on the Prospekt controller unit.

Water samples were preconcentrated on 10 mm × 1.5 mm I.D. precolumns packed with PLRP-S (15–25 μm) styrene–divinylbenzene copolymer (Spark Holland). A MicroMetric pump from Milton Roy (Riviera Beach, FL, USA) was used for delivering the desorption solvent ethyl acetate, which was collected in a GC autosampler vial (Chrompack). Prior to use the cartridges were conditioned with 500 μl of ethyl acetate and 2.5 ml of HPLC-grade water. A 10- or 50-ml water sample was preconcentrated at a flow-rate of 5 ml/min, and, next, clean-up was carried out with 1 ml of HPLC-grade water. The cartridge was dried by 30 min of nitrogen gas purging at 3 bar. Finally desorption was carried out with 500 μl of ethyl acetate at a flow-rate of 100 μl/min.

Table 1
AED parameters used for GC–AED

Element	Wavelength (nm)	Scavenger gas	Make-up flow (He, ml/min)
C	193.0	H_2, O_2	40
S	181.4	H_2, O_2	40
N	174.2	H_2, O_2	40
P	185.9	H_2	80
Cl	480.2	O_2	40
Br	478.6	O_2	40

Spectrometer purge rate: 2 l/min of nitrogen; transferline temperature: 300°C; cavity temperature: 300°C; window purge flow-rate: 40 ml/min; solvent vent time: 7 min; waterbath temperature: 65°C.

3. Results and discussion

3.1. Large-volume injections: system ruggedness and performance

The first aim of the study was to test the robustness and analytical performance of the GC–AED system or, rather, of the AED system as a detector when using large-volume injections. As regards the latter aspect, studying element responses in terms of linearity, repeatability and analyte detectability appeared to be good criteria. The injection volume selected was 100 μl, because this is a typical volume for both LC–GC heart-cut and SPE–GC desorption operations. Besides, the two-order magnitude difference with 1-μl injections should create sufficient trace-enrichment potential.

Preliminary experiments using the original set-up —i.e. without an early solvent vapour exit— showed that the injection of 100-μl samples in ethyl acetate did not cause any flame-outs [13]. However, the evaporation rate through the AED solvent vent was rather low. Consequently, too much time was required to evaporate the solvent and early-eluting compounds were lost in the

solvent peak. However, if a second, so-called early solvent vapour exit (SVE, cf. Fig. 2) was inserted between the retention gap and the retaining precolumn, the solvent evaporation rate became sufficiently high to prevent such problems. At an oven temperature of 100°C, the evaporation of 100 μl of ethyl acetate now took 78 s. The SVE was closed after 90 s.

With the complete set-up of Fig. 2, the ruggedness of the GC–AED set-up under large-volume-injection conditions turned out to be excellent. No plasma flame-outs occurred even after 300 injections. The combined chromatograms obtained after three injections (the C, S and N channels can be monitored simultaneously, as can the Cl and Br channels; the P channel had to be monitored separately) of 100 μl of a standard solution of the eleven OPPs (100 pg/μl in ethyl acetate or 10 ng injected per compound) is shown in Fig. 3. The six traces shown are all of good quality. As regards the analytes, bromophos-ethyl is the most interesting compound because it shows up in five out of the six traces. The repeatability obtained for these injections was comparable with the repeatability obtained with 1-μl injections (see Table 2). Actually, the R.S.D. values themselves are quite satisfactory for all but the N channel. This may well be due to the fact that the injected amounts were rather close to the detection limit with this relatively insensitive channel (10 ng corresponds to S/N ratios of 3–10; see Table 3 below). We have no explanation for the poor repeatability observed for tetrachlorvenphos with 100-μl, but *not* 1-μl, injections on all three relevant channels.

The linearity of the AED response was tested in the 0.5–50-ng range both for 100-μl and 1-μl injections for all six elements monitored (six data points; $n = 2$). For the C, S and N channels, the regression coefficients, R^2, were equal to or better than 0.992, 0.9981 and 0.9968, respectively. There was one exception only, viz. pyrazophos (N channel) with $R^2 = 0.9647$ for 1-μl as against, fortunately, $R^2 = 0.9996$ for 100-μl injections. The R^2 values for the Cl, Br and P channels were at least 0.9984, 0.9998 and 0.9974, respectively. Actually, the results for the 100-μl injections were slightly better than those for the 1-μl studies.

In Table 3 the absolute detection limits (S/N = 3) of all OPPs for 100-μl injections are given, both per compound and per element. It is evident, as is also known from literature [1,14], that from among the six channels tested, the S and P channels display the best sensitivity. With analyte detection limits of below 100 pg (S) and 50–300 pg (P), respectively, for most of the OPPs tested, GC–AED with 100-μl injections

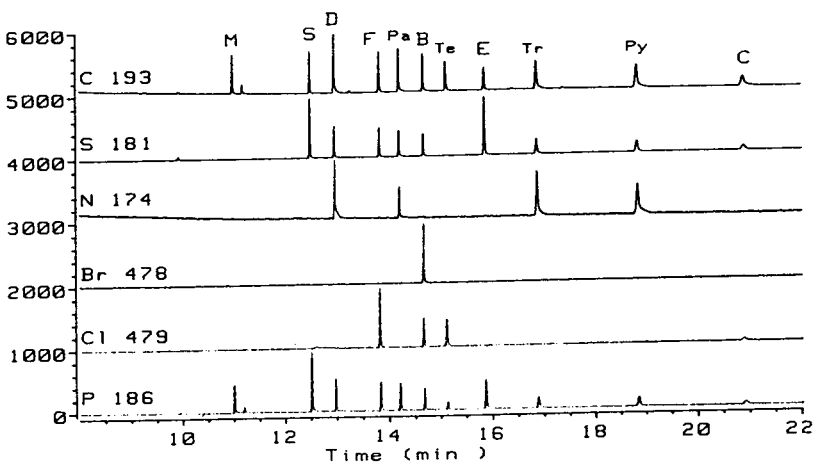

Fig. 3. GC–AED chromatogram (recording of the C, S, N, Cl, Br and P traces) obtained after 100-μl injections of OPPs in ethyl acetate (100 pg/μl). Peaks; M = mevinphos; S = sulphotep; D = diazinon; F = fenchlorphos; Pa = parathion-ethyl; B = bromophos-ethyl; Te = tetrachlorvinphos; E = ethion; Tr = triazophos; Py = pyrazophos; C = coumaphos.

Table 2
Relative standard deviations (R.S.D.s; $n = 8$) of 100-μl/1-μl injections of OPP mixture in ethyl acetate

Compound	R.S.D. (%) for channel:					
	C	S	N	Cl	Br	P
Mevinphos	2.2/1.6	–	–	–	–	3.7/3.2
Sulphotep	1.8/0.9	2.0/1.9	–	–	–	3.9/2.7
Diazinon	1.9/1.0	2.7/1.9	12/6.6	–	–	5.1/3.1
Fenchlorphos	3.1/2.1	2.7/3.2	–	2.4/1.6	–	4.1/3.2
Parathion-ethyl	2.8/5.0	2.9/2.1	10/13	–	–	5.2/3.7
Bromophos-ethyl	2.6/3.7	2.6/2.9	–	2.9/2.3	1.4/3.2	3.7/5.0
Tetrachlorvinphos	9.9/3.7	–	–	14/4.2	–	21/5.7
Ethion	2.9/1.9	2.9/2.8	–	–	–	3.7/3.6
Triazophos	3.6/3.5	5.0/4.2	17/13	–	–	7.0/6.7
Pyrazophos	3.0/5.1	4.3/7.4	26/13	–	–	4.8/8.0
Coumaphos	3.6/4.9	4.8/5.8	–	6.8/17	–	5.5/6.1

Analyte concentrations 100 pg/μl and 10 ng/μl for 100- and 1-μl injections, respectively; i.e., injected amount, 10 ng.

obviously becomes attractive for (selective) trace-level environmental analysis. Further it should be noted that the relatively high detection limits observed for the late-eluting pyrazophos and coumaphos are caused by their larger peak width rather than due to a lower element response.

Finally, a direct comparison of the conventional 1-μl and large-volume 100-μl approach was made by injecting all OPPs in standard solutions containing 10 ng/μl and 100 pg/μl of analyte, respectively. That is, the injected amount of the analytes was the same, i.e. 10 ng, in both series. The results showed that the AED response for the 1- and 100-μl injections was the same within 10–20% for all channels and all analytes tested. In other words, the expected 100-fold increase in analyte detectability (in terms of concentration units) was indeed found.

3.2. Off-line SPE–GC–AED

In order to demonstrate the usefulness of 100-μl injection GC–AED and to provisionally explore the potential of on-line SPE–GC–AED, large-volume GC–AED was combined off-line with SPE, using spiked surface and tapwater as real-life samples. As a first test, the analyte

Table 3
Detections limits (pg; $S/N = 3$) per compound (element) for 100-μl injections of OPPs in ethyl acetate

Compound	Detection limit (pg) for channel					
	C	S	N	Cl	Br	P
Mevinphos	575 (220)	–	–	–	–	250 (35)
Sulphotep	300 (90)	20 (4.0)	–	–	–	40 (8)
Diazinon	225 (100)	40 (4.0)	975 (90)	–	–	80 (9)
Fenchlorphos	175 (50)	40 (4.0)	–	240 (80)	–	80 (7)
Parathion-ethyl	325 (140)	40 (4.5)	2000 (100)	–	–	110 (12)
Bromophos-ethyl	375 (110)	60 (4.5)	–	330 (60)	560 (110)	120 (10)
Tetrachlorvinphos	1250 (410)	–	–	860 (330)	–	370 (30)
Ethion	500 (140)	20 (6.0)	–	–	–	75 (12)
Triazophos	1100 (510)	90 (9.0)	1650 (220)	–	–	360 (35)
Pyrazophos	850 (380)	140 (12)	3000 (330)	–	–	450 (35)
Coumaphos	1550 (730)	240 (21)	–	3900 (380)	–	900 (75)

Table 4
Recoveries (and R.S.D.s; $n = 5$) of eleven OPPs in off-line SPE–GC–AED

Compound	Recovery (%)	R.S.D. (%)
Mevinphos	87	7
Sulphotep	95	6
Diazinon	110	9
Fenchlorphos	85	4
Parathion-ethyl	95	10
Bromophos-ethyl	42	22
Tetrachlorvinphos	86	9
Ethion	72	11
Triazophos	104	5
Pyrazophos	96	4
Coumaphos	102	18

For experimental details, see text.

recoveries and the repeatability of the procedure were determined by spiking HPLC-grade water with 1 μg/l of all eleven OPPs and preconcentrating 10 ml of the spiked sample on a SPE cartridge. For desorption, 500 μl of ethyl acetate proved to be sufficient. From the eluate, 100 μl (or 20%) were injected into the GC–AED system. The results which were determined using the P 186 channel and which are reported in Table 4 show that good recoveries (85–110%) were obtained for all but two test analytes (ethion and bromophos), while the R.S.D. values are satisfactory for such trace-level work. Since demonstration of the general usefulness of the procedure rather than a dedicated application was the primary aim of the study, no attempt was made to improve the recoveries of ethion and bromophos.

As a real-life application, the off-line SPE–GC–AED chromatograms recorded for 10 ml of river Rhine water without and with a 1-μg/l OPP spike are shown in Fig. 4. It is obvious that the detection limits are in the order of 0.1–0.5 μg/l for all compounds; that is, they are below the alert and alarm levels for pesticides in surface water, which are 1 and 3 μg/l, respectively. It is also clear that none of the selected OPPs is present in the surface water sample at such levels.

As another example, 50 ml of tap water were preconcentrated using the same procedure as before, the only difference being that 340 μl of ethyl acetate were now used for desorption. Chromatograms of blank tap water, and tap water spiked with 0.1 μg/l of triphenylphosphine oxide (TPPO) are shown in Fig. 5. The obvious presence of TPPO at a concentration of 0.05 μg/l was confirmed by means of on-line SPE–

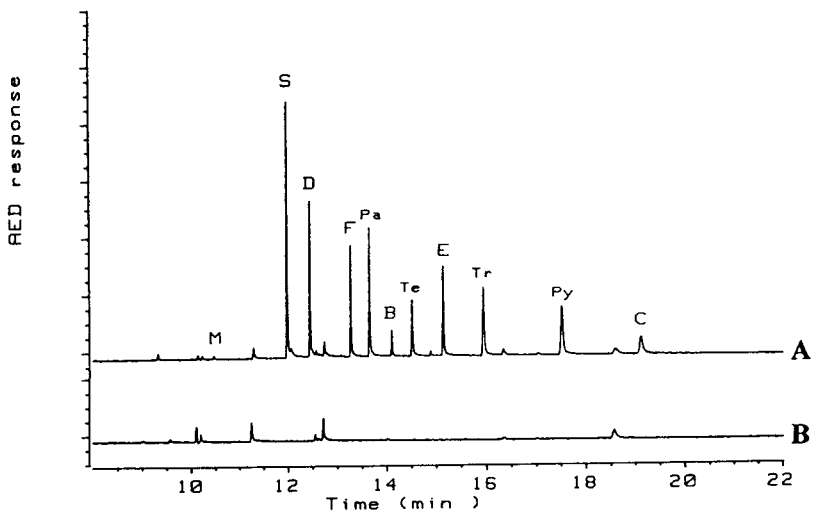

Fig. 4. GC–AED chromatograms (P trace) obtained after injection of a 100-μl aliquot (20%) of the ethyl acetate extract, resulting from preconcentration by means of SPE, of 10 ml of river Rhine water: (A) spiked with 1 μg/l of OPPs (for peak assignment, see Fig. 3), (B) blank.

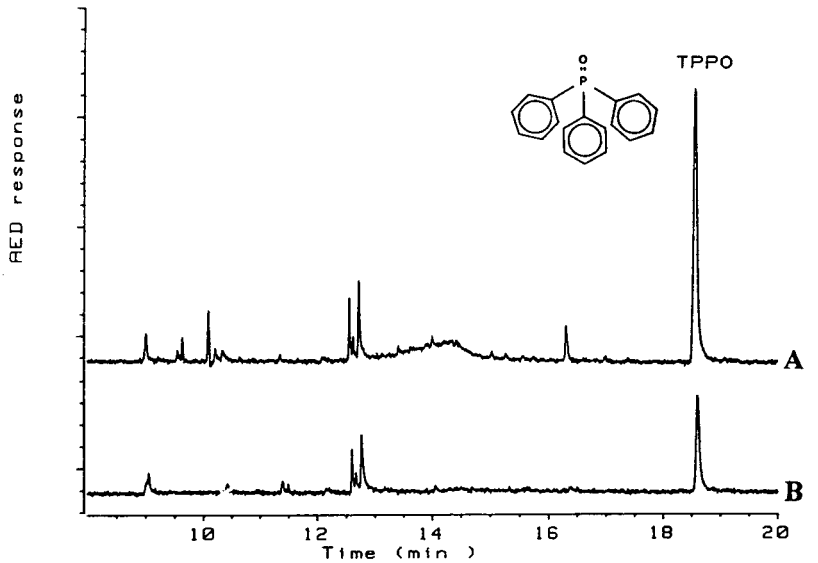

Fig. 5. GC–AED chromatograms (P trace) obtained after injection of a 100-μl aliquot (30%) of the ethyl acetate extract, resulting from preconcentration by means of SPE, of 50 ml Amsterdam tap water: (A) spiked with 0.1 μg/l of TPPO, (B) blank.

GC–MS (data not shown). From Fig. 5B one can calculate that the detection limit under the experimental conditions used (30% analyte transfer from SPE to GC–AED) is ca. 0.02 μg/l.

A final example deals with the analysis of a sample from the river Meuse in which benzothiazole (for structure, see Fig. 6) was suspected to be present [15]. 10 ml of river Meuse water were preconcentrated on a cartridge and after desorption with ethyl acetate, a 20% aliquot was injected and analysed by monitoring the C, N and S channels of the GC–AED system. The traces of Fig. 6A–C nicely illustrate the identification power of the present procedure in real-life samples, and the quantification potential even at around the 1 μg/l level (Fig 6D). Of course, the additional advantage that the three element channels can be covered in one run, will not be encountered in every study!

4. Conclusions

Contrary to what is often suggested, large-volume injections of up to 100 μl can be used in GC–AED to enhance analyte detectability without any experimental (flame-out) or maintenance problems. Linearity and repeatability are according to expectations. Two real-life applications (dealing with surface water) illustrate that environmental pollutants such as organophosphorus pesticides and benzothiazole can be identified at, typically, the 0.1–0.5 μg/l level when using 10-ml samples. In tapwater TPPO could be identified at the 0.05 μg/l level when using 50-ml samples.

The present preliminary studies on SPE combined off-line with GC–AED, with an analyte transfer of typically some 20%, strongly suggest that on-line SPE–GC–AED using 10–50-ml water samples will be a useful addition to the list of sophisticated procedures for the trace-level analysis of organic pollutants in water samples. Current research is aimed at setting up such a system.

Acknowledgement

The present work was carried out within the framework of the Rhine Basin Program (Amsterdam/Waldbronn). The authors thank Hew-

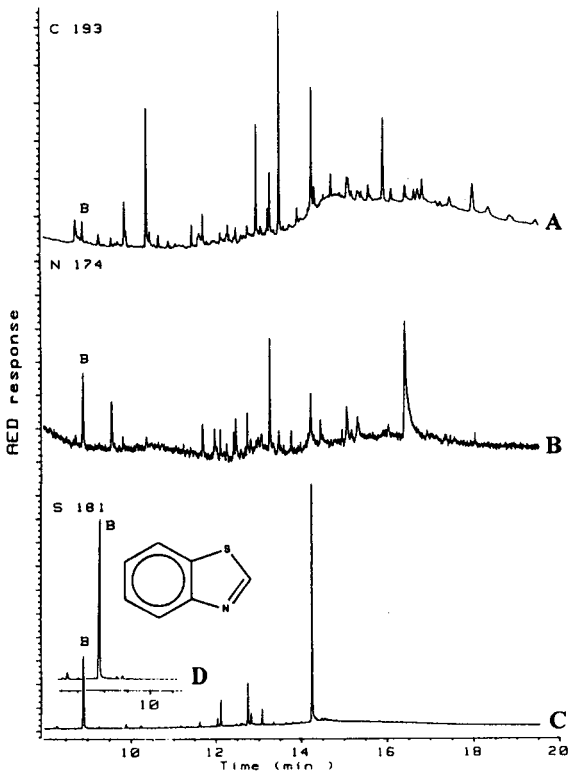

Fig. 6. GC–AED chromatograms (P trace) obtained after injection of a 100-μl aliquot (20%) of the ethyl acetate extract, resulting from preconcentration by means of SPE, of 10 ml of river Meuse water; (A) C trace, (B) N trace, (C) S trace; (D) S trace of the chromatogram obtained after injection of 100 μl of benzothiazole in ethyl acetate (20 pg/l).

lett-Packard for putting the GC–AED combination at their disposal.

References

[1] P.L. Wylie and B.D. Quimby, *J. High Resolut. Chromatogr.*, 12 (1989) 813–818.
[2] P.C. Uden, in P.C. Uden (Editor), *Element Specific Detection by Atomic Emission Spectroscopy (ACS Symposium Series*, No. 479), American Chemical Society, Washington, DC, 1992, pp. 1–24.
[3] W. Wardencki and B. Zygmunt, *Anal. Chim. Acta*, 255 (1991) 1–13.
[4] K. Grob, *J. Chromatogr.*, 626 (1992) 25–32.
[5] J.J. Vreuls, A.J.H. Louter and U.A.Th. Brinkman, in H.-J. Stan (Editor), *Chemistry of Plant Protection*, Springer, Berlin, (1994) in press.
[6] J.J. Vreuls, R.T. Ghijsen, G.J. de Jong and U.A.Th. Brinkman, *J. Assoc. Off. Anal. Chem.*, 77 (1994) 306–327.
[7] I.L. Davies, M.W. Raynor, J.P. Kithinji, K.D. Bartle, P.T. Williams and G.E. Andrews, *Anal. Chem.*, 60 (1988) 683A–702A.
[8] J.C. Moltó, Y. Picó, G. Font and J. Mañes, *J. Chromatogr.*, 555 (1991) 137–145.
[9] P.J.M. Kwakman, J.J. Vreuls, U.A.Th Brinkman and R.T. Ghijsen, *Chromatographia*, 34 (1992) 41–47.
[10] A.J. Bulterman, J.J. Vreuls, R.T. Ghijsen and U.A.Th. Brinkman, *J. High Resolut. Chromatogr.*, 16 (1993) 397–403.
[11] J. Mañes, J.C. Moltó, C. Igualda and G. Font, *J. Chromatogr.*, 472 (1989) 365–370.
[12] A.J.H. Louter, U.A.Th. Brinkman, R.T. Ghijsen, *J. Microcol. Sep.*, 5 (1993) 303–315.
[13] E.C. Goosens, D. de Jong, F.D. Rinkema, G.J. de Jong, R.T. Ghijsen and U.A.Th. Brinkman, in preparation.
[14] P.L. Wylie and R. Oguchi, *J. Chromatogr.*, 517 (1990) 131–142.
[15] A.J.H. Louter, F.D. Rinkema, R.T. Ghijsen and U.A.Th. Brinkman, *Int. J. Environ. Anal. Chem.*, 54 (1994) in press.

ELSEVIER

Journal of Chromatography A, 678 (1994) 299–312

JOURNAL OF CHROMATOGRAPHY A

Carboxylic anhydrides–orthoesters —novel reagent systems for derivatization of aminoalkanephosphonic acids for characterization by gas chromatography and mass spectrometry. III☆

Zbigniew H. Kudzin[a,*], Marek Sochacki[b], Józef Drabowicz[b]

[a]*Department of Organic Chemistry, University of Łódź, Narutowicza 68, Łódź 90-136, Poland*

[b]*Centre of Molecular and Macromolecular Studies, Polish Academy of Sciences, Sienkiewicza 112, Łódź 90-363, Poland*

First received 26 January 1994; revised manuscript received 3 May 1994

Abstract

Studies of the derivatization of aminoalkanephosphonic acids by means of carboxylic anhydrides–trialkyl orthoester systems are reported. Gas chromatographic separations of mixtures of derivatized 1-aminoalkanephosphonic acids and low-resolution electron impact mass spectra for the derivatives studied are presented.

1. Introduction

Phosphonic acids bearing amino functions have been found to possess substantial importance in pure, applied and environmental chemistry owing to their chelating [1,2] and biological properties [3,4]. For these reasons, their determination, mainly based on chromatographic methods, is of current interest in the analytical chemistry of organophosphorus compounds [5–7].

Recently we reported on the scope of the derivatization of 1-aminoalkanephosphonic acids (**1**) by means of trialkyl orthoformates [8,9], according to the equation

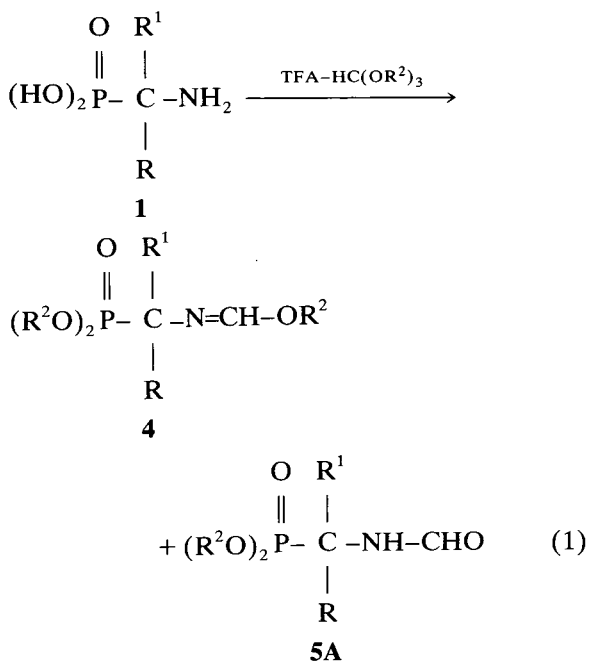

(1)

* Corresponding author.

☆ Dedicated to Professor E. Wenschuh on the occasion of his 60th birthday. Presented at the *3rd Symposium of ECOBAPHOS, Düsseldorf, April 1994.*

0021-9673/94/$07.00
SSDI 0021-9673(94)00455-I

where TFA = trifluoroacetic acid. The volatile derivatives **4** and **5** have been found to be the suitable models for analysis by gas chromatography–mass spectrometry (GC–MS), similarly to their amino ester analogues **3** [10]. However, the formation of two sets of derivatives **4** and **5** during the derivatization of **1** is a limitation of this procedure, especially in the analysis of more complex mixtures of **1**.

In this paper, we report another approach, involving the derivatization of 1-aminoalkanephosphonic acids (**1**) into the volatile N-acylaminoalkanephosphonates (**5**), which is based on the use of carboxylic anhydride–trialkyl orthoformate systems. This two-step, one-pot procedure is described by the general scheme presented in Eq. 2.

{The 1-(N-formylamino)alkanephosphonates **2AA*** and **2AB*** were described in previous papers [8,9].} An illustration of the GC–MS characteristics of the N-acylaminoalkanophosphonates **5** is also presented.

2. Experimental

2.1. Materials

Acetic acid, acetic anhydride, trimethyl orthoacetate, triethyl orthoformate, trimethyl orthoformate, trifluoroacetic acid and trifluoroacetic anhydride were purchased from Aldrich (Milwaukee, WI, USA). 1-Aminoalkanephosphonic acids (**1**) were prepared according to Ref. [11] and phosphonoglycine (**1a**) according to Ref. [12]. All aminoalkanephosphonic acids were of the purity reported previously [11,12].

2.2. Preparation of derivatives 5

The conversions of 1-aminoalkanephosphonic acids (**1**) into the volatile derivatives **5** were carried out in a Wheaton 1-ml micro product V-vial, equipped with a spin vane, placed in a thermostated oil-bath.

In order to prepare a series of 1-(N-acetylamino)alkanephosphonates (**5B**), samples of **1** (0.1–5 mg) were dissolved in acetic acid (0.05 ml)–acetic anhydride (0.05 ml) and the resulting solutions were heated with stirring at 100°C for 10 min. Then the reaction mixture was cooled to ca. 40–50°C and trialkyl orthoformate (0.4 ml) or trialkyl orthoacetate (0.4 ml) was added. The resulting mixtures were stirred at 100°C for 1.5 h (the derivatizations were usually completed after 1 h) and after this time the reaction mixtures were analysed by GC and/or GC–MS.

For the preparation of 1-(N-trifluoroacetylamino)alkanephosphonates (**5C**), samples of **1** (0.1–5 mg) were dissolved in trifluoroacetic acid (TFA) (0.05 ml)–trifluoroacetic anhydride (0.05 ml) and the solutions were heated with stirring for 10 min at 30–40°C. Then trialkyl orthoformate (0.40 ml) was carefully added and the resulting mixtures were stirred at 100°C for 1.5 h (the derivatizations were usually completed after 1 h).

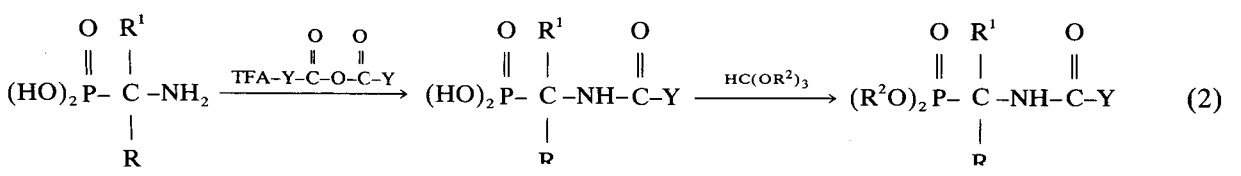

(2)

1

2

2B (Y = Me)

2C (Y = CF_3)

5

5BA* (Y = Me, R^2 = Me)

5BB* (Y = Me, R^2 = Et)

5CA* (Y = CF_3, R^2 = Me)

5CB* (Y = CF_3, R^2 = Et)

2.3. Gas chromatography–mass spectrometry

A Finnigan MAT 95 mass spectrometer was used for GC–MS analysis of the multi-component mixture of derivatives. Sample introduction was via a Varian 3400 gas chromatograph equipped with a 30 m × 0.25 mm I.D. capillary column coated with BP-17. The column temperature was 100°C for 3 min, then increased at 10°C min^{-1} to 250°C. The injector temperature was maintained at 200°C and the transfer line temperature was 250°C. The column was introduced directly into the ion source of the mass spectrometer. Mass spectra were recorded at an electron energy of 70 eV.

2.4. ^{31}P NMR

^{31}P NMR spectra were recorded on a Bruker AC 200 spectrometer operating at 81.01 MHz.

3. Results and discussion

3.1. Derivatization

The esterification of aminoalkanephosphonic acids (**1**) by means of trialkyl orthoformates afforded a mixture of forminoalkoxy (**4**) and N-formyl derivatives (**5**) according to Eq. 1 [8,9]. It was found that both the structure of **1** and the nature of the acidic catalyst exert a substantial influence on the course and the rate of derivatization [9]. Thus, 1-aminoalkanephosphonic acids with primary and secondary amino groups reacted with the TFA–trialkyl orthoformate system smoothly, with formation of corresponding amido esters. On the other hand, the esterification of 1-(N,N-dialkylamino)alkanephosphonic acids occurs much more slowly [8], which suggests that the formylation of the amino group in **1** constitutes the key step in the whole esterifica-

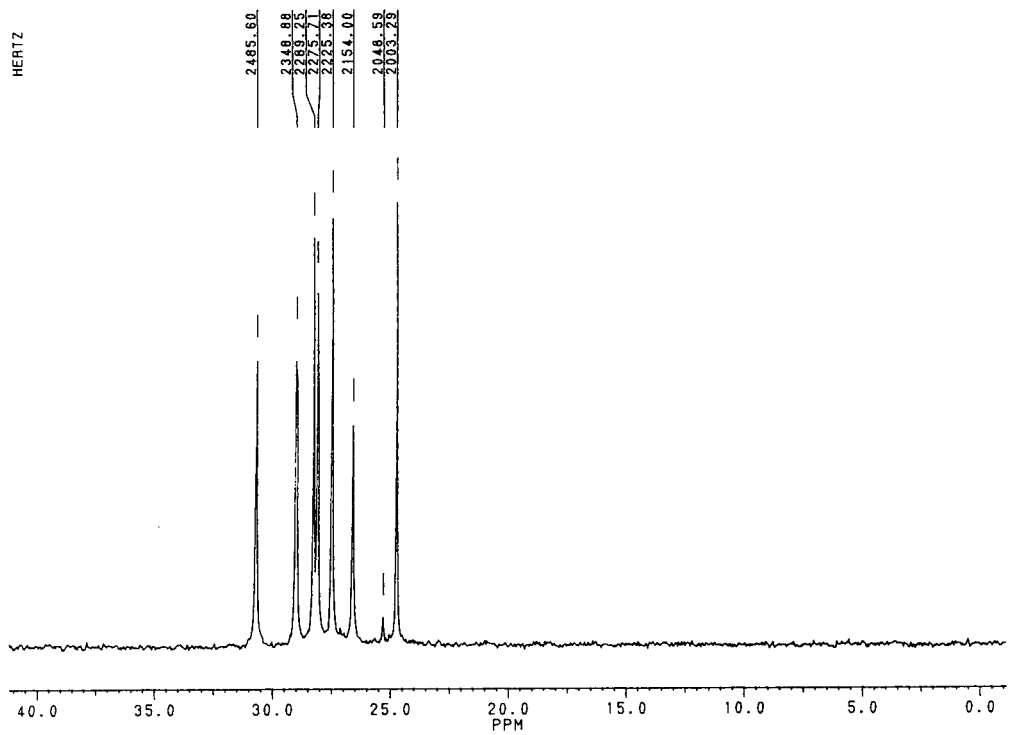

Fig. 1. ^{31}P NMR spectrum of the derivatization products **5BA*** (**a–g**) of the mixture of aminophosphonic acids [aminomethylenephosphonic (**1a**), 1-aminoethanephosphonic (**1b**), 1-aminopropanephosphonic (**1c**), 1-amino-1-methylethanephosphonic (**1d**), 1-aminopentanephosphonic (**1e**), 1-aminophenylmethanephosphonic (**1f**) and 1-amino-2-phenylethanephosphonic acid (**1g**)] obtained by means of acetic acid–acetic anhydride and trimethyl orthoacetate. Conditions as described under Experimental.

tion process of 1-aminoalkanephosphonic acids by means of orthoformates. Based on this observation (the results on the reaction course of various types of aminophosphonic acids with trialkyl orthoformates will be presented elsewhere) and in order to facilitate the conversion of **1** into their **5**, we pretreated **1** with carboxylic acid–acid anhydrides mixtures to induce the in situ formation of the N-acyl derivatives **2**. Subsequent treatment of the intermediates **2** with orthoesters afforded the desired 1-amidoalkanephosphonates (**5**) with almost quantitative NMR yields (Figs. 1 and 2).

When the N-acylation of **1** was carried out in TFA (owing to the good solubility of **1** in TFA)–acetic anhydride mixture (TFA–Ac_2O, 10 min, 40–50°C), followed by O-alkylation of the intermediate **2** with triethyl orthoformate, N-acetylaminoalkanephosphonates (**5BB***) and N-trifluoroacetylaminoalkanephosphonates (**5CB***) were found in the reaction mixture, presumably owing to the formation of mixed trifluoroacetyl–acetic anhydrides:

$$CF_3C(O)OH + CH_3C(O)OC(O)CH_3 \longrightarrow$$

$$CH_3C(O)OH + CF_3C(O)OC(O)CH_3 \qquad (3)$$

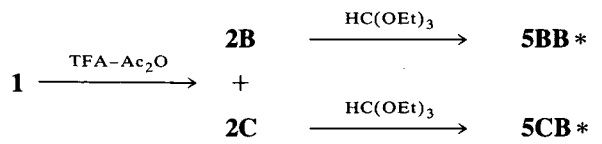

(4)

In order to determine the relative rate of esterification of amino acids **1** by means of trimethyl and triethyl orthoformates, the starting amino acids **1** were converted into 1-(N-TFA-amino)alkanephosphonic acids (**2**) and these were esterified with the mixture of trimethyl and triethyl orthoesters (1:1):

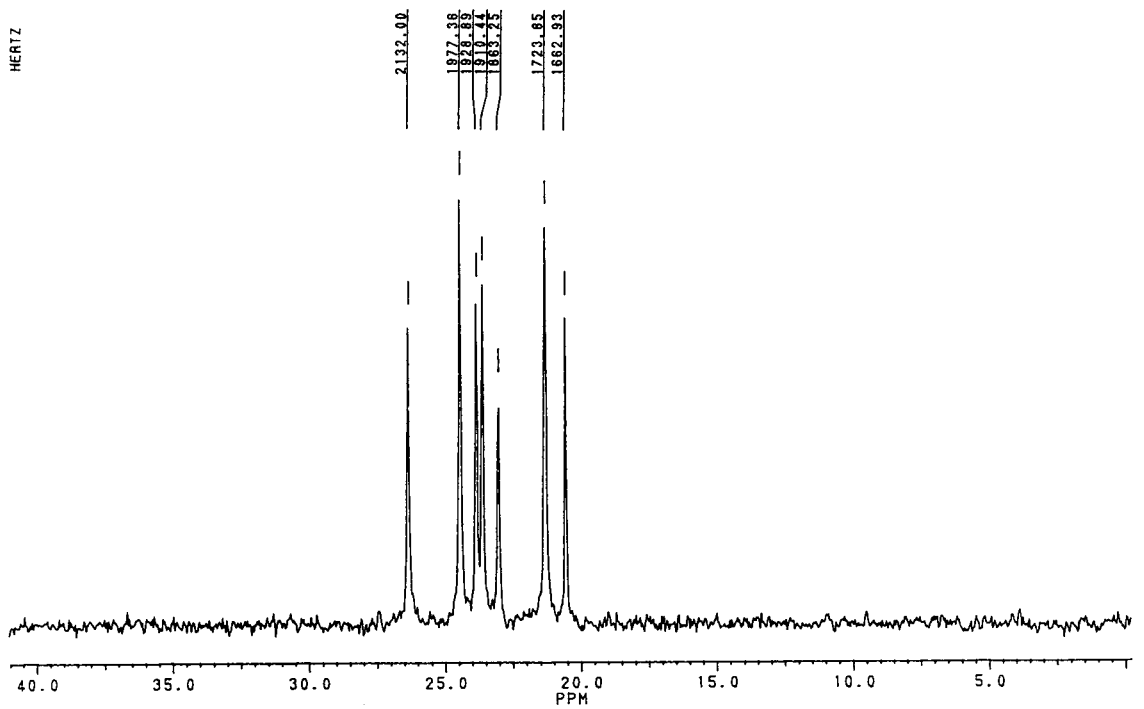

Fig. 2. ^{31}P NMR spectrum of the derivatization products **5CB*** (**a–g**) of the mixture of aminophosphonic acids **1a**, **1b**, **1c**, **1d**, **1e**, **1f** and **1g** obtained by means of trifluoroacetic acid–trifluoroacetic anhydride and triethyl orthoformate. Conditions as described under Experimental.

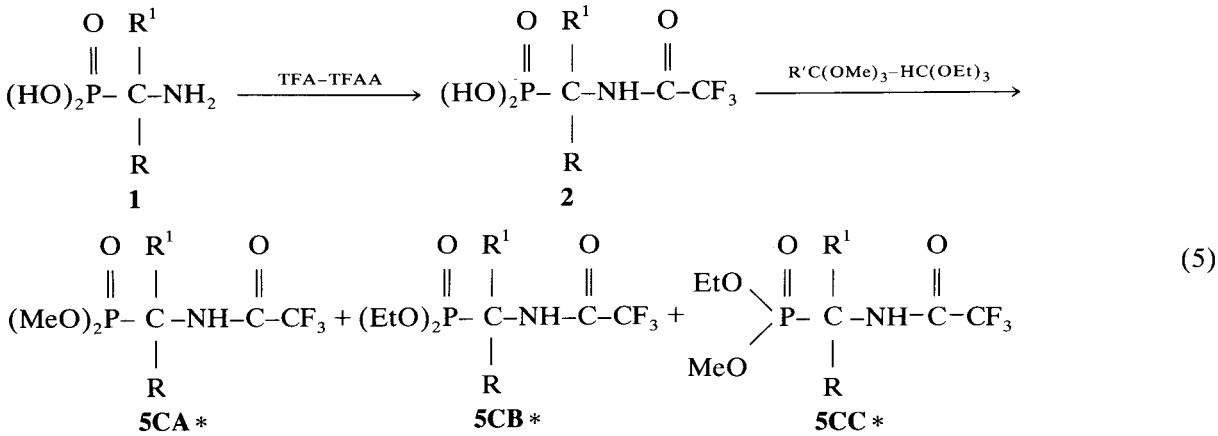

(5)

The relative amounts of the amido esters **5CA*** (O,O-dimethyl), **5CB*** (O,O-diethyl) and mixed **5CC*** (O-methyl-O-ethyl) formed reflected the alkylation capability of all the types of orthoesters applied towards the phosphonic function. Thus, the alkylation rate of derivatives **2** by means of these orthoesters generally exhibit the orders $HC(OMe)_3 < HC(OEt)_3 \approx MeC(OMe)_3$ for N-TFA-aminoalkanephosphonic acids (**2C**) and $HC(OMe)_3 \approx MeC(OMe)_3 < HC(OEt)_3$ for N-acetylaminoalkanephosphonic acids (**2B**).

A similar approach based on the prior trifluoroacetylation of **1** in the two-stage procedures for their esterification was also applied in the methods elaborated by Ruppel *et al.* [13] and

Table 1
Comparison with other methods of aminoalkanephosphonic acid derivatization

Conversion to derivative	Reagent	Time (h)	Temperature (°C)	Range (mg)	Ref.
(I) O,O-Dibutyl 1-(N-TFA-amino)alkane phosphonate	(Ms. pr.)	ca. 3		0.25–10	[13]
	(1) TFA–TFAA	1	40		
	(2) Diazobutane	0.2	20		
(II) O,O-Diethyl 1-(N-TFA-amino)alkane phosphonate	(Ms. pr.)	ca. 10		10	[14]
	(1) TFA–TFAA	1	20		
	(20 $HC(OEt)_3$	8	>130		
(III) O,O-Diethyl 1-(N-formylamino)alkane phosphonate	(One-pot pr.) $TFA–HC(OEt)_3$	2	120	0.1–5	[9]
(IV)	(One-pot pr.)	ca. 2		0.1–5	This work
(IVa) O,O-Dialkyl 1-(N-acetylamino) alkanephosphonate	(1) $AcOH–Ac_2O$	0.2	100		
	(1a) $HC(OR)_3$ or $MeC(OR)_3$	1.5	100		
(IVb) O,O-Dialkyl 1-(N-TFA-amino)alkane phosphonates	(1) TFA–TFAA	0.2	30–40		
	(1a) $HC(OR)_3$	1.5	100		

Abbreviations: Ac = acetyl; Ac_2O = acetic anhydride; TFA = trifluoroacetic acid; TFAA = trifluoroacetic anhydride; N-TFA = N-trifluoroacetyl; Ms. pr. = multi-stage procedure; One-pot pr. = one-pot procedure.

Huber [14]. The comparison of the present method with those procedures is given in Table 1.

Optimization of the reaction conditions was carried out using ^{31}P NMR monitoring. These investigations revealed the complete conversion of aminoalkanephosphonic acids **1** into the corresponding diester derivatives **5**. The ^{31}P NMR spectra of the derivatization products (**5BA*** and **5CB***) of **1** obtained with the carboxylic anhydride–orthoester systems are presented in Figs. 1 and 2. The phosphorus chemical shifts for all the derivatives obtained, **5BA***, **5BB***, **5CA*** and **5CB***, are given in Tables 2 and 3.

Table 2
^{31}P NMR chemical shifts (δ, ppm) of N-acetylaminoalkanephosphonates **5B** (**5BA*** and **5BB***)

Starting amino acid **1**		**5B** derivatives	
No.	R ($R^1 \neq H$)	$P(O)(OMe)_2$	$P(O)(OEt)_2$
1a	H	26.6	23.2
1b	Me	29.1	25.6
1c	Et	28.3	25.0
1d	Me (Me)	31.0	27.6
1e	Bu	28.1	24.7
1f	Ph	24.8	21.6
1g	$PhCH_2$	27.5	24.1

Table 3
^{31}P NMR chemical shifts (δ, ppm) of N-trifluoroacetylaminoalkanephosphonates **5C** (**5CA*** and **5CB***)

Starting amino acid **1**		**5C** derivatives	
No.	R ($R^1 \neq H$)	$P(O)(OMe)_2$	$P(O)(OEt)_2$
1a	H	25.4	21.3
1b	Me	26.8	24.4
1c	Et	26.3	23.8
1d	Me (Me)	28.5	26.3
1e	Bu	26.0	23.6
1f	Ph	22.6	20.5
1g	$PhCH_2$	24.6	23.0

3.2. Chromatographic properties of derivatives 5

The derivatives **5** can be stored for several weeks at 0°C without extensive decomposition (^{31}P NMR) and have been found to be suitable for characterization by means of GC. These compounds give reproducible retention data. The separation of derivatives **5** from derivatization of the mixture of 1-aminoalkanephosphonic acids **1a**, **1b**, **1c**, **1d**, **1e**, **1f** and **1g**, achieved on a DB-17 column, is presented in Figs. 3 and 4.

The DB-17 column was suitable for the separations of all the N-acylaminoalkanephosphonates **5BA*** and **5BB***. The higher polarity of N-trifluoroacetylamino derivatives **5CA*** and **5CB*** had the result that, in two cases (Fig. 4) (**5CB*d** and **5CB*b**; **5CB*a** and **5CB*c**), the overlapping effect occurred. This suggests that, for better separation, a column of higher polarity should be used (e.g., DB-225).

The elution of the amidoalkanephosphonates **5** did not follow the order of their molecular masses. The derivatives **5d** appeared first, then the others in the order **5b**, **5c**, **5a**, **5e**, **5f** and **5g** (in all four series of derivatives **5**, i.e. **5BA***, **5BB***, **5CA*** and **5CB***). The comparison of the retention times of acetyl (**5B**) and trifluoroacetyl derivatives (**5C**), and also different O-alkyl amidoalkanephosphonates (**5CA***, **5CB*** and **5CC***) revealed the following orders of increasing retention times: **5B** > **5C** and **5CA*** < **5CC*** < **5CB***.

3.3. Mass spectral properties of N-acylaminoalkanephosphonates 5

The partial mass spectra of N-acyl derivatives **5** are summarized in Tables 4–8.

The N-acylaminoalkanephosphonates **5** present distinct structural differences caused by (a) the constitution of the acyl group, (b) the type of O-alkyl phosphonate function and (c) the type of hydrocarbon side-chain attached to C_α. However, in spite of these structural differences, the whole group present some common features, which are reflected in their fragmentation patterns, and consequently determine the shape of all the mass spectra.

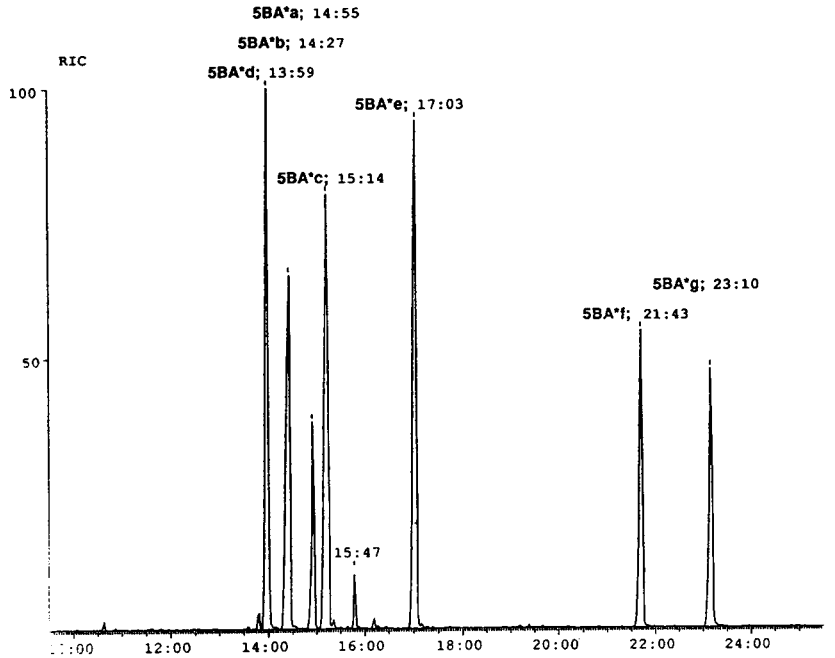

Fig. 3. GC–MS analysis of the derivatization products **5BA** * **(a–g)** of the mixture of aminophosphonic acids **1a**, **1b**, **1c**, **1d**, **1e**, **1f** and **1g** obtained by means of acetic acid–acetic anhydride and trimethyl orthoacetate. Conditions as described under Experimental. The ^{31}P NMR spectrum of the derivatization products of this reaction mixture is presented in Fig. 1.

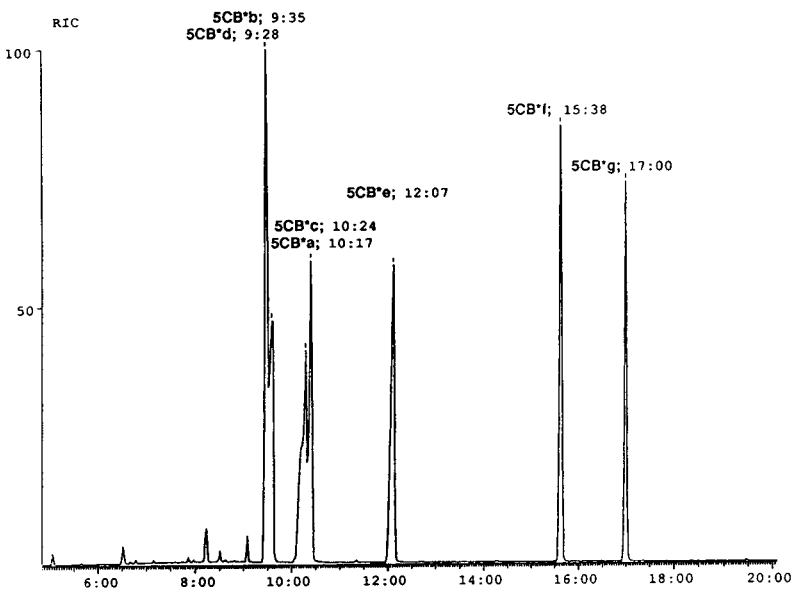

Fig. 4. GC–MS analysis of the derivatization products **5CB** * **(a–g)** of the mixture of aminophosphonic acids **1a**, **1b**, **1c**, **1d**, **1e**, **1f** and **1g** obtained by means of trifluoroacetic acid–trifluoroacetic anhydride and triethyl orthoformate. Conditions as described under Experimental. The ^{31}P NMR spectrum of the derivatization products of this reaction mixture is presented in Fig. 3.

Table 4
Reduced mass spectra of O,O-dimethyl 1-(acetylamino)alkanephosphonates **5BA***

No.	R ($R^1 \neq H$)	Molecular formula (mass)	Mass spectrometry: *m/z* (relative intensity, %)										
			M	M − MeO [M − 31]	M − R	[M − 42]	M − Ac [M − 43]	M − NHAc [M − 58]	M − $(MeO)_2PO$ [M − 109]	Phosphonyl-derived ions[a]			$RCH{=}NH_2^+$ [R + 29]
										[110]	[95]	[79]	
5BA*a	H	$C_5H_{12}NPO_4$	181	150	180	140	139	124	72	110	95	79	30
		(181.1)	(4.2)	(8.9)	(−)	(0.2)	(2.0)	(10)	(31)	(90)	(13)	(21)	(100)
5BA*b	CH_3	$C_6H_{14}NPO_4$	195	164	180	153	152	138	86	110	95	79	44
		(195.1)	(2.0)	(0.5)	(0.5)	(0.5)	(6.5)	(2.6)	(64)	(17)	(3.5)	(6.1)	(100)
5BA*c	C_2H_5	$C_7H_{16}NPO_4$	209	178	180	167	166	152	100	110	95	80	58
		(209.2)	(1.7)	(0.2)	(0.2)	(0.2)	(1.6)	(0.5)	(56)	(8.2)	(1.7)	(2.9)	(100)
5BA*d	$CH_3(CH_3)$	$C_7H_{16}NPO_4$	209	178	180	167	166	152	100	110	95	80	58
		(209.2)	(0.5)	(0.5)	(−)	(0.1)	(2.5)	(2.4)	(74)	(5.0)	(1.3)	(2.0)	(100)
5BA*e	n-C_4H_9	$C_9H_{20}NPO_4$	237	206	180[b]	195[c]	194	166	128	110	95	80	86
		(237.2)	(1.8)	(0.1)	(0.2)	(0.9)	(1.3)	(2.5)	(64)	(4.6)	(1.0)	(1.7)	(100)
5BA*f	C_6H_5	$C_{11}H_{18}NPO_4$	257	226	180	215[c]	214	200	148	110	95	80	106
		(257.2)	(7.2)	(0.1)	(0.1)	(2.9)	(5.1)	(1.6)	(61)	(3.0)	(0.9)	(1.3)	(100)
5BA*g	$C_6H_5CH_2$	$C_{12}H_{2O}NPO_4$	271	240	180	229	228	214	162	110	95	80	120
		(271.2)	(2.2)	(0.2)	(4.8)	(0.1)	(0.5)	(2.9)	(26)	(4.5)	(0.2)	(1.8)	(100)

[a] $(MeO)_2POH$ [110], (MeO)P(O)(OH) [95], PO_3 [79].
[b] [181]; (1.3%).
[c] $[M - CH_2CO]$.

Table 5
Reduced mass spectra of O,O-diethyl 1-(acetylamino)alkanephosphonates **5BB***

No.	R ($R^1 \neq H$)	Molecular formula (mass)	Mass spectrometry: m/z (relative intensity, %)										
			M	M − EtO [M − 45]	M − R	[M − 42]	M − Ac [M − 43]	M − NAc [M − 57]	M − $(EtO)_2PO$ [M − 137]	Phosphonyl-derived ions[a]			$RCH{=}NH_2^+$ [R + 29]
										[138]	[111]	[82]	
5BB*a	H	$C_7H_{16}NPO_4$	209	164	208	167[b]	166	152	72	138	111	82	30
		(209.2)	(54)	(14.0)	(−)	(5.8)	(7.4)	(6.2)	(23)	(100)	(54)	(21)	(−)
5BB*b	CH_3	$C_8H_{18}NPO_4$	223	178	208	181	180	166	86	138	111	82	44
		(223.2)	(7.8)	(3.8)	(0.2)	(1.4)	(23.0)	(1.8)	(73)	(30)	(33)	(15)	(100)
5BB*c	C_2H_5	$C_9H_{20}NPO_4$	237	192	208	195	194	180	100	138	111	82	58
		(237.1)	(5.9)	(1.7)	(0.2)	(0.4)	(3.1)	(0.7)	(70)	(12)	(12)	(5)	(100)
5BB*d	$CH_3(CH_3)$	$C_9H_{20}NPO_4$	237	192	208	195	194	180	100	138	111	82	58
		(237.1)	(2.6)	(2.4)	(−)	(0.3)	(8.2)	(2.5)	(74)	(5.0)	(7.1)	(4.6)	(100)
5BB*e	n-C_4H_9	$C_{11}H_{24}NPO_4$	265	220	208	223[b]	222	208	128	138	111	82	86
		(265.3)	(3.2)	(1.2)	(0.4)	(2.3)	(2.8)	(0.4)	(64)	(5.4)	(5.6)	(3.7)	(100)
5BB*f	C_6H_5	$C_{13}H_{20}NPO_4$	285	240	208	243[b]	242	228	148	138	111	82	106
		(285.3)	(9.2)	(0.9)	(−)	(1.8)	(5.1)	(−)	(61)	(1.4)	(2.9)	(3.0)	(100)
5BB*g	$C_6H_5CH_2$	$C_{14}H_{22}NPO_4$	299	254	208	257	256	242[c]	162[d]	138	111	82	120
		(299.3)	(5.3)	(1.7)	(5.7)	(−)	(0.3)	(0.2)	(26)	(20)	(4.2)	(4.2)	(80)

[a] $(EtO)_2POH$ [138], $(EtO)P(H)(OH)_2$ [111], H_3PO_3 [82].
[b] $M - CH_2CO$.
[c] [241]; (0.2%) and [240]; (18%).
[d] [161]; (100%).

Table 6
Reduced mass spectra of O,O-dimethyl 1-(trifluoroacetylamino)alkanephosphonates **5CA***

No.	R ($R^1 \neq H$)	Molecular formula (mass)	Mass spectrometry: *m/z* (relative intensity, %)											
			M	M − MeO [M − 31]	M − R	M − CF_3 [M − 69]	M − TFA [M − 97]	M − $(MeO)_2PO$ [M − 109]	Phosphonyl-derived ions[a]				CF_3 [69]	$RCH{=}NH_2^+$ [R + 29]
									[110]	[95]	[80]	[79]		
5CA*a	H	$C_5H_9F_3NPO_4$	235	204	234	166	140	126	110[d]	95	80	79	69	30
		(235.1)	(16.0)	(2.3)	(−)	(66.0)	(4.7)	(26)	(100)	(17)	(22)	(44)	(19)	(−)
5CA*b	CH_3	$C_6H_{11}F_3NPO_4$	249	217	234	180	154	140	110	95	80	79	69	44
		(249.1)	(1.4)	(−)	(−)	(0.8)	(0.3)	(20)	(100)	(8.9)	(17)	(14)	(9.8)	(0.4)
5CA*c	C_2H_5	$C_7H_{13}F_3NPO_4$	263	232	234	194	166	154	110	95	80	79	69	58
		(263.1)	(2.7)	(0.2)	(1.1)	(1.1)	(0.3)	(22)	(100)	(5.0)	(11)	(9.7)	(5.1)	(0.2)
5CA*d	$CH_3(CH_3)$	$C_7H_{13}F_3NPO_4$	263	232	234[b]	194	166	154	110	95	80	79	69	58
		(263.1)	(4.6)	(0.2)	(−)	(0.7)	(4.0)	(91)	(100)	(7.8)	(18)	(13)	(11)	(0.5)[e]
5CA*e	*n*-C_4H_9	$C_9H_{17}F_3NPO_4$	291	260	234[c]	222	194	182	110	95	80	79	69	86
		(291.2)	(0.4)	(0.2)	(0.4)	(0.5)	(0.2)	(17)	(100)	(3.4)	(22)	(8.4)	(22)	(0.2)
5CA*f	C_6H_5	$C_{11}H_{15}F_3NPO_4$	311	280	234	242	214	202	110	95	80	79	69	106[f]
		(311.2)	(29.0)	(0.2)	(−)	(−)	(1.6)	(100)	(16)	(1.8)	(4)	(12)	(4.2)	(0.1)
5CA*g	$C_6H_5CH_2$	$C_{12}H_{17}F_3NPO_4$	325	294	234	256	228	215	110	95	80	79	69	120
		(325.2)	(25.0)	(2.5)	(2.5)	(−)	(−)	(100)	(11)	(1.6)	(2.3)	(6.1)	(1.7)	(1.3)

[a] $(MeO)_2POH$ [110], (MeO)P(O)(OH) [95], HPO_3 [80], PO_3 [79].
[b] [248]; (1.1%).
[c] [235]; (7.1%).
[d] [109]; (60%).
[e] [59]; (24%).
[f] [107]; (16%).

Table 7
Reduced mass spectra of O,O-diethyl 1-(trifluoroacetylamino)alkanephosphonates **5CB**∗

No.	R ($R^1 \neq H$)	Molecular formula (mass)	Mass spectrometry: m/z (relative intensity, %)											
			M	M − R	M − EtO [M − 45]	M − CF_3 [M − 69]	M − TFA [M − 97]	M − NHTFA [M − 112]	M − $(EtO)_2PO$ [M − 138]	Phosphonyl-derived ions[a]			CF_3 [69]	$RCH{=}NH_2^+$ [R + 29]
										[138]	[111]	[82]		
5CB∗a	H	$C_7H_{13}F_3NPO_4$	263	262	218	194	156	150	126	138	111	82	69	30
		(263.2)	(54.0)	(−)	(18.0)	(4.6)	(0.6)	(1.9)	(55)	(100)	(50)	(34)	(22)	(5.4)
5CB∗b	CH_3	$C_8H_{15}F_3NPO_4$	277	262	232	208	180	164	140	138	111	82	69	44
		(277.2)	(3.5)	(−)	(5.0)	(1.0)	(1.7)	(0.1)	(29)	(100)	(56)	(34)	(10)	(2.0)
5CB∗c	C_2H_5	$C_9H_{17}F_3NPO_4$	291	262[b]	246	222	194	179	154	138	111	82	69	58
		(291.1)	(6.1)	(0.3)	(3.7)	(0.7)	(0.3)	(0.2)	(32)	(100)	(61)	(19)	(6.6)	(0.5)
5CB∗d	$CH_3(CH_3)$	$C_9H_{17}F_3NPO_4$	291	262[c]	246	222	194	179	154	138	111	82	69	58
		(291.1)	(4.0)	(−)	(4.2)	(1.0)	(2.4)	(1.5)	(18)	(100)	(68)	(29)	(6.6)	(0.6)
5CB∗e	n-C_4H_9	$C_{11}H_{21}F_3NPO_4$	319	262[d]	274	250	222	207	182	138	111	82	69	86
		(319.3)	(1.0)	(0.2)	(2.7)	(0.2)	(0.2)	(3.1)	(6.4)	(100)	(43)	(13)	(2.3)	(0.2)
5CB∗f	C_6H_5	$C_{13}H_{19}F_3NPO_4$	339	262	294	270	242	227	202	138	111	82	69	106[f]
		(339.3)	(53.0)	(−)	(2.6)	(0.3)	(2.0)	(0.3)	(100)	(56)	(40)	(15)	(8.5)	(0.5)
5CB∗g	$C_6H_5CH_2$	$C_{14}H_{21}F_3NPO_4$	353	262	308	284	256	241[e]	215	138	111	82	69	120
		(353.3)	(25.0)	(2.8)	(2.5)	(0.2)	(0.1)	(4.4)	(100)	(66)	(37)	(12)	(3.8)	(2.0)

[a] $(EtO)_2POH$ [138], $(EtO)P(H)(OH)_2$ [111], H_2PO_3 [82].
[b] [263]; (1.3%).
[c] [276]; (0.3%).
[d] [263]; (8.2%).
[e] [240]; (13%).
[f] [107]; (15%).

Table 8
Reduced mass spectra of O-methyl-O-ethyl 1-(trifluoroacetylamino)alkanephosphonates **5CC***

No.	R ($R^1 \neq H$)	Molecular formula (mass)	Mass spectrometry: m/z (relative intensity, %)												
			M	M − EtO[a] [M − 45]	M − R	M − CF_3 [M − 69]	M − TFA [M − 97]	M − HNTFA [M − 112]	M − $(RO)_2PO$ [M − 123]	Phosphonyl-derived ions[a]				CF_3 [69]	RCH=NH_2^+ [R + 29]
										[124]	[97]	[96]	[79]		
5CC*a	H	$C_6H_{11}F_3NPO_4$	249	204	248	180	152	137	126	124	97	96[f]	79	69	30
		(249.2)	(33.0)	(29.0)	(−)	(84.0)	(53.0)	(1.0)	(55)	(83)	(65)	(90)	(55)	(38)	(6.9)
5CC*b	CH_3	$C_7H_{13}F_3NPO_4$	263	218	248	194	166	151	140	124	97	96	79	69	44
		(263.2)	(2.3)	(4.3)	(−)	(1.2)	(4.2)	(0.2)	(36)	(100)	(54)	(61)	(9.6)	(12)	(1.6)
5CC*d	$CH_3(CH_3)$	$C_8H_{15}F_3NPO_4$	277	232	−[c]	208	180	165	154	124	97	96	79	69	58
		(277.1)	(10)	(4.7)	−	(1.6)	(6.7)	(1.4)	(85)	(100)	(64)	(62)	(7.7)	(10)	(0.6)
5CC*f	C_6H_5	$C_{12}H_{17}F_3NPO_4$	325	280	248	256	228	213	202	124	97	96	79	69	114
		(325.3)	(29.0)	(1.0)	(−)	(0.2)	(1.5)	(1.3)	(100)	(18)	(16)	(18)	(11)	(6.4)	(0.2)
5CC*g	$C_6H_5CH_2$	$C_{13}H_{19}F_3NPO_4$	339	294	248	270	242	227[d]	216[e]	124	97	96	79	69	128
		(339.3)	(8.3)	(1.2)	(1.5)	(0.2)	(−)	(2.4)	(14)	(19)	(18)	(13)	(13)	(3.2)	(1.6)

[a] The ions [M − MeO, (M − 31)] exhibited intensity <0.2%.
[b] (EtO)(MeO)POH [124], $(MeO)P(H)(OH)_2$ [97], $(MeO)P(OH)_2$ [96], PO_3 [79].
[c] [262]; (0.9%).
[d] [226]; (7.8%).
[e] [215]; (100%).
[f] [95]; (100%).

3.4. Mass spectral properties of N-acetylaminoalkanephosphonates 5B

The molecular ions $[M]^{+\cdot}$ of these derivatives were observed in low abundance, except the lowest homologue **5Ba** derived from phosphonoglycine (**1a**, Gly^P). Charge localization on the nitrogen atom produced ions $[M-(R^2O)_2P(O)]^+$ and $[M-R]^+$ ions (R is the alkyl chain at C_α) resulting from α-cleavage. The ions $[RCH{-}NH_2]^+$ or $[M-(R^2O)_2P(O)]^+$ constitute the base peaks for the majority of N-acyl derivatives **5BA*** and **5BB***. The ions $[M-1]^+$ and/or $[M-R]^+$, excluding compound **5BB*g**, derived from phosphonophenylalanine (**1f**, Phe^P) were not observed or were observed in very low abundances.

The ions resulting from the competitive charge localization on the phosphonate moiety were very abundant. Thus, the ions at *m/z* 138, 137, 110 and 82 were characteristic of the presence of the O,O-diethyl phosphonate system and had the mechanism of formation reported previously [15]. The ions at *m/z* 110, 109, 95 and 79 were characteristic of the presence of the O,O-dimethyl phosphonate system.

Cleavage of the acetate or acetamide group from the molecular ions of derivatives **5B** gave rise to the ions at $[M-43]^+$ or $[M-57]^+$, respectively. Ions at $[M-42]^{+\cdot}$ which were more abundant for derivatives of **5BB*** than for **5BA***, were produced by the loss of ketene ($CH_2{=}C{=}O$) from $[M]^{+\cdot}$. Considerable scrambling between the acetate methyl hydrogens and the amide hydrogen accompanied these eliminations.

Cleavage of the alkoxy group of the phosphonate moiety from the molecular ions of derivatives **5B** afforded the ions $[M-31]^+$ or $[M-45]^+$.

3.5. Mass spectral properties of N-trifluoroacetylaminoalkanephosphonates 5C

The molecular ions $[M]^{+\cdot}$ of these derivatives were observed in abundances varying from 0.4% (for **5CA*e**) to over 50% (for **5CB*a** and **5CB*f**). Generally the highest abundances occurred for O,O-diethyl derivatives **5CB*** and the lowest for O,O-dimethyl derivatives **5CA***. Charge localization on the nitrogen atom produced ions $[M-(R^2O)_2P(O)]^+$ and $[M-R]^+$ ions (R is the alkyl chain at C_α) resulting from α-cleavage. The ions $[M-(R^2O)_2P(O)]^+$ represent the base peaks for most of the N-trifluoroacetyl derivatives **5BA*** and **5BB***. The ions $[M-1]^+$ were not observed or were observed in very low abundances. The ions $[M-R]^+$ appeared for R > Et and $R = PhCH_2$, and were of low abundance.

The ions resulting from competitive charge localization on the phosphonate moiety were very abundant. Thus, the ions at *m/z* 138, 137, 110 and 82 were characteristic of the presence of the O,O-diethyl phosphonate system. The ions at *m/z* 124, 97, 96 and 81 indicated the presence of the O-ethyl-O-methyl phosphonate system and the ions at *m/z* 110, 109, 95 and 79 were characteristic of the presence of the O,O-dimethyl phosphonate system. The ions $[(R^2O)_2POH]^{+\cdot}$ at *m/z* 138, 124 and 110 constitute the base peaks of derivatives **5CB***, **5CC*** and **5CA***, respectively.

Cleavage of the trifluoromethyl, the trifluoroacetyl or the trifluoroacetamide group from the molecular ions of derivatives **5C** gave rise to ions at $[M-69]^+$, $[M-97]^+$ or $[M-112]^+$, respectively. The ions $[RCH{=}NH_2]^{+\cdot}$ appeared at low abundances, if they were observed at all.

Cleavage of the alkoxy group of the phosphate moiety from the molecular ions of derivatives **5CA*** afforded the ions $[M-31]^+$. The corresponding cleavage in the derivatives **5CB*** and **5CC*** gave rise to the ions $[M-45]^+$.

4. Conclusions

A general derivatization method for aminoalkanephosphonic acids using carboxylic anhydrides–trialkyl orthoesters has been developed. ^{31}P NMR spectroscopic investigations confirmed the complete conversion of 1-aminoalkanephosphonic acids into the volatile diester

derivatives **5** within 2 h. The ester products of this reaction, N-acetyl (**5B**) or N-trifluoroacetyl (**5C**) derivatives of aminoalkanephosphonates are satisfactory for characterization by both GC and GC–MS. The mass spectra of these derivatives were structurally informative. Ions characteristic of the phosphonate system were present in the mass spectra of all derivatives **5**, permitting rapid identification of these compounds.

References

[1] L. Maier, *Chimia*, 23 (1969) 323.
[2] K.A. Pietrov, V.A. Chauzov and T.S. Erokhina, *Usp. Khim.*, 43 (1974) 2045.
[3] P. Kafarski, B. Lejczak and P. Mastalerz, *Beitrage Wirkstofforschung*, 25 (1985) 1.
[4] P. Kafarski and P. Mastalerz, *Beitr. Wirkstofforschung*, 21 (1984) 1.
[5] F. Eisenberg in M. Halmann (Editor), *Analytical Chemistry of Phosphorous Compounds*, Wiley-Interscience, New York, 1972, p. 69.
[6] Y. Kiso, H. Kobayashi and Y. Kitaoka, in M. Halmann (Editor), *Analytical Chemistry of Phosphorus Compounds*, Wiley-Interscience, New York, 1972, p. 93.
[7] M. Horiguchi, in M. Halmann (Editor), *Analytical Chemistry of Phosphorus Compounds*, Wiley-Interscience, New York, 1972, p. 703.
[8] Z.H. Kudzin, M. Sochacki and W. Kopycki, *Phosphorus Sulfur Silicon*, 77 (1993) 207.
[9] Z.H. Kudzin, M. Sochacki and W. Kopycki, *J. Chromatogr. A*, 655 (1993) 346.
[10] Z.H. Kudzin and A. Kotyński, *Synthesis*, (1984) 1028.
[11] Z.H. Kudzin and W.J. Stec, *Synthesis*, (1978) 469.
[12] B. Gallenkamp, W. Hofer, B.W. Kruger, F. Haurer and T. Pfister, in M. Regitz (Editor), *Methoden der Organischen Chemie (Houben–Weyl)*, Vol. III, Georg Thieme, Stuttgart, 1982, p. 300.
[13] M.L. Ruppel, C.A. Suba and J.T. Marvel, *Biomed. Mass Spectrom.*, 9 (1976) 28.
[14] J.W. Huber, *J. Chromatogr.*, 152 (1978) 220.
[15] T. Nishiwaki, *Tetrahedron*, 23 (1967) 2187.

ELSEVIER

Journal of Chromatography A, 678 (1994) 313–318

JOURNAL OF CHROMATOGRAPHY A

Determination of the semi-volatile compounds nitrobenzene, isophorone, 2,4-dinitrotoluene and 2,6-dinitrotoluene in water using solid-phase microextraction with a polydimethylsiloxane-coated fibre

Jang-Yeun Horng, Shang-Da Huang*

Department of Chemistry, National Tsing Hua University, Hsinchu 30043, Taiwan

First received 2 March 1994; revised manuscript received 11 May 1994

Abstract

Aqueous samples of the semi-volatile compounds nitrobenzene, isophorone, 2,4-dinitrotoluene and 2,6-dinitrotoluene, listed in the US Environmental Protection Agency (EPA) Method 609, were analysed by solid-phase microextraction (SPME) with a polydimethylsiloxane-coated fibre. SPME is a technique to extract organics from an aqueous matrix into a stationary phase immobilized on a fused-silica fibre. The analytes are thermally desorbed directly into the injector of a gas chromatograph. The sensitivity of this method decreased with increasing concentration of methanol and absorption temperature and increased with increasing concentration of Na_2SO_4. Samples of lake water were analysed using calibration graphs based on deionized water. The relative standard deviations of these analytes were 1–2% for analytes in deionized water and 2–4% for analytes in lake water. The detection limits were 9 ng/ml for nitrobenzene and 15 ng/ml for the other three analytes.

1. Introduction

Sample pretreatment is generally required for determination of trace organic pollutants in water. Liquid–liquid extraction and solid-phase extraction are the most commonly used techniques for semi-volatile and non-volatile compounds. The traditional method of liquid–liquid extraction requires large volumes of solvent for extraction and is protracted and tedious. Solid-phase extraction [1,2] requires less solvent, but for trace analysis a large volume of sample is generally required for preconcentration, and probably much time is required to load the sample solution. Contaminants may be eluted from the solid-phase packing [3].

Solid-phase microextraction (SPME) [4–16], recently developed by Pawliszyn and co-workers, eliminates most of the drawbacks in the preparation of an aqueous sample. SPME involves exposing a fused-silica fibre previously coated with a stationary phase [12] (or even a bare fused-silica fibre) to an aqueous solution containing organic compounds. The organic compounds partition between water and the stationary phase until equilibrium is reached. The fibre

* Corresponding author.

0021-9673/94/$07.00
SSDI 0021-9673(94)00457-K

is then removed from the solution and the analytes are thermally desorbed into the injector of a gas chromatograph. The fibre is contained in a syringe to facilitate handling. The amounts of analytes absorbed on the fibre are linearly related to the concentrations of analytes in the aqueous sample. SPME, which takes only a few minutes for extraction and thermally desorbs analytes from the fibre coating, requires no solvents, is inexpensive, simple and readily adapted to automation [5].

The applications of SPME, studied by Pawliszyn and co-workers, include substituted benzenes in water [5,8,9] and headspace [11], caffeine in beverages [10], chlorinated compounds listed in the USA Environmental Protection Agency (EPA) Method 624 [7], polyaromatic hydrocarbons and selected polychlorinated biphenyls (PCBs) in water [6,16] and phenols listed in EPA Methods 604 and 625 [14,15]. Several fibre coatings, such as polydimethylsiloxane [8,11,16], polyacrylate [13,15] and polyimide [6], have been developed. The polydimethylsiloxane-coated fibre, the most successful, is the first kind of fibre available commercially (from Supelco) for an SPME fibre assembly [17].

It is of interest to establish whether SPME can also be used to determine other organic pollutants in water. In this work, we determined the semi-volatile priority pollutants listed in EPA Method 609 using the SPME fibre assembly. The desorption–time profile was explored. The effects of methanol, Na_2SO_4, duration of absorption and absorption temperature were investigated. The detection limits were 9 ng/ml for nitrobenzene and 15 ng/ml for isophorone, 2,4-dinitrotoluene and 2,6-dinitrotoluene. This method was applied to an environmental sample (lake water).

2. Experimental

The SPME fibre assembly was purchased from Supelco. The microextraction fibre was coated with polydimethylsiloxane (100 μm). The fibre was conditioned at 210°C before use.

SPME involves a few simple steps [4–7]. The fibre is withdrawn into the needle of the syringe (Hamilton Model 7005) and the needle is used to penetrate the septum of a sample vial (4 ml). The fibre is then inserted into the sample by depressing the plunger. The fibre coated with polydimethylsiloxane is completely immersed in the sample solution (3 ml). The sample solution in the vial is stirred with a stirring bar by the magnetic stirrer. The organic analytes become partitioned between the water and the stationary phase until equilibrium is reached (10 min). The plunger is withdrawn to retract the fibre into the needle and the syringe needle is then removed from the vial. For desorption, the needle is inserted into the GC injection port and then the fibre is exposed for 5 min. The injection position must be kept at a constant depth in all injections [5].

A gas chromatograph (Shimadzu GC 9-AM) with a split–splitless system, flame ionization detector and capillary column (Shimadzu CBP-10, 25 m × 0.2 mm I.D., film thickness 0.25 μm) were used. The fibre was desorbed in the GC injector at 210°C for 5 min. As the fibre began its desorption, the column temperature was kept isothermal at 70°C for 5 min, then increased at 7°C/min to 175°C and held isothermal at 175°C for 10 min. The detector temperature was 280°C. The carrier gas was nitrogen of purity 99.99%, further purified by passage through a gas purifier (Alltech) containing molecular sieve 5A and indicating Drierite and an oxygen-adsorbing gas purifier (OxiClear). The pressure of the carrier gas was 150 kPa and the flow-rate of make-up gas was 60 ml/min. The split flow-rate was 60 ml/min and the flow-rate for the septum purge was 2 ml/min. The GC temperature programme used for analysis the lake water was modified to avoid the interference peak that appeared near the 2,6-dinitrotoluene peak; the column was kept isothermal at 70°C for 5 min, then increased at 7°C/min to 120°C, at 1°C/min to 139°C and at 15°C/min to 175°C, and held isothermal at 175°C for 2 min. The same modified GC temperature programme was used to obtain the calibration graph for analytes in deionized water and lake water.

Stock standard solutions of nitrobenzene, iso-

phorone, 2,4-dinitrotoluene and 2,6-dinitrotoluene (TCI, Japan) were prepared in acetone (2000 μg/ml). Methanol (Optima grade; Fisher) and disodium sulfate (Osaca, Japan) were used to prepare the sample solution. Deionized water was prepared using a Millipore Milli-Q SP purification system. Lake water from National Tsing Hua University served as the environmental sample.

3. Results and discussion

A chromatogram of the mixed standard in water (1 μg/ml each) using SPME is shown in Fig. 1. Sharp peaks and good resolution were obtained under the analytical conditions used.

The absorption–time profile (Fig. 2) was obtained by monitoring the peak-area counts as a function of duration of exposure. The equilibrium period was 10 min for isophorone and 3 min for nitrobenzene, 2,4-dinitrotoluene and 2,6-dinitrotoluene. Factors that influence the equilibrium period were investigated by Pawliszyn and co-workers [4,5,9]. The equilibrium period is limited by mass transfer of the analytes through a thin, static aqueous layer at the fibre–solution interface. The equilibrium period increased with increasing distribution constant of the analyte and with increasing thickness of the fibre coating, but the equilibrium period decreased for the stirred solution [4,5,9]. As we analysed the sample under the constant conditions (the same thickness of fibre coating and stirring conditions), and the peak-area of isophorone was even smaller than that of nitrobenzene and 2,6-dinitrotoluene, we concluded that there must be other factors that affect the equilibrium period. The solubility [18] of isophorone in water (12 g/l) is much greater than that of nitrobenzene (1.9 g/l) and dinitrobenzene (about 0.3 g/l). These data imply that the extent of hydration of isophorone may be significantly greater than those of the others, such that diffusion of isophorone through the thin, static aqueous layer at the fibre–solution interface is slower than that of the others; hence the equilibrium period of isophorone is greater. In order to improve the sensitivity and precision, and extraction period of 10 min was chosen for subsequent experiments.

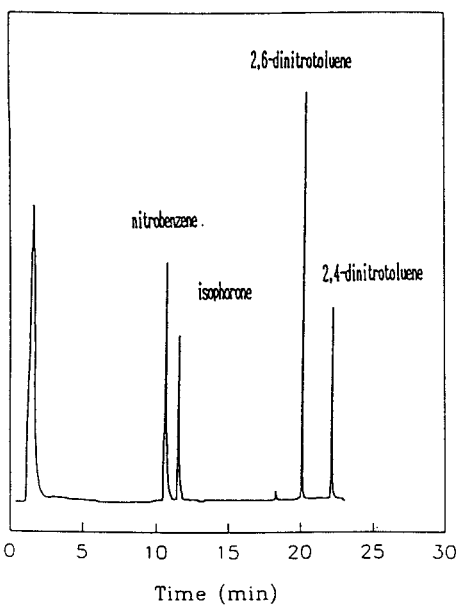

Fig. 1. Chromatogram of nitrobenzene, isophorone, 2,4-dinitrotoluene, 2,6-dinitrotoluene extracted from deionized water (1 μg/ml) by SPME for 10 min and desorbed in the GC injection port at 210°C for 5 min.

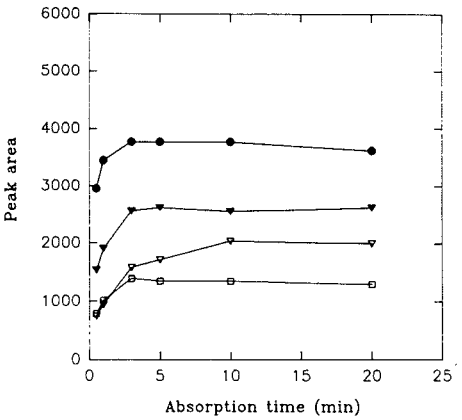

Fig. 2. Effect of absorption period on peak area of (●) nitrobenzene, (▽) isophorone, (□) 2,4-dinitrotoluene and (▼) 2,6-dinitrotoluene. Deionized water containing the analytes (0.4 μg/ml each) was extracted by SPME and desorbed in the GC injection port at 210°C for 3 min.

The desorption–time profile is shown in Fig. 3. Quantitative desorption of nitrobenzene and

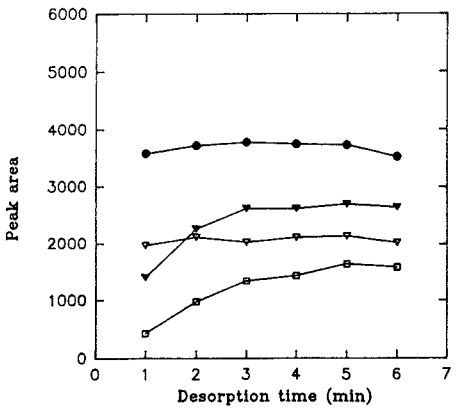

Fig. 3. Effect of desorption period on the peak area of the four analytes (symbols as in Fig. 2). Deionized water containing analytes (0.4 μg/ml each) was extracted by SPME for 10 min and desorbed in the GC injection port at 210°C.

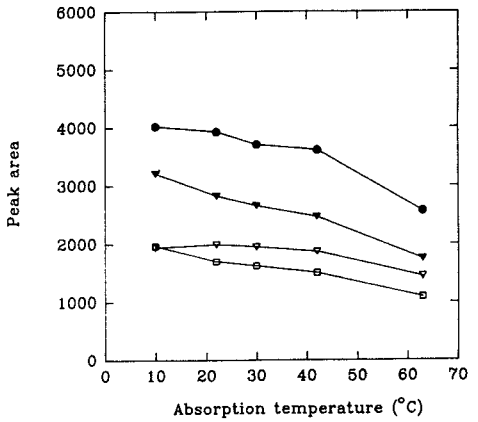

Fig. 4. Effect of temperature of absorption on the peak area of the four analytes (symbols as in Fig. 2). The sample solution (0.4 μg/ml each) was extracted by SPME for 10 min and desorbed in the GC injection port at 210°C for 5 min.

isophorone from the stationary phase of the fibre was achieved in 1 min or less, as the boiling points of the analytes [18] were near the desorption temperature. The period (5 min) required to desorb completely the less volatile analytes, 2,4- and 2,6-dinitrotoluene (b.p. 250 and 280°C), was much greater. Peak broadening of the analytes was avoided by cryofocusing of the analytes at the inlet of the GC column.

There was concern that the adsorbed semi-volatile analytes might not be efficiently removed from the fibre during thermal desorption for 5 min, and might thus contaminate the fibre for analysis of subsequent samples. To determine whether analyte retention was a significant source of error, the SPME fibre was inserted into the GC injection port a second time after analysis of the aqueous sample was completed. No carryover of analyte species was observed in the second GC analysis, demonstrating that 5 min were sufficient for thermal desorption.

The absorption–temperature profile is shown in Fig. 4. The amount of analytes absorbed decreased with increasing temperature of absorption. The distribution constant decreased with increasing temperature because absorption is generally an exothermic process; therefore, the amount of analytes adsorbed decreased with increasing temperature if equilibrium was reached. The rate of diffusion of the analyte species through the static aqueous layer at the fibre–solution interface decreases with decreasing temperature [5], such that less analyte is absorbed at a lower temperature if equilibrium was not reached. No effect of absorption temperature on the rate of diffusion was observed.

The effect of methanol on peak area is shown in Fig. 5. The amounts of 2,4- and 2,6-di-

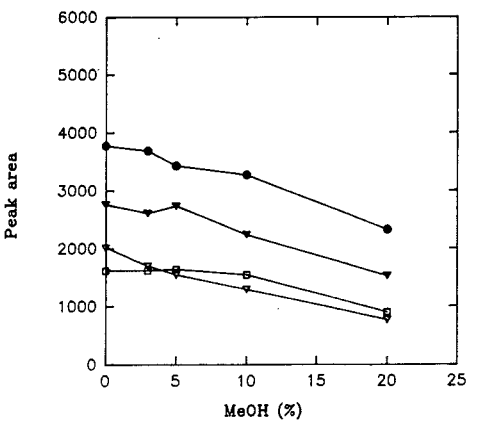

Fig. 5. Effect of methanol on the peak area of the four analytes (symbols as in Fig. 2). The sample solution (0.4 μg/ml each) was extracted by SPME for 10 min and desorbed in the GC injection port at 210°C for 5 min.

nitrotoluene adsorbed were little affected by methanol at concentrations less than 5% and 10%, respectively. The amount of nitrobenzene and isophorone absorbed on the fibre decreased with increasing concentration of methanol. An increased proportion of methanol in aqueous solution decreased the polarity of the aqueous sample so that the distribution constant decreased [5]. The more soluble analytes (isophorone and nitrobenzene) were more readily affected by methanol than the less soluble analytes (dinitrobenzene).

The effect on Na_2SO_4 on peak area is shown in Fig. 6. An increased Na_2SO_4 concentration in an aqueous sample increased the distribution constant of the analyte so that the amount of absorbed analyte increased [5]. Adding Na_2SO_4 to the sample solution may improve the sensitivity and the detection limit of SPME, but the amount of Na_2SO_4 added should be well controlled.

The precision of SPME for the determination of these analytes in deionized water and lake water was investigated. The relative standard deviations are given in Table 1. The values were about 1% for samples based on deionized water and 2% for samples of lake water, except for 2,4-dinitrotoluene, for which the values were 2% and 4%, respectively.

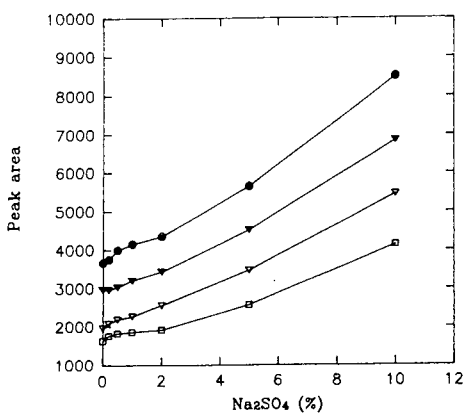

Fig. 6. Effect of Na_2SO_4 on the peak area of the four analytes (symbols as in Fig. 2). The sample solution (0.4 μg/ml each) was extracted by SPME for 10 min and desorbed in the GC injection port at 210°C for 5 min.

Table 1
Relative standard deviations (R.S.D.s) for the four analytes in lake water and deionized water

Compound	R.S.D. (%)[a]	
	Lake water	Deionized water
Nitrobenzene	0.8	1.7
Isophorone	0.5	0.5
2,4-Dinitrotoluene	0.9	2.1
2,6-Dinitrotoluene	2.0	4.4

[a] Data obtained for the concentrations of the four analytes from 0.4 to 10 μg/ml ($n = 15$).

The detection limits for the analytes in deionized water (0.05 μg/ml), calculated as three times the standard deviations of seven replicate runs, were 9 ng/ml for nitrobenzene and 15 ng/ml for the other three analytes.

Various amount of analytes (0.1, 0.4, 1, 2, 5 and 10 μg/ml) were added to deionized water and lake water to obtain the calibration graphs. The linearities were satisfactory. The slopes based on deionized water and lake water were almost identical, so that we were able to determine the analytes in lake water using calibration graphs based on deionized water.

4. Conclusions

Aqueous samples of the semi-volatile compounds nitrobenzene, isophorone, 2,4-dinitrotoluene and 2,6-dinitrotoluene were readily analysed using SPME with a polydimethylsiloxane-coated fibre. The sensitivity of this method decreased with increasing concentration of methanol and temperature of absorption and increased with increasing concentration of Na_2SO_4. Samples of lake water were analysed using calibration graphs based on deionized water. The relative standard deviations for these analytes were 1–2% in deionized water and 2–4% in lake water. The detection limits were 9 ng/ml for nitrobenzene and 15 ng/ml for the other three analytes.

Acknowledgements

This work was supported by the National Science Council of the Republic of China (NSC 83-0208-M007-67).

References

[1] M. Zief and R. Kiser, *Am. Lab.*, 22 (1990) 70.
[2] G.M. Hearne and D.O. Hall, *Am. Lab.*, 25 (1993) H28.
[3] G.A. Junk, M.J. Avery and J.J. Richard, *Anal. Chem.*, 60 (1988) 1347.
[4] D. Louch, S. Motlagh and J. Pawliszyn, *Anal. Chem.*, 64 (1992) 1187.
[5] C.L. Arthur, L.M. Killam, K.D. Buchholz and J. Pawliszyn, *Anal. Chem.*, 64 (1992) 1960.
[6] C.L. Arthur and J. Pawliszyn, *Anal. Chem.*, 62 (1990) 2145.
[7] C.L. Arthur, K. Pratt, S. Motlagh and J. Pawliszyn, *J. High Resolut. Chromatogr.*, 15 (1992) 741.
[8] C.L. Arthur, L.M. Killam, S. Motlagh, M. Lim, D.W. Potter and J. Pawliszyn, *Environ. Sci. Technol.*, 26 (1992) 979.
[9] D.W. Potter and J. Pawliszyn, *J. Chromatogr.*, 625 (1992) 247.
[10] S.B. Hawthorne, D.J. Miller, J. Pawliszyn and C.L. Arthur, *J. Chromatogr.*, 603 (1992) 185.
[11] Z. Zhang and J. Pawliszyn, *Anal. Chem.*, 65 (1993) 1843.
[12] C.L. Arthur, D.W. Potter, K.D. Buchholz, S. Motlagh and J. Pawliszyn, *LC · GC*, 10 (1992) 656.
[13] R.P. Belardi and J. Pawliszyn, *Water Pollut. Res. J. Can.*, 24 (1989) 179.
[14] K.D. Buchholz and J. Pawliszyn, *Environ. Sci. Technol.*, 27 (1993) 2844.
[15] K.D. Buchholz and J. Pawliszyn, *Anal. Chem.*, 66 (1994) 160.
[16] D.W. Potter and J. Pawliszyn, *Environ. Sci. Technol.*, 28 (1994) 298.
[17] *Instruction Sheet, 100 μm Polydimethylsiloxane Solid Phase Micro Extraction Fiber Assemblies, T713018A*, Supelco, Bellefonte, PA, 1993.
[18] J.H. Montgomery and L.M. Welkom, *Groundwater Chemical Desk Reference*, Lewis, Chelsea, MI, 1990.

ELSEVIER

Journal of Chromatography A, 678 (1994) 319–325

JOURNAL OF CHROMATOGRAPHY A

Determination of (methylcyclopentadienyl)manganesetricarbonyl in gasoline by capillary gas chromatography with alternating current plasma emission detection

Jackson M. Ombaba, Eugene F. Barry*

Department of Chemistry, University of Massachusetts Lowell, Lowell, MA 01854, USA

First received 6 July 1993; revised manuscript received 17 May 1994

Abstract

(Methylcyclopentadienyl)manganesetricarbonyl (MMT) commonly used as an antiknock agent in gasoline is determined by capillary gas chromatography with an alternating current plasma (ACP) detector. The ACP selectivity, the ratio of the peak area response of MMT per gram Mn to the peak area response for a hydrocarbon per gram of carbon, was found to exceed five orders of magnitude. Detection limits for MMT and a closely related organomanganese analyte, bis(pentamethylcyclopentadienyl)manganese (BPM), were calculated to be 62 and 69 pg/s (as Mn), respectively. Precision of the methodology was 6.6% relative standard deviation ($n = 10$) for both MMT and BPM.

1. Introduction

(Methylcyclopentadienyl)manganesetricarbonyl (MMT), $CH_3C_5H_4Mn(CO)_3$ and chemically similar compounds are currently used as substitutes for tetraethyllead to improve the octane rating of unleaded gasoline [1,2]. MMT is also used in aircraft fuels and in the production of heating oil to reduce flue-gas smoke [3]. Build up of Mn_3O_4 deposits may also decrease the efficiency of catalytic converters. Although 1 g of Mn as MMT is as effective in improving octane rating as 3.22 g of Pb as tetraethyllead [4], atmospheric manganese emissions are unfavorable and may offer a potential health risk. Levels above 5 μg Mn/l have been reported to lead to chronic manganese poisoning and manganese-induced pneumonia [5].

Because of the underlying toxicological properties of MMT and other closely related compounds, sensitive chromatographic detectors have been employed. One common method for the determination of MMT and other gasoline additives has been to interface various element-selective detectors with gas chromatography (GC). Uden et al. [6] reported a detection limit for MMT of 3 ng Mn by utilizing a direct GC interface to a d.c. plasma emission detector. Aue et al. [7] used a commercially available flame photometric detector resulting in the determi-

* Corresponding author.

0021-9673/94/$07.00
SSDI 0021-9673(94)00472-L

nation of MMT at the 0.6 ppm (w/w) level in gasoline. With a hydrogen atmosphere flame ionization detector, Dupuis and Hill [4] reported a MMT detection limit of $1.7 \cdot 10^{-14}$ g/s. Coe et al. [8] were able to analyze MMT in air samples from underground parking garages achieving detection of 0.05 ng MMT m^{-3}. Atmospheric pressure microwave plasma detection has also been utilized for the determination of MMT [9]. Other approaches that have been investigated in the analysis of MMT include atomic absorption spectroscopy (AAS) with a nitrous oxide–hydrogen flame [10], AAS with a heated vapor technique [11], carbon-filament AAS [3], neutron activation analysis, spark source mass spectrometry and X-ray fluorescence [12], and GC with flame ionization detection [13].

In this report an alternating current plasma (ACP) detector developed in our laboratory [14–18] is described for the selective determination of MMT in gasoline. A gas chromatograph is interfaced with an ACP detector through a quartz discharge tube which encloses a helium-sustained plasma. Observation of the optical emission spectrum resulting from the fragmentation and excitation of the organomanganese species entering the plasma affords sensitive, elemental-selective detection. A further advantage offered by the present design is the capability to view light emitted from the plasma axially with an appropriate light-collecting lens. With the earlier work in which the helium plasma was viewed transversely through the walls of the discharge tube, deposition of materials on the walls of the discharge tube and devitrification of the quartz resulted in gradual attenuation of detector response with time.

2. Experimental

2.1. Materials

Stock solutions of MMT and bis(pentamethylcyclopentadienyl)manganese (BPM) (Strem Chemical, Newburyport, MA, USA) were prepared by dissolving the appropriate amount of the analyte in acetone and subsequent standard solutions were prepared by serial dilution of the stock solution. The selectivity response mixture contained *n*-dodecane (Aldrich, Milwaukee, WI, USA) and MMT in acetone. Gasoline samples obtained locally were stored in amber bottles until needed. Gasoline samples were diluted 1 to 10 with acetone prior to GC in order to avoid saturation of the detector with hydrocarbons.

2.2. Instrumentation

The GC–ACP detector system has been described in detail elsewhere [14,18] and its experimental arrangement is illustrated in Fig. 1. Table 1 lists the components, model/type, manufacturer and the corresponding optimum operating conditions used throughout the study, unless otherwise noted. A megabore fused-silica capillary column employed for the entire study was a HP-1 30 m × 0.530 μm I.D. column with a film thickness of 0.25 μm (Hewlett-Packard, Avondale, PA, USA). The detector interface employed featured the megabore capillary column as the interface tube which extended from the GC oven, through a heated column jacket, into the ACP detector. The column jacket was clamped to a mount on the optical bench to

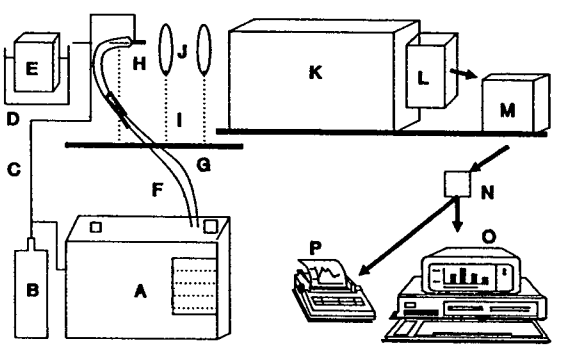

Fig. 1. Schematic representation of the GC–ACP detector instrumentation. A = Gas chromatograph; B = helium make gas; C = helium gas conduit; D = transformer water cooling jacket; E = transformer; F = GC–ACP detector interface column jacket (flexible tubing); G = optical bench; H = discharge tube; I = optical mount; J = focusing lens; K = monochromator; L = photomultiplier tube; M = picoammeter; N = resistor/capacitor low pass filter; O = data acquisition system; P = integrator.

Table 1
Components and operating conditions for GC–ACP detector

Components	Model/manufacturer	Experimental conditions
Gas chromatograph	Hewlett-Packard 5890A	Injector temperature: 160°C, interface temperature: 170°C, linear velocity: 30 cm/s, split ratio 10:1
ACP Power supply	Webster ignition transformer, Sta-Rite, Frankfort, KY, USA	Output: 285 W; 14 000 V, 23 mA
Monochromator	EU-700, 0.35 m; McPherson, Acton, MA, USA	Slit width: 30 μm, slit height: 5 mm
Photomultiplier tube (PMT)	R758, Hamamatsu Co., Middlesex, NJ, USA	Voltage: −1000 V d.c.
PMT Power supply	Model 7640, McPherson, Acton, MA, USA	
Picoammeter	414-S, Keithley Instruments, Cleveland, OH, USA	$3.0 \cdot 10^{-6}$–$10 \cdot 10^{-6}$ A
Focusing lens	Fused silica, Plano convex, Oriel Corp., Stratford, CT, USA	25.4 mm dia., 150 mm f.l.
Discharge tube	Laboratory constructed	End-on configuration, 2 cm × 1 mm I.D × 6 mm O.D.
Data acquisition Software	LabCalc, Galactic Industies, Salem, NH, USA	5 Hz
Computer	IBM-AT Compatible	
Resistor/capacitor low pass filter	Laboratory constructed	Time constant: 0.2 s

permit easy alignment and also to prevent any possible shift in optical alignment due to vibration. The capillary column was inserted through the center of one of the electrodes. Approximately 0.5 cm of the capillary column extended into the 2 cm × 6 mm O.D. × 1 mm I.D. quartz discharge tube which contains the plasma. The polyimide coating from this 0.5 cm segment was removed prior to insertion. In this arrangement, the column effluent was introduced directly into the plasma plume, minimizing band broadening.

The plasma was viewed in an axial position and focused on the entrance slit of the monochromator by means of two serial fused-silica biconvex lenses (25.4 mm diameter, 150 mm focal length). The output of the picoammeter was electrically filtered (time constant 0.2 s) and collected by the data acquisition system at a sampling rate of 5 Hz.

The total helium flow-rate through the discharge tube (column flow-rate plus plasma support flow-rate of helium) was adjusted slightly higher than the optimum value. The plasma was initiated by momentarily inserting the tip of a small diameter piece of copper wire, which acted as the second electrode, a few millimeters into the end of the discharge tube. After 2 min this combined helium flow-rate was readjusted to the optimum flow-rate of 1800 ml/min. The ACP detector was allowed to equilibrate after ignition for approximately 5 min to ensure stable, reproducible behavior.

3. Results and discussion

The analytical emission lines of manganese were focused on the monochromator by two methods. First, an ultrasonic nebulizer (a common room humidifier) was used to generate a headspace vapor of MMT which was transported to the ACP by helium flow. This procedure

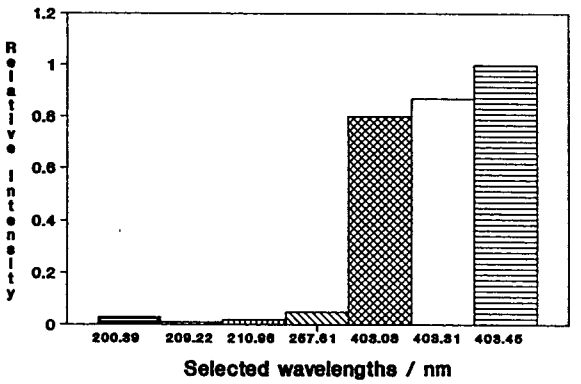

Fig. 2. Relative intensities of prominent Mn emission lines.

provided a constant mass introduction of manganese vapor into the plasma and the corresponding emission wavelengths of manganese were observed, as illustrated in Fig. 2. The 403.45-nm line was selected as the analytical wavelength for this study because of its favorable relative intensity and location with respect to the background emission spectrum where no interference from OH, N_2, NH, He and O is observed. Secondly, a manganese hollow-cathode lamp, typically employed in AAS, was employed to confirm the analytical emission line (403.45 nm) by positioning the lamp such that its emission lines were incident on the entrance slit of the monochromator. The carbon backbone of MMT was eliminated as the source of molecular emission in this spectral region because a scan of *n*-dodecane vapor in the ACP did not produce any major emission bands.

The ACP emission response at 403.45 nm resulting from a 0.5-μl injection of a standard solution of MMT in acetone solution (230 ng/μl) at a column temperature of 130°C is shown in Fig. 3A. On the other hand, BPM proved to be rather air-sensitive. When standard solutions of

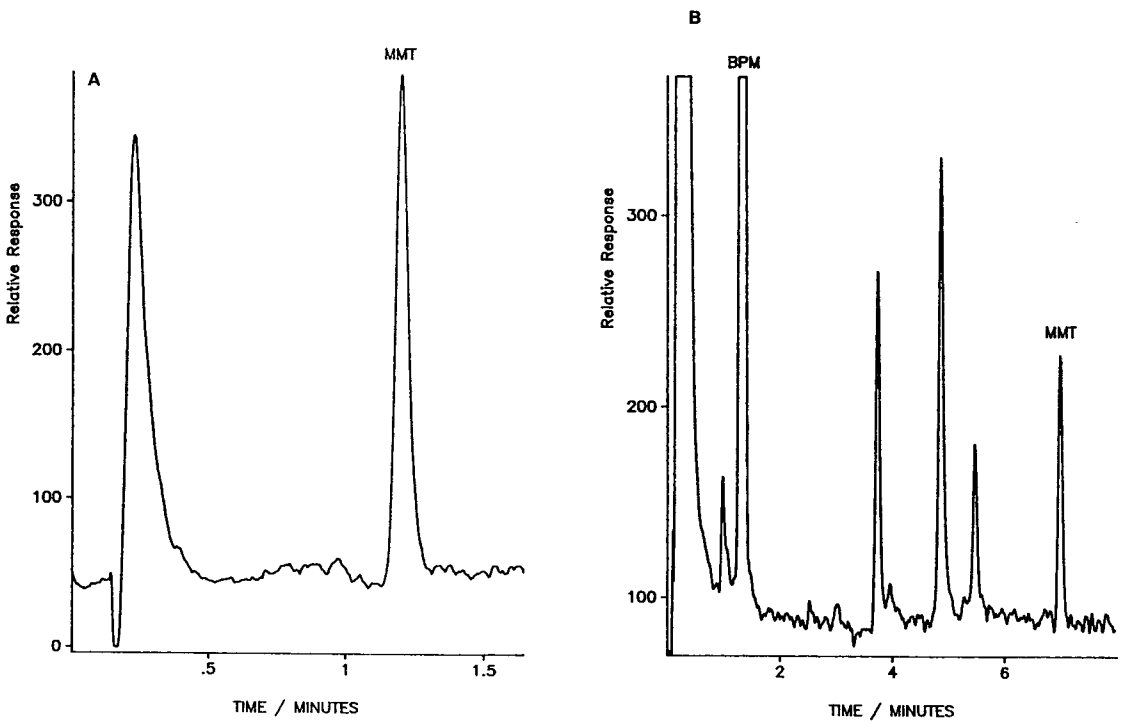

Fig. 3. (A) Isothermal separation at 130°C with ACP detector system of a standard solution of MMT in acetone; MMT peak corresponds to 1.15 ng Mn. (B) Temperature-programmed separation of BPM solution in acetone; conditions: 50°C (1 min) to 130°C at 10°C/min.

BPM were prepared in acetone, the formation of a brown flocculent precipitate was noted and suggestive of degradation. Fig. 3B illustrates a temperature-programmed separation of a acetone solution of BPM and its organomanganese degradation products which interestingly include MMT. In the chromatograms the pronounced negative response immediately after injection is associated with perturbation in the plasma due to the passage of a large volume of solvent through the plasma. The ACP detector can tolerate large volumes of eluted solvent without extinguishing and, thus, requires no venting valve, important advantages which suggest that an ACP detector can also be employed with packed GC columns.

3.1. Linearity and detection limits

A calibration plot of MMT and BPM for the ACP detector was constructed for the determination of the linear dynamic range, linearity and detection limits by making repetitive injections of known amounts of analyte into the GC–ACP system. The linear dynamic range for MMT and BPM extended over 3.5 orders of magnitude. Correlation coefficients of the log–log plots were found to be 0.9999 for both MMT and BPM. The detection limits of MMT and BPM were estimated based on integrated baseline noise [19,20]. Detection limit may be defined as the amount of analyte needed to produce a signal that is three times the standard deviation of the baseline noise divided by the sensitivity whereas sensitivity is defined as the slope of the calibration plot [21,22] multiplied by the peak-width at half height of the analyte peak to account for k' [23]. The detection limit was calculated to be 62 and 69 pg/s (as Mn) for MMT and BPM, respectively. The precision in response at twice the detection limit was under 6.6% relative standard deviation ($n = 10$) for MMT. The detection limit of BPM should be viewed cautiously in lieu of the inherent instability of BPM.

3.2. Selectivity

A mixture containing MMT and *n*-dodecane in acetone was used to establish the detector selectivity for MMT at a slit width of 30 μm. The selectivity can be defined as the ratio of the peak area response of the ACP detector toward MMT at 403.45 nm per gram of elemental manganese to the response of the detector to *n*-dodecane per gram of carbon. The selectivity toward manganese was then established by means of a response mixture that contained 1150 ng/μl of *n*-dodecane as internal standard and 1.74 ng/μl of MMT. A 0.2-μl aliquot was injected using a split ratio of 10:1 and a column temperature of 130°C, after which the responses at 403.45 nm of the hydrocarbon probe and MMT were compared. The average selectivity ratio for MMT resulting from a series of ten injections was $5.2 \cdot 10^5$. The ACP selectivity obtained in this study for MMT compares favorably with selectivity obtained by GC–flame photometric detection [7], even in the absence of background correction.

3.3. Analytical applications

Two applications were performed in order to demonstrate the selectivity of the ACP detection towards MMT in gasoline which represents a potentially interfering matrix. Old commercial regular unleaded gasoline containing no detectable amount of MMT was diluted one to ten with acetone. A 400-μl portion of this diluted gasoline sample was then spiked with a 200-μl aliquot of a solution containing 92 μg MMT and 142 μg BPM; a 0.2-μl volume of the resulting solution was injected into the chromatographic system. Several illustrative chromatograms appear in Fig. 4 which depict the ACP selectivity. Fig. 4A and B show chromatograms with ACP detection at 403.45 nm of unspiked and spiked regular grade unleaded gasoline, respectively, whereas a parallel chromatogram with flame ionization detection is displayed in Fig. 4C. The rapid coelution of many hydrocarbons is responsible for the irregular appearance at the beginning of the chromatogram in Fig. 4A, resulting in plasma instability and carbon background emission [15–18]. Commercial fuel samples were purchased locally and analyzed for MMT content; these results are presented in Table 2. The

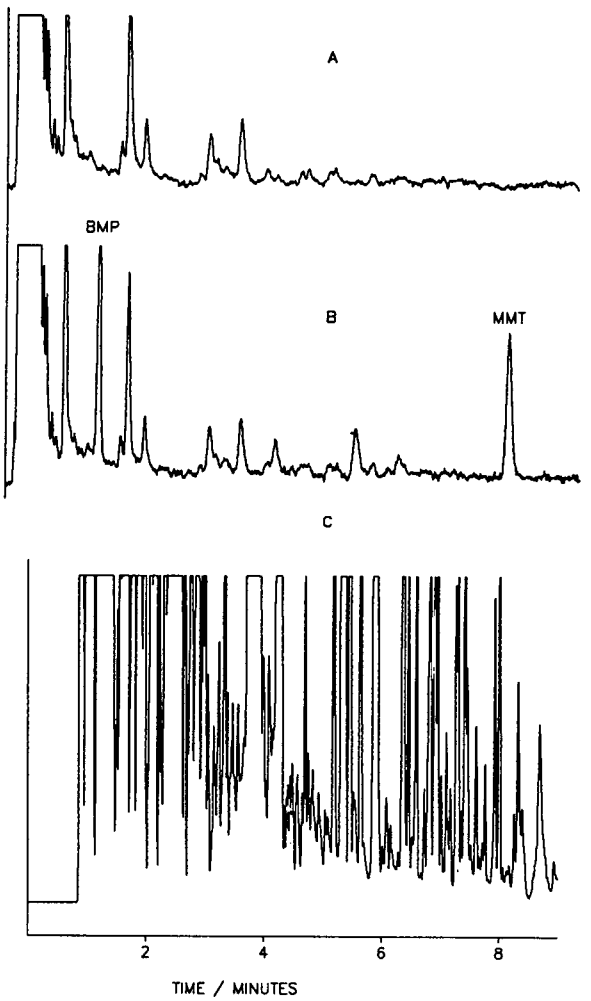

Fig. 4. (A) Chromatogram of unspiked old regular gasoline with ACP detection at 403.45 nm; (B) chromatogram of same gasoline spiked with MMT and BPM with ACP detection; (C) parallel flame ionization detection chromatogram of same sample as in (B); conditions: 30°C (1 min) to 130°C at 10°C/min.

MMT levels in the examined samples ranged from 9.74 to 16.9 μg/ml and compare favorably with the value of 7 μg MMT/ml in premium unleaded gasoline reported in a recent study [7].

4. Conclusions

The system described here provides a versatile element-selective detector for the determination of organomanganese additives in gasolines. Although the commercial GC–atomic emission spectroscopy system offers a more favorable organomanganese detection limit of 1.6 pg/s [24], the detector described here is easily assembled and interfaced with chromatographic equipment at moderate cost. The ACP detector exhibits a remarkably stable signal because the plasma is self-seeding, reigniting itself every half cycle which is 120 times per second for the 60-Hz power supply. A tesla coil is not required to commence operation of the plasma if the a.c. voltage is greater than the breakdown voltage. As a result, the ACP can tolerate high mass of solvent without extinguishing and, thus, requires no venting valve which lends itself to a less complex interface design and minimizes band broadening. The inclusion of signal-to-noise enhancement devices such as background correction components and more elaborate signal filtering could greatly improve the performance of the detector.

Table 2
Measured level of MMT in fuels

Fuel	μg/ml
Premium unleaded gasoline	9.73 (1.9)[a]
Regular unleaded gasoline	16.9 (2.3)
No. 2 Fuel Oil	16.4 (0.9)

[a] Values in parentheses represent average relative standard deviation of five replicate injections for six samples of each type of fuel obtained locally.

Acknowledgements

One of us (J.M.O.) wishes to acknowledge the Graduate School at the University of Massachusetts Lowell for a research fellowship. The authors are also appreciative of the data acquisition system donated by Galactic Industries.

References

[1] D.R. Bailey, F.J. Cordera and R.G. Tuell, *Belg. Pat.*, 613 117 (1963); *Chem. Abstr.*, 59 (1963) 7289b.

[2] A.T. Rolfe, *US Pat.*, 3 443 916 (1969); *Chem. Abstr.*, 71 (1969) 24558e.
[3] G.C. Everett, T.S. West and R.W. Williams, *Anal. Chim. Acta*, 70 (1974) 204.
[4] M.D. Dupuis and H.H. Hill, *Anal. Chem.*, 51 (1979) 292.
[5] J.W. Hwang, *Anal. Chem.*, 44 (1972) 20A.
[6] P.C. Uden, R.M. Barnes and F.P. Disanzo, *Anal. Chem.*, 50 (1978) 852.
[7] W.A. Aue, B. Millier and X.Y. Sun, *Anal. Chem.*, 62 (1990) 2453.
[8] M. Coe, R. Cruz and J.C. Van Loon, *Anal. Chim. Acta.*, 120 (1980) 171.
[9] B.D. Quimbly, P.C. Uden and R.M. Barnes, *Anal. Chem.*, 50 (1978) 2112.
[10] R.J. Lukasiewicz and B.E. Buell, *Appl. Spectrosc.*, 31 (1977) 541.
[11] W.K. Robbins, *Anal. Chem.*, 46 (1974) 2177.
[12] D.J. Von Lehmden, R.H. Jungers and R.E. Lee, *Anal. Chem.*, 46 (1974) 239.
[13] R.P. Hanzlik, C.E. Harkness and S. Arnoldi, *J. Chromatogr.*, 171 (1979) 279.
[14] R.B. Costanzo and E.F. Barry, *Anal. Chem.*, 60 (1988) 826.
[15] R.B. Costanzo and E.F. Barry, *J. High Resolut. Chromatogr.*, 12 (1989) 522.
[16] J.M. Ombaba and E.F. Barry, *J. Chromatogr.*, 598 (1992) 97.
[17] R.B. Costanzo and E.F. Barry, *J. Chromatogr.*, 467 (1989) 373.
[18] L.A. Colon and E.F. Barry, *J. High Resolut. Chromatogr.*, 14 (1991) 608.
[19] H.C. Smith and H.L. Walg, *Chromatographia*, 8 (1975) 311.
[20] C.H. Gast, J.C. Kraak, H. Poppe and J.M. Maessen, *J. Chromatogr.*, 185 (1979) 549.
[21] *Nomenclature, Symbols, Units and Their Usage in Spectrochemical Analysis II: Data Interpretation, Spectrochim. Acta.*, 33B (1978) 241.
[22] W.P. Carey and B.R. Kowalski, *Anal. Chem.*, 58 (1986) 3077.
[23] R.P.W. Scott, *Liquid Chromatography Detectors*, Elsevier, Amsterdam, New York, 2nd ed., 1986, p. 18.
[24] P.C. Uden, in P.C. Uden (Editor), *Element-Specific Chromatographic Detection by Atomic Emission Spectroscopy*, American Chemical Society, Washington, DC, 1992, p. 10.

ELSEVIER

Journal of Chromatography A, 678 (1994) 327–332

JOURNAL OF CHROMATOGRAPHY A

Effect of physico-chemical properties and molecular structure on the micelle–water partition coefficient in micellar electrokinetic chromatography

Nong Chen[a,*], Yukui Zhang[a], Shigeru Terabe[b], Terumichi Nakagawa[c]

[a]*National Chromatographic R & A Centre, Dalian Institute of Chemical Physics, Academia Sinica, Dalian 116011, China*

[b]*Faculty of Science, Himeji Institute of Technology, Kamigori, Hyogo, Japan*

[c]*Faculty of Pharmaceutical Sciences, Kyoto University, Sakyo-ku, Kyoto 606, Japan*

First received 7 February 1994; revised manuscript received 25 April 1994

Abstract

Quantitative structure–migration relationship (QSMR) analyses for neutral compounds were carried out in micellar electrokinetic chromatography (MEKC) with sodium dodecyl sulfate solution. Linear log–log relationships were found between both the micelle–water partition coefficient (log P_{mc}) and the capacity factor and the octanol–water partition coefficient (log P_{oct}). The quantitative relationship between log P_{mc} for neutral compounds and the solvatochromic parameters is described. The relationships developed from this work were used to predict micelle–water partition coefficients in MEKC.

1. Introduction

Micellar electrokinetic chromatography (MEKC) is a branch of high-performance capillary electrophoresis (HPCE) that allows electrically neutral substances that cannot be separated in principle by conventional free-solution capillary electrophoresis to be effectively separated. MEKC is a relatively recent and important modification of capillary zone electrophoresis (CZE) [1–5].

Resolution in MEKC can be enhanced through careful manipulation of the micelle–water partition coefficient, which is directly related to the capacity factor, and through extending the migration time window (i.e., reducing the ratio of the migration time of the aqueous phase to the micellar phase). The selectivity for neutral solutes in MEKC is determined almost exclusively by micelle–water partition coefficients, which gives useful information about the partition mechanism of the analyte between the micellar phase and the aqueous buffer. MEKC allows the calculation of the partition coefficient between the micelle and the surrounding aqueous phase, and is more suitable than micellar liquid chromatography for calculation of the micelle–water partition coefficient [4,5].

The micelle–water partition coefficient gives very interesting characteristics of selectivity to MEKC with regard to the separation of many neutral solutes. An accurate knowledge of mi-

* Corresponding author. Present address: Department of Material Science, Faculty of Science, Himeji Institute of Technology, Hyogo 671-22, Japan.

0021-9673/94/$07.00
SSDI 0021-9673(94)00399-T

celle–water partition coefficients is essential for a better understanding of the separation mechanisms and in designing optimization strategies [3,4]. Accurate prediction of this value from physico-chemical parameters and molecular structures of the solute is useful in elucidating the migration mechanism in MEKC, which will be especially advantageous for studies of quantitative structure migration–relationships (QSMR).

QSMRs result from applying the methodology used for quantitative structure–biological activity relationships (QSAR) to the analysis of capillary electrophoretic data [6–9]. To obtain valuable QSARs, reliable input data must be provided and a stringent statistical analysis should be carried out. Quantitative retention–biological activity relationship studies by micellar liquid chromatography have been reported [7–10]. Capillary electrophoresis (CE) is now able readily to yield a great amount of unequivocally precise and reproducible data. In the CE process, all electrophoretic conditions can be kept constant, so structural parameters of the solutes such as the charge and molecular size become the single independent variable in the system [11,12]. QSMRs can be utilized for testing the applicability of individual structural parameters for property description, which may be applicable to biological or biomedical QSARs. In MEKC, the migration parameter can be well represented by the capacity factor or the micelle–water partition coefficient. In this study, QSMR analyses for neutral compounds in MEKC were carried out and the thermodynamic equation for the correlation between the micelle–water partition coefficient (log P_{mc}) and the octanol–water partition coefficient (log P_{oct}) was established. A quantitative relationship between the micelle–water partition coefficient and solvatochromic parameters of the solutes was established by utilizing the linear solvation energy relationship (LSER). The relationships developed from this work were used for the prediction of micelle–water partition coefficients and also capacity factors in MEKC. All the MEKC capacity factors and log P_{mc} values were taken from published data [4,5,13,14].

2. Results and discussion

2.1. Linear relationship between micelle–water and octanol–water partition coefficients

According to the well known equation in chromatography in which the capacity factor is related to the partition coefficient (P_{mc}), the capacity factor in MEKC can be expressed by

$$k' = P_{mc}V_{mc}/V_{aq} \quad (1)$$

where k' is the capacity factor, V_{mc} and V_{aq} are the volumes of the micelle and the remaining aqueous phase, respectively, and P_{mc} is the micelle–water parition coefficient.

According to an extrathermodynamic relationship [8,9], a linear relationship between the partitioning behaviour in micelle–water and octanol–water is generally observed, hence an approximately linear relationship between log P_{mc} and log P_{oct} is obtained and can be expressed by the Collander equation:

$$\log P_{mc} = a_1 \log P_{oct} + a_0 \quad (2)$$

where P_{mc} and P_{oct} are micelle–water and octanol–water partition coefficients, respectively, and a_0 and a_1 are constants.

In addition, an approximately linear relationship between log k' and log P_{oct} can also be obtained:

$$\log k' = a_0 + \log V_{mc}/V_{aq} + a_1 \log P_{oct} \quad (3)$$

Logarithmic plots of the sodium dodecyl sulfate (SDS)–water partition coefficients vs. octanol–water partition coefficients for six and nine neutral compounds are shown in Figs. 1 and 2.

The effect of temperature (T) on the micelle–water partition coefficient follows the Van 't Hoff equation:

$$\log P_{mc} = -\Delta H^0/RT + \Delta S^0/R \quad (4)$$

where ΔH^0 is the standard enthalpy change of transfer between the micelle and water and ΔS^0 is the corresponding standard entropy change.

The observed parallel linear relationships between log P_{mc} and $1/T$ [5] implies that the micelle–water partition process is mainly gov-

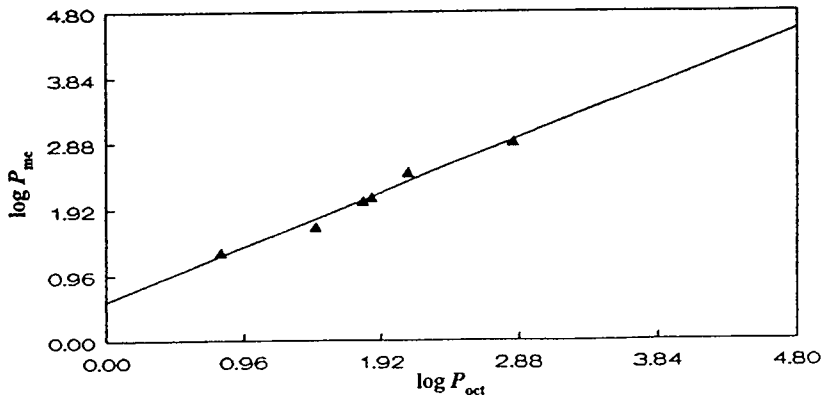

Fig. 1. Linear relationship between log P_{mc} and log P_{oct} for six neutral compounds in SDS–buffer system. Log P_{mc} values from Ref. [5], log P_{oct} from Ref. [15]. 100 m*M* borate–50 m*M* phosphate buffer (pH 7.0), 25°C. The linear regression is log $P_{mc} = 0.579 + 0.825$ log P_{oct} ($n = 6$, $r = 0.989$).

erned by the contribution of the entropy term, and the MEKC selectivity factors are independent of the temperature applied, which is different from that in RP-HPLC [16]. Better linear relationships between log P_{mc} and log P_{oct} at different temperature were obtained. The following are the results of linear regression analyses between log P_{mc} and log P_{oct} for resorcinol, phenol, *p*-nitroaniline, nitrobenzene, toluene and 2-naphthol at five different column temperatures:

30°C: log $P_{mc} = 0.816$ log $P_{oct} + 0.553$, $n = 6$, $r = 0.987$;

35°C: log $P_{mc} = 0.801$ log $P_{oct} + 0.533$, $n = 6$, $r = 0.983$;

40°C: log $P_{mc} = 0.784$ log $P_{oct} + 0.539$, $n = 6$, $r = 0.981$;

45°C: log $P_{mc} = 0.785$ log $P_{oct} + 0.498$, $n = 6$, $r = 0.977$.

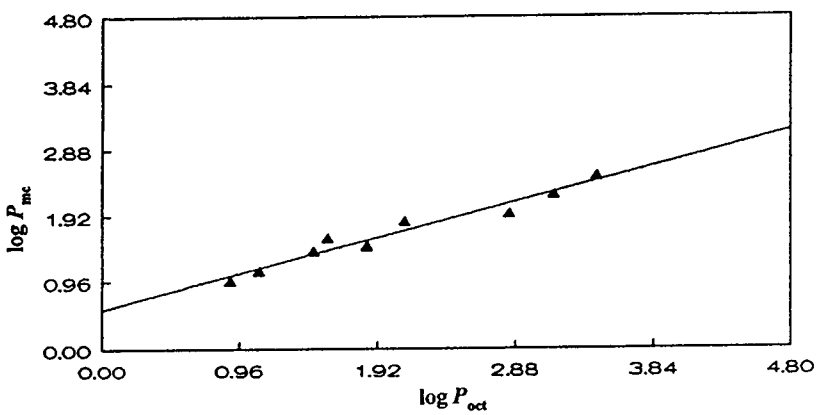

Fig. 2. Linear relationship between log P_{mc} and log P_{oct} for nine neutral compounds in SDS–buffer system. The regression equation is log $P_{mc} = 0.555 + 0.541$ log P_{oct} ($n = 9$, $r = 0.977$). See Table 1 for details.

It was shown by Nielsen and Foley [14] that a buffer solution containing magnesium dodecyl sulfate [$Mg(DS)_2$] exhibited electroosmotic velocities one third to half that of an SDS solution, and the migration time window for $Mg(DS)_2$ was independent of the percentage of organic modifier in the buffer solution while the migration time window for SDS increased as the percentage of organic modifier increased. Fig. 3 shows linear log–log plots between log k' and log P_{oct} for seven neutral compounds in two surfactant systems. The parallel linear relationships between log k' and log P_{oct} in the two surfactant systems implies that the retention mechanisms are similar and the selectivities are the same. From the linear relationships between log k' and log P_{oct} in both surfactant systems, it is interesting to note that the $Mg(DS)_2$ micelle is more hydrophobic than the SDS micelle, which agrees well with the results of hydrophobic selectivity found by Nielsen and Foley [14].

2.2. Quantitative relationship between the micelle–water partition coefficient in MEKC and the solvatochromic parameters

The effect of molecular parameters on log P_{mc} can be studied based on the LSERs, where for neutral compounds the solvent-dependent properties depend on four types of terms and the general LSER for solutes takes the form [17–21]

$$SP = SP_0 + m\nu + d\pi + b\beta + a\alpha \quad (5)$$

where SP represents solvent-dependent properties and here it refers to log P_{mc}, ν is the molar volume or Van der Waals volume ($\nu_w/100$), π is a measure of the solute dipolarity/polarizability, β is the hydrogen bond donor ability, α is the hydrogen acceptor ability and m, d, b and a are constants. Therefore, log P_{mc} can be given by the following equation:

$$\log P_{mc} = SP_0 + m\nu + d\pi + b\beta + a\alpha \quad (6)$$

For structurally related compounds whose solvatochromic parameters π, β and α are almost the same, a linear relationship between log P_{mc} and ν can be derived. Fig. 4 shows the linear relationship between log P_{mc} and ν for six structurally related alkylphenols in an SDS–buffer system.

The sign of the coefficients in Eq. 6 is determined by whether the term represents an exoergic or endoergic situation in the micelle–water partitioning process. The hydrophobic volume of a neutral solute makes a positive contribution to log P_{mc}. Therefore, there is general trend that as the solute becomes increas-

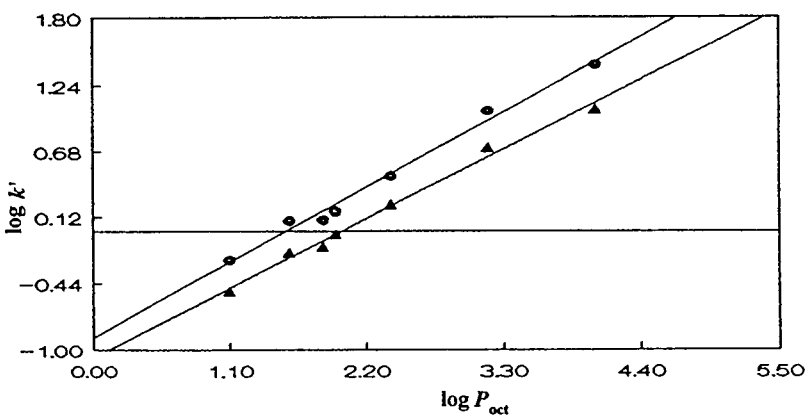

Fig. 3. Linear relationships between log k' and log P_{oct} for seven neutral compounds (benzyl alcohol, acetophenone, nitrobenzene, nitrophenyl acetate, *m*-nitrotoluene, benzophenone and biphenyl) in (▲) SDS and (●) $Mg(DS)_2$ systems. Log P_{mc} values from Ref. [14], log P_{oct} from Ref. [15]. Buffer: 50 m*M* surfactant–10% acetonitrile–5 m*M* phosphate–4 m*M* EDTA at pH 7.2. The regression equations in SDS and $Mg(DS)_2$ buffer systems are log $k' = -1.067 + 0.533$ log P_{oct} ($n = 7$, $r = 0.996$) and log $k' = -0.899 + 0.576$ log P_{oct} ($n = 7$, $r = 0.994$), respectively.

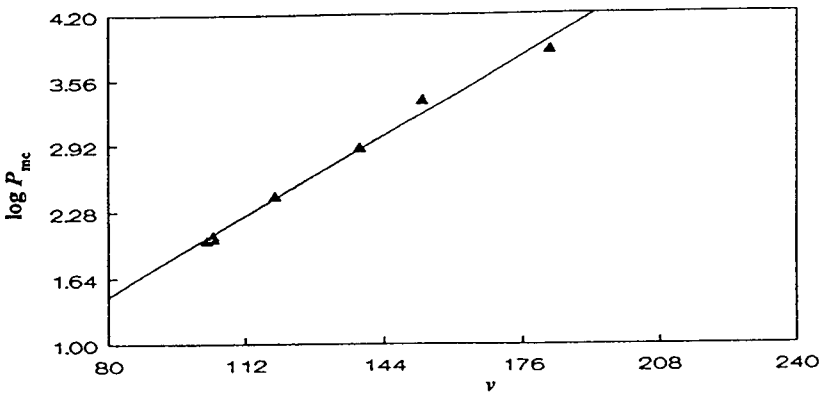

Fig. 4. Linear relationship between log P_{mc} and molar volume for seven structurally related alkylphenols (*o*-cresol, *m*-cresol, *p*-cresol, 2,4-xylenol, *p*-propylphenol, *p*-butylphenol and *p*-amylphenol) in SDS–buffer system (100 m*M* borate–50 m*M* phosphate buffer, pH 7.0) at 30°C. Log P_{mc} values from Ref. [5]. The regression equation is log $P_{mc} = 0.0242v - 0.475$ ($n = 7$, $r = 0.995$).

ingly hydrophobic, log P_{mc} will become increasingly positive, which is consistent with the practical observations in MEKC. For complex compounds with different functional groups, a quantitative relationship between the micelle–water partition coefficient and the solvatochromic parameters was found. Table 1 shows the solvatochromic parameters for eleven compounds and a comparison of the experimentally measured log P_{mc} and the values calculated from the solvatochromic parameters. The resulting equation obtained by least-squares regression is

$$\log P_{mc} = -0.0033 + 4.057v_w/100 - 0.542\pi - 1.534\beta - 0.397\alpha \quad (7)$$
$$n = 11,\ r = 0.991$$

In this and all the regression equations in this

Table 1
Values of solvatochromic parameters and comparison of the experimental log P_{mc} and the predicted values for eleven neutral compounds in SDS–buffer system

Compound[a]	$v_w/100$	π	β	α	Log P_{mc}		Difference
					Exptl.	Calc.	
1	0.562	0.73	0.50	0.26	0.96	1.01	0.05
2	0.536	0.72	0.33	0.61	1.04	1.03	−0.01
3	0.634	0.99	0.52	0.39	1.10	1.08	−0.02
4	0.606	0.92	0.44	0.00	1.39	1.28	−0.11
5	0.631	1.01	0.30	0.00	1.47	1.55	0.08
6	0.788	1.30	0.58	0.00	1.55	1.60	0.05
7	0.690	0.90	0.49	0.04	1.58	1.54	−0.04
8	0.592	0.55	0.11	0.00	1.83	1.93	0.10
9	0.581	0.71	0.07	0.00	1.94	1.86	−0.08
10	0.668	0.53	0.12	0.00	2.22	2.24	0.02
11	0.753	0.70	0.15	0.00	2.49	2.44	−0.05

Solvatochromic parameters taken from Ref. [17]. Data recalculated from Ref. [13], log P_{oct} from Ref. [15]. 25 m*M* borate buffer at pH 8.5 with SDS concentrations of 30, 70, 110 and 150 m*M*; fused-silica capillary (57 cm × 75 μm I.D.); 25°C.

[a] Nos. 1–11 denote aniline, phenol, benzyl alcohol, benzaldehyde, nitrobenzene, phenylacetone, acetophenone, toluene, chlorobenzene, ethylbenzene, naphthalene, respectively.

paper, n is the number of data points in the regression, r is the regression coefficient and ν_w is the Van der Waals volume.

The calculated log P_{mc} values are consistent with the experimental values. The contribution of the ν_w term is very significant; the ν_w term makes a positive contribution to log P_{mc}, whereas the π, β and α terms make negative contributions, indicating that there is a general trend that as the solute becomes increasing hydrophobic, log P_{mc} will become increasingly positive. In contrast, as the solute becomes more polar or stronger to accept or donor the hydrogen bonding, log P_{mc} will decrease when other conditions remain the same, which is similar to the effects observed in RP-HPLC [17,18,20].

Acknowledgements

N.C. and Y.Z. are most grateful for financial support from the National Natural Science Foundation of China and the Young Postdoctoral Foundation of Liaoning Province. N.C. also thanks Dr. Norio Matsubara of Himeji Institute of Technology for his kind assistance with the preparation of the manuscript.

References

[1] S. Terabe, K. Otsuka, K. Ichikawa, A. Tsuchiya and T. Ando, *Anal. Chem.*, 56 (1984) 111.
[2] S. Terabe, K. Otsuka and T. Ando, *Anal. Chem.*, 57 (1985) 834.
[3] S. Terabe, N. Chen and K. Otsuka, in A. Chrambach, M.J. Dunn and B.J. Radola (Editors), *Advances in Electrophoresis: Micellar Electrokinetic Chromatography*, VCH, Weinheim, 1994, in press.
[4] A.S. Kord, J.K. Strasters and M.G. Khaledi, *Anal. Chim. Acta*, 246 (1991) 131.
[5] S. Terabe, T. Katsura, Y. Okada, Y. Ishihama and K. Otsuka, *J. Microcol. Sep.*, 5 (1993) 23.
[6] R. Kaliszan, *Anal. Chem.*, 64 (1992) 619A.
[7] E.D. Breyer, J.K. Strasters and M.G. Khaledi, *Anal. Chem.*, 63 (1991) 828.
[8] M.G. Khaledi and E.D. Breyer, *Anal. Chem.*, 61 (1989) 1041.
[9] C. Treiner and A.K. Chattopadhyay, *J. Colloid Interface Sci.*, 109 (1986) 101.
[10] M. Valsara, *Sep. Sci. Technol.*, 25 (1990) 369.
[11] N. Chen, L. Wang and Y.K. Zhang, *Chromatographia*, 37 (1993) 429.
[12] N. Chen, L. Wang and Y.K. Zhang, *J. Chromatogr.*, 644 (1993) 175.
[13] J. Vindevogel, R. Szucs and P. Sandra, *J. Microcol. Sep.*, 4 (1992) 399.
[14] K.R. Nielsen and J.P. Foley, *J. Microcol. Sep.*, 5 (1993) 347.
[15] A. Leo, C. Hansch and D. Elkins, *Chem. Rev.*, 71 (1971) 525.
[16] N. Chen, Y.K. Zhang and P.C. Lu, *J. Chromatogr.*, 603 (1992) 25.
[17] M.J. Kamlet, R.M. Doherty, M.H. Abraham, Y. Marcus and R.W. Taft, *J. Phys. Chem.*, 92 (1988) 5244.
[18] P.W. Carr, R.M. Doherty, M.J. Kamlet, R.W. Taft, W. Melander and Cs.Horváth, *Anal. Chem.*, 58 (1986) 2674.
[19] D.E. Leahy, P.W. Carr, R.S. Pearlman, R.W. Taft, W. Melander and Cs. Horváth, *Chromatographia*, 21 (1980) 473.
[20] N. Chen, Y.K. Zhang and P.C. Lu, *J. Chromatogr.*, 606 (1992) 1.
[21] N. Chen, Y.K. Zhang and P.C. Lu, *J. Chromatogr.*, 633 (1993) 31.

ELSEVIER

Journal of Chromatography A, 678 (1994) 333–342

JOURNAL OF CHROMATOGRAPHY A

Chiral separation of drugs by capillary electrophoresis using β-cyclodextrin polymer

Hiroyuki Nishi*, Kouji Nakamura, Hideo Nakai, Tadashi Sato

Analytical Chemistry Research Laboratory, Tanabe Seiyaku Co., Ltd., 16-89, Kashima 3-chome, Yodogawa-ku, Osaka 532, Japan

First received 21 February 1994; revised manuscript received 29 April 1994

Abstract

The direct separation of enantiomers of trimetoquinol hydrochloride, related substances and some other drugs was investigated by capillary electrophoresis employing six kinds of cyclodextrins (CDs). Enantiomeric recognition of trimetoquinol and related substances was successfully achieved by using β-cyclodextrin (β-CD), heptakis(2,6-di-O-methyl)-β-cyclodextrin (DM-β-CD) and β-CD polymer. β-CD polymer was especially effective for the separation of both enantiomers and different solutes. The effects of the amount of β-CD polymer added to the background electrolyte, the pH of the buffer solution and some additives such as an organic solvent or a surfactant on the resolution of enantiomers were examined. The best enantioseparation was obtained by employing 5–7% β-CD polymer in an acidic solution with a surfactant.

1. Introduction

Capillary electrophoresis (CE) has become a powerful and a popular separation technique because of the fast separation and high resolution achieved [1–3]. Several different separation modes, from capillary gel electrophoresis (CGE) to micellar electrokinetic chromatography (MEKC) [4,5], have been developed and consequently a wide variety of substances such as ions, drugs and biopolymers can now be investigated by CE, according to the physico-chemical properties of the analyte.

The synthesis of chiral compounds and recognition of molecular chirality are important subjects, especially in the pharmaceutical industry, because stereochemistry can have a significant effect on the biological activity of a drug. Further, it is necessary to develop a chiral separation method for the determination of the optical purity of drugs from the viewpoint of quality control, because the antipode of a chiral drug is regarded as one of the impurities. Chromatographic approaches, particularly those using high-performance liquid chromatography (HPLC), are the most successful for the analysis of enantiomers [6,7]. HPLC is also suitable for biomedical samples.

Concerning the separation of enantiomers, CE techniques can take advantage of the ultra-high separation efficiency, easy changes of separation media, extremely small volumes of the sample and the media, etc., in comparison with HPLC. In the development of a CE chiral separation

* Corresponding author.

0021-9673/94/$07.00
SSDI 0021-9673(94)00456-J

method, one can easily alter the separation solution to find the optimum separation medium and can also use an expensive chiral selector because of the small amount required.

Recently much work has been reported on the direct resolution of enantiomers by capillary zone electrophoresis (CZE) employing cyclodextrins (CDs) (CD-CZE) [8–10]. CDs have also been used successfully in chiral separations by CGE [11] or MEKC (CD-MEKC) [12,13]. CDs are cyclic oligosaccharides with truncated cylindrical molecular shapes. Differential inclusion complex formation between CDs and the solute provides differential solute migration and chiral recognition. CD immobilized stationary phases for HPLC or GC are now widely used and most of them are commercially available. Chiral separation by CE using a CD immobilized capillary tube (for GC) has been also reported [14].

In this paper, chiral separation of trimetoquinol hydrochloride and related substances by CD-CZE, especially employing β-CD polymer, is described. Cyclodextrin polymers have been used in chromatographic separations for the improvement of selectivity or optical resolution [15–18]. The effects of β-CD polymer concentration on the migration time and chiral recognition were investigated. The effects of some additives, such as an organic solvent, other CDs or a surfactant, and the buffer pH on the separation of enantiomers were also examined. A comparison between β-CD polymer and β-CD as chiral selectors in CD-CZE is briefly discussed.

2. Experimental

2.1. Apparatus

Most of the experiment was carried out with the following laboratory-made apparatus: a fused-silica capillary of 40 cm length (effective length 25 cm) and 50 μm I.D. (Scientific Glass Engineering, Ringwood, Victoria, Australia) was used as the separation tube, a Model HCZE-30PN0.25 high-voltage d.c. power supply (Matsusada Precision Devices, Kusatsu, Shiga, Japan) delivering from −25 to +25 kV was used to drive the separation, the migrating solutes were detected by the on-column measurement of UV absorption at 220 nm with an SPD-6A spectrophotometer (Shimadzu, Kyoto, Japan) at a time constant of 0.05 s using a laboratory-made cell holder and a slit and a Chromatopac C-R5A (Shimadzu, Kyoto, Japan) was used for data processing. Other apparatus and experimental procedures were the same as reported previously [19]. Some of the experiments were performed on a Beckman P/ACE system 5510 equipped with a UV detector adjusted to 214 nm. A capillary tube of 57 cm total length (effective length 50 cm) and 75 μm I.D. was used in the system for the separation. The separation obtained from the laboratory-made apparatus showed a noisy baseline compared with the P/ACE system.

2.2. Reagents

Five types of CDs, α-CD, β-CD, heptakis-(2,6-di-O-methyl)-β-CD (DM-β-CD), heptakis-(2,3,6-tri-O-methyl)-β-CD (TM-β-CD) and γ-CD, were obtained from Nacalai Tesque (Kyoto, Japan). Water-soluble β-CD polymer, which was synthesized by condensation of β-CD molecules with epichlorohydrin (see Fig. 1), was purchased from Wako (Osaka, Japan). Up to a 10% β-CD polymer solution can be prepared. All other reagents and solvents were of analytical-reagent grade from Katayama Kagaku Kogyo (Osaka, Japan). Water was purified with a Milli-RO 60 water system (Millipore Japan, Tokyo, Japan). CD solution was prepared by dissolving each CD in a 25 m*M* phosphate buffer solution (pH 2.7 or

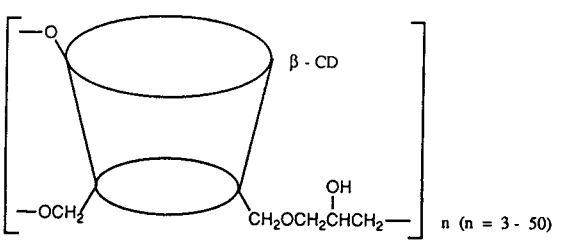

Fig. 1. Structure of β-CD polymer.

6.5) containing 2 *M* urea. The solution was passed through a membrane filter of 0.45-μm pore size (Gelman Science Japan, Tokyo, Japan) and degassed by sonication with a Branson B-2200 ultrasonic cleaner (Yamato, Tokyo, Japan) prior to use.

The structures of samples are shown in Fig. 2. Enantiomers of denopamine, trimetoquinol hydrochloride and the positional isomer of the hydroxy group of trimetoquinol were obtained from Tanabe Seiyaku (Osaka, Japan). Other racemic compounds with structures similar to that of trimetoquinol were purchased from Aldrich (Milwaukee, WI, USA). The samples were dissolved in methanol–water (50:50) at an approximate concentration of 0.1–1 mg/ml so that adequate peak heights could be obtained. Sample injection was performed by siphoning for the laboratory-made apparatus and by the pressure mode for the P/ACE 5510 system.

3. Results and discussion

3.1. Chiral recognition by CDs

The separation model of CD-CZE has been described by Wren and Rowe [20,21]. The difference in electrophoretic mobilities between two enantiomers pairs, $\Delta\mu$, is given by

$$\Delta\mu = \frac{[C](\mu_f - \mu_c)(K_1 - K_2)}{1 + [C](K_1 + K_2) + K_1K_2[C]^2} \quad (1)$$

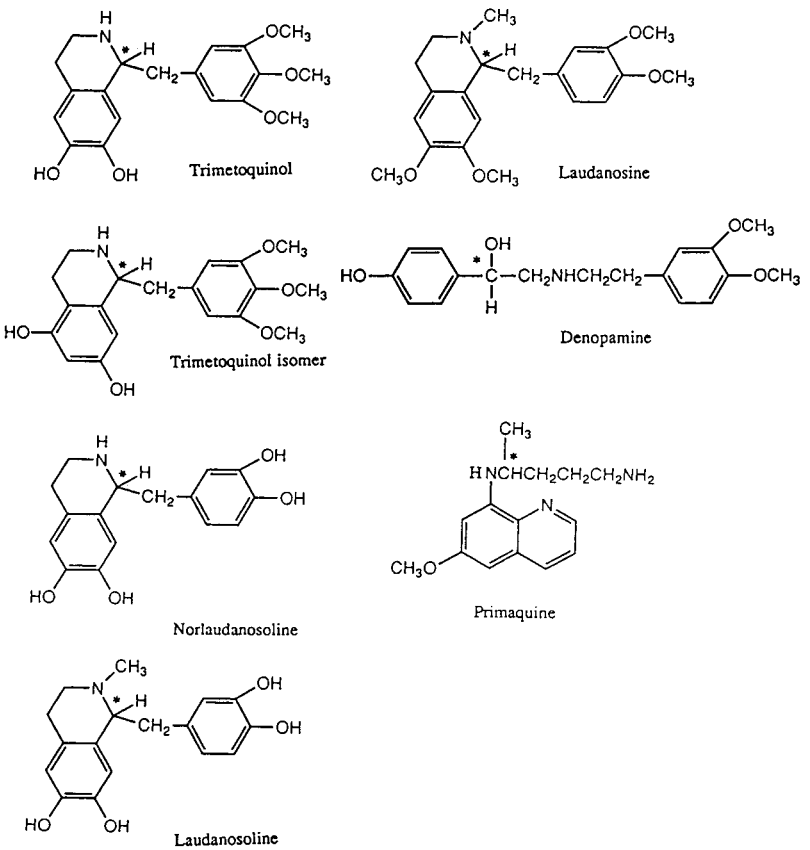

Fig. 2. Structures of samples.

where μ_f is the electrophoretic mobility of the enantiomers in free solution, μ_c is the electrophoretic mobility of the CD-complexed enantiomers, K_1 and K_2 are formation constants of the inclusion complexes of two enantiomers and [C] is the concentration of CD.

Eq. 1 shows the dependence of $\Delta\mu$ on the difference in the mobilities between the free and the CD-complexed enantiomer, $\mu_f - \mu_c$, the formation constants, K_1 and K_2, and the concentration of CD. It is obvious that the larger is the difference $\mu_f - \mu_c$ the greater is $\Delta\mu$. Therefore, an acidic buffer solution was selected to decrease the electroosmotic flow, leading to a small μ_c value. The effect of the type of CD on the chiral recognition of the samples was then investigated by using a 25 m*M* phosphate buffer solution of pH 2.7 containing 2 *M* urea and 20 m*M* of each CD or 1% β-CD polymer. The applied voltage was 15 kV. Urea was added to increase the solubility of the CDs in the aqueous phase [22].

The results are summarized in Table 1 together with the result of MEKC using sodium taurodeoxycholate (STDC) [23]. Chiral recognition was observed with all CDs except α-CD. Chiral recognition depended on the type of CD and DM-β-CD showed the widest enantioselectivity for these solutes. A typical separation using DM-β-CD is shown in Fig. 3. Chiral recognition of denopamine and laudanosine in CD-CZE was only successful when employing DM-β-CD. Chiral separation of denopamine, primaquine and some other drugs by CD-CZE with DM-β-CD has been reported in detail previously [24].

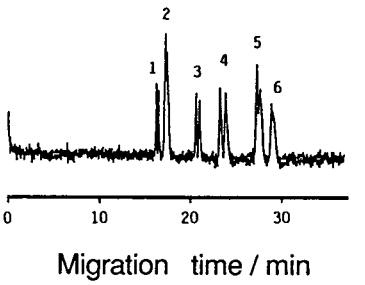

Fig. 3. Separation of enantiomers by CD-CZE using DM-β-CD. Solutes: 1 = primaquine; 2 = laudanosine; 3 = trimetoquinol; 4 = denopamine; 5 = trimetoquinol isomer; 6 = 6-chlorodiltiazem. Conditions: buffer, 25 m*M* phosphate buffer of pH 2.7 containing 2 *M* urea and 20 m*M* DM-β-CD; separation tube; 40 cm (effective length 25 cm) × 50 μm I.D.; applied voltage, 15 kV; detection, 220 cm (0.08 AUFS); temperature, ambient.

Separation of the enantiomers of trimetoquinol hydrochloride was achieved by using β-CD, DM-β-CD or β-CD polymer. Chiral separation of trimetoquinol-related compounds was also successful with the same β-type CDs, having a 7–8 Å diameter cavity. However, the chiral recognition of these solutes by TM-β-CD was

Table 1
Chiral recognition by cyclodextrins

CD	Concentration	Solute[a]						
		1	2	3	4	5	6	7
α-CD	20 m*M*	×	–	×	×	×	×	×
β-CD	20 m*M*	○	○	○	○	×	×	×
γ-CD	20 mM	×	–	×	×	△	×	○
DM-β-CD	20 m*M*	○	△	○	○	△	○	○
TM-β-CD	20 m*M*	×	△	×	×	×	△	○
β-CD polymer	1%	○	○	○	○	×	×	×
STDC[b]		○	–	△	×	○	×	–

Buffer, 25 m*M* phosphate (pH 2.7) containing 2 *M* urea and each CD. Conditions: applied voltage, 15 kV; temperature, ambient; detection, 220 nm.

[a] Solutes: 1 = trimetoquinol; 2 = trimetoquinol isomer; 3 = norlaudanosoline; 4 = laudanosoline; 5 = laudanosine; 6 = denopamine; 7 = primaquine. Symbols: ○ = $R_s > 0.5$; △ = $0.5 > R_s > 0.1$; × = not separated; – = not examined.

[b] From Ref. [23].

not successful. This can probably be interpreted by the steric hindrance due to the 3-O-methyl group: it is known that the introduction of a methyl group into a hydroxy group at the 3-position of the glucose unit in CDs causes strain of CD cavity [25], leading to interference with the penetration of the solute into the CD cavity. The cavity size of α-CD (cavity diameter 5–6 Å) and γ-CD (cavity diameter 9–10 Å) was not suited to the molecular size of these substances. The dimensions of CDs and trimetoquinol hydrochloride are summarized in Fig. 4. Chiral separation of laudanosoline, which was not successful by MEKC with STDC [23], was achieved by CD-CZE, although the chiral recognition of laudanosine was decreased.

3.2. Comparison between β-CD and β-CD polymer as a chiral selector

The molecular mass (M_r) of β-CD polymer has a range because of the wide range of the degree of polymerization (3–50) of β-CD (M_r 1135). However, the M_r of one unit of water-soluble β-CD polymer (1135 + 55; see Fig. 1) is almost the same as that of β-CD, indicating that a solution having the same concentration in mass percentage units has almost the same numbers of β-CD units, which is an essential factor for chiral recognition.

The effect of β-CD and β-CD polymer on the separation of enantiomers of trimetoquinol and related compounds was investigated by using a buffer solution of pH 2.7 containing 2 *M* urea and the following CDs: 20 m*M* of β-CD (0.23 g per 10 ml) and 2% of β-CD polymer. The selectivities (α) and resolution (R_s) between the two enantiomers were calculated with the following equations:

$$\alpha = t_2/t_1 \quad (2)$$

$$R_s = 2\,(t_2 - t_1)/(w_2 + w_1) \quad (3)$$

where t is the migration time and w the peak width. The results obtained for three substances are summarized in Table 2. Good enantiomeric resolution (>1) was obtained by using β-CD polymer, indicating that a polymer-type CD is a useful chiral selector. The high stereoselectivity in the chlorination of aromatic compounds was also observed with α-CD polymer in comparison with α-CD [26].

The great enantioselectivity of β-CD polymer

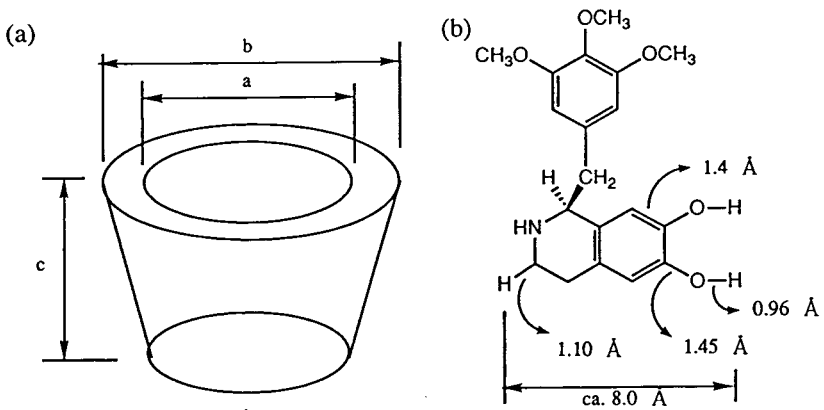

(Å)

	a	b	c
α	5.7	13.7	7.8
β	7.8	15.3	7.8
γ	9.5	16.9	7.8

Fig. 4. Dimensions of (a) CDs and (b) trimetoquinol.

Table 2
Comparison between β-CD and β-CD polymer as a chiral sector

Solute	Buffer containing			
	20 m*M* β-CD		2% β-CD polymer	
	α	R_s	α	R_s
Trimetoquinol	1.024	1.1	1.027	1.2
Laudanosoline	1.031	1.3	1.049	1.6
Norlaudanosoline	1.033	0.9	1.053	1.8

Buffer, 25 m*M* phosphate (pH 2.7) containing 2 *M* urea and CDs.

can probably be ascribed to its large M_r. It is clear that the electrophoretic mobility of β-CD polymer is smaller than that of β-CD, and this will cause a greater difference $\mu_t - \mu_c$ (Eq. 1). In addition to M_r, polymerization, i.e., the structure of β-CD polymer, may be an important factor for the enantioselectivity. A decrease in the free rotation of the β-CD unit, a constant distribution of β-CD (regular length interval) or hydrophobic interactions, hydrogen bonding, etc., in the polymeric β-CD network will probably contribute to the chiral recognition. However, the migration times of the enantiomers of trimetoquinol and related substances in CZE with 2% β-CD polymer or 20 m*M* β-CD were almost the same, showing no successful separation of both enantiomers and different solutes. It must be necessary to use a higher concentration of the chiral selector.

3.3. *Influence of concentration of β-CD polymer*

The simultaneous enantiomeric separation of trimetoquinol hydrochloride and related substances was investigated by using β-CD polymer because of its high capability as a chiral selector. The concentration of CD is an important factor influencing the selectivity and chiral recognition, as shown in Eq. 1, and there is an optimum CD concentration for the enantiomeric separation [20]. The effects of β-CD polymer concentration (over the concentration range 1–7%) on the migration time and the chiral recognition were investigated by using 25 m*M* phosphate buffer solution of pH 2.7 containing 2 *M* urea. The results are summarized in Table 3. The resolution and the migration time increased as the concentration increased. However, the separation of enantiomers of laudanosine was not successful. A resolution of >3 was obtained for other solutes by using a 7% β-CD polymer solution. A typical electropherogram using a 5% β-CD polymer solution is shown in Fig. 5. The selectivity for the solutes was considerably improved as the concentration increased, although the separation between laudanosoline and norlaudanosoline was not successful.

Under acidic conditions (pH 2.7), the velocity of electroosmotic flow (EOF) is very low compared with the electrophoretic velocity of cationic solutes. As CD is not charged, CD is transported by the EOF, indicating that a slowly eluted solute is more effectively included in CD. In Fig. 5, the migration time of the positional isomer (5,7-dihydroxy) of trimetoquinol was largest and greatly prolonged as the β-CD polymer concentration increased. On the other had, laudanosine, which has two bulky methoxy groups in the tetrahydroisoquinoline structure (6- and 7-positions), migrated fast. The dependence of the migration time of laudanosine on the β-CD polymer concentration is relatively small compared with other solutes. These results suggest that the molecules of trimetoquinol hydrochloride analogues penetrate the CD cavity from the tetrahydroisoquinoline side. Fig. 6 shows a schematic illustration of a possible

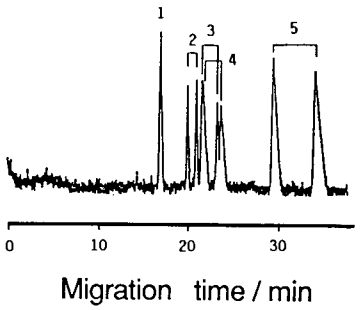

Fig. 5. Separation of enantiomers of trimetoquinol and related compounds by CD-CZE using β-CD polymer. Solutes: 1 = laudanosine; 2 = trimetoquinol; 3 = laudanosoline; 4 = norlaudanosoline; 5 = trimetoquinol isomer. Buffer, 25 m*M* phosphate (pH 2.7) containing 2 *M* urea and 5% β-CD polymer. Other conditions as in Fig. 3.

complex. Trimetoquinol isomer can penetrate more deeply into the CD cavity than trimetoquinol because it is free from steric hindrance at the 6-hydroxy group, as illustrated in Fig. 6.

3.4. Effect of additives on selectivity and chiral recognition

The effects of some additives such as an organic solvent, other CDs or a surfactant on the migration time and the resolution of the enantiomers were investigated to manipulate the selectivity, leading to successful simultaneous enantiomeric separation. As already pointed out previously [21], the addition of an organic modifier is a useful method for manipulating the selectivity. However, the addition of methanol (10–20%) to a 2% β-CD polymer solution of pH 2.7 caused a decrease in the selectivity and theoretical plate number for these solutes, with

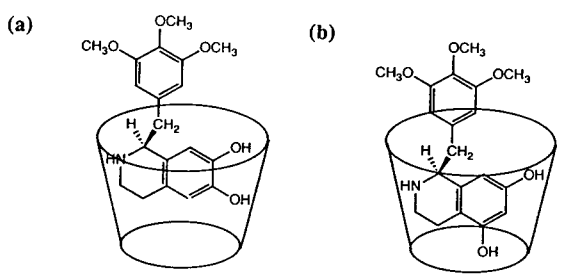

Fig. 6. Schematic illustration of the complexation of (a) trimetoquinol and (b) its isomer in β-CD.

increased migration times. The addition of 20 m*M* DM-β-CD to a 5% β-CD polymer solution of pH 2.7 containing 2 *M* urea did not affect the separation in Fig. 5. In contrast, chiral recognition of denopamine was impaired with the use of both 20 m*M* DM-β-CD and 5% β-CD polymer, compared with Fig. 3.

The addition of a surfactant was investigated by employing STDC, which shows a wide enantioselectivity in MEKC using bile salts [19,27], and sodium dodecyl sulphate (SDS). The separation of four solutes and each enantiomeric separation were successfully achieved in a single run through the addition of 10 m*M* SDS to a 5% β-CD polymer solution of pH 2.7, as shown in Fig. 7. However, the addition of 10 m*M* STDC to the same β-CD polymer solution (5%) was not successful for the separation between laudanosoline and norlaudanosoline. The addition of 10 m*M* STDC was effective for the separation of the two when the concentration of β-CD polymer was 7%. These two were not baseline resolved by only changing β-CD polymer (1–7%). The addition of 30 m*M* STDC to a 7% β-CD polymer solution of pH 2.7 caused a change in elution order, i.e., both enantiomers of laudanosoline eluted faster than those of norlaudanosoline. The results are summarized in Table 4.

The successful separation of both enantiomers and different solutes by CD-MEKC probably depends on the difference in the interaction between the solute and the micelle (micellar

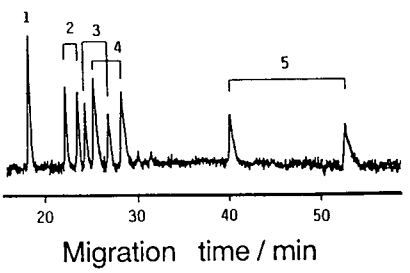

Fig. 7. Simultaneous enantiomeric separation of trimetoquinol and related compounds by CD-MEKC using β-CD polymer and SDS. Solutes numbers and buffer as in Fig. 5, except for the addition of 10 m*M* SDS. Other conditions are as in Fig. 3.

Table 3
Effect of concentration of β-CD polymer on the migration time and chiral recognition

Solute	Concentration of polymer (%)													
	1			2			3			5			7		
	t_R (min)	α	R_s	t_R (min)	α	R_s	t_R (min)	α	R_s	t_R (min)	α	R_s	t_R (min)	α	R_s
Laudanosine	15.11	1.0	–	15.18	1.0	–	15.20	1.0	–	17.86	1.0	–	19.19	1.0	–
Trimetoquinol	15.81	1.018	0.9	16.67	1.026	1.2	17.10	1.032	2.0	21.46	1.053	3.1	24.40	1.075	4.0
	16.10			17.10			17.64			22.60			26.24		
Laudanosoline	16.45	1.033	1.2	17.10	1.044	1.6	17.78	1.064	2.2	23.28	1.085	3.1	27.68	1.094	4.0
	17.00			17.85			18.92			25.25			30.28		
Norlaudanosoline	16.50	1.044	1.3	17.10	1.053	1.8	17.96	1.072	1.8	23.46	1.097	2.9	27.83	1.112	3.9
	17.22			18.00			19.25			25.74			30.95		
Trimetoquinol isomer	–			–			–			29.29	1.132	3.3	38.68	1.150	4.1
										33.17			44.50		

Buffer, 25 m*M* phosphate (pH 2.7) containing 2 *M* urea and β-CD polymer.

Table 4
Effect of surfactant addition on the selectivity of the enantiomer

Solute	Buffer containing								
	5% polymer + 10 m*M* SDS			7% polymer + 10 m*M* STDC			7% polymer + 30 m*M* STDC		
	t_R (min)	α	R_s	t_R (min)	α	R_s	t_R (min)	α	R_s
Laudanosine	18.36	1.0	–	19.81	1.0	–	23.10	1.0	–
Trimetoquinol	22.38	1.060	2.9	24.55	1.069	3.5	28.83	1.046	2.6
	23.72			26.25			30.16		
Laudanosoline	24.49	1.100	4.9	27.79	1.098	4.0	31.21	1.077	3.1
	26.94			30.52			33.62		
Norlaudanosoline	25.38	1.119	3.2	28.40	1.112	3.4	33.75	1.111	5.0
	28.40			31.59			37.50		
Trimetoquinol isomer	40.22	1.312	9.3	41.47	1.232	6.1	49.44	1.500	14.4
	52.76			51.08			74.16		

Buffer, 25 m*M* phosphate (pH 2.7) containing 2 *M* urea and β-CD polymer. Applied voltage, 15 kV; temperature, ambient; detection, 220 nm.

solubilization) in the presence of the surfactant, whose concentration is greater than the critical micelle concentration. Norlaudanosoline interacted more strongly than laudanosoline with the micelle, judging from the increase in the migration time of norlaudanosoline on addition of the surfactant. Anyhow, it was found that the addition of a surfactant to a buffer solution, i.e., MEKC mode, is a useful method for manipulating the selectivity, leading to a simultaneous separation.

3.5. Effect of buffer pH on migration time and chiral recognition

The effects of buffer pH on the migration time and chiral recognition were investigated by using a 25 m*M* phosphate buffer solution of pH 6.5 containing 2 *M* urea and 3–5% β-CD polymer. The solutes tested were laudanosine, trimetoquinol, laudanosoline and trimetoquinol isomer. The results are summarized in Table 5. A typical electropherogram obtained with the P/ACE 5510 system (3% β-CD polymer and an applied voltage of 20 kV) is shown in Fig. 8.

Enantiomers of norlaudanosoline migrated with almost the same velocity as those of laudanosoline. The migration times of the solute decreased with increase in pH. This can be interpreted by the increase in the velocity of EOF at high pH. In Fig. 8, all solutes migrated faster than the velocity of EOF (t_0), which is traced by the negative signal of methanol on the electropherogram. The same enantioselectivity was observed using β-CD at pH 6.5, although the chiral recognition was worse than that in β-CD polymer.

Chiral recognition of trimetoquinol-related compounds was successful even at high pH (6.5), although the resolution was lower than in the separation at pH 2.7. At pH 6.5, the addition of SDS was also effective for improving the selectivity. However, the chiral separation of other solutes, which were enantioresolved by a β-CD polymer solution of pH 2.7, was not achieved at pH 6.5. In previous work [24], the same results were obtained for the basic compounds. That is, the enantioselectivity decreased with increase in pH. Lower pH values gave a higher enantioseparation for basic solutes as discussed regarding Eq. 1. It is recommended to use a solution of low pH, i.e., under the condition of low velocity of EOF, for chiral separation by CD-CZE. However, for trimetoquinol-related compounds, a solution of high pH was better for fast enantioseparation.

Table 5
Effect of buffer pH on the migration time and enantiomer recognition

Solute	Buffer containing								
	3% polymer			5% polymer			5% polymer + 10 m*M* SDS		
	t_R (min)	α	R_s	t_R (min)	α	R_s	t_R (min)	α	R_s
Laudanosine	6.75	1.0	–	6.73	1.0	–	8.52	1.0	–
Trimetoquinol	7.14	1.017	1.1	7.21	1.022	1.2	9.23	1.024	1.3
	7.26			7.37			9.45		
Laudanosoline	7.51	1.027	1.4	7.72	1.028	1.4	9.82	1.038	1.3
	7.71			7.94			10.19		
Trimetoquinol isomer	8.02	1.041	2.2	8.21	1.038	2.5	11.07	1.067	2.9
	8.35			8.52			11.81		
EOF (t_0)	9.90			9.89			12.58		

Buffer, 25 m*M* phosphate (pH 6.5) containing 2 *M* urea and β-CD polymer. Applied voltage, 15 kV; temperature, ambient.

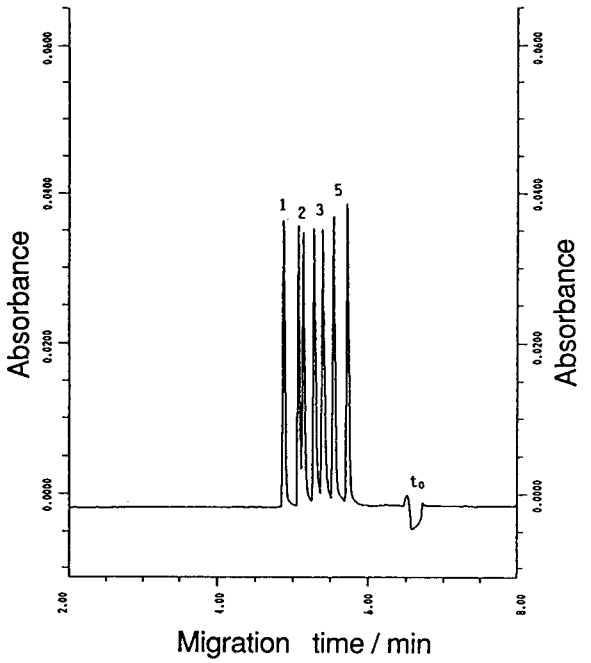

Fig. 8. Separation of enantiomers of trimetoquinol and related compounds by CD-CZE using a pH 6.5 buffer solution. Conditions: buffer, 25 m*M* phosphate (pH 6.5) containing 2 *M* urea and 3% β-CD polymer; separation tube, 57 cm (effective length 50 cm) × 75 μm I.D.; applied voltage, 20 kV; detection, 214 nm (0.06 AUFS); temperature, 23°C. Solute numbers as in Fig. 5.

In conclusion, it was found that β-CD polymer is useful for the enantioseparation of trimetoquinol and related compounds. The higher the concentration of β-CD polymer, the greater is the resolution. The addition of a surfactant was effective for the manipulation of selectivity in CD-CZE using β-CD polymer. The best enantioseparation was obtained by employing 5–7% β-CD polymer in an acidic solution containing the surfactant. On the other hand, the first enantioseparation was achieved by using a high pH solution, although the resolution was slightly decreased. The separation of different solutes and the corresponding enantiomers will be optimized by changing the type and concentration of CD, the pH of the buffer and adding a surfactant.

References

[1] P.D. Grossmann and J.C. Colburn (Editors), *Capillary Electrophoresis —Theory and Practice*, Academic Press, New York, 1992.
[2] S.F.Y. Li, *Capillary Electrophoresis —Principle, Practice and Applications*, Elsevier, Amsterdam, 1992.
[3] N.A. Guzman (Editor), *Capillary Electrophoresis Technology*, Marcel Dekker, New York, 1993.
[4] S. Terabe, *Trends Anal. Chem.*, 8 (1989) 129.
[5] J. Vindevogel and P. Sandra, *Introduction to Micellar Electrokinetic Chromatography*, Hüthig, Heidelberg, 1992.
[6] A.M. Krstulovic (Editor), *Chiral Separation by HPLC*, Ellis Horwood, Chichester, 1989.
[7] W. Lindner, *Chromatographia*, 24 (1987) 97.
[8] S. Fanali, *J. Chromatogr.*, 474 (1989) 441.
[9] S. Fanali and P. Boček, *Electrophoresis*, 11 (1990) 757.
[10] J. Snopek, H. Soini, M. Novotony, E. Smolková-Keulemansová and I. Jelinek, *J. Chromatogr.*, 559 (1991) 215.
[11] A. Guttman, A. Paulus, A.S. Cohen, N. Grinberg and B.L. Karger, *J. Chromatogr.*, 448 (1989) 41.
[12] H. Nishi, T. Fukuyama and S. Terabe, *J. Chromatogr.*, 553 (1991) 503.
[13] T. Ueda, F. Kitamura, R. Mitchell, T. Metcalf, T. Kuwana and A. Nakamoto, *Anal. Chem.*, 63 (1991) 2981.
[14] S. Mayer and V. Schurig, *J. High Resolut. Chromatogr.*, 15 (1992) 129.
[15] N. Wiedenhof, *Staerke*, 21 (1969) 119.
[16] A. Harada, M. Furue and S. Nozakura, *J. Polym. Sci., Polym. Chem. Ed.*, 16 (1978) 189.
[17] T. Cserhati, B. Bordas, E. Fenyvesi and J. Szejtli, *J. Chromatogr.*, 259 (1983) 107.
[18] W.L. Hinze, *Sep. Purif. Methods*, 10 (1981) 159.
[19] H. Hishi, T. Fukuyama, M. Matsuo and S. Terabe, *J. Microcol. Sep.*, 1 (1989) 234.
[20] S.A.C. Wren and R.C. Rowe, *J. Chromatogr.*, 603 (1992) 235.
[21] S.A.C. Wren and R.C. Rowe, *J. Chromatogr.*, 609 (1992) 363.
[22] D.Y. Pharr, Z.S. Fu, T.K. Smith and W.L. Hinze, *Anal. Chem.*, 61 (1989) 275.
[23] H. Nishi, T. Fukuyama, M. Matsuo and S. Terabe, *Anal. Chim. Acta*, 236 (1990) 281.
[24] H. Nishi, Y. Kokusenya, T. Miyamoto and T. Sato, *J. Chromatogr. A*, 659 (1994) 449.
[25] K. Uekama and F. Hirayama, *Kagaku to Kogyo*, 59 (1985) 443.
[26] R. Breslow, H. Kohn and B. Siegel, *Tetrahedron Lett.*, (1976) 1645.
[27] H. Nishi, T. Fukuyama, M. Matsuo and S. Terabe, *J. Chromatogr.*, 515 (1990) 233.

ELSEVIER

Journal of Chromatography A, 678 (1994) 343–350

JOURNAL OF CHROMATOGRAPHY A

Migration behaviour of triiodinated X-ray contrast media containing diol groups as borate complexes in capillary electrophoresis

Hoang H. Thanh[1]

Department of Analytical and Physical Chemistry, Exploratory Research, Nycomed Imaging AS, P.O. Box 4220 Torshov, N-0401 Oslo, Norway

First received 27 August 1993; revised manuscript received 26 May 1994

Abstract

The migration behaviour of several triiodinated X-ray contrast media containing diol groups was examined by capillary electrophoresis as borate complexes. A basic pH and a high concentration of borate buffer appeared to facilitate the complexation reaction and hence enhance the electrophoretic mobility and the resolution of solutes. Further, addition of organic modifiers to the background electrolyte was found to affect the resolution by decreasing the magnitude of the electroosmotic flow. A correlation between migration order and structure of the solutes is discussed in terms of degree of complex formation.

1. Introduction

Modern triiodinated X-ray contrast media (XCM) containing small diol groups have been developed, as the second generation of non-ionic contrast media, in succession to metrizamide (Amnipaque; Nycomed Imaging, Oslo, Norway). The compounds have high water solubility and chemical stability, low osmolality and significantly improved biological safety when compared with metrizamide [1].

Owing to their highly hydrophillic character (>50%, w/w), reversed-phase HPLC has been used routinely in the qualitative and quantitative analysis of these pharmaceuticals [2–5]. Recently, capillary electrophoresis (CE) has been developed as a potent and complementary tool to HPLC for analytical purposes [6,7]. One of the most common formats of CE is capillary zone electrophoresis (CZE), which primarily allows the separation of ionizable compounds. Interestingly, CZE has been extended to the analysis of certain non-ionizable compounds, through dynamic complexation [8]. This approach involves an in situ transformation of neutral solutes into negatively charged complexes, using borate buffer as a complexing additive in the background electrolyte. The concept has been applied in the separation of diol-containing compounds, including catechols [8], catecholamines [9], carbohydrates [10] and flavonoid-O-glycosides [11].

The objective of this work was to adopt the borate complexation concept to enable triiodinated XCM containing diol groups to be de-

* Present address: Pharmaceutical Research and Development, Merck Frosst Canada Inc., P.O. 1005, Pointe Claire–Dorval, Quebec H9R 4P8, Canada.

0021-9673/94/$07.00
SSDI 0021-9673(94)00502-Z

termined by CE. The compounds include iosemide, iopentol, ioversol, iopamidol and iohexol (Fig. 1). The emphasis was placed on studies of the effect of pH and concentration of borate buffer on the migration behaviour of solutes. Attempts to lower the electroosmotic flow and thereby affect the resolution was done by addition of organic modifiers. A correlation between migration order and structure of solutes was also elucidated.

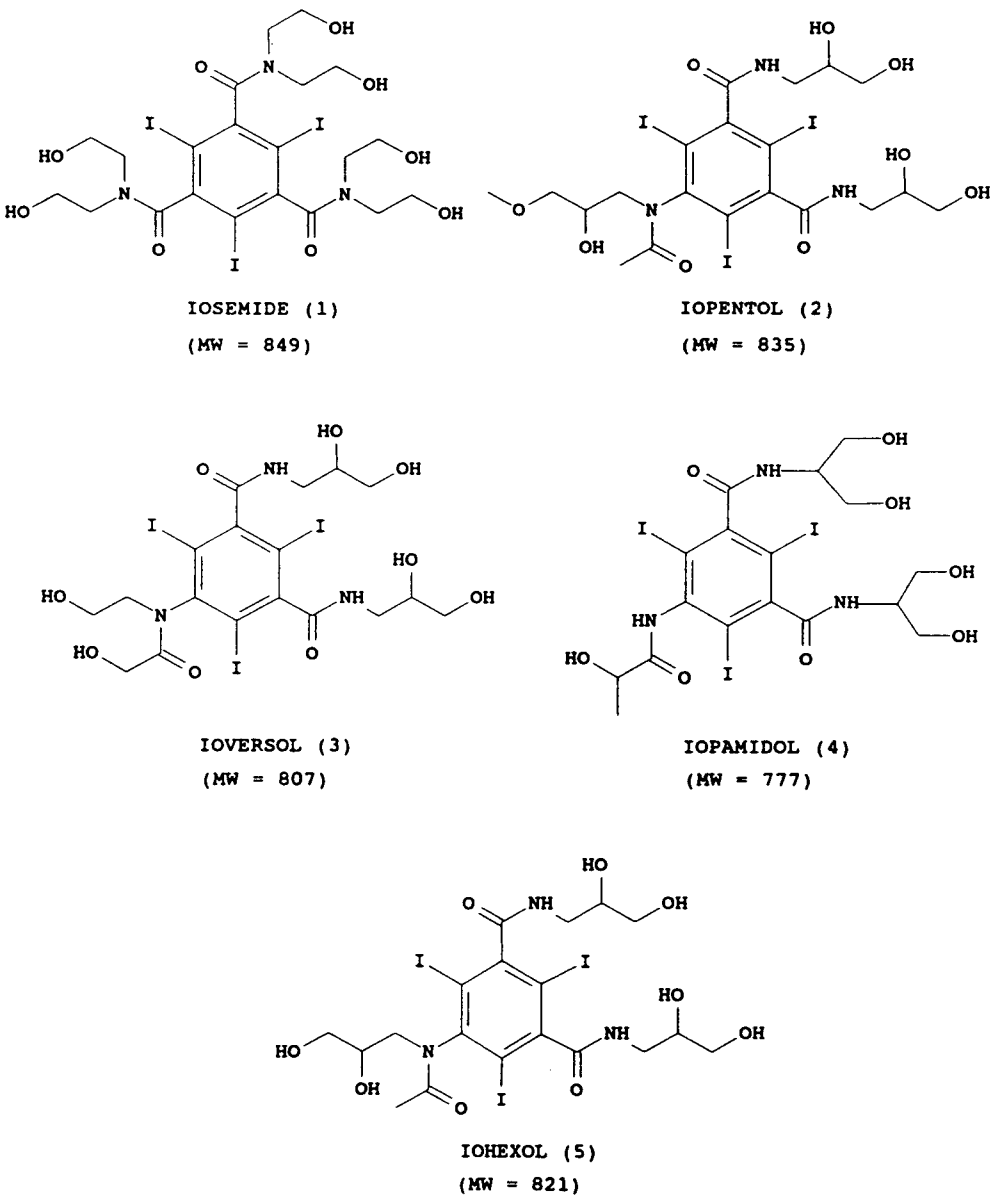

Fig. 1. Structures and molecular masses of the non-ionic XCM.

2. Experimental

2.1. Materials

Iohexol (Omnipaque) and iopentol (Imagopaque) were obtained from the laboratory stocks (Nycomed Imaging). Iopamidol (Iopamiro; Astra Tech, Sweden) and ioversol (Optiray, Mallinckrodt, St. Louis, MO, USA) were isolated from the commercially available pharmaceutical products. Iosemide was synthesized according to the method proposed by Gries et al. [12]. Borax (disodium tetraborate decahydrate), HPLC-grade methanol and 2-propanol were supplied by Merck (Darmstadt, Germany). Tris-(hydroxymethyl)aminomethane hydrochloride (Tris) and benzyl alcohol (as neutral marker) were purchased from Fluka (Buchs, Switzerland).

2.2. Buffers and sample preparation

Tris and borate buffer were prepared in Milli-Q-purified water with the pH adjusted with 0.1 *M* NaOH or 0.1 *M* HCl (Titrisol; Merck) and filtered through a 0.45-μm filter (Millipore, Bedford, MA, USA) before use. Approximately 0.1 mg/ml sample solutions were prepared in Milli-Q-purified water.

2.3. Apparatus

An Applied Biosystems (San Jose, CA, USA) Model 270A-HT capillary electrophoresis system was used. All experiments were performed in a 72 cm (50 cm from injection to detection) × 50 μm I.D. fused-silica capillary (Applied Biosystems).

The injection cycle was started with flushing of the capillary with 0.1 *M* NaOH for 2 min, followed by the applied buffer for 2 min. Samples were introduced at the anode (+) by hydrodynamic injection using a controlled vacuum system for 2 s and detected by UV measurement at 245 nm with a 0.5-s rise time. A constant voltage of 20 kV was applied and the oven temperature was maintained at 25°C. A Perkin-Elmer Model LCI-100 integrator was used to record the electropherograms. The attenuation was set at 16 mV and the chart speed at 1 cm/min.

3. Results and discussion

3.1. Evidence for borate complexation of the XCM

Initial experiments were performed to confirm the borate complexation of the XCM, using 50 m*M* Tris and 50 m*M* borate buffer, both at pH 9.2. Benzyl alcohol was used to measure the electroosmotic flow (EOF). Fig. 2 shows the electropherograms of the XCM obtained with these buffers.

As electrically neutral compounds, the XCM

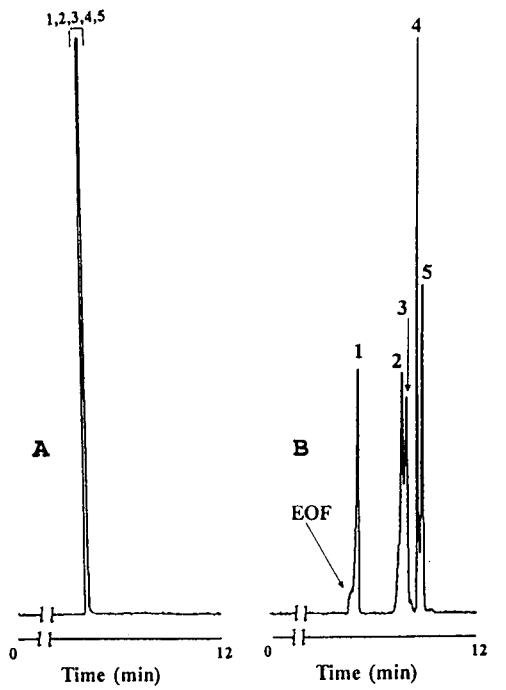

Fig. 2. Electropherograms of the XCM obtained with (A) 50 m*M* Tris and (B) 50 m*M* borate buffer, both at pH 9.2. Constant voltage, 20 kV; detection wavelength, 254 nm; temperature, 25°C. Peaks 1–5 as indicated in Fig. 1.

migrated with the same velocity as that of the EOF in CZE with the non-complexing Tris buffer. Interestingly, when borate buffer was applied, the migration pattern changed considerably. All compounds studied, except for iosemide, migrated more slowly than the EOF. This indicated that the compounds had to possess negative charges, presumably resulting from the complexation of borate with the diol groups of XCM.

According to the complexation mechanism postulated by Lorand and Edwards [13], the complexation involves a change of boric acid into borate anion on ionization and subsequent reaction with diols to yield a complex. As each XCM studied contains at least two diol moieties, the complexation of borate with XCM is considered to involve several equilibria, as illustrated in Fig. 3. In this figure, iohexol is assumed not to have any enantiomeric preference (*R* or *S*) for the borate complexation as the compound was eluted as a single peak under the conditions tested. Moreover, the complexation of the XCM with borate should be governed by the pH and concentration of the borate buffer. It was therefore of great interest to examine the effects of these parameters on the migration behaviour of the compounds.

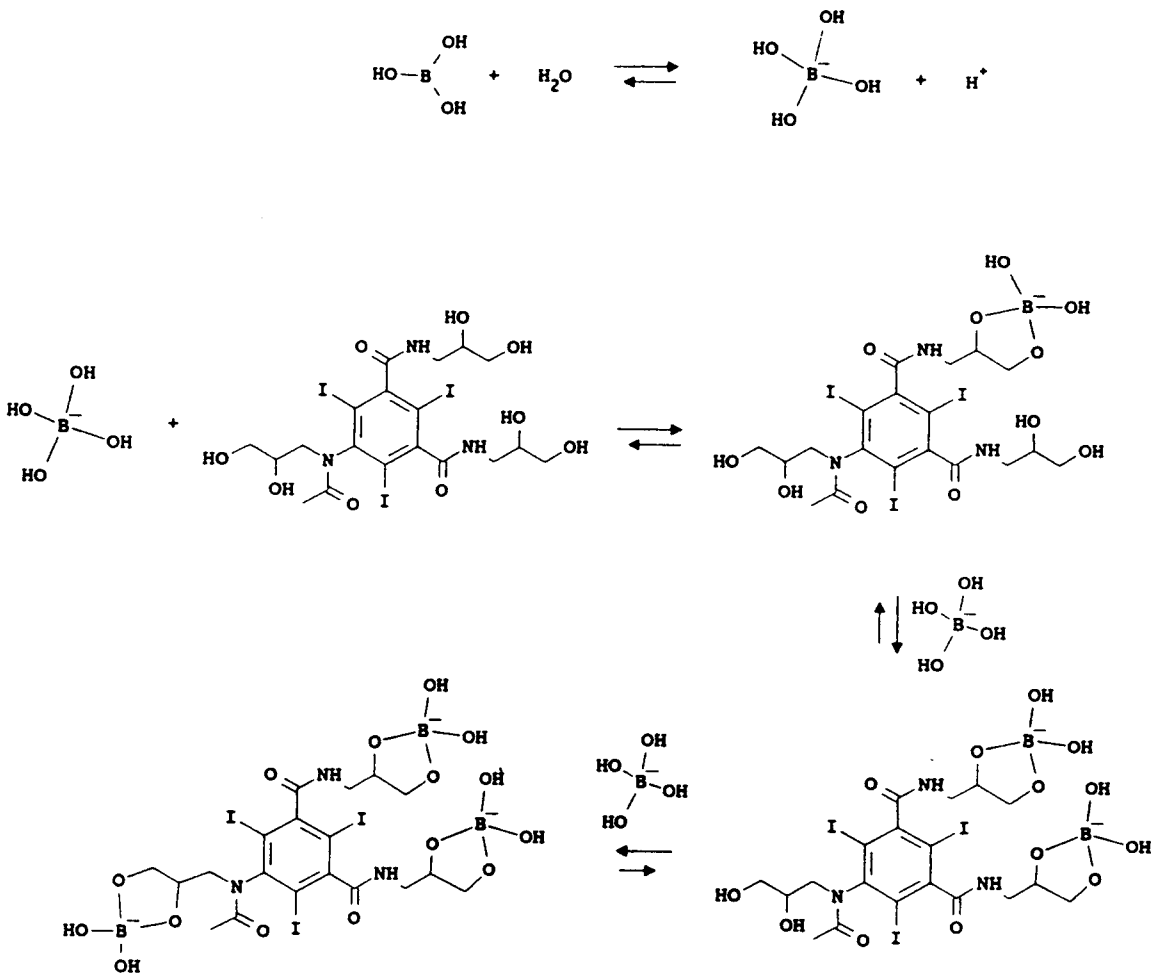

Fig. 3. Equilibria between boric acid, anionic borate and iohexol in aqueous medium.

3.2. Effect of pH

To verify the effect of buffer pH on the migration behaviour of the XCM, experiments were performed with 50 m*M* borate buffer. The results are shown in Fig. 4. The effective electrophoretic mobilities, μ(ep) in $cm^2\ V^{-1}\ s^{-1}$, were calculated using $\mu(ep) = L_{(d)}L_{(t)}/V[1/t_{eo)} - 1/t_{(m)}]$, where $L_{(t)}$ (cm) is the total length of the capillary, $L_{(d)}$ (cm) the distance between the inlet of the capillary and the detector, V (V) the applied voltage, $t_{(eo)}$ (s) the migration time of the neutral marker and $t_{(m)}$ (s) the migration time of the solute.

The co-migration of the XCM with the EOF observed at pH 7 suggested that no complexation occurred at this pH. When the pH was made more basic, a structural preference for the formation of borate complexes was observed. The complexation of iosemide seemed to occur at pH 9.2, whereas the corresponding processes for the other XCM were observed at pH 8. Further raising the pH towards 10 led to a general increase in the electrophoretic mobility of the XCM. This can be explained in terms of an increase in the overall concentration of anionic borate that is active in the complex formation. Accordingly, the complex formation was facilitated at basic pH and the electrophoretic mobility of the solutes towards the anode was enhanced. Further, increasing the pH brought about an improved resolution of iopentol and ioversol, but at the expense of a loss of resolution of iopamidol and iohexol.

3.3. Effect of borate concentration

A plot of electrophoretic mobility of the XCM vs. borate buffer concentration at pH 9.2 is given in Fig. 5. As stated above, increasing borate concentration in the background electrolyte would favour the complex formation and result in more negative mobilities of the compounds.

Notably, high borate concentration appeared to improve the resolution of the four late-eluting XCM. The best separation of these four XCM was achieved with 75 m*M*. However, some small and unidentified peaks were also observed with this buffer.

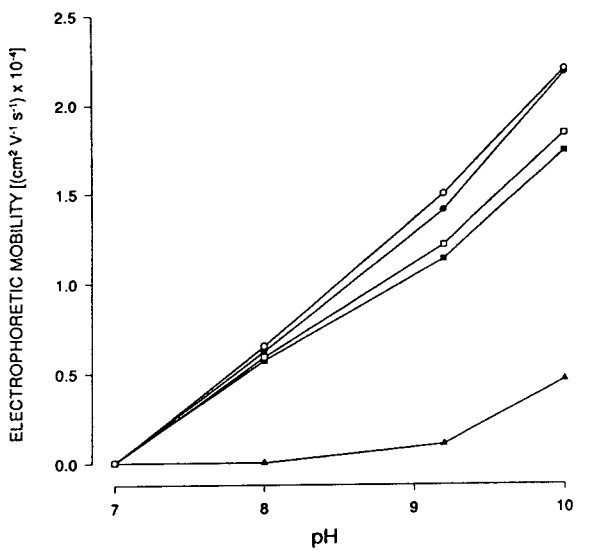

Fig. 4. Effect of buffer pH on the electrophoretic mobility of the XCM. Buffer concentration, 50 m*M* borate; other conditions as in Fig. 2. ○ = Iohexol; ● = iopamidol; □ = ioversol; ■ = iopentol; ▲ = iosemide.

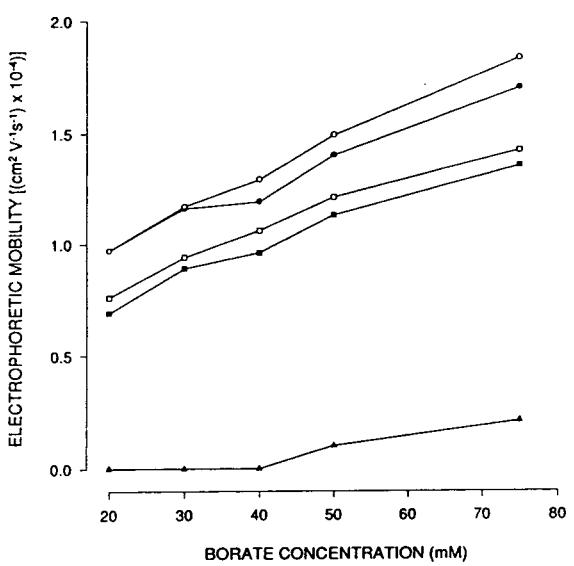

Fig. 5. Effect of borate concentration on the electrophoretic mobility of the XCM at pH 9.2. Other conditions as in Fig. 2. Symbols as in Fig. 4.

3.4. Effect of organic additives

So far, pH and borate concentration were observed to affect the resolution of the XCM, solely by increasing the differences in the electrophoretic mobilities. Alternatively, the resolution of solutes could be improved by decreasing the magnitude of the EOF according to Jorgenson and Lukacs [14]. A decrease in the EOF may be achieved by addition of an organic modifier to the background electrolyte [15].

The addition of up to 5% (v/v) of 2-propanol to 50 m*M* borate buffer (pH 9.2) was shown to lower the EOF, without having a significant effect on the resolution. A similar effect on the EOF was also observed when methanol was applied, but the resolution of iopamidol (**4**) and iohexol (**5**) was remarkably improved, particularly at 10% methanol (Fig. 6; for comparison, see Fig. 2B). Further increasing the concentration of methanol to 20% led to a greater resolution of iopamidol (**4**) and iohexol (**5**) at the cost of a slight loss of resolution of ioversol (**3**) and iopamidol (**4**).

3.5. Migration order and structure of solutes

When attempting to understand the migration order of the XCM observed in Fig. 2B, it is important to emphasize that the electrophoretic mobility of an ion in CE depends on its charge-to-size ratio. In the borate complexation mode, the magnitude of this ratio depends on the type and numbers of diol being complexed, as the complexation results in a slight increase in molecular mass and imparts negative charges to the molecule. Further, the borate complexation with the XCM is governed by equilibria between the uncomplexed and complexed forms. It is believed that the reaction equilibrium is probably achieved at high borate concentration. To confirm this, a solution of the XCM prepared in 50 m*M* borate (pH 10) was analysed by CE (50 m*M* borate buffer, pH 10, as background electrolyte) after 0, 4 and 24 h of continuous stirring. The results showed a constant migration time for the individual XCM at those time intervals. This indicated an instantaneous establishment of equilibria in the complex formation of the XCM

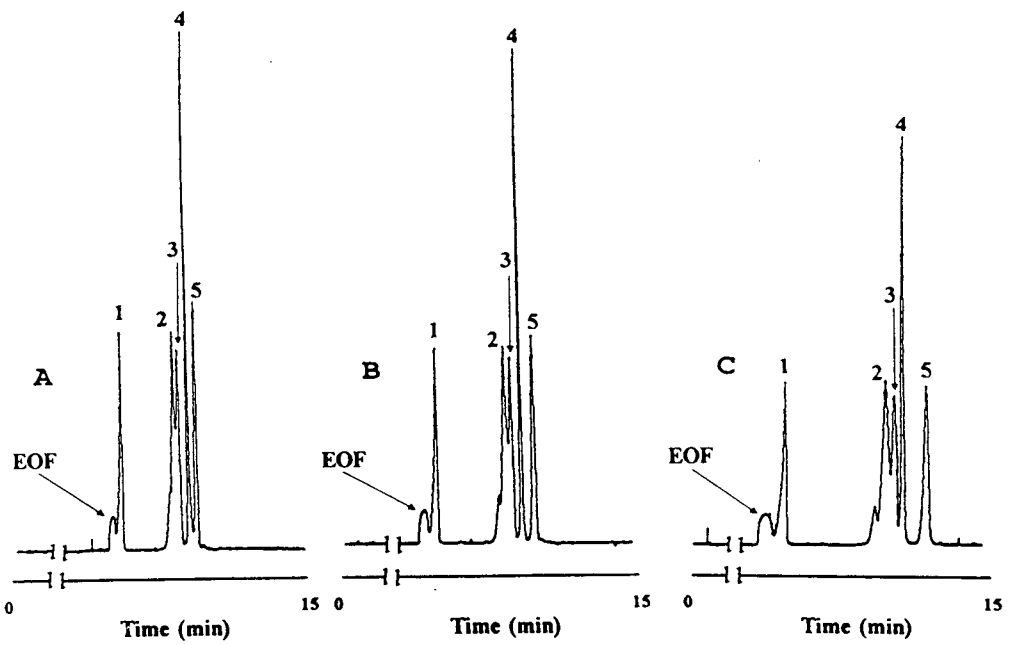

Fig. 6. Electropherograms of the XCM obtained with addition of (A) 5, (B) 10 and (C) 20% (v/v) methanol to 50 m*M* borate buffers at pH 9.2. Other conditions as in Fig. 2. Peaks 1–5 as indicated in Fig. 1.

at high borate concentration. Throughout the study, the borate complexation of iosemide was observed to take place only if the borate concentration was high enough. The resultant complex would have an eight-membered ring structure. Owing to the ring size and strain generally existing in such a ring structure [16], the complexation reaction is considered to be unfavorable. As a result, it is most probable that only a 1:1 iosemide–borate complex was formed at equilibrium. The iosemide–borate complex would therefore have the lowest charge density among the XCM and migrate fastest through the capillary, as observed in this study.

In contrast, the other XCM possess either 1,2-diol or 1,3-diol groups, all of which could react smoothly with borate [17–19], to form almost strainless five- or six-membered rings, respectively. As there are two such diol moieties in iopentol, ioversol and iopamidol, 1:2 solute–borate complexes were expected to be formed at high borate concentration. These complexes have the same charge density and the migration order is dependent on their masses, i.e. iopentol (**2**) > ioversol (**3**) > iopamidol (**4**). It should be noted that ioversol contains a third diol group, namely $N(COCH_2OH)(CH_2CH_2OH)$, in addition to the two 1,2-diol groups. An eight-membered ring, similar to that of iosemide, could in principle be formed on complexation. Unlike the diol of iosemide, which formed a borate complex at high borate concentration, the corresponding reaction of that of ioversol was not observed. If it took place, ioversol would have an overall charge density similar to that of iohexol and migrate more slowly than iohexol because of its lower mass. Under all conditions tested, ioversol was observed to migrate faster than iohexol, indicating that ioversol must have a lower charge density than iohexol. In other words, ioversol has only two 1,2-diol groups which are active in the borate complexation.

Lastly, iohexol, with its three 1,2-diol moietities, would possess the highest charge density of the XCM studied on complexation. It would therefore migrate the slowest through the capillary in spite of clearly being a larger solute than ioversol (**3**) or iopamidol (**4**).

4. Conclusions

The results demonstrate that CE is a useful technique for the rapid and efficient separation of non-ionic triiodinated XCM containing diol groups as borate complexes. Further, CE gives only a single peak for the individual XCM whereas multiple peaks are usually observed in HPLC, owing to the restricted rotation in amides [2]. This makes CE more attractive for both qualitative and quantitative analysis of these pharmaceuticals.

Acknowledgements

The author thanks Kebo Lab (Oslo, Norway) for lending the CE instrument and Professor A. Rogstad for critically reading the manuscript.

References

[1] T. Renaa and T. Jacobsen, *Acta Radiol., Suppl.*, 370 (1987) 9.
[2] A. Berg and R. Fagervoll, *Acta Radiol., Suppl.*, 370 (1987) 13.
[3] K. Skinnemoen, R. Fagervoll and T. Jacobsen, *Acta Radiol., Suppl.*, 370 (1987) 23.
[4] I.J. Alonso-Silva, J.M. Carretero, J.L. Martin and A.M. Sanz, *J. Chromatogr.*, 507 (1990) 293.
[5] A.T. Andresen, P.B. Jacobsen and K.E. Rasmussen, *J. Chromatogr.*, 575 (1992) 93.
[6] A. Wainright, *J. Microcol. Sep.*, 2 (1990) 166.
[7] D. Perrett and G. Ross, *Trends Anal. Chem.*, 11 (1992) 157.
[8] R.A. Wallingford and A.G. Ewing, *J. Chromatogr.*, 441 (1988) 299.
[9] T. Kaneta, S. Tanaka and H. Yoshida, *J. Chromatogr.*, 538 (1991) 385.
[10] S. Hoffstetter-Kuhn, A. Paulus, E. Gassmann and H.M. Widmer, *Anal. Chem.*, 63 (1991) 1541.
[11] P. Morin, F. Villard, M. Dreux and P. Andre, *J. Chromatogr.*, 628 (1993) 161.
[12] H. Gries, H. Pfeiffer, U. Speck and W. Muetzel, *Ger. Pat. Appl.*, DE 3001292 (1981).
[13] J.P. Lorand and J.O. Edwards, *J. Org. Chem.*, 24 (1959) 769.
[14] J.W. Jorgenson and K.D. Lukacs, *Anal. Chem.*, 53 (1981) 1298.
[15] B.B. Vanorman, G.G. Liversidge, G.L. McIntire, T.M. Olefirowicz and A.G. Ewing, *J. Microcol. Sep.*, 2 (1990) 176.

[16] J. Dale, *Stereochemistry and Conformation Analysis*, Universitetsforlaget, Oslo, 1975, Ch. 5, p. 182.
[17] A.J. Hubert, B. Hargitay and J. Dale, *J. Chem. Soc.*, (1961) 931.
[18] M.V. Duin, J.A. Peters, A.P.G. Kieboom and H.V. Bekkum, *Tetrahedron*, 40 (1984) 2901.
[19] M.V. Duin, J.A. Peters, A.P.G. Kieboom and H.V. Bekkum, *Tetrahedron*, 41 (1985) 3411.

ELSEVIER

Journal of Chromatography A, 678 (1994) 351–358

JOURNAL OF CHROMATOGRAPHY A

Electrophoretic behaviour and infrared spectra of dihydroxyboryl compounds in aqueous di- and tricarboxylic acids: paper electrophoresis as a tool for determining the chemical states of a substance in solution

Mitsue Kobayashi*, Yoshinori Kitaoka, Yoshiko Tanaka, Keizo Kawamoto

Research Reactor Institute, Kyoto University, Kumatori-cho, Sennan-gun, Osaka, Japan

First received 3 August 1993; revised manuscript received 23 March 1994

Abstract

p-Dihydroxyborylphenylalanine behaved as an anion in aqueous 0.1 mol dm^{-3} oxalic acid and 0.1 mol dm^{-3} citric acid in paper electrophoresis, but as a cation in aqueous 0.1 mol dm^{-3} fumaric, malic, tartaric, succinic, maleic and malonic acid. A similar electrophoretic behaviour was observed for boric acid. These results indicate that dihydroxyboryl compounds form complexes with oxalic and citric acid. The complex formation was confirmed by the infrared spectra of boric acid in the two aqueous carboxylic acids. The spectral behaviour was fully consistent with the migration behaviour in paper electrophoresis. It was confirmed that paper electrophoresis is a useful technique for determining the chemical states of a compound in solution.

1. Introduction

Electrophoresis is a useful technique for separating ionizable substances in solution. In electrophoresis, the mobility of a migrant depends on its net charge and apparent molecular mass. The net charge depends on both the pK_a value of the migrant and the pH of the supporting solution. The apparent molecular mass is influenced by the association of a migrant molecule with other molecules such as solute and solvent molecules. In principle, electrophoresis is useful for studying the chemical nature of a compound in solution [1,2]. Using electrophoretic data, stability constants of chelate compounds [3] and dissociation constants of acids [4] have been determined. Elucidation of the chemical form of a compound is also possible. We observed that so-called phenylphosphonous acid (**I**) had two dissociable protons in aqueous solution, by analysing the mobility-pH curve in electrophoresis, [5] and assigned the chemical form of phenylphosphonic acid to phenylphosphinic acid (**II**) in aqueous solution.

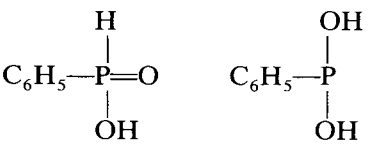

I **II**

* Corresponding author.

0021-9673/94/$07.00
SSDI 0021-9673(94)00464-K

On the basis of the above, we adopted paper electrophoresis for studying the chemical nature of *p*-dihydroxyborylphenylalanine (*p*-boronophenylalanine; BPA) in aqueous solution [6]. BPA has been used clinically in the boron neutron capture therapy (BNCT) for malignant melanoma as a boron carrier [7], and a knowledge of the solution chemistry of medicines is essential in pharmacokinetics.

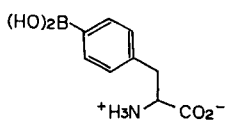

p-Boronophenylalanine (BPA)

In the course of previous studies, we noticed that BPA behaved as an anion in aqueous 0.05 mol dm^{-3} oxalic acid [8]. Recently we preliminarily showed that BPA behaved as an anion in aqueous 0.1 mol dm^{-3} citric acid, but as a cation in aqueous 0.1 mol dm^{-3} fumaric, malic, tartaric, succinic, maleic and malonic acid [9]. The pH values of the aqueous carboxylic acid solutions are estimated to be <3. In such acidic solutions, BPA should be a cation owing to the protonated amino group (NH_3^+). Hence we proposed that BPA formed a negatively charged complex with oxalic or citric acid.

Many workers have studied the complexation of dihydroxyboryl compounds (DHBCs) with *cis*-diols [10], and the resulting complexes have been utilized in affinity chromatography especially for the purification of diverse biomolecules [11]. Although studies on the complexation of DHBC with di- and/or polycarboxylic acids are limited, the complexation reactions of boric acids with some carboxylic acids such as oxalic [12] and tartaric [13] acid have been reported.

To obtain more evidence for complexation, we tried to elucidate the chemical form of the complex by infrared spectrometry, which is a useful technique for investigating solute–solute [14] and solute–solvent [15,16] interactions in solution. As BPA was scarcely soluble in water, we chose orthoboric acid as a candidate of DHBCs. The spectral behaviour was fully consistent with the migration behaviour in electrophoresis. This means that paper electrophoresis is a useful technique for determining the chemical states of a substance in solution.

2. Experimental

2.1. Reagent and materials

Boric acid, oxalic acid dihydrate, citric acid monohydrate, malonic acid, succinic acid and maleic acid of guaranteed grade and oxalate pH standard solution (pH 1.68 at 25°C) were purchased from Wako (Osaka, Japan). BPA (^{10}B-enriched) was supplied by Eagle Pitcher Research Laboratory (Miami, FL, USA). Ion-exchanged water was used after distillation. Toyoroshi No. 51A filter-paper (40 × 1 cm) was used as a support in electrophoresis.

2.2. Electrophoresis

The apparatus and procedures have been described previously [1,2,6]. The supporting solutions were aqueous 0.1 mol dm^{-3} oxalic, citric, fumaric, malic, tartaric, succinic, maleic and malonic acid. A 5-μl volume of sample (BPA and orthoboric acid) solution (about $5 \cdot 10^{-3}$ mol m^{-3}) or picric acid ($5 \cdot 10^{-3}$ mol dm^{-3}) (the standard migrant) was spotted at three different positions on a paper strip (A, 5 cm to the cathodic side from the centre of the strip; B, the centre; C, 5 cm to the anodic side from the centre) for checking the movement of a migrant due to the capillary action of the paper, the technique being named the "three-spot method" [6]. Six strips of the support (three pairs of sample solutions and standard solution) were set in parallel in *n*-hexane in the migration chamber and the electrode cells containing 0.1 mol dm^{-3} NaCl solution. A constant electric voltage gradient (1000 V per 30 cm) was applied to the two pairs for 30 min at constant temperature. One pair was allowed to remain in the migration chamber without applying an electric voltage to determine the effect of the capillary action of the support on the movement of a migrant.

BPA on the support was detected by spraying with ninhydrin solution and boric acid with alcoholic curcumin solution.

2.3. IR spectra

Infrared spectra of boric acid in the aqueous carboxylic acids were recorded in the frequency range 1000–2000 cm^{-1} with a Perkin-Elmer Model 1830 Fourier transform IR spectrometer, employing solution cells of 0.025 mm path length with calcium fluoride windows, at ambient temperature (22°C).

3. Results and discussion

3.1. Electrophoretic behaviour of DHBCs

The migration distances (mobilities) of BPA in aqueous solutions of various carboxylic acids are shown in Fig. 1, where a positive distance denotes movement towards the anode and a negative distance towards the cathode. The pH of the supporting solutions was calculated from the pK_a and the concentration of the carboxylic acids, and is given in Fig. 1. The pK_a values [17,18] and the chemical forms of the carboxylic acids are summarized in Table 1.

In paper electrophoresis, the observed mobility suffers from the influence of capillary action and the electroosmotic flow caused by the filter-paper as a support. The electroosmotic flow arises from the dissociation of the carboxylic acids in the filter-paper [19]. Hence the effect of the electroosmotic flow is unavoidable in the solutions of pH > 2.5. The influence of the capillary action was checked by the three-spot method. Normally it is minimized by spotting the sample solution in the middle of the filter-paper.

The mobility of a migrant primarily depends on its net charge (Z), which is a function of the pK_a of the migrant and the pH of the supporting solution. In previous studies [1,2], we showed that the relationship between Z and pH can be expressed to a good approximation by a hyperbolic tangent function:

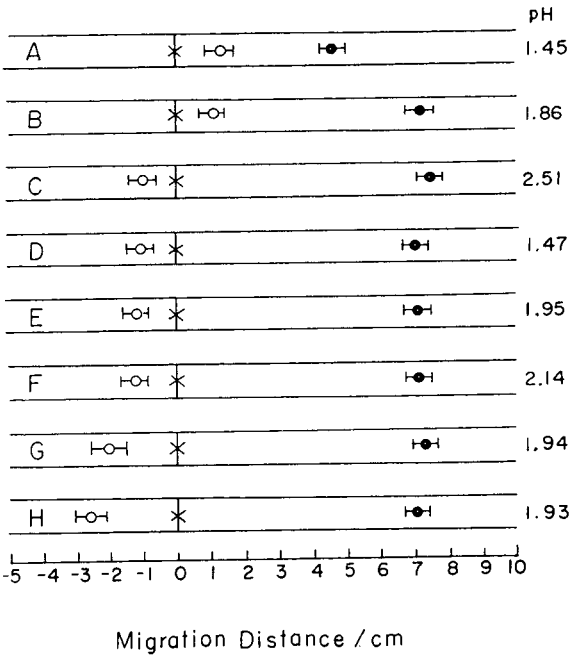

Fig. 1. Observed migration distances of BPA in carboxylic acids: Migrants: ● = picric acid (PA); ○ = BPA. Electrophoretic conditions: 1000 V per 30 cm; time, 30 min; migration temperature, 25°C; support, Toyoroshi No. 51A; spotting position, centre of the support (×); supporting solutions, 0.1 mol dm^{-3} carboxylic acids (lettered as in Table 1).

$$Z = -\tfrac{1}{2}\sum_{i=1}^{n}\left\{1+\tanh\left[\frac{2.303}{2}(\mathrm{pH}-\mathrm{p}K_{a_i})\right]\right\} \quad (1)$$

where K_{a_i} is one of the consecutive dissociation constants of an acid.

The pK_a values of BPA are 2.46, 8.46 and 9.76 [18] for the dissociation reactions of

$$-\mathrm{COOH} \rightleftharpoons -\mathrm{COO}^- + \mathrm{H}^+ \quad (2)$$

$$-\mathrm{B(OH)_2} + \mathrm{OH}^- \rightleftharpoons -\mathrm{B(OH)_3^-} \quad (3)$$

$$-\mathrm{NH_3^+} \rightleftharpoons -\mathrm{NH_2} + \mathrm{H}^+ \quad (4)$$

The net charge of BPA in a solution of a certain pH was calculated using Eq. 1 and plotted against pH (Fig. 2). In acidic solutions of pH < 3, BPA has a positive charge owing to the NH_3^+ group. In neutral solutions (pH 4–7.5) BPA has no charge as an amphoteric ion. With increasing pH the negative charge of BPA in-

Table 1
Structural formulae and pK_a values of carboxylic acids, BPA and boric acid

Name		Structural formula	pK_a
(A)	Oxalic acid	HOOC–COOH	1.04; 3.82
(B)	Citric acid	CH_2–C(OH)–CH_2 HOOC COOH COOH	2.87; 4.35; 5.69
(C)	Fumaric acid	*trans*-HOOC–HC=CH–COOH	2.85; 4.10
(D)	Malic acid	HOOC–CH–CH_2–COOH OH	3.24; 4.71
(E)	Tartaric acid	HOOC–CH–CH–COOH OH OH	2.82; 3.95
(F)	Succinic acid	HOOC–CH_2–CH_2–COOH	4.00; 5.24
(G)	Maleic acid	*cis*-HOOC–CH=CH–COOH	1.75; 5.83
(H)	Malonic acid	HOOC–CH_2–COOH	2.65; 5.28
	BPA	*p*-$(HO)_2$B–C_6H_4–CH_2–CH(NH_2) COOH	2.46; 8.46; 9.76
	Boric acid	$B(OH)_3$	9.24

creases according to the reactions 3 and 4. In solutions of pH > 11, BPA has an approximately divalent negative charge.

The closed circles in Fig. 2 show the observed migration distances of BPA at pH 4.0, 6.88 and 9.18 [8]. As expected from the net charge-pH curve, BPA showed negative movement at pH 2. Although BPA has approximately no charge in solutions of pH 4–7, it showed negative movement at pH 4.0 and 6.88. The movement was

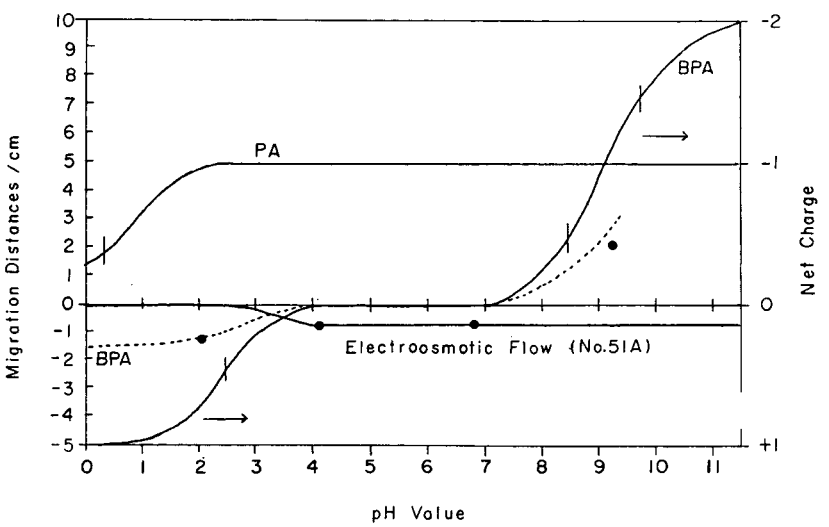

Fig. 2. Net charge and the corrected migration distances of migrants (BPA, PA) at 15°C plotted against pH. The movement due to an electroosmotic flow is shown. Small vertical lines, pK_a; ● = observed migration distances of BPA at pH 2.0, 4.0, 6.88 and 9.18 [8]; dashed line, migration curve of BPA.

caused by the electroosmotic flow. Based on the observed distances, the electroosmotic flow–pH curve for BPA was obtained. The dashed line in Fig. 2 is the corrected migration curve of BPA for the electroosmotic flow.

The migration distances of BPA in the aqueous carboxylic acids are plotted against pH in Fig. 3. The distances deviate substantially from the migration curve in aqueous oxalic (A) and citric (B) acids, where BPA behaves as an anion. Both oxalic and citric acid are typical ligands [20], and hence it is likely that BPA forms complexes of negative charge with oxalic and citric acids.

In aqueous succinic (F), maleic (G) and malonic (H) acid, the migration distances are in good agreement with those calculated from the migration curve. This indicates no complexation between BPA and each of the three acids.

In aqueous fumaric (C), malic (D) and tartaric (E) acid, BPA behaves as a cation. However, the migration distances deviate somewhat from the migration curve.

Based on the electrophoretic behaviour, the carboxylic acids can be classified into three groups: (i) acids forming complexes of negative charge with BPA (oxalic and citric acids); (ii) acids forming complexes of positive charge with BPA (fumaric, malic and tartaric acid); and (iii) acids not forming complexes with BPA (succinic, maleic and malonic acid).

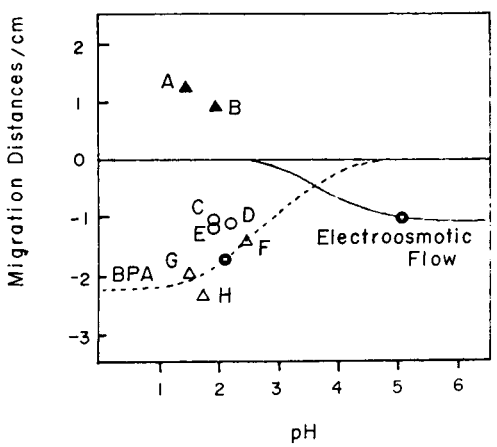

Fig. 3. Observed migration distances of BPA in aqueous 0.1 mol dm^{-3} oxalic acid, citric acid, fumaric acid, malic acid, tartaric acid, succinic acid, maleic acid and malonic acid (lettered as in Table 1). Dashed line, migration curve of BPA.

3.2. IR spectra of DHBCs in aqueous carboxylic acids

In order to obtain further evidence for the complex formation, we tried to elucidate the chemical form of the complex by IR spectrometry. As mentioned in the Introduction, orthoboric acid was used as a candidate of DHBCs owing to its moderate solubility in water. Similarly to BPA, orthoboric acid behaved as a cation in oxalic and citric acid but not in maleic acid [21].

Fig. 4 shows the IR spectra of boric acid in water and in aqueous $NaHCO_3$–Na_2CO_3 solution (pH ≈ 8.5) in the frequency range 1000–

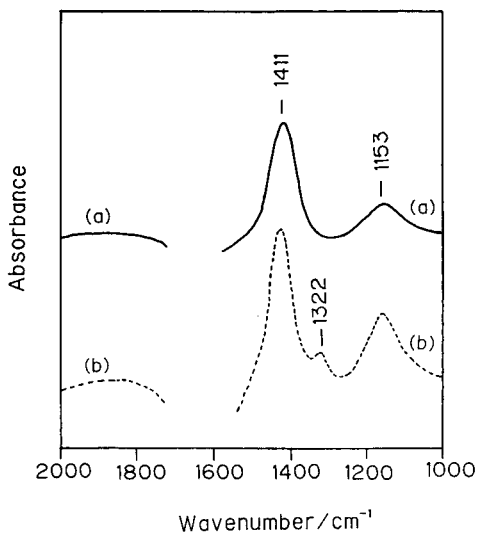

Fig. 4. IR spectra of boric acid in (a) water and (b) aqueous solution of $NaHCO_3$–Na_2CO_3 (pH ≈ 8.5). Concentration of boric acid, 0.1 mol dm^{-3}. Reference: (a) water; (b) aqueous solution of $NaHCO_3$–Na_2CO_3. Band assignment: 1411 cm^{-1} = antisymmetric B–O stretching for H_3BO_3; 1151 cm^{-1} = antisymmetric B–O–H bending for H_3BO_3; 1322 cm^{-1} = antisymmetric B–O stretching for $B(OH)_4^-$. The strong absorption due to the normal water prohibited the spectral measurement in the frequency range 1575–1725 cm^{-1}.

2000 cm^{-1}. The bands at 1411, 1151 and 1322 cm^{-1} are assigned to the antisymmetric B–O stretching for H_3BO_3, the antisymmetric B–O–H bending for H_3BO_3 [22] and the antisymmetric B–O stretching for $B(OH)_4^-$ [23], respectively.

The IR spectra of H_3BO_3 in aqueous 0.1 mol dm^{-3} malonic, succinic and maleic acid are shown in Fig. 5. No spectral change was observed in the three acids, indicating that interaction between the dihydroxyboryl compound and each of the three acids was negligible. This coincided with the result of electrophoresis for BPA, namely that the migration distance of BPA towards the cathode approximately agreed with that expected from the charge of the three solutions.

Fig. 6 shows the IR spectra of H_3BO_3 in aqueous oxalic acid. The ratio of oxalic acid molecules to boron atoms (CA/B ratio) ranges from 0.33 to 8.

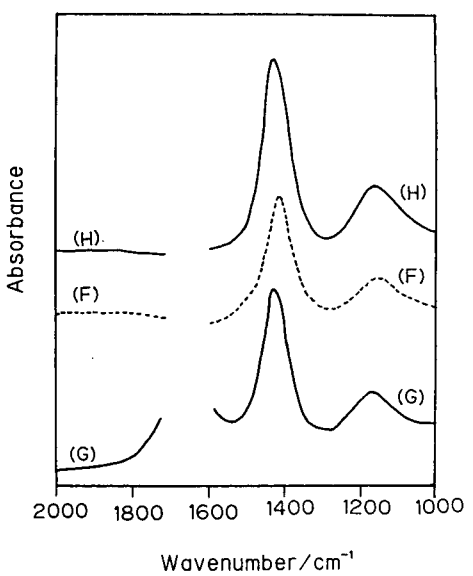

Fig. 5. IR spectra of boric acid in aqueous 0.1 mol dm^{-3} (H) malonic acid, (F) succinic acid and (G) maleic acid. Concentration of boric acid, 0.1 mol dm^{-3}; ratio of carboxylic acid molecules to boron atoms (CA/B) = 1; reference, aqueous solution of the corresponding carboxylic acid.

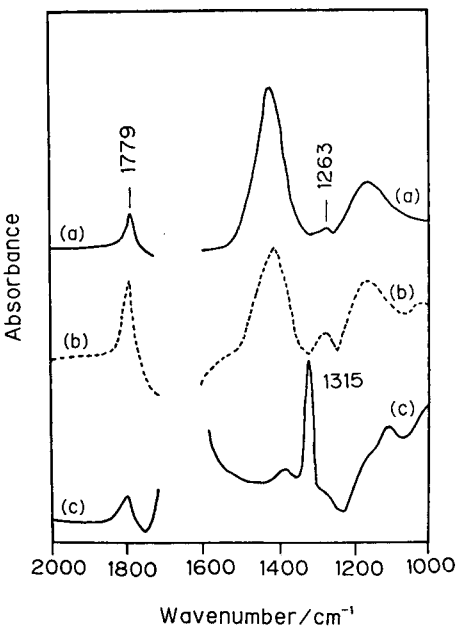

Fig. 6. IR spectra of boric acid in aqueous (a) 0.1, (b) 0.2 and (c) 0.2 mol dm^{-3} oxalic acid. Ratio of carboxylic acid molecules to boron atoms (CA/B): (a) 0.33; (b) 4.0; (c) 8.0. Reference: aqueous (a) 0.1, (b) 0.2 and (c) 0.2 mol dm^{-3} oxalic acid.

The spectrum of H_3BO_3 in a solution with CA/B = 0.33 showed new bands at 1779 and 1263 cm^{-1}, the assignment of which is currently under investigation. In the spectrum for CA/B = 4, the B–O stretching band decreased, whereas the two new bands increased. In the spectrum for CA/B = 8, the two bands due to H_3BO_3 (B–O stretching and B–O–H bending) disappeared almost completely. Instead, the band at 1315 cm^{-1} due to the $B(OR)_4^-$ group increased.

The spectral behaviour can be explained as follows. In solutions of lower CA/B ratio, boric acid and oxalic acid form a complex (complex **III**), in which the boron atom is trivalent. The complex **III** bonds to another oxalic acid molecule in the solutions of larger CA/B ratio, giving another complex (complex **IV**) with tetrahedral boron.

For the complexes of boric acid with oxalic acid, Van Duin et al. [24] proposed the following chemical species:

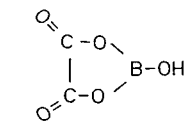

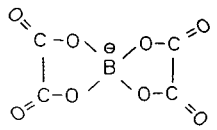

It is possible to identify the complex **III** with a chemical form comparable to the top formula and the complex **IV** to the bottom formula. Taking the spectral result into account, we explain the electrophoretic behaviour as follows: many oxalate ions are located around the dihydroxyboryl compounds in the background solution in electrophoresis, and hence the boron compounds form complexes such as the complex **IV** with negative charge.

Based on the spectral behaviour of boric acid and the migration distance of BPA in aqueous citric acid, we propose the following chemical form for the complex of BPA with oxalic acid:

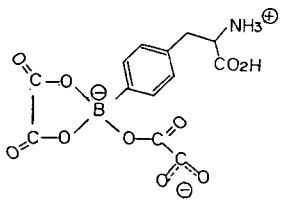

In aqueous citric acid, similar spectral changes were observed with increasing CA/B ratio, as shown in Fig. 7. Clearly, boric acid formed a tetrahedral boron complex with citric acid.

Fig. 8 shows that boric acid forms complexes with fumaric, malic and tartaric acid. However, no evidence was detected for tetrahedral boron complexes.

In conclusion, complex formation of dihydroxyboryl compounds with oxalic and citric acid

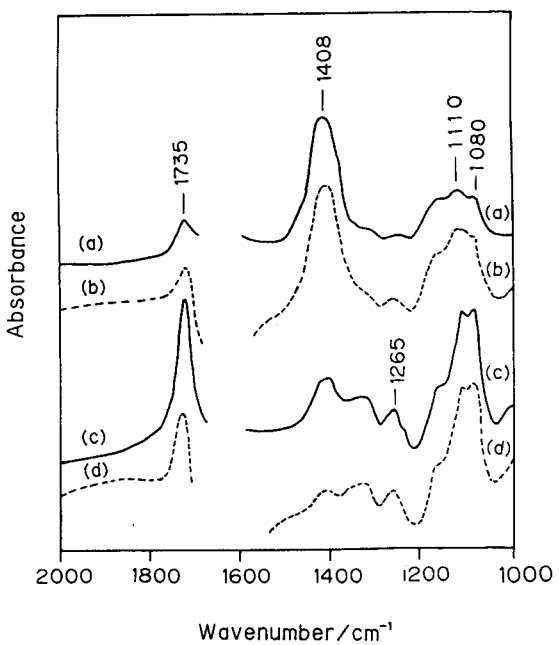

Fig. 7. IR spectra of boric acid in aqueous (a) 0.1, (b) 0.1, (c) 0.2 and (d) 0.2 mol dm^{-3} citric acid. Concentration of boric acid: (a) 0.2; (b) 0.1; (c) 0.05; (d) 0.025 mol dm^{-3}. Ratio of carboxylic acid molecules to boron atoms (CA/B): (a) 0.5, (b) 1.0; (c) 4.0, (d) 8.0.

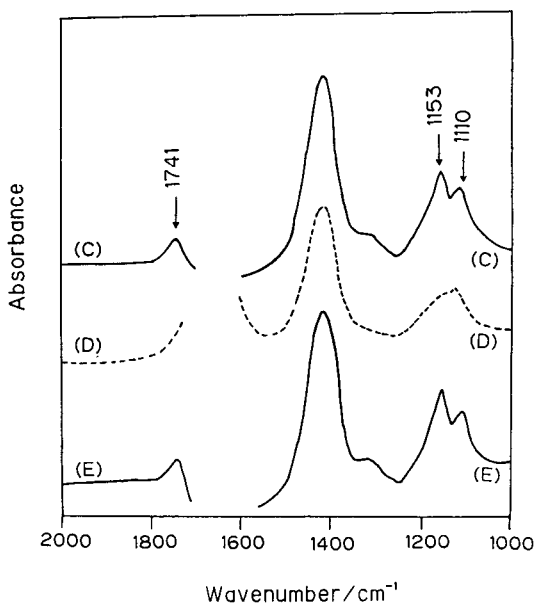

Fig. 8. IR spectra of boric acid in aqueous 0.1 mol dm^{-3} (C) fumaric acid, (D) malic acid and (E) tartaric acid. Concentration of boric acid: (C) 0.13; (D) 0.1; (E) 0.13 mol dm^{-3}. Ratio of carboxylic acid molecules to boron atoms (CA/B): (C) 0.75; (D) 1.0; (E) 0.75.

and also with fumaric, malic and tartaric acid was predicted by paper electrophoresis and was proved by IR spectrometry. No appreciable interaction was detected between boric acid and succinic, maleic or malonic acid. The spectral behaviour was fully consistent with the migration behaviour in paper electrophoresis. It was confirmed that electrophoresis is useful not only for separating substances but also for elucidating the chemical states of a compound in solution.

4. References

[1] Y. Kiso, M. Kobayashi, Y. Kitaoka, K. Kawamoto and J. Takada, *J. Chromatogr.*, 36 (1968) 215.
[2] Y. Kiso, M. Kobayashi and Y. Kitaoka, in M. Halmann (Editor), *Analytical Chemistry of Phosphorus Compounds*, Wiley-Interscience, New York, 1972, Ch. 3.
[3] P. Gebauer and P. Boček, *Folia Fac. Sci. Nat. Univ. Purkynianae Brun.*, 26 (1985) 37.
[4] Y. Hirokawa and Y. Kiso, *J. Chromatogr.*, 628 (1993) 283.
[5] Y. Kiso, M. Kobayashi, Y. Kitaoka, K. Kawamoto and J. Takada, *J. Chromatogr.*, 33 (1968) 561.
[6] M. Kobayashi, Y. Kitaoka and Y. Ujeno, *KURRI-TR (Technical Report of the Research Reactor Institute, Kyoto University)*, No. 354, 1991, p. 63.
[7] Y. Mishima (Editor), *Selective Thermal Neutron Capture, Treatment of Malignant Melanoma Using its Specific Metabolic Activity, KURRI-TR*, No. 260, 1985.
[8] Y. Kitaoka, M. Kobayashi and Y. Ujeno, *J. Chromatogr.*, 585 (1991).
[9] Y. Kitaoka, M. Kobayashi and Y. Ujeno, *Annu. Rept. Res. Reactor Inst. Kyoto Univ.*, 25 (1992) 95.
[10] R.P. Singhal and S.S.M. DeSilva, *Adv. Chromatogr.*, 31 (1993) 293.
[11] R.P. Singhal, B. Ramamurthy, N. Govindraj and Y. Sarwar, *J. Chromatogr.*, 543 (1991) 17.
[12] M. Van Duin, J.A. Peter, A.P.G. Kieboom and H. Van Bekkum, *Tetrahedron*, 40 (1984) 2901.
[13] J.O. Edwards, G.C. Morrison, V.F. Ross and I.W. Schultz, *J. Am. Chem. Soc.*, 77 (1955) 266.
[14] M. Kobayashi, *Annu. Rep. Res. Reactor Inst. Kyoto Univ.*, 19 (1986) 99.
[15] M. Kobayashi and M. Kobayashi, *J. Phys. Chem.*, 84 (1980) 781.
[16] M. Kobayashi and R. Matsushita, *J. Phys. Chem.*, 94 (1990) 2789.
[17] Chemical Society of Japan, *Kagakubenran Kisohen II*, Maruzen, Tokyo, 1984, p. 339.
[18] Y. Mori, A. Suzuki, K. Yoshino and H. Kakihana, *Pigment Cell Res.*, 2 (1989) 273.
[19] J.R. Whitaker, in G. Zweig and J.R. Whitaker (Editors), *Paper Chromatography and Electrophoresis*, Vol. 1, Academic Press, New York, 1967, p. 11.
[20] Chr.K. Jørgenson, *Inorganic Complexes*, Academic Press, New York, 1963.
[21] Y. Kitaoka, M. Kobayashi, M. Kirihata and I. Ichiomoto, *Annu. Rep. Res. Reactor Inst. Kyoto Univ.*, 26 (1993) 143.
[22] L. Andrews and T.R. Burkholder, *J. Chem. Phys.*, 97 (1992) 7203.
[23] J.O. Edwards, G.C. Morrison, V.F. Ross and I.W. Shultz, *J. Am. Chem. Soc.*, 77 (1955) 266.
[24] M. van Duin, J.A. Peter, A.P.G. Kieboom and H. van Bekkum, *Tetrahedron*, 40 (1984) 2901.

ELSEVIER

Journal of Chromatography A, 678 (1994) 359–363

JOURNAL OF CHROMATOGRAPHY A

Short Communication

High-performance liquid chromatographic determination of equine estrogens with ultraviolet absorbance and electrochemical detection

Jasmina Novaković[a], Eva Tvrzická[b,*], Věra Pacáková[a]

[a]*Department of Analytical Chemistry, Faculty of Natural Sciences, Charles University, Albertov 2030, 128 40 Prague 2, Czech Republic*

[b]*4th Department of Medicine, 1st Faculty of Medicine, Charles University, U Nemocnice 2, 128 08 Prague 2, Czech Republic*

First received 3 February 1994; revised manuscript received 24 May 1994

Abstract

The simultaneous separation of a mixture of equine estrogens containing estrone, equilin, equilenin and their corresponding 17α-diols was accomplished by reversed-phase high-performance liquid chromatography (RP-HPLC) on a Nucleosil C_{18} column with a mobile phase composed of methanol–water–2-propanol–dichloromethane (45:42.5:7.5:5, v/v). UV absorbance and electrochemical detection were used for the analysis of a standard mixture of equine estrogens. RP-HPLC with UV absorbance detection was applied to the determination of these compounds in pharmaceutical drug substances and drug products after acid hydrolysis of their sodium sulfate esters.

1. Introduction

Conjugated estrogens are defined in the USP XXII [1] as a mixture of sodium estrone sulfate and sodium equilin sulfate obtained synthetically or isolated from equine urine. They may contain other pharmacologically active conjugated estrogenic substances, such as equilenin, 17α-estradiol, 17α-dihydroequilin and 17α-dihydroequilenin, and traces of the corresponding 17β-diols.

The official USP XXII method [1] for the determination of conjugated estrogens is based on the GC of trimethylsilyl ethers of estrone and equilin after enzymatic hydrolysis of their sodium sulfate esters. Recently, capillary GC [2] and densitometry [3,4] of underivatized equine estrogens in drug substances and drug products have been reported. HPLC has been described for the determination of the estrogens after hydrolysis of the conjugates and formation of dansyl derivatives [5]. RP-HPLC of conjugated forms of equine estrogens was proposed by Flann and Lodge [6], but the quantitative evaluation of the method was not reported. Townsend et al. [7] developed an RP-HPLC determination of conjugated and free forms of estrone and equilin with UV absorbance detection. The separation of nine equine estrogens by RP-HPLC has been reported by Desta [8].

This paper describes an RP-HPLC method with UV absorbance and electrochemical detec-

* Corresponding author.

0021-9673/94/$07.00
SSDI 0021-9673(94)00507-6

tion (ED) for the determination of estrone (ES), equilin (EQ), equilenin (EQN), 17α-estradiol, 17α-dihydroequilin (DHEQ) and 17α-dihydroequilenin (DHEQN) after acid hydrolysis of their conjugates. This method was applied to pharmaceutical drug substances and drug products.

2. Experimental

2.1. Apparatus and operating conditions

The HPLC measurements with UV absorbance detection were carried out by using a Chrompack (Middelburg, Netherlands) HPLC Gras system equipped with CP UV-VAR detector and an injection valve with a 20-μl loop (Chrompack), interfaced with an IBM PC/2 Model 30 computer, connected to an Epson LQ 550 recorder (Seico Epson, Japan) and a Chrompack BD 70 recorder (Kipp and Zonen, Delft, Netherlands). The mobile phase consisted of methanol–water–2 - propanol–dichloromethane (45:42.5:7.5:5, v/v). The flow-rate was 0.7 ml/min and UV absorption detection was performed at 280 nm.

The HPLC–ED measurements were carried out by using an LC-XPD pump (Pye Unicam) equipped with an injection valve with a 3-μl loop and an ADLC 2 amperometric detector (Laboratorní Přístroje, Prague, Czech Republic) connected with a TZ 4620 line recorder (Laboratorní Přístroje). Ag–AgCl was used as the reference electrode, carbon fibre as the working electrode and stainless steel as the counter electrode. $Na_2HPO_4 \cdot 12H_2O$ (0.6%) was added to the above mobile phase, which was adjusted to pH 6.0–6.05 with acetic acid.

All separations were performed on a Nucleosil C_{18} stainless-steel column (250 × 4.6 mm I.D., 3-μm particle size) (Chrompack).

2.2. Materials

ES, EQ, EQN and estriol [internal standard (I.S.)] were obtained from Sigma (St. Louis, MO, USA) and ESD, DHEQ and DHEQN were gifts from Diosynth (Oss, Netherlands). Drug substance containing 604 mg/g of conjugated estrogens was obtained from Diosynth, Hormopleks sugar-coated tablets, each containing 1.25 mg of conjugated estrogens, from Galenika (Zemun, Yugoslavia) and Oestro-Feminal capsules, each containing 1.25 mg of conjugated estrogens, from Heinrich Mach (Illertisen, Germany).

2.3. Calibration plots

Stock standard solutions of ES, EQ, EQN, ESD, DHEQ, DHEQN and the I.S. were prepared at a concentration of 0.5 mg/ml in methanol and stored at 4°C. Working standard solutions for obtaining calibration graphs were prepared by transferring 1 ml of I.S. stock standard solution into 10-ml volumetric flasks and diluting to the mark with methanol. The final concentrations of estrogens in the working standard solutions for calibration were 0.005, 0.01, 0.02, 0.05, 0.1, 0.15, 0.2 and 0.3 mg/ml.

2.4. Sample preparation

Acid hydrolysis of conjugated estrogens and extraction of the 3-phenol forms of equine estrogens from drugs were carried out as described previously [4]. A 2.5-ml volume of I.S. stock standard solution (0.5 mg/ml in methanol) was added to the hydrolysate previously cooled to room temperature. The estrogens were extracted with 2 × 10 and 1 × 5 ml of chloroform and the combined extracts were washed with 5 ml of water, passed through 1 g of anhydrous sodium sulfate and evaporated to dryness under a nitrogen stream and the residue was dissolved in 25 ml of methanol–water (1:1).

3. Results and discussion

According to the results of Carignan and Lodge [9] and Clairns et al. [10], there is no significant difference between acid and enzymatic hydrolysis of conjugated estrogens. The separation of all compounds was achieved within less than 25 min and the retention times of the I.S., DHEQN, DHEQ, ESD, EQN, EQ and ES

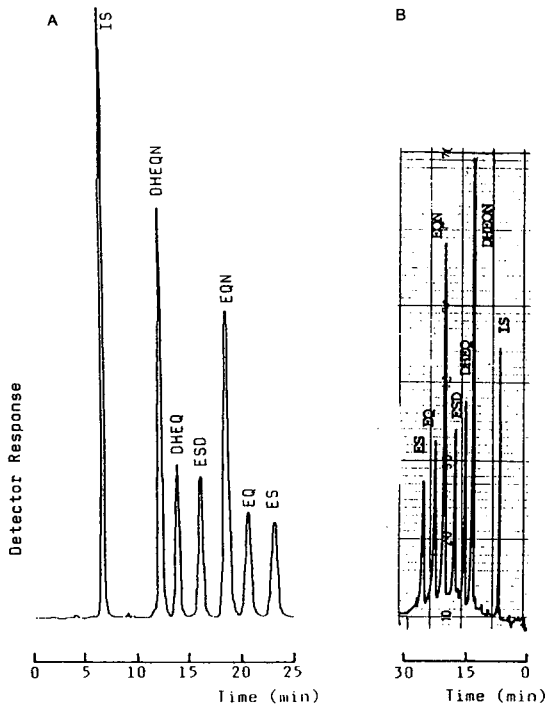

Fig. 1. Typical chromatograms of the standard calibration mixture of equine estrogens containing 0.05 mg/ml each of the I.S., DHEQN, DHEQ, ESD, EQN, EQ and ES obtained by (A) HPLC–UV detection and (B) HPLC–ED. Chromatographic conditions: (A) column, Nucleosil C_{18} (250 × 4.6 mm I.D.), mobile phase, methanol–water–2-propanol–dichloromethane (45:42.5:7.5:5, v/v); flow-rate, 0.7 ml/min; loop injection (20 μl); UV absorbance detection at 280 nm; (B) mobile phase, as above but containing 0.6% of $Na_2HPO_4 \cdot 12H_2O$; loop injection (3 μl); applied potential, 1.1 V; 100 nA full-scale; other conditions as in (A).

were 6.44, 11.85, 13.36, 15.14, 18.59, 20.59 and 23.18 min, respectively. Details of the separation will be presented in a separate paper [11]. ED requires the use of a conducting mobile phase, which is why 0.06% of $Na_2HPO_4 \cdot 12H_2O$ was added to the mobile phase.

Fig. 1 represents typical chromatograms of a calibration mixture containing 0.05 mg/ml of the I.S., DHEQN, DHEQ, ESD, EQN, EQ and ES obtained by (A) RP-HPLC with UV absorbance detection and (B) RP-HPLC with ED detection. The potential of the electrochemical detector was set at 1.1 V vs. Ag–AgCl. On increasing the potential, the detector response showed a plateau.

Statistical evaluation of the calibration data obtained by UV absorbance and electrochemical detection is given in Tables 1 and 2, respectively.

Estriol meets all the requirements for an ideal I.S. [12], as its UV absorption maximum (280 nm) and electrochemical properties are similar to those of the analyte compounds. As ED depends critically on numerous experimental conditions [12], RP-HPLC–UV detection was applied to the determination of equine estrogens in drugs. The better selectivity of ED might be of benefit in the determination of these compounds in biological materials. HPLC–ED has been used successfully for the determination of catechol estrogens [13,14] and estriol glucuronides [15] in biological fluids. By this means the tedious clean-up procedure was avoided [15]. To our knowledge, the

Table 1
Statistical evaluation of the calibration data obtained by RP-HPLC with UV absorbance detection

Compound	$y = a + bx$[a]	r[b]	Range of linearity[c]	LOD[d]
DHEQN	$y = -0.0534 + 1.1266x$	0.9994	0.005–0.3	0.002
DHEQ	$y = -0.0460 + 0.4736x$	0.9988	0.005–0.3	0.004
ESD	$y = -0.0363 + 0.4986x$	0.9982	0.005–0.3	0.004
EQN	$y = -0.0859 + 1.3526x$	0.9993	0.005–0.3	0.002
EQ	$y = -0.0389 + 1.4757x$	0.9989	0.010–0.3	0.004
ES	$y = -0.0529 + 0.4868x$	0.9985	0.010–0.3	0.004

[a] y = Relative detector response (estrogen/I.S. peak-area ratio); x = concentration of the estrogen in the calibration solution divided by I.S. concentration; a = intercept on the ordinate; b = slope.
[b] r = Correlation coefficient.
[c] In mg/ml, which corresponds to injected amounts from 0.1 ng DHEQN, DHEQ, ESD, EQN (0.2 ng EQ, ES) to 6 ng in 20 μl.
[d] Limit of detection (mg/ml) at a signal-to-noise ratio of 3.

Table 2
Statistical evaluation of the calibration data obtained by RP-HPLC with ED

Compound	$y = a + bx$[a]	r[b]	Range of linearity[c]	LOD[d]
DHEQN	$y = 0.1783 + 1.4641x$	0.9960	0.005–0.05	0.002
DHEQ	$y = 0.0147 + 0.7241x$	0.9992	0.005–0.05	0.004
ESD	$y = 0.0178 + 0.5921x$	0.9995	0.005–0.05	0.004
EQN	$y = 0.1437 + 1.2096x$	0.9969	0.005–0.05	0.002
EQ	$y = 0.0726 + 0.4704x$	0.9965	0.010–0.05	0.004
ES	$y = 0.0452 + 0.3907x$	0.9986	0.010–0.05	0.004

[a] y = Relative detector response (estrogen/I.S. peak-height ratio); x = concentration of the estrogen in the calibration solution divided by I.S. concentration; a = intercept on the ordinate; b = slope.
[b] r = Correlation coefficient.
[c] In mg/ml, which corresponds to injected amounts from 0.015 ng DHEQN, DHEQ, ESD, EQN (0.03 ng EQ, ES) to 0.15 ng in 3 μl.
[d] Limit of detection (mg/ml) at a signal-to-noise ratio of 3.

Table 3
Determination of equine estrogens by RP-HPLC–UV absorbance detection in drugs

Compound	Drug substance			Hormopleks tablets			Oestro-Feminal capsules		
	D[a] (%)	F[b] (%)	R.S.D.[c] (%)	D[a] (%)	F[b] (%)	R.S.D.[c] (%)	D[a] (%)	F[b] (%)	R.S.D.[c] (%)
ES	55.29	56.76	1.54	–[d]	54.93	0.99	70–90	82.36	1.57
EQ	29.80	27.69	5.21	–	26.17	1.64	8–15	8.39	1.94
EQN	2.66	4.28	6.19	–	4.79	4.25	≤4	2.09	5.37
ESD	5.93	5.42	6.00	–	5.76	3.44		2.22	6.11
DHEQ	4.90	3.85	5.92	–	6.17	5.54	2–8[e]	2.29	8.13
DHEQN	1.42	1.86	3.73	–	2.32	2.51		1.48	6.24

[a] Declared amount.
[b] Found amount.
[c] Relative standard deviation of ten determinations.
[d] Not specified.
[e] Total amount of ESD, DHEQ and DHEQN.

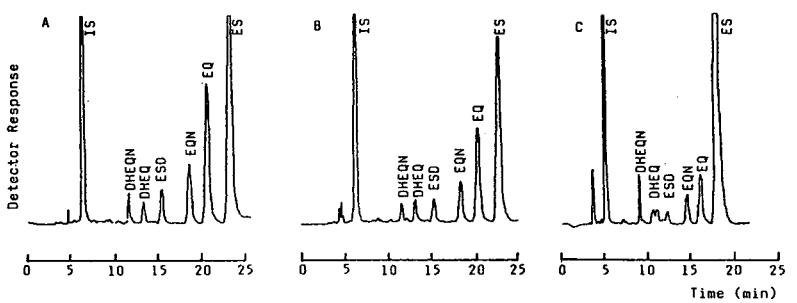

Fig. 2. Typical chromatograms of (A) the drug substance, (B) Hormopleks tablets and (C) Oestro-Feminal capsules. Chromatographic conditions as in Fig. 1A.

determination of equine estrogens by HPLC–ED detection has not previously been reported.

The results of the determination of equine estrogens in drugs by HPLC–UV detection are given in Table 3 and the chromatograms are presented in Fig. 2. The results imply that the HPLC–UV detection method can replace the official USP XXII assay for the determination of conjugated estrogens in drugs.

References

[1] *The United States Pharmacopeia XXII Revision*, US Pharmacopeial Convention, Rockville, MD, 1990, pp. 535–536.
[2] J. Novaković and E. Tvrzická, *J. High Resolut. Chromatogr.*, 14 (1991) 495.
[3] J. Novaković, D. Agbaba, S. Vladimirov and D. Živanov-Stakić, *J. Pharm. Biomed. Anal.*, 8 (1990) 253.
[4] J. Novaković, J. Kubeš and I. Němec, *J. Planar Chromatogr.*, 3 (1990) 521.
[5] R.W. Roos and C.A. Lau Cam, *J. Pharm. Sci.*, 74 (1985) 201.
[6] B. Blann and B. Lodge, *J. Chromatogr.*, 360 (1987) 273.
[7] R.W. Townsend, V. Keuth, K. Embil, G. Mullersman, J.H. Perin and H. Derendorf, *J. Chromatogr.*, 450 (1988) 414.
[8] B. Desta, *J. Chromatogr.*, 435 (1988) 358.
[9] G. Carignan and B.A. Lodge, *J. Pharm. Sci.*, 69 (1980) 1453.
[10] T. Clairns, E. Siegmund and B. Rader, *Anal. Chem.*, 53 (1981) 1271.
[11] J. Novaković, E. Tvrzická, L. Feltl and V. Pacaková, in preparation.
[12] C.F. Poole and S.K. Poole, *Chromatography Today*, Elsevier, Amsterdam, 1991.
[13] K. Shimada, T. Tanaka and T. Nambara, *J. Chromatogr.*, 178 (1979) 350.
[14] K. Shimada, T. Tanaka and T. Nambara, *J. Chromatogr.*, 223 (1981) 33.
[15] K. Shimada, F. Xie and T. Nambara, *J. Chromatogr.*, 232 (1982) 13.

ELSEVIER

Journal of Chromatography A, 678 (1994) 364–369

JOURNAL OF CHROMATOGRAPHY A

Short Communication

Analysis of fluoride, acetate and formate in Bayer liquors by ion chromatography

T.J. Cardwell*, W.R. Laughton

Centre for Scientific Instrumentation, School of Chemistry, La Trobe University, Bundoora, Victoria 3083, Australia

First received 28 February 1994; revised manuscript received 16 May 1994

Abstract

Fluoride, acetate and formate in Bayer liquors have been separated on an AS5A column by suppressed ion chromatography using a very weak sodium hydroxide eluent before a rapid change in the eluent composition was required to elute the remaining liquor components. Fluoride data for four liquor samples analysed by ion chromatography with conductivity detection correlated well with potentiometric data obtained by a fluoride ion-selective electrode. Acetate and formate were analysed by conductivity and spectrophotometric detection and reasonable agreement was achieved.

1. Introduction

Bauxite used to produce pure alumina in the Bayer process contains quantities of chloride, fluoride, sulfate, phosphate, organic matter and traces of many metals. The organic matter is oxidised progressively to oxalate within the process liquors and this, along with the soluble components, accumulates in the liquors. Many of these components require constant monitoring of the liquors as the purity and yield of the final product may be affected adversely [1].

Currently in the aluminium industry, fluoride is assayed quantitatively using a fluoride ion-selective electrode (ISE). An ionic strength adjustment buffer allows the ISE potential to be correlated directly to concentration rather than to the activity of the analyte by ensuring a constant ionic strength for each solution. These buffers also adjust the sample pH to ca. 5 or 8.5 (depending upon the particular buffer) to eliminate hydroxide ion interference in the fluoride ISE measurements at room temperature. Ionic strength adjustment buffers also contain a complexing agent, although some conjecture exists as to which particular complexing agent should be employed [2]. These reagents complex aluminium and iron(III) in particular, releasing any fluoride bound to these metals [3,4]. The choice of buffer is dependent on the interfering components and the aluminium levels in the sample.

Although the potentiometric procedure is quite reliable, ion chromatography (IC) [5] is a more useful technique because anions such as fluoride, chloride, sulfate and phosphate, as well as organic acids including oxalate and tartrate, can be analysed simultaneously and, after optimal conditions for peak separation have been obtained, with minimal user intervention.

Several communications have been published

* Corresponding author.

0021-9673/94/$07.00
SSDI 0021-9673(94)00526-F

regarding chloride, phosphate, sulfate and oxalate analysis in Bayer liquors using IC with conductivity detection [6–8], but the chromatographic analysis of fluoride in these liquors has not been reported presumably because of interference from early-eluting organic acids present in the liquor sample. This paper describes the development of an elution program for the separation of fluoride from early-eluting organic acids and the application of this program to the analysis of some Bayer liquors in order to explain the discrepancy in fluoride levels determined by potentiometry and chromatography.

2. Experimental

2.1. Ionic strength adjustment buffers

The following buffers were prepared fresh before use.

Citrate buffer (pH 8.9). Citric acid monohydrate (60 g), sodium citrate dihydrate (210 g), ammonium chloride (53.5 g) and ammonia solution (67 ml) were made up to 1 l in deionised water.

TISAB IV (pH 8.8). Concentrated hydrochloric acid (84 ml), TRIZMA base (Tris; Sigma, St. Louis, MO, USA; 242 g) and sodium tartrate dihydrate (230 g) were made up to 1 l in deionised water.

Modified TISAB IV (pH 8.0). As for TISAB IV above, but 150 ml concentrated hydrochloric acid was added.

All glassware was soaked in caustic detergent (Pyroneg, Diversey) and rinsed thoroughly with deionised water before use. All solutions were prepared using deionised NANOpure water purified on a Sybron/Barnstead filtration system.

2.2. Fluoride standards

A 1000 mg/l fluoride stock solution was prepared from anhydrous sodium fluoride and transferred immediately to a polyethylene container for storage. Fresh standards, 10 mg/l or below, were prepared weekly.

2.3. Sodium hydroxide eluents

A 50% (w/v) stock solution of NaOH was prepared and allowed to stand in a closed polypropylene container for about 48 h until insoluble sodium carbonate had settled. Eluents 200 and 0.75 m*M* sodium hydroxide were prepared daily by adding the necessary volume of 50% (w/v) NaOH stock solution to deoxygenated water. Before starting a series of chromatographic runs, the eluents were sparged with helium for ca. 15 min each day to prevent possible carbonate contamination.

2.4. Samples

Two spent liquors (samples 1 and 2) and two pregnant liquors (samples 3 and 4) were available for analysis.

2.5. Instrumentation

Chromatography was carried out on a Dionex 4500i ion chromatograph fitted with an AS5A column (150 × 5 mm), an AG5A guard column (50 × 5 mm) and an AMMS micromembrane suppressor. IC data were acquired and stored using a WYSE ECM 5400 personal computer and DAPA Chromatography System VI.40 software. Detection of fluoride, formate and acetate was achieved on the Dionex conductivity detector and detection of formate and acetate was performed on a Hewlett-Packard 1050 spectrophotometric detector at 200 nm.

For ISE fluoride determinations, an Orion EA-940 expandable ion analyser was used in conjunction with an Orion 94-09 fluoride ISE and an Orion 90-02 double-junction reference electrode. Measurements of pH were made using an Orion research microprocessor Ionalyzer Model 901 digital pH/mV meter in conjunction with an Activon combination pH (glass/calomel) electrode.

2.6. Determination of fluoride by potentiometry

Equal volumes of an ionic strength adjustment buffer and a standard (or sample) were mixed. The potential for each mixture was measured and a calibration curve of potential versus log concentration of fluoride was plotted. Spent liquors and pregnant liquors were diluted to yield fluoride concentrations in the 10-100 mg/l region and to dilute the aluminate concentration, thus reducing possible aluminium interference [4,9].

2.7. Determination of fluoride, formate and acetate by IC

For the determination of fluoride, formate and acetate the calibration graph method was used. Spent liquors were diluted by a factor of at least 1000 and pregnant liquors by a factor of at least 400. Recalibrations were performed regularly; a stable temperature is essential as fluctuations throughout the day affect reproducibility of peak areas.

The IC elution program developed for resolution of fluoride, acetate and formate at a flow-rate of 1 ml/min using two eluents, eluent 1 (0.75 m*M* NaOH) and eluent 2 (200 m*M* NaOH), was as follows: 0–6.0 min, 100% eluent 1; 6.0–6.5 min, linear gradient to eluent 1–eluent 2 (50:50); 6.5–13.5 min, eluent 1–eluent 2 (50:50); 13.5–14.0 min, linear gradient down to 100% eluent 1; 14.0–33.0 min, 100% eluent 1. The initial isocratic conditions (until 6 min) permitted the elution and resolution of fluoride, acetate and formate. The increase in eluent strength beyond 6 min ensured rapid elution of other components of the liquor before the column was re-equilibrated in preparation for the next injection.

Continuous regeneration of the AMMS suppressor was achieved using 20 m*M* sulfuric acid at a flow-rate of ca. 10 ml/min. For these particular samples containing a high aluminium content, it is necessary to flush the AMMS regularly with a strongly acidic reagent (1 *M* HCl) otherwise precipitation of $Al(OH)_3$ may result.

3. Results and discussion

3.1. Determination of fluoride by potentiometry

For the determination of fluoride in Bayer liquors, the currently adopted industrial method of analysis involves the calibration graph method using a fluoride ISE. A high-pH buffer is required in order to decrease potential aluminium interference and to ensure the buffer capacity is sufficiently strong to cater for the highly caustic liquors [9]. Three high-pH buffers examined in this work were a citrate buffer (pH 8.9), TISAB IV (pH 8.8) and modified TISAB IV (pH 8.0).

Nicholson and Duff [4] recommended that a complexing time of at least 20 min and preferably 24 h should be used with TISAB buffers before measurement of the electrode potential in fluoride analysis. They observed an initial rapid potential change due to the release of fluoride arising from complexation of the aluminium, thus supporting the need to delay the measurement for 20 min. In the present work, complexing time dependence studies were carried out on two of the Bayer liquor samples by taking measurements at various intervals from 3 min to 24 h after addition of one of the above buffers. In the case of the citrate buffer, the measured fluoride concentration increased slightly and remained constant after about 2 h. No significant differences in the fluoride concentration were found for the TISAB buffers after 3 min and there seemed to be no improvement in the detection range using the pH 8.0 buffer. All subsequent measurements were taken 5 min after addition of TISAB IV (pH 8.8) buffer.

A calibration plot for a series of standards was found to be linear over the range 10–1000 mg/l fluoride. Recovery studies were conducted by addition of known amounts of fluoride to previously analysed liquor samples and, in all cases, recoveries of 100% were obtained.

3.2. Fluoride by IC

Using 35 m*M* NaOH as eluent, the fluoride peak at ca. 1.3 min in the chromatogram of a dilute liquor sample was found to be relatively unsymmetrical, which suggested that other solutes were co-eluting with fluoride. Furthermore, initial quantitation of the nominated fluoride peak yielded a fluoride concentration at least four times that obtained by potentiometric measurements. Fig. 1 shows a typical chromatogram obtained with an elution program which commences with 0.75 m*M* NaOH to separate three components which co-elute with the eluent used in the preliminary studies above. The elution program includes a rapid change to a stronger eluent to elute more strongly retained components of the liquors and these are observed in Fig. 1 at retention times greater than 8 min.

Small organic acids such as acetic, formic and gluconic are often present in Bayer liquors [1] and these acids are well known to elute very early in IC. The co-elution of these species with fluoride using 35 m*M* NaOH was highly likely. Under the conditions employed in Fig. 1, spiking of the sample suggests that the first peak at 3.8 min is fluoride, the second peak at 5.0 min is acetate and the third peak at 7.2 min is formate. However, further confirmation of these assignments is presented later in the paper.

The fluoride peak in the chromatogram of a liquor sample displays noticeable band broadening compared to that in a standard, but the effect does not extend so prominently to the acetate and formate peaks. One explanation for this discrepancy may be a matrix effect because the standards are prepared in deionised water of pH $\approx$ 5 and the diluted liquor is pH $\approx$ 11. Injection of a standard results in direct adsorption of fluoride and elution with the 0.75 m*M* NaOH eluent (pH $\approx$ 10.8) whereas the pH of a liquor sample is slightly higher than that of the eluent and hence there may be some preliminary elution of fluoride which appears as band broadening. An alternative explanation for the apparent band broadening of the liquor sample is that band compression may be occurring on the column after injection of a standard of low ionic strength but it may be absent in the samples which have high ionic strength.

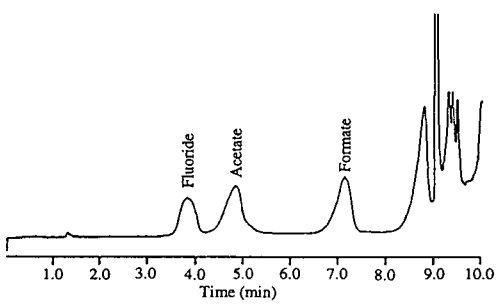

Fig. 1. Ion chromatogram of diluted sample 2 (spent liquor). Elution program as in Experimental section; flow-rate, 1 ml/min; column, Dionex AS5A (150 × 5 mm); guard column, AG5A (50 × 5 mm); sample loop, 25 μl; conductivity detector sensitivity, 100 μS.

Calibration plots of peak area vs. fluoride concentration were more reliable than peak height plots and they were linear over the range 1–4 mg/l fluoride. IC and ISE data for fluoride in four samples are presented in Table 1; the linear regression equation for these data is $y = 0.993x + 4.01$, with $r = 0.999$, which indicates excellent agreement between these two sets of data. The precision of ISE measurements (0.9–1.9%) is slightly better than the IC precision (1.3–3.2%), although the latter is quite acceptable for Bayer liquor analysis [6].

3.3. Determination of acetate and formate by IC

The carboxylate functional groups of carboxylic acids are known to absorb in the low 200 nm region [10,11], as do their conjugate bases COO^-. However, molar absorption coefficients are extremely low and detection of these species at low concentrations would be difficult [10]. UV detection was attempted by connecting a spectrophotometric detector directly to the outlet of the conductivity detector with a minimum length of connection tubing to minimise dispersion. This approach revealed two peaks at similar retention times to those observed for peaks 2 and 3 by conductivity detection and this supports their assignment as acetate and formate. As fluoride does not absorb at 200 nm, the absence of a peak

Table 1
Bayer liquor fluoride concentrations obtained by IC–conductivity detection and ISE potentiometry

Sample	IC		ISE	
	mg/l	R.S.D. (%)	mg/l	R.S.D. (%)
1	920	3.2 ($n = 38$)	930	0.9 ($n = 12$)
2	1550	1.4 ($n = 18$)	1540	0.7 ($n = 13$)
3	180	2.6 ($n = 16$)	180	1.8 ($n = 8$)
4	330	2.1 ($n = 14$)	330	1.8 ($n = 8$)

Chromatographic conditions as in Fig. 1. In potentiometry, electrode potentials were taken 5 min after addition of TISAB IV (pH 8.8) buffer.

Table 2
Acetate and formate in Bayer liquors obtained by IC–conductimetric and spectrophotometric detection

Sample	Acetate (mg/l)		Formate (mg/l)	
	UV	Conductivity	UV	Conductivity
1	18 700	19 600	6400	6300
R.S.D. (%, $n = 17$)	2.7	2.3	3.3	2.7
2	21 000	21 600	7500	6800
R.S.D. (%, $n = 10$)	2.6	2.9	4.1	2.4

Chromatographic conditions as in Fig. 1.

close to 3.8 min is consistent with its assignment as fluoride by conductivity detection.

The calibration plot for acetate was linear over the range 0–20 mg/l using conductivity detection and linear over the range 0–40 mg/l by UV detection. The plot for formate was linear over the range 0–5 mg/l by conductivity detection and linear over the range 0–20 mg/l by UV detection. The IC analytical data for acetate and formate in samples 1 and 2 by UV and conductivity detection appear in Table 2. There is good agreement in the data derived from the two different modes of detection and either of the two detection methods is recommended for the analysis of acetate and/or formate in Bayer liquors.

4. Conclusions

The main development in this paper was the successful analysis of fluoride in Bayer liquors by suppressed IC. An elution program was devised to separate fluoride from acetate and formate. The fluoride data correlated well with ISE measurements and the acetate and formate data showed good agreement with on-line UV spectrophotometric data. ISE studies also revealed TISAB IV as the most appropriate buffer for potentiometric analysis of fluoride in Bayer liquors.

Acknowledgements

We wish to thank Alcoa of Australia Ltd. (Kwinana, Australia) and Comalco Research Centre (Thomastown, Australia) for the supply of samples for analysis. We thank Dr. G.R. O'Connell for useful discussions.

References

[1] T.G. Pearson, *The Chemical Background to the Aluminium Industry*, Royal Institute of Chemistry, London, 1955.
[2] D.E. Davey, D.E. Mulcahy, T.J. Muggleton and G.R. O'Connell, *Anal. Lett.*, 25 (1992) 607.
[3] E. Pungor, G. Nagy and K. Toth, in A.K. Covington (Editor), *Ion-Selective Electrode Methodology*, Vol. 2, CRC Press, Boca Raton, FL, 1979, p. 78.
[4] K. Nicholson and E.J. Duff, *Anal. Lett.*, 14, No. A7 (1981) 493.
[5] P.R. Haddad and P.E. Jackson, *Ion Chromatography —Principles and Applications* (*Journal of Chromatography Library*, Vol. 46), Elsevier, Amsterdam, 1990.
[6] K. The and R. Roussel, *Light Metals (Warrendale, PA)*, (1984) 115.
[7] K.H. Jansen, *GIT Fachz. Lab.*, 22 (1979) 1062.
[8] *Application Note 5*, Dionex, Sunnyvale, CA.
[9] W.F. Pickering, *Talanta*, 33 (1986) 661.
[10] P.R. Haddad and P.E. Jackson, *J. Chromatogr.*, 447 (1988) 155.
[11] G. Albarran and C.H. Collins, *J. Chromatogr.*, 395 (1987) 623.

ELSEVIER

Journal of Chromatography A, 678 (1994) 370–374

JOURNAL OF CHROMATOGRAPHY A

Short Communication

Comparison of two esterified γ-cyclodextrins with some other chirally selective gas chromatographic phases using volatile oil constituents

T.J. Betts

School of Pharmacy, Curtin University of Technology, GPO Box U1987, Perth, Western Australia 6001, Australia

First received 16 May 1994; revised manuscript received 26 May 1994

Abstract

Twenty-six different volatile oil constituents were used as solutes to check some chirally selective gas chromatographic phases for similar behaviour. Some diverse monoterpenoids and aromatics gave almost the same relative retention times on three differently esterified γ-cyclodextrins. However, rigid molecular bicyclic monoterpenes yielded different results on the trifluoroacetyl ester phase, and caused a changed elution sequence. This phase was equivalent to the previously used propionyl ester for some solutes, with increase in values, when compared to an α-cyclodextrin ester phase, remaining over 100% for most bicyclics. The γ-cyclodextrin butyryl ester was equivalent to Chirasil-Val for several solutes, but not for some bicyclic terpenes and aromatics, and it did not give as good an analysis of patchouli oil sesquiterpenes.

1. Introduction

This author has previously compared the behaviour of various solutes found in volatile oils on sets of dipentylated cyclodextrins which were either esterified or unesterified (with the 3-OH remaining). Relative retention times, using the three cyclodextrin ring sizes [1–3] allowed deductions to be made concerning the chemical nature of each solute peak. Percentage increases in these values on changing to γ-unesterified cyclodextrin from the corresponding α-modification (both dipentylated) were very indicative of whether monoterpenoids were bicyclic, monocyclic or acyclic. These results were partly seen with the esterified cyclodextrins, although here a different ester was used on the α- and γ-rings, trifluoroacetyl and propionyl respectively [3]. The latter was used for its claimed temperature stability (the manufacturer's booklet [4] has to give directions for regenerating the trifluoroacetyl cyclodextrins after high-temperature "misuse"), "enhanced selectivity" and "increased sensitivity" [4]. In case this change of esterifying acid had influenced the observations, it was desirable to check what would occur using the γ-trifluoroacetate ester instead of the propionate dipentylated γ-cyclodextrin [3]. These phases were introduced in 1990 and subsequently [3] to resolve enantioners, but that is not the purpose of this work.

Besides this recently introduced γ-propionate phase, the manufacturers have provided γ-butyrylester cyclodextrin, which is "nonpolar and has temperature stability. It is considered a good alternative to the L-valine *tert.*-butylamide

0021-9673/94/$07.00
SSDI 0021-9673(94)00511-7

phase (Chirasil-Val, which has a methylpolysiloxane backbone and contains no cyclodextrin). The influence of the inclusion mechanism on selectivity is much reduced" [4]. A comparison of new observations on butyryl and trifluoroacetyl γ-(dipentylated) cyclodextrins with previous results on propionyl γ-cyclodextrin [3] and Chirasil-Val [5] would thus be interesting.

2. Experimental

2.1. Apparatus

A Hewlett-Packard 5790A gas chromatograph was used, fitted with a capillary control unit and a splitter injection port. This latter and the flame ionisation detector, were both used at 215°C. Helium was the mobile phase, used at 0.6–1.2 ml min^{-1}, and as "make-up" gas to the detector.

The Chiraldex modified cyclodextrin capillaries used were purchased from Advanced Separation Technologies (Whippany, NJ, USA) and were all 10 m × 0.25 mm I.D. with film thickness given as 0.125 μm ± 10%. They were G-TA (trifluoroacetyl, dipentyl, γ-cyclodextrin), and G-BP (butyryl, dipentyl, γ-cyclodextrin). The previously used [3] G-PN (propionyl, dipentyl, γ-cyclodextrin) and A-TA (trifluoroacetyl, dipentyl, α-cyclodextrin) were from the same supplier. The Chirasil-Val capillary [5] was from Alltech (Deerfield, IL, USA) and was 25 m × 0.25 mm I.D. with 0.16 μm film thickness. All capillaries were heated and cooled at less than 10°C min^{-1} to avoid damaging the phases.

2.2. Methods

Solutes from various commercial sources were used. Trace residues from an "emptied" syringe were injected. Holdup times, obtained by extrapolating to methane the retention times for *n*-heptane and *n*-hexane on semi-logarithmic graph paper, were deducted from observed retention times. Relative retention times to *n*-undecane or to linalol were calculated, having been found previously to be more significant for this work than retention indices [2]. These were very reproducible; for example, repeated determinations for cuminal and menthol on Chiraldex G-TA gave identical different relative retention times given in Table 1. Results for fenchone and some other solutes were ±0.02. Similarly, 4-terpineol and estragole on G-BP gave identical values shown in Table 2. Results for fenchone on this phase, and for some other solutes were ±0.01.

3. Results and discussion

Table 1 lists new results as relative retention times against *n*-undecane for the modified γ-cyclodextrins Chiraldex G-TA (trifluoracetyl ester) and G-BP (butyryl ester). They are compared with previous results on the propionyl ester G-PN and on the α-cyclodextrin trifluoracetyl ester A-TA. Some solutes give similar values on all three γ-ester phases at 125°C. These are the aromatics *p*-cymene, estragole and cuminal; the acyclic monoterpenoids myrcene, linalol, citronellal, (citral and citronellol on two phases); and the monocyclic hydrocarbons α-terpinene, limonene and γ-terpinene (columns 3, 5 and 7, Table 1). Estragole is distinctive in showing the lowest relative retention time (by a small amount) for the three γ-esters on G-TA, which usually has the highest values. Such are distinctively shown by the rigid molecular bicyclics α-pinene, camphene, cineole and fenchone. Three of these even appear earlier in the solute elution sequence from the other two phases. Their percentage increase in relative retention going from G-BP (usually the lowest values) to G-TA (usually the highest) ranges from 63–88% (column 6, Table 1). The other bicyclics, 3-carene and thujone, which has a rotatable three-carbon side-chain, give only 17 and 33% increase, respectively. These values are similar to those of the monocyclics menthone and 4-terpineol, respectively, which also have such a side-chain. "No" increase (less than ±8%) is shown by three monocyclic terpene hydrocarbons, three acyclic monoterpenoids;

Table 1
Relative retention times (*n*-undecane = 1.00) on esterified dipentyl cyclodextrin capillaries at three temperatures

Solute	Type[a]	Column No. in this table								
		3: Chiraldex G-TA at 125°C	4: % increase ← G-PN to TA (columns 3/5)	5: Chiraldex G-PN at 125°C (Ref. [3])	6: % increase G-PB to TA (columns 3/7)	7: Chiraldex G-BP at 125°C	8: Chiraldex G-BP at 110°C	9: Chiraldex G-BP at 140°C	10: Chiraldex A-TA at 125°C (Ref. [3])	11: % increase A- to G-TA (columns 3/10)
Piperitone	M	8.01	12	7.17					*3.60*[b]	122
Citronellol	N	6.75	3	6.54					*4.74*	42
Citral	N	6.66	5	6.33					6.03	10
Cuminal	A	6.53	−1	↑ *6.55*[b]				5.24	4.88	34
Menthol	M	6.13	11	5.54					3.59	71
4-Terpineol	M	5.01	14	4.39	30	3.85[c]	4.28	3.41	*2.77*	81
Estragole	A	3.65	−7	3.93	−3	3.75[c]	4.12	3.38	2.82	29
Fenchone	B	3.35	29	*2.59*	74	*1.93*[c]	*2.03*	*1.83*	*1.16*	189
Thujone	B	3.32	16	*2.85*	33	*2.49*[c]	*2.75*	*2.22*	*1.26*	163
Menthone	M	3.30	6	3.12	18	2.80[c]	3.08	2.52	*1.72*	92
Citronellal	N	2.45	−1	2.46	7	2.28[c]	2.48	2.08	1.77	38
Linalol	N	2.37	−2	2.42	6	2.24[c]	2.48	2.00	1.44	65
Cineole	B	2.07	49	1.39	88	1.10	*1.05*		0.76	172
Camphene	B	1.27	55	*0.82*	87	*0.68*	*0.62*		*0.42*	202
γ-Terpinene	M	1.17	3	1.14	5	1.11[c]	1.11	1.11	0.74	58
Limonene	M	1.07	8	0.99	8	0.99	0.92		0.67	60
3-Carene	B	1.03	13	0.91	17	0.88	0.80		0.59	75
p-Cymene	A	1.01	−3	↑ *1.04*	−2	↑ *1.03*	↑ *1.00*		↑ *0.68*	48
α-Terpinene	M	0.91	5	0.87	5	0.87	0.80		0.56	62
α-Pinene	B	0.88	38	*0.64*	63	*0.54*	*0.56*		*0.37*	138
Myrcene	N	0.71	6	0.67	6	0.67	0.63		0.43	65

Using γ-(G) or α-(A) cyclodextrins which are dipentylated with 3-0 esterified: trifluoroacetyl (-TA), butyryl (-BP) or propionyl (-PN).
[a] A = Aromatic; B = bicyclic; M = monocyclic; N = acyclic.
[b] Values in italics are not in the elution sequence from Chiraldex G-TA (lower, unless with upward pointing arrow).
[c] Estimated from columns 8 and 9.

Table 2
Relative retention times (linalol = 1.00) on butyryl-esterified dipentyl γ-cyclodextrin compared with those from Chirasil-Val [5] at two temperatures and with two other esterified dipentyl γ-cyclodextrins at a third temperature

Solute	Type[a]	Column No. in this table								
		3: Chiraldex G-BP at 110°C	4: % increase ← columns 3/5	5: Chirasil-Val at 110°C	6: Chiraldex G-BP at 140°C	7: % increase ← columns 6/8	8: Chirasil-Val at 140°C	9: Chiraldex G-BP at 125°C	10: Chiraldex G-PN at 125°C	11: Chiraldex G-TA at 125°C
Caryophyllene	B				4.25	19	3.56			
Anethole	A				3.01	27	2.36			
Cuminal	A				2.62	20	2.19		2.71	2.75
Isoborneol	B				2.47	43	*1.73*[b]			
α-Terpineol	M				2.11	9	1.94			
Camphor	B	1.82	55	*1.17*[b]	1.69	27	*1.33*			
4-Terpineol	M	1.71	4	1.65	1.70	6	1.61	1.71	1.81	2.11
Estragole	A	1.65	22	1.35	1.69	19	1.42	1.67	1.62	1.54
Thujone	B	1.10						1.11	1.18	1.40
Citronellal	N	1.01	3	0.98	1.04	−2	1.06	1.02	1.02	1.03
Fenchone	B	0.85	15	0.74	0.91	−2	0.89	0.86	↑ *1.07*[b]	↑ *1.41*[b]
γ-Terpinene	M	0.44	−2	0.45	0.56	4	0.54	0.49	0.47	0.49
Cineole	B	0.42	2	0.41				0.49	↑ *0.57*	↑ *0.87*
p-Cymene	A	0.40	3	0.39				0.46	0.43	0.43
Limonene	M	0.38	5	0.36				0.44	0.41	↑ *0.45*
3-Carene	B	0.32						0.39	0.38	0.43
Camphene	B	0.25						0.30	0.34	↑ *0.54*
α-Pinene	B	0.20						0.24	0.26	0.37

[a,b] See footnotes to Table 1.

and by two aromatics which give a slight decrease.

A purpose of this study was to compare the ester phases G-TA and G-PN. A number of solutes give almost the same relative retention times on both phases —"no" increase, as before (column 4, Table 1). This group now includes menthone, all five acyclics and all three aromatics. The four rigid bicyclics are again distinctive with the largest increases (PN to TA) of 29–55%, leaving five other cyclic monoterpenes exhibiting "in-between" increases of 11–16%. Thus G-PN is not equivalent to G-TA for all solutes, particularly rigid bicyclic molecules which presumably are able to form transient inclusion complexes with the TA phase, but not the PN. There are a few changes in solute elution sequence, too. The monoterpenoid bicyclics α-pinene, camphene, thujone and fenchone are delayed, relatively, on TA, whilst the aromatics *p*-cymene and cuminal elute relatively quicker (see Table 1).

Previously [3], results on the dipentylated γ-cyclodextrin ester G-PN were compared with those from the α-ester A-TA. Now comparing G-TA with A-TA (column 11, Table 1) there is still [3] over 100% increase in relative retention time for nearly all bicyclics (not 3-carene which falls in a group of cyclic and acyclic monoterpenes ranging from 58–92% increase). As before, the monocyclic piperitone (122%) is grouped with the bicyclics. Three terminally oxygenated acyclics continue to exhibit low increases (less than 45%), particularly citral. Three aromatics also give increases less than 50%.

A second intention of this study was to compare Chiraldex G-BP phase with Chirasil-Val. The results are given in Table 2 as relative retention times to linalol at two temperatures as before [5]. Values are virtually the same (±9%) for the acyclic citronellal, four monocyclics, the bicyclics cineole and fenchone (at 140°C) and the aromatic hydrocarbon *p*-cymene. Despite having an identical polarity rating by *c* value [6] of 0.46, which is "fairly low", the Chiraldex G-BP phase gives increases in relative retention time at 140°C of 19–43% for three bicyclics and 19–27% for three aromatics. Increases seen at 110°C are 15–55%. Thus this Chiraldex is not an exact alternative to Chirasil-Val for all solutes, including the sesquiterpene caryophyllene. At 130°C, the helium flowrate on G-BP was adjusted to yield an uncorrected retention time of 5.30 min for caryophyllene, as was obtained from Chirasil-Val [5]. Two other sesquiterpene hydrocarbons, longifolene and humulene, then emerged at 5.35 and 6.60 min, respectively, from G-BP (5.07 and 6.10 min from Chirasil-Val). Using the conditions previously determined for patchouli oil (8 min isothermally at 130°C, then programmed up at 5°C min^{-1}) gave an inferior chromatogram from Chiraldex G-BP, which could not be improved by changing the conditions. The pairs of sesquiterpenes α-patchoulene/seychellene and β-patchoulene/α-gurjunene would not resolve. Thus for this author's purpose, the phases were not equivalent.

Comparing columns 9–11 of Table 2, nearly half the solutes yield virtually constant relative retention times at 125°C on the three Chiraldex G ester phases. Where this is not so, they usually increase from G-BP to -PN to -TA. The rise is particularly seen on the lattermost with the bicyclic terpenoids. The aromatic estragole behaves in reverse fashion, as seen in Table 1.

The most significant fact from this work is that Chiraldex G-TA is valuable for indicating bicyclic terpenoids when relative retention times are compared to values from another γ-cyclodextrin ester phase, particularly G-BP. Increase relative to undecane of over 60% suggests a rigid bicyclic molecule. A slight decrease may indicate an aromatic solute.

References

[1] T.J. Betts, *J. Chromatogr.*, 639 (1993) 366.
[2] T.J. Betts, *J. Chromatogr. A*, 653 (1993) 167.
[3] T.J. Betts, *J. Chromatogr. A*, 672 (1994) 254.
[4] *Chiraldex Capillary GC Columns*, ASTEC, Whippany, NJ, 1993.
[5] T.J. Betts, *J. Chromatogr. A*, 664 (1994) 295.
[6] T.J. Betts, *J. Chromatogr.*, 628 (1993) 138.

ELSEVIER

Journal of Chromatography A, 678 (1994) 375–379

JOURNAL OF CHROMATOGRAPHY A

Short Communication

Determination of thiobencarb residues in water and soil using solid-phase extraction discs

M.J. Redondo, M.J. Ruiz, R. Boluda, G. Font*

Laboratori de Toxicologia, Facultat de Farmàcia, Universitat de València, 46100 Burjassot, València, Spain

First received 3 March 1994; revised manuscript received 6 June 1994

Abstract

The movement and degradation of the herbicide thiobencarb was monitored in a rice field near Lake Albufera (Valencia, Spain). This area constitutes an ecological unit of great environmental interest. Soil samples were collected from the surface and the subsurface of the rice field treated with this herbicide. Soil characterization tests for pH, organic matter, moisture and texture were also carried out. At the same time, samples of water were taken from the inundated plot 10 cm below the surface. Both types of sample were extracted by solid-phase extraction using 47-mm discs of octyl-bonded silica sorbent and eluted with ethyl acetate, with average recoveries for this compound of 63 and 93% from soil and water, respectively. The analyses were carried out by gas chromatography with nitrogen–phosphorus detection. Sample components were separated with a 30 m × 0.25 mm I.D. fused-silica capillary column coated with 50% phenylmethylsilicone (DB-17).

1. Introduction

Thiobencarb [(*S*)-4-chlorobenzyl diethylthiocarbamate)] is a carbamate herbicide that has been widely used for weed control in rice crops. It is normally applied directly on the soil surface or by inundating the rice fields. After application, thiobencarb is distributed in the sediments and water of rice fields.

It has been stated that almost all of the pesticides applied in agriculture fails to reach the target and enters the environment unnecessarily [1]. Research has begun to focus on factors such as selectivity, reduction of application rates and the environmental fate of chemicals. Soil and surface waters are interesting matrices for these environmental studies. Monitoring samples for pesticide residues requires rapid, simple, accurate and reliable methods for determining the most common polluting pesticides.

Chromatographic analyses are preceded by sample preparation to extract the analyte compounds. This step is more difficult for complex samples, such as soil, than for water samples, so the selection of the extraction process may be one of the most important factors in the optimization of pesticide analyses.

Numerous methods exist for determining carbamate residues in both soil and water samples, but most of them involve partitioning by liquid–liquid extraction or solid-phase extraction. Prior to the partitioning it is necessary, for soil samples, to prepare a supernatant liquid by

* Corresponding author.

SSDI 0021-9673(94)00528-H

adding the soil to an organic or aqueous solvent, or a combination of the two, and shaking [2–7].

A wide variety of solvents have been used for the extraction of carbamates by traditional liquid–liquid extraction methods. The primary criteria for choosing the solvent have been extraction efficiency, selectivity (reducing the amount of unwanted co-extractives) and reproducibility of residue recovery. Partitioning with methylene chloride for carbamate insecticides [8–10], with chloroform for aldicarb [11] or with *n*-hexane for thiobencarb [12] has been proposed.

Because liquid–liquid extraction can be tedious and time consuming, solid-phase extraction is gaining popularity, principally for water samples [13–15]. The results obtained from application of solid-phase extraction techniques to the extraction of other groups of pesticides from soil samples [16–20] reveal important benefits of using them for carbamate determinations [21].

The purpose of this work was to develop a simple and rapid procedure for the determination of carbamate herbicides in agricultural soil and water samples. This procedure was used to monitor the movement and degradation of thiobencarb in a rice field near Lake Albufera (Valencia, Spain).

2. Experimental

2.1. Chemicals and reagents

Ethyl acetate and acetone, both of pesticide grade, were obtained from Promochem (Wesel, Germany) and methanol from Romyl (Leics., UK). The herbicide standard used was thiobencarb (98.9% purity) from Promochem.

2.2. Apparatus

A standard Millipore 47-mm filtration apparatus equipped with 47-mm discs of Empore octyl-bonded silica (Analytichem International, Harbor City, CA, USA) was used.

2.3. Gas chromatographic analyses

Gas chromatography was performed with a Hewlett-Packard Model 5890 Series II chromatograph equipped with a nitrogen–phosphorus detector, a Model H-P 7673 automatic injector, an HP 3365 integrator and a 30 m × 0.25 mm I.D. DB-17 capillary column with a film thickness of 0.25 μm. The injector and detector temperatures were 285 and 300°C, respectively.

Injection was performed in the splitless mode with the column oven at 50°C. This temperature was held for 1 min and was then increased at 30°C min^{-1} to 140°C, held for 2 min, then increased at 5°C min^{-1} to 280°C, which was held for 10 min. Helium was used as the carrier gas at 1.6 ml min^{-1}. The detector gases were air at 70.9 ml min^{-1}, hydrogen at 3.5 ml min^{-1} and helium (make-up) at 18.3 ml min^{-1}.

2.4. Collection and sample preparation

The plot was treated with thiobencarb at a rate of 3.6 kg ha^{-1}. Samples from the same sampling sites had been analysed prior to application and no pesticides could be detected.

Soil samples were taken from three different locations in the plot, from 0–15, 15–30 and 30–45 cm layers. The collection of samples was carried out five times in a period of 4 weeks. After collection the samples were stored at 4°C until analysis.

These samples were thoroughly mixed, and stones and plant materials were removed. Two 5-g portions were drawn, one of which was used for determining the herbicide residues and the other for determining the moisture content, by heating at 105°C for 24 h.

The soils used differ with respect to organic matter content, soil pH levels, sand, silt and clay content. These characteristics are listed in Table 1 and were determined according to the official method [22].

Factors such as temperature and moisture also affect the persistence and rate of degradation of thiobencarb. They ranged from 20 to 26°C and from 24.6 to 37.3%, respectively. The moisture

Table 1
Characteristics of soil samples

Depth (cm)	Organic matter (%)	pH (H_2O)[a]	Sand (%)	Silt (%)	Clay (%)
0–15	2.9	7.9	42.1	37.8	20.1
15–30	2.4	8.2	39.9	37.3	22.8
30–45	1.9	8.5	12.7	49.3	38.0

[a] pH (H_2O) is the pH measured in a water–soil suspension.

not only changes with the depth of the soil layer, but also with the study time.

Water samples were taken from the inundated plot 10 cm below the surface. These samples were filtered to remove plant materials and stored at 4°C until analysed.

2.5. Extraction procedure

Extraction of soil samples

The method used has been described elsewhere [23]. Briefly, 5 g moist soil sample were added to 5 ml of distilled water and shaken by sonication for 15 min. It was then added to 5 ml acetone and shaken for another 15 min. The suspension was filtered through a Whatman No. 40 filter and washed twice with 5 ml of distilled water.

The polar solution was diluted to about 500 ml with distilled water and passed through a conditioned 47-mm disc of octyl-bonded silica sorbent. The adsorbed residues were eluted with 10 ml of ethyl acetate. The extract was concentrated at 45°C to 1 ml and 1-μl samples were injected into the gas chromatograph. The residues were determined by capillary gas chromatography with a nitrogen–phosphorus detector.

Extraction of water samples

A volume of 1 l of filtered water was passed through the conditioned solid sorbent and the residues was eluted with 10 ml of ethyl acetate. The extract was concentrated to 1 ml and 1-μl samples were injected into the gas chromatograph.

3. Results and discussion

In order to judge the efficiency of the analytical procedure, recovery experiments were performed by spiking with thiobencarb soil and water samples that had not received treatment with this herbicide. The spiked concentration levels were 0.06 $\mu g\ g^{-1}$ and 0.2 $\mu g\ l^{-1}$, respectively. The samples were extracted by the methods described above.

The recoveries (mean ± R.S.D., $n = 5$) were 62.6 ± 4.9% for soil and 92.5 ± 3.2% for water. These values were lower for soil than for water samples owing to adsorption in the soil, a complex phenomenon which makes it difficult to extract the residues. Similar carbamate recoveries were obtained from soil samples using a traditional method involving liquid–liquid extraction with methylene chloride [9,24], as reported in a previous paper [23].

The detection limits are 11.5 ng g^{-1} in soil and 34.0 ng l^{-1} water. These limits were calculated by extrapolation and represent amounts that produce a chromatographic peak with a height equal to three times the standard deviation of the baseline noise.

Figure 1 shows typical chromatograms of an extract, obtained by the solid-phase extraction procedure described, from a real soil sample before and after treatment with thiobencarb. Similar chromatograms were obtained from a real water sample containing thiobencarb, as illustrated in Fig. 2.

The GC peak with a retention time 26.8 min was identified as the herbicide thiobencarb. Owing to the high selectivity of nitrogen–phosphorus detection, no further purification was

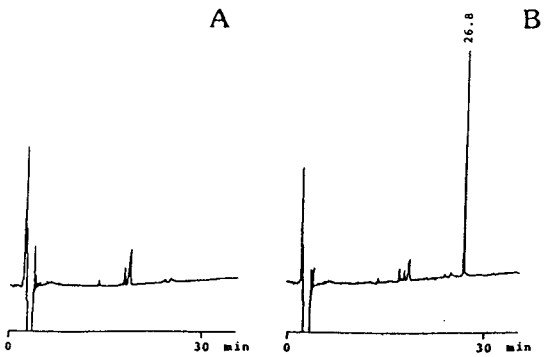

Fig. 1. Chromatograms of extracts obtained by SPE with a C_8 disc from (A) a real soil sample prior to treatment and (B) a real soil sample from the same plot treated with thiobencarb.

needed. The concentrations determined in the soil and water samples are given in Table 2. The herbicide residue levels in a soil sample were subjected to a correction based on the moisture content of the sample and were expressed on a dry mass basis. In Table 2 it can be seen that there was a rapid initial dissipation followed by a slower rate of dissipation from the second sampling to the end of the experiment.

The movement of thiobencarb is considerably less in soil with increased organic matter content (see Table 1), because organic matter is the most important factor involved in adsorption of this herbicide [25]. However, the dissipation was slower below the soil surface than at the surface, which proves that thiobencarb can move vertically, reaching the deeper layers some days after the application owing to the leaching of the pesticide through the soil. In addition, in the top layer, the combination of degradation and movement leads to a rapid decrease in thiobencarb concentration. Generally, the degradation process of the pesticides is favoured by the presence of oxygen and by aerobic microorganisms [25].

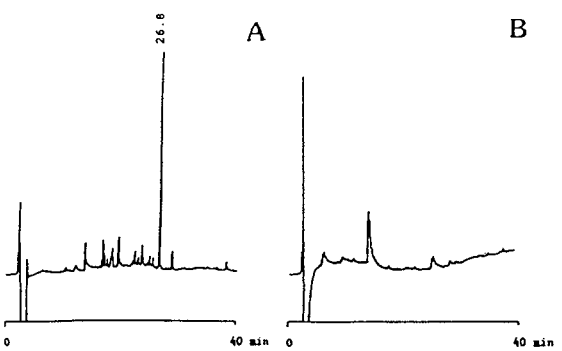

Fig. 2. (A) Chromatogram of an extract obtained by solid-phase extraction with a C_8 disc from a real water sample taken from the inundated plot and (B) blank.

Table 2
Total thiobencarb concentrations in soil and water

Days after application	Depth (cm)	Concentration in soil (ng g^{-1})	Concentration in water ($\mu g\ l^{-1}$)
5	0–15	743.0	
	15–30	247.2	36.3
	30–45	115.0	
10	0–15	425.3	
	15–30	189.1	10.5
	30–45	121.9	
14	0–15	332.3	
	15–30	135.4	9.9
	30–45	83.5	
21	0–15	291.1	
	15–30	147.2	8.0
	30–45	42.0	
28	0–15	237.2	
	15–30	143.5	4.6
	30–45	42.1	

The estimated field half-life was 12 days in the soil surface. This does not agree with values in the literature, which ranged from 14 to 21 days [26]. This can easily be explained by the fact that this parameter is closely linked to the soil characteristics, climate factors and agricultural methods.

4. Conclusions

The methodology proposed may be useful in pesticide residue programmes because it is suitable for the rapid analysis of a large number of samples. The effectiveness of the sorbent discs for extraction and clean-up in the determination of thiocarbamates in soil and water samples has been demonstrated. The application of the method to soil and water samples from an inundated

rice field made it possible to monitor the thiobencarb concentration under field conditions and to determine its rate of dissipation.

Acknowledgements

The authors thank CICYT (NAT 91-1129) for financial support of this project, the Generalitat Valenciana, Conselleria de Cultura, Educación y Ciencia for a grant to M.J. Redondo and the Science and Education Ministry for a grant to M.J. Ruiz.

References

[1] I.J. Graham-Bryce, *Agrochemicals in Soils*. Pergamon Press, Oxford, 1980.
[2] N.D. Westcott and B.L. Worobey, *J. Agric. Food Chem.*, 33 (1985) 58–60.
[3] F.A. Elhag, W.N. Yule and W.D. Marshall, *Bull. Environ. Contam. Toxicol.*, 42 (1989) 172–176.
[4] K.W. McDougall, G. Singh, C.R. Harris and F.R. Higginson, *Bull. Environ. Contam. Toxicol.*, 39 (1987) 286–293.
[5] H. Wan, F.R. Higginson, C.R. Harris and K.W. McDougall, *Bull. Environ. Contam. Toxicol.*, 42 (1989) 177–180.
[6] A.M. Balinova and I. Balinov, *Fresenius' J. Anal. Chem.*, 339 (1991) 409–412.
[7] M. Venkatramesh and V. Agnihothudu, *Bull Environ. Contam. Toxicol.*, 41 (1988) 548–555.
[8] K.D. Racke and J.R. Coats, *J. Agric. Food Chem.*, 36 (1988) 1067–1972.
[9] B.C. Leppert, J.C. Markle, R.C. Helt and G.H. Fujie, *J. Agric. Food Chem.*, 31 (1983) 220–223.
[10] L.W. Getzin, C.G. Cogger and P.R. Bristow, *J. Assoc. Off. Anal. Chem.*, 72 (1989) 361–364.
[11] Y. Picó, C. Albelda, J.C. Moltó, G. Font and J. Mañes, *Food Addit. Contam.*, 7 (1990) S29–S34.
[12] J.M. Carrasco, M. Planta, V. Gómez-Casals and V. Moragues, *J. Assoc. Off. Anal. Chem.*, 70 (1987) 752–753.
[13] R.G. Nash, *J. Assoc Off. Anal. Chem.*, 73 (1990) 438–442.
[14] T. McDonnell and J. Rosenfeld, *J. Chromatogr.*, 629 (1993) 41–53.
[15] L.S. Chiron and D. Barceló, *J. Chromatogr.*, 645 (1993) 125–134.
[16] L.Q. Huang and C.R. Frink, *Bull. Environ. Contam. Toxicol.*, 43 (1989) 159–164.
[17] P.R. Loconto, *LC·GC Int.*, 4 (1991) 12–15.
[18] L.Q. Huang, *J. Assoc. Off. Anal. Chem.*, 72 (1989) 349–354.
[19] H. Weil and K. Haberer, *Fresenius' J. Anal. Chem.*, 339 (1991) 405–408.
[20] M.S. Mills and E.M. Thurman, *Anal. Chem.*, 64 (1992) 1985–1990.
[21] K.L. Crepeau, G. Walker and W. Winterlin, *Bull. Environ. Contam. Toxicol.*, 46 (1991) 512–518.
[22] *Official Methods of the Spanish Ministry of Agriculture, Fisheries and Food, Vol. 3, Spanish Ministry of Agriculture, Fisheries and Food, Madrid*, 1986, *p.* 178.
[23] M.J. Redondo, M.J. Ruiz, R. Boluda and G. Font, *Chromatographia*, 36 (1993) 187–190.
[24] S.Y. Szeto and K.M.S. Sundaram, *J. Chromatogr.*, 200 (1980) 179–184.
[25] S.U. Khan, in R.J. Wakeman (Editor), *Pesticides in the Soil Environment*, Elsevier, Amsterdam, 1980, p. 29.
[26] R.D. Wauchope, T.M. Buttler, A.G. Harnsby, P.W.M. Augustijn-Beckers and J.P. Burt, *Rev. Environ. Contam. Toxicol.*, 123 (1992) 1–163.

ELSEVIER

Journal of Chromatography A, 678 (1994) 380

JOURNAL OF CHROMATOGRAPHY A

Erratum

Characterization of stationary phases used in reversed-phase and hydrophobic interaction chromatography [*Journal of Chromatography A*, 668 (1994) 301–312]

G. Rippel, E. Alattyani, L. Szepesy

Page 312 of this article was erroneously left blank. The text on this page should read:

[33] R.M. Smith, *J. Chromatogr.*, 236 (1982) 313.
[34] R.M. Smith, *Anal. Chem.*, 56 (1984) 256.
[35] B.A. Bidlingmeyer, S.N. Deming, W.P. Price, B. Sachok and M. Petrusek, *J. Chromatogr.*, 186 (1979) 419.
[36] P.J. Schoenmakers, H.A.H. Billiet and L. de Galan, *J. Chromatogr.*, 185 (1979) 179.
[37] T.L. Hafkenscheid and E. Tomlinson, *J. Chromatogr.*, 264 (1983) 47.
[38] P.J. Schoenmakers, *Optimization of Chromatographic Selectivity*, Elsevier, Amsterdam, 1986, p. 64.
[39] P.J. Schoenmakers, A. Bartha and H.A.H. Billiet, *J. Chromatogr.*, 550 (1991) 425.
[40] L. Szepesy and G. Rippel, *Chromatographia*, 34 (1992) 391.
[41] G. Rippel and L. Szepesy, *J. Chromatogr. A*, 664 (1994) 27.
[42] A. Drouen, J.W. Dolan, L.R. Snyder, A. Poile and P.J. Schoenmakers, *LC · GC Int.*, 5, No. 2 (1992) 28.
[43] L. Szepesy and G. Rippel, *J. Chromatogr. A*, 668 (1994) 337.

SSDI 0021-9673(94)00616-4

Author Index

Flow-Through (Bio)Chemical Sensors

By **M. Valcárcel** and **M.D. Luque de Castro**, Department of Analytical Chemistry, University of Córdoba, 14004 Córdoba, Spain

Techniques and Instrumentation in Analytical Chemistry Volume 16

Flow-through sensors are more suitable than classical probe-type sensors for addressing real (non-academic) problems. The external shape and operation of flow-through (bio)chemical sensors are of great practical significance as they facilitate sample transport and conditioning, as well as calibration and sensor preparation, maintenance and regeneration, all of which result in enhanced analytical features and a wider scope of application.
This is a systematic presentation of flow-through chemical and biochemical sensors based on the permanent or transient immobilization of any of the ingredients of a (bio)chemical reaction (i.e. the analyte, reagent, catalyst or product) where detection is integrated with the analytical reaction, a separation process (dialysis, gas diffusion, sorption, etc.) or both.

The book deals critically with most types of flow-through sensors, discussing their possibilities and shortcomings to provide a realistic view of the state-of-the-art in the field. The large numbers of figures, the wealth of literature references and the extensive subject index complement the text.

© 1994 332 pages Hardbound
Price: Dfl. 355.00 (US$ 202.75)
ISBN 0-444-89866-2

ORDER INFORMATION
ELSEVIER SCIENCE B.V.
P.O. Box 330
1000 AH Amsterdam
The Netherlands
Fax: (+31-20) 5862 845
For USA and Canada
P.O. Box 945
Madison Square Station
New York, NY 10159-0945
Fax: (212) 633 3680
US$ prices are valid only for the USA & Canada and are subject to exchange rate fluctuations; in all other countries the Dutch guilder price (Dfl.) is definitive. Customers in the European Union should add the appropriate VAT rate applicable in their country to the price(s). Books are sent posttree if prepaid.

ELSEVIER SCIENCE

Send your article on floppy disk!

All articles may now be submitted on computer disk, with the eventual aim of reducing production times and improving the reliability of proofs still further. Please follow the guidelines below.

With revision, your disk plus one final, printed and exactly matching version (as a printout) should be submitted together to the editor. **It is important that the file on disk to be processed and the printout are identical.** Both will then be forwarded by the editor to Elsevier.

The accepted article will be regarded as final and the files will be processed as such. Proofs are for checking typesetting/editing: only printer's errors may be corrected. No changes in, or additions to the edited manuscript will be accepted.

Illustrations should be provided in the usual manner and, if possible, on a **separate** floppy disk as well.

Please follow the general instructions on style/arrangement and, in particular, the reference style of this journal as given in the "Guide for Authors".

The preferred storage medium is a 5¼ or 3½ inch disk in MS-DOS or Macintosh format, although other systems are also welcome.

Please label the disk with your name, the software & hardware used and the name of the file to be processed.

For further information on the preparation of compuscripts please contact:

Elsevier Science B.V.
Journal of Chromatography A
P.O. Box 330
1000 AH Amsterdam, The Netherlands
Phone: (+31-20) 5862 793 Fax: (+31-20) 5862459

ELSEVIER SCIENCE

PUBLICATION SCHEDULE FOR THE 1994 SUBSCRIPTION

Journal of Chromatography A and *Journal of Chromatography B: Biomedical Applications*

MONTH	1993	J–J	J	A	S	O	
Journal of Chromatography A	652–657	Vols. 658–672	673/1 673/2 674/1 + 2 675/1 + 2 676/1	676/2 677/1 677/2 678/1	678/2 679/1 679/2 680/1	680/2	The publication schedule for further issues will be published later.
Bibliography Section		Vol. 681			682/1		
Journal of Chromatography B: Biomedical Applications		Vols. 652–656	657/1 657/2	658/1 658/2	659	660/1 660/2	

INFORMATION FOR AUTHORS

(Detailed *Instructions to Authors* were published in *J. Chromatogr. A*, Vol. 657, pp. 463–469. A free reprint can be obtained by application to the publisher, Elsevier Science B.V., P.O. Box 330, 1000 AH Amsterdam, Netherlands.)

Types of Contributions. The following types of papers are published: Regular research papers (full-length papers), Review articles, Short Communications and Discussions. Short Communications are usually descriptions of short investigations, or they can report minor technical improvements of previously published procedures; they reflect the same quality of research as full-length papers, but should preferably not exceed five printed pages. Discussions (one or two pages) should explain, amplify, correct or otherwise comment substantively upon an article recently published in the journal. For Review articles, see inside front cover under Submission of Papers.

Submission. Every paper must be accompanied by a letter from the senior author, stating that he/she is submitting the paper for publication in the *Journal of Chromatography A* or *B*.

Manuscripts. Manuscripts should be typed in **double spacing** on consecutively numbered pages of uniform size. The manuscript should be preceded by a sheet of manuscript paper carrying the title of the paper and the name and full postal address of the person to whom the proofs are to be sent. As a rule, papers should be divided into sections, headed by a caption (*e.g.*, Abstract, Introduction, Experimental, Results, Discussion, etc.). All illustrations, photographs, tables, etc., should be on separate sheets.

Abstract. All articles should have an abstract of 50–100 words which clearly and briefly indicates what is new, different and significant. No references should be given.

Introduction. Every paper must have a concise introduction mentioning what has been done before on the topic described, and stating clearly what is new in the paper now submitted.

Experimental conditions should preferably be given on a *separate* sheet, headed "Conditions". These conditions will, if appropriate, be printed in a block, directly following the heading "Experimental".

Illustrations. The figures should be submitted in a form suitable for reproduction, drawn in Indian ink on drawing or tracing paper. Each illustration should have a caption, all the *captions* being typed (with double spacing) together on a *separate sheet*. If structures are given in the text, the original drawings should be provided. Coloured illustrations are reproduced at the author's expense, the cost being determined by the number of pages and by the number of colours needed. The written permission of the author and publisher must be obtained for the use of any figure already published. Its source must be indicated in the legend.

References. References should be numbered in the order in which they are cited in the text, and listed in numerical sequence on a separate sheet at the end of the article. Please check a recent issue for the layout of the reference list. Abbreviations for the titles of journals should follow the system used by *Chemical Abstracts*. Articles not yet published should be given as "in press" (journal should be specified), "submitted for publication" (journal should be specified), "in preparation" or "personal communication".

Vols. 1–651 of the *Journal of Chromatography*; *Journal of Chromatography, Biomedical Applications* and *Journal of Chromatography, Symposium Volumes* should be cited as *J. Chromatogr.* From Vol. 652 on, *Journal of Chromatography A* (incl. Symposium Volumes) should be cited as *J. Chromatogr. A* and *Journal of Chromatography B: Biomedical Applications* as *J. Chromatogr. B.*

Dispatch. Before sending the manuscript to the Editor please check that the envelope contains four copies of the paper complete with references, captions and figures. One of the sets of figures must be the originals suitable for direct reproduction. Please also ensure that permission to publish has been obtained from your institute.

Proofs. One set of proofs will be sent to the author to be carefully checked for printer's errors. Corrections must be restricted to instances in which the proof is at variance with the manuscript.

Reprints. Fifty reprints will be supplied free of charge. Additional reprints can be ordered by the authors. An order form containing price quotations will be sent to the authors together with the proofs of their article.

Analytical Applications of Circular Dichroism

Edited by **N. Purdie** and **H.G. Brittain**

Techniques and Instrumentation in Analytical Chemistry Volume 14

Circular dichroism is a special technique which provides unique information on dissymmetric molecules. Such compounds are becoming increasingly important in a wide variety of fields, such as natural products chemistry, pharmaceutics, molecular biology, etc. The content of this book has been selected in order to feature the unique aspects of circular dichroism, and how these strengths can be of assistance to workers in the field.

Substantial discussions have been provided regarding the particular phenomena associated with dissymmetric compounds which give rise to the circular dichroism effect. Reviews are also given of the type of instrumentation available for the measurement of these effects. A number of chapters cover the wide range of applications illustrating the power of the method.

Owing to its broad appeal, the book will be of interest to workers in all areas of chemistry and pharmaceutical science.

Contents:

© 1994 360 pages Hardbound
Price: Dfl. 355.00 (US $ 202.75)
ISBN 0-444-89508-6

ORDER INFORMATION

For USA and Canada
ELSEVIER SCIENCE INC.
P.O. Box 945
Madison Square Station
New York, NY 10160-0757
Fax: (212) 633 3880

In all other countries
ELSEVIER SCIENCE B.V.
P.O. Box 330
1000 AH Amsterdam
The Netherlands
Fax: (+31-20) 5862 845

US$ prices are valid only for the USA & Canada and are subject to exchange rate fluctuations; in all other countries the Dutch guilder price (Dfl.) is definitive. Customers in the European Community should add the appropriate VAT rate applicable in their country to the price(s). Books are sent postfree if prepaid.

ELSEVIER SCIENCE B.V.

0021-9673(19940902)678:2;1-M